Université de Strasbourg

UNIVERSITÉ DE STRASBOURG

École doctorale Sciences de la vie et de la santé | ED 414 Université de Strasbourg

ÉCOLE DOCTORALE DES SCIENCES DE LA VIE ET DE LA SANTÉ

Immunologie, Immunopathologie et Chimie Thérapeutique - CNRS UPR 3572

&

INSTITUTE OF BIOLOGY II

CIBSS - Centre for Integrative Biological Signalling Studies

THÈSE présentée par :

Yubing GUO

soutenue le : **17 Octobre 2023**

pour obtenir le grade de : **Docteur de l'université de Strasbourg**

Discipline/ Spécialité : Aspects Moléculaires et Cellulaires de la Biologie/ Immunologie

The impact of the *P. aeruginosa* lectin LecB on wound healing processes with a particular focus on the immune response

THÈSE dirigée par :

M. MUELLER Christopher	DR1, Université de Strasbourg
M. RÖMER Winfried	Prof., Albert-Ludwigs-Universität Freiburg

RAPPORTEURS :

Mme ORIAN-ROUSSEAU Veronique	Prof., Karlsruher Institut für Technologie
M. BODIN Stephane	MCF., Université de Montpellier

AUTRES MEMBRES DU JURY :

M. GROS Frédéric	MCF., Université de Strasbourg

The impact of the *P. aeruginosa* lectin LecB on wound healing processes with a particular focus on the immune response

Inaugural-Dissertation
to obtain the doctoral degree at the Faculty of Biology
of the Albert-Ludwigs-University Freiburg im Breisgau
and Doctoral School of Life and Health Sciences (ED414)
of the Université de Strasbourg

presented by

Yubing Guo
born in Dalian, China

at the
Albert-Ludwigs-University Freiburg, Germany

Freiburg im Breisgau, August 2023 of submission of the thesis

Joint supervision (co-tutelle) by:

Prof. Winfried Römer

DR1-CNRS Christopher G. Mueller

Examiners:

Prof. Veronique Orian-Rousseau

Lecturer Dr. Stephane Bodin

Lecturer Dr. Frédéric Gros

Date of the oral exam: 17th October 2023

Acknowledgements

This thesis work was conducted between October 2019 and October 2023 at the CIBSS Centre For Integrative Biological Signalling Studies, Freiburg University, and IBMC Institute of Molecular and Cellular Biology, Strasbourg University.

Studies under the direct supervision of Prof. Dr. Winfried Römer, Freiburg University, and DR Christopher Mueller, Strasbourg University, where I became immersed in two research projects, mentored students, academic conferences, and cherished the academic discourse. My sincerest gratitude goes to my supervisors Prof. Dr. Winfried Römer and DR Christopher Mueller, who trusted me with many opportunities to develop creative and inspiring projects and collaborations! I am appreciated that Prof. Dr. Alexander Titz kindly provided me LecB inhibitor, DH445, to support my project. Many thanks to Prof. Veronique Orian-Rousseau, Dr. Stephane Bodin and Dr. Frédéric Gros, who attend my Ph.D. defense as examiners to give me comments.

I had the great pleasure of working with my current and former lab members of AG Römer, which unwavering support accompanied me during my Ph.D. journey! Particularly helpful and encouraging to me during this time were Dr. Valera Melendez, Dr. Alessia Landi, Dr. Annette Brandel, Dr. Marco Frensch, Dr. Ramin Omidvar, Dr. Francesca Rosato, Sarah Frisancho Mariscal, Anna-Sophia Kittel, Jana Tomisch, Stella Glauz, Lena Wolter, Kai Stober, Celine Enderle, Shengnan Zou and Carmen Senin. I also had the great pleasure of working with my current and former lab members of AG Mueller, Dr. Abdouramane Camara, Dr. Vincent Flacher, Alice C. Lavanant, Lutfir Hamzam, Zinaida Igamberdieva, Raquel Sal-Carro, Dr. Benjamin Neighbor, Shadrack Owusu, Astrid Host, and Dr. Wacym Boufenghou. Many thanks to Fabien Lhericel and Delphine Lamon, who helped me to inject LecB into mice and isolate lymph nodes, bones, and spleen from mice.

I would like to give gratitude to my parents, Xianming Guo and Dong He, and my boyfriend, Fan Xu. Many thanks to my closest friends, Zhenyu Yang, Huanyu Ma, Jia Wang, Yixin Zhang and Yiqing Zhang, and so on. I am incredibly grateful for your tremendous support during the difficulties of this journey.

Last but not least, my thesis has received funding from the China Scholarship Council, No. 202008080232, and the German-French University, a co-doctoral financial aid, No. CT-07-20. I also received traveling funding from the PROCOPE Mobility fellowship from July to September 2021.

Declaration

1. I herewith declare that I have prepared the present work without any unallowed help from third parties and without using any aids beyond those given. All data and concepts taken directly or indirectly from other sources are indicated along with a notation of the source. In particular, I have not used any paid assistance from exchange or consulting services (doctoral degree advisors or other persons). I have yet to receive remuneration from anyone, either directly or indirectly, for work related to the content of the present dissertation.

2. The work has not been submitted in this country or abroad to any other examination board in this or similar form.

3. The provisions of the doctoral degree examination procedure of the Faculty of Biology of the University of Freiburg are known to me. In particular, I am aware that before awarding the final doctoral degree, I am not entitled to use the title of Dr.

Part A of this thesis is an unpublished manuscript.
Part B of this thesis is a reprint of the following published research article.

Contents

Summary

Pseudomonas aeruginosa (*P. aeruginosa*) can cause a wide variety of infections, which encompass all organs of the human body, such as ventilator-associated pneumonia and acute lung injury. Due to the extracellular toxin and multi-drug resistance of *P. aeruginosa*, it is virulent to the host cells or organs. To date, several shreds of evidence show that *P. aeruginosa* lectin LecB is an important virulence factor. From our previous works, LecB can block epithelial cell wound healing and lung cancer cell migration with the reduction of β-catenin level. However, the molecular mechanisms induced by LecB are unclear. Besides, LecB also causes B cell receptor (BCR)-dependent activation-induced death of B cells *in vitro*, however, its impact on the immune system remains incompletely understood. Here, my Ph.D. projects are separated into two parts to investigate these questions. One part is about the effect of LecB on cell adhesion and cell migration *in vitro*, and another part is regarding the impact of LecB on immune response *in vivo*, such as dendritic cells (DCs) and T cells.

In my first part of the project, our findings revealed that LecB, as a bacterial adhesin, severely attenuated cell migration and enhanced cell adhesion in human non-small cell lung cancer cells H1299. I unraveled that LecB had less capability to increase cell adhesion and decrease cell migration with the knockout of flotillin-1 or the knockdown of flotillin-2 alone expression in H1299 cells. I used fibronectin instead of streptavidin and LecB-Biotin to mimic the microenvironment. I found that LecB increased fibronectin-dependent cell adhesion ability, which was also mediated by flotillin-1. Moreover, I found the colocalization and co-precipitation between LecB and flotillin-1/2. Furthermore, I introduced ß1-integrin as another interactor of LecB. I found that ß1-integrin could indirectly interact with flotillin-1 but not with flotillin-2 induced by LecB. Meanwhile, the silencing of flotillin-1/2 could postpone the intracellular trafficking of ß1-integrin triggered by LecB. Consequently, I identified that LecB facilitied the recruitment of flotillins, especially flotillin-1, as an essential molecular factor of LecB. LecB also induced FAK-Src complex, and LecB changed the localization of FAK from the leading edge of cells to the cytoplasm. The knockout of flotillin-1 rescued the decreased FA number induced by LecB. Moreover, LecB induced the nuclear accumulation of ß-catenin, which was blocked by the silencing of flotillin-1/2. With the knockout of flotillin-1 or the knockdown of flotillin-2, there was no accumulation of ß-catenin in nuclei, but most ß-catenin was in the cytoplasm in perinuclear regions. Thus, I revealed that LecB could trigger ß1-integrin/FAK-Src signaling and its downstream signal ß-catenin mediated by flotillin-1.

In my second part of the project, I found that LecB-triggered restriction of cell migration in mice. LecB colocalized with lymphatic vessels in mice and endothelial cell (ECs) in humans. After the skin-draining LecB into lymph nodes, LecB interfered with migration of DCs and subsequent T cell activation *in vivo*. Meanwhile, I also employed DH445, a derivative of L-fucose, as a LecB inhibitor to investigate if DH445 can block LecB regarding immune responses. The results depicted that DH445 could rescue LecB-mediated inhibition of DC migration into the T cell zone, and it reversed the reduced T cell activation induced by LecB. Thus, DH445 may find an application to *P. aeruginosa* infections. Then, I found that LecB-triggered cell migration could be reproduced in an *in vitro* endothelial transmigration assay. By studying human

umbilical vein endothelial cells (HUVECs) in more detail, I found that LecB triggered the endocytic degradation of VE-cadherin, changes in FAK subcellular location, the formation of a cortical F-actin rim, and reduced phosphorylation of myosin light chain. Notably, the degradation of VE-cadherin was not due to LecB toxicity-induced cell apoptosis. From the results of MTT and caspase-3 assay, LecB did not affect the cell viability of HUVECs, compared with positive controls, such as staurosporine inducing cell apoptosis and serum-free inhibiting cell growth. Moreover, untreated cells exhibited actin dynamics concomitant with cell motility, and the 3 h LecB treatment left the cells sessile with low levels of polymerized actin, which was quantified via Image J. Thus, I found that LecB could inhibit DC migration and T cell activation *in vivo*, and LecB changed cytoskeletal proteins, such as FAK and F-actin, resulting in the blockage of endothelial transmigration.

Overall, I focused on the effect of *P. aeruginosa* lectin LecB on cell migration. One part concerns lung cancer cell migration *in vitro*, and another is about immune cell migration *in vivo*. I highlighted a new light on the function of LecB regarding cell migration not only *in vitro* but also *in vivo*. It depicted that LecB could block either lung cancer cell migration *in vitro* and immune cell migration *in vivo*, resulting in diminished tissue repair and reduced immune responses, respectively. L-fucose and DH445 can rescue the cellular functions induced by LecB, underlining the importance of LecB antagonism to cell migration and immune response against *P. aeruginosa* infection.

Résumé

Pseudomonas aeruginosa (P. aeruginosa) peut être à l'origine d'une grande variété d'infections qui touchent tous les organes du corps humain, telles que la pneumonie sous ventilation assistée et les lésions pulmonaires aiguës. En raison de sa toxine extracellulaire et de sa multirésistance aux médicaments, P. aeruginosa est virulente pour les cellules ou les organes de l'hôte. À ce jour, plusieurs éléments de preuve montrent que la lectine LecB de P. aeruginosa est un facteur de virulence important. D'après nos travaux antérieurs, LecB peut bloquer la cicatrisation des cellules épithéliales et la migration des cellules cancéreuses du poumon en réduisant le niveau de β-caténine. Cependant, les mécanismes moléculaires induits par LecB ne sont pas clairs. En outre, LecB provoque également la mort des cellules B in vitro par activation dépendante du récepteur des cellules B (BCR), mais son impact sur le système immunitaire reste incomplètement compris. Ici, mes projets de doctorat sont divisés en deux parties afin d'étudier ces questions. La première partie concerne l'effet de LecB sur l'adhésion cellulaire et la migration cellulaire in vitro, et la seconde partie concerne l'impact de LecB sur la réponse immunitaire in vivo, comme les cellules dendritiques (DCs) et les cellules T.

Dans la première partie de mon projet, nos résultats ont révélé que LecB, en tant qu'adhésine bactérienne, atténuait fortement la migration cellulaire et renforçait l'adhésion cellulaire dans les cellules humaines de cancer du poumon non à petites cellules H1299. J'ai découvert que la LecB avait moins de capacité à augmenter l'adhésion cellulaire et à diminuer la migration cellulaire avec le knock-out de la flotilline-1 ou le knock-out de la flotilline-2 seule dans les cellules H1299. J'ai utilisé de la fibronectine à la place de la streptavidine et de la LecB-Biotin pour reproduire le microenvironnement. J'ai constaté que LecB augmentait la capacité d'adhésion cellulaire dépendante de la fibronectine, qui était également médiée par la flotilline-1. En outre, j'ai constaté la colocalisation et la co-précipitation entre LecB et la flotilline-1/2. En outre, j'ai introduit la ß1-intégrine comme un autre interacteur de LecB. J'ai constaté que la ß1-intégrine pouvait interagir indirectement avec la flotilline-1 mais pas avec la flotilline-2 induite par LecB. Par ailleurs, l'inhibition de la flotilline-1/2 pouvait retarder le trafic intracellulaire de la ß1-intégrine déclenché par LecB. Par conséquent, j'ai identifié que LecB facilitait le recrutement des flotillines, en particulier la flotilline-1, comme un facteur moléculaire essentiel de LecB. LecB induit également le complexe FAK-Src, et LecB modifie la localisation de FAK du bord d'attaque des cellules vers le cytoplasme. L'inactivation de la flotilline-1 a permis de remédier à la diminution du nombre de FA induite par la LecB. De plus, LecB a induit l'accumulation nucléaire de la ß-caténine, qui a été bloquée par l'inhibition de la flotilline-1/2. Avec le knock-out de la flotilline-1 ou le knock-out de la flotilline-2, il n'y avait pas d'accumulation de ß-caténine dans les noyaux, mais la plupart de la ß-caténine se trouvait dans le cytoplasme dans les régions périnucléaires. Ainsi, j'ai révélé que LecB pouvait déclencher la signalisation ß1-intégrine/FAK-Src et son signal en aval, la ß-caténine, par l'intermédiaire de la flotilline-1.

Dans la deuxième partie de mon projet, j'ai découvert que la LecB déclenchait une restriction de la migration cellulaire chez la souris. LecB se colocalise avec les vaisseaux lymphatiques chez la souris et les cellules endothéliales (CE) chez l'homme. Après avoir drainé la peau dans les ganglions lymphatiques, LecB

interfère avec la migration des DC et l'activation subséquente des cellules T in vivo. Parallèlement, j'ai également utilisé le DH445, un dérivé du L-fucose, comme inhibiteur de la LecB afin d'étudier si le DH445 pouvait bloquer la LecB en ce qui concerne les réponses immunitaires. Les résultats ont montré que le DH445 pouvait remédier à l'inhibition de la migration des CD dans la zone des cellules T médiée par la LecB, et qu'il inversait l'activation réduite des cellules T induite par la LecB. Le DH445 pourrait donc trouver une application dans les infections à P. aeruginosa. J'ai ensuite constaté que la migration cellulaire déclenchée par le LecB pouvait être reproduite dans un essai de transmigration endothéliale in vitro. En étudiant plus en détail les cellules endothéliales de la veine ombilicale humaine (HUVEC), j'ai découvert que LecB déclenchait la dégradation endocytique de la VE-cadhérine, des changements dans la localisation subcellulaire de FAK, la formation d'une bordure corticale de F-actine et une réduction de la phosphorylation de la chaîne légère de myosine. Notamment, la dégradation de la VE-cadhérine n'était pas due à l'apoptose cellulaire induite par la toxicité de la LecB. D'après les résultats des tests MTT et caspase-3, le LecB n'a pas affecté la viabilité cellulaire des HUVEC, par rapport aux contrôles positifs, tels que la staurosporine qui induit l'apoptose cellulaire et le sérum libre qui inhibe la croissance cellulaire. En outre, les cellules non traitées présentaient une dynamique de l'actine concomitante à la motilité cellulaire, et le traitement au LecB pendant 3 heures a laissé les cellules sessiles avec de faibles niveaux d'actine polymérisée, ce qui a été quantifié via Image J. Ainsi, j'ai découvert que le LecB pouvait inhiber la migration des DC et l'activation des cellules T in vivo, et que le LecB modifiait les protéines du cytosquelette, telles que FAK et F-actine, ce qui entraînait le blocage de la transmigration endothéliale.

Dans l'ensemble, je me suis concentré sur l'effet de la lectine LecB de P. aeruginosa sur la migration cellulaire. Une partie concerne la migration des cellules cancéreuses du poumon in vitro et une autre la migration des cellules immunitaires in vivo. J'ai jeté un nouvel éclairage sur la fonction de LecB concernant la migration cellulaire non seulement in vitro mais aussi in vivo. Il en ressort que LecB peut bloquer la migration des cellules cancéreuses du poumon in vitro et la migration des cellules immunitaires in vivo, ce qui entraîne une diminution de la réparation des tissus et une réduction des réponses immunitaires, respectivement. Le L-fucose et le DH445 peuvent sauver les fonctions cellulaires induites par la LecB, soulignant l'importance de l'antagonisme de la LecB pour la migration cellulaire et la réponse immunitaire contre l'infection par P. aeruginosa.

List of figures

Part A:

Part B:

Supplementary figures:

List of abbreviations

Abbreviation	Definition
ac-LDL	acetylated low density lipoprotein
AFM	atomic force microscopy
AJs	adherens junctions
AKT	protein kinase B
ALCAM	activated leukocyte cell adhesion molecule
AMPK	AMP-activated protein kinase
AP1	activator protein 1
APCs	antigen presenting cells
BCAM	basal cell adhesion molecule
BCR	B cell receptor
BECs	blood vessel endothelial cells
BMDCs	DCs from bone marrow precursors
CAMs	cell adhesion molecules
CC	coiled-coil
CCJs	cell-cell junctions
CCL	C-C linked chemokine
CCR	CC chemokine receptor
CD40L	CD40 ligand
CF	cystic fibrosis
CFSE	carboxyfluorescein succinimidyl ester
CIE	clathrin independent endocytosis
CKIα	casein Kinase Iα
CLCA1	Calcium activated chloride channel regulator 1
CLEVER1	common lymphatic endothelial and vascular receptor 1
CPs	cryptopatches
CRAC	cholesterol recognition amino acid consensus
CTLA-4	cytotoxic T lymphocyte antigen-4
DCs	dendritic cells
D-Gal	D-galactose
Dvl	dishevelled
dLN	draining lymph node
ECs	endothelial cells
ECM	extracellular matrix
EE	early endosome

EEA1	early endosome antigen 1
EGFR	epidermal growth factor receptor
EMT	epithelial mesenchymal transition
EPAC	exchange protein directly activated by cAMP
EPCAM	epithelial cell adhesion molecule
EPS	extracellular polymeric substances
ER	endoplasmic reticulum
FA	focal adhesion
FAK	focal adhesion kinase
FCS	fetal calf serum
F_d	detachment force
FERM	protein, ezrin, radixin, moesin
FRCs	fibroblastic reticular cells
GALT	gut-associated lymphoid tissue
GJ	gap junctions
Grb2	growth factor receptor-bound protein 2
GSK3	glycogen synthase kinase 3
HBSS	Hanks' balanced salt solution
HEV	high endothelial venules
hFlt3L	human fms related tyrosine kinase 3 ligand
HUVECs	human umbilical vein endothelial cells
IACs	integrin adhesion complexes
ICAM1	intercellular adhesion molecule 1
Ig	immunoglobulin
IGF1R	insulin like growth factor 1 receptor
ILFs	isolated lymphoid follicles
JAM1	junctional adhesion molecule 1
JNK	c-Jun N-terminal kinase
KD	knockdown
LasA, staphylolysin	elastase A
LasB, pseudolysin	elastase B
LE	late endosome
LECs	lymphatic endothelial cells
LNs	lymph nodes
LPS	Lipopolysaccharide
LVs	lymphatic vessels
LYVE-1	lymphatic vessel endothelial hyaluronan receptor-1
MAPK	mitogen activated protein kinases

MBL	mannan binding lectin
MDCK	Madin-Darby canine kidney strain cell line
MET	mesenchymal epithelial transition
MHC	major histocompatibility complex
MRSA	methicillin-resistant *S. aureus*
NEAA	non-essential amino acids solution
NF-κB	nuclear factor kappa-light-chain-enhancer of activated B cells
NK	natural killer
NT	untreated
OVA	ovalbumin
P. aeruginosa	*Pseudomonas aeruginosa*
PAMPs	pathogen associated molecular patterns
PD	photodiode
PDPN	podoplanin
PECAM1	platelet endothelial cell adhesion molecule1
PI3K	phosphoinositide 3-kinase
PIV	protease IV
PKC	protein kinase C
PNAd	peripheral node addressins
PROX1	prospero homeobox 1
PTEN	phosphatase and tensin homolog
PTK2	protein tyrosine kinase 2
RAS homologue	Rho GTPases
RE	recycling endosome
RNAi	RNA interference
RPMI	Roswell Park Memorial Institute
S. aureus	*Staphylococcus aureus*
SCFS	single cell force spectroscopy
SCS	subcapsular sinus
SEM	standard error of the mean
SPFH	stomatin/prohibitin/flotillin/HflC/K
S. pneumoniae	*Streptococcus pneumoniae*
SSTIs	skin and soft tissue infections
T3SS	type III secretion system
TCF/LEF	T cell factor/lymphoid enhancer factor
TCR	T cell receptor
TGN	trans-Golgi network
TJ	tight junctions

Tinagl1	tubulointerstitial nephritis antigen-like 1
TMD	transmembrane domain
TRAFs	TNFR associated factors
Tregs	regulatory T cells
Vav3	vav guanine nucleotide exchange factor 3
VCAM1	vascular cell adhesion protein 1
VE-cadherin	vascular endothelial cadherin
VEGFR-3	vascular endothelial growth factor receptor-3

1. General Introduction

1. 1. *Pseudomonas aeruginosa*

Pseudomonas aeruginosa (*P. aeruginosa*) is a Gram-negative bacterium and one of the main opportunistic pathogens that have a vital role in nosocomial, acute, and chronic infections [1]. It is often isolated from plants, fruits, soil, and water environments, such as rivers and lakes [2]. *P. aeruginosa* is also known to cause a wide variety of other infections, which encompass all organs of the human body, including soft tissue infection in burns, open wounds, cystic fibrosis (CF), and postsurgery [3]. Notably, it can lead to acute and chronic lung infections, particularly prevalent in individuals with CF. Furthermore, *P. aeruginosa* is associated with urinary tract infections, often linked to the use of urinary catheters. Diabetics are at risk of foot infections caused by this bacterium, while ear infections may arise from tissue injuries or water blockage. Additionally, *P. aeruginosa* can cause keratitis, especially in individuals who wear contact lenses for extended periods or use contaminated contact lenses. This wide array of infections caused by *P. aeruginosa* underscores the importance of vigilant monitoring and appropriate medical interventions to address these diverse clinical challenges [3]. Due to the widespread role of this bacterium in causing various infections and increasing antibiotic resistance, treatment failure of *P. aeruginosa* infection has become a major global problem [1]. It also belongs to the ESKAPE pathogens (*Enterococcus faecium*, *Staphylococcus aureus* (*S. aureus*), *Klebsiella pneumoniae*, *Acinetobacter baumannii*, *P. aeruginosa*, and *Enterobacter species*) and is listed by the World Health Organization as one of the most critical bacterial pathogens [4]. Due to the extracellular toxin and multi-drug resistance of *P. aeruginosa*, it is virulent to the host cells or organs, including wound healing and the immune system.

1. 1.1. *P. aeruginosa* and wound healing

P. aeruginosa is a frequently encountered pathogen that induces severe lung infections such as ventilator-associated pneumonia and acute lung injury [5]. After the colonization of bacteria, bacterial virulence factors, such as *S. aureus* virulence protein A [6], allow a range of activities: penetration of surface epithelia, attachment to cell surfaces and/or the extracellular matrix, invasion of intracellular compartments, acquisition of iron, evasion of host-defense mechanisms and transmission to another host [7]. Epithelial tissues are the first guards that protect organs from pathogens, while opened wounds represent an ideal niche for bacterial colonization when the epithelial integrity is damaged. *S. aureus* and *P. aeruginosa* are the most frequent pathogens isolated from chronic wounds, and increasing resistance to antibiotics has become a major issue [8]. It has been reported that *P. aeruginosa* and its virulence proteins can impede wound healing [9–11] and alter repair processes, leading to chronic wounds and infections [5][12]. A remarkable reduction of cell metabolic activity of the HaCaT cell (a kind of keratinocyte cell line) pool is found after preincubation with the extracellular adherence protein of *Streptococcus pneumoniae* (*S. pneumoniae*) [13]. In my project, I also present findings of other bacteria or baterial products, such as *P. aeruginosa* and LecB.

Most wounds are contaminated by bacteria, and colonization of wounds can result in delayed or impaired wound healing (Fig. 1)[8], and among them, cell migration is essential for wound healing and tissue homeostasis [14]. For example, *P. aeruginosa* lectins can block cell migration [5][10], and other virulence proteins from *P. aeruginosa* have similar functions. *P. aeruginosa* pseudolysin and protease IV impede cutaneous wound healing [11], and *P. aeruginosa* utilizes type III secretion system (T3SS) virulence structure to induce tissue damage in the wounds of diabetic mice [15]. Not only *P. aeruginosa* blocks wound healing, but also other pathogens, such as *S. pneumoniae* [16] and *S. aureus* [17]. It has been demonstrated that *S. pneumoniae* and *S. aureus* can delay epithelial wound healing *in vivo* [16, 17] Wound healing is an intricate and dynamic process encompassing four clearly defined stages such as hemostasis, inflammation, repair, and remodeling [11]. However, infections with *P. aeruginosa* can result in the failure of tissue repair and wound healing [5][9]. After that, *P. aeruginosa* can cause apoptosis of neutrophils, macrophages, and mast cells leading to impaired phagocytosis, resulting in dysfunction of the immune system.

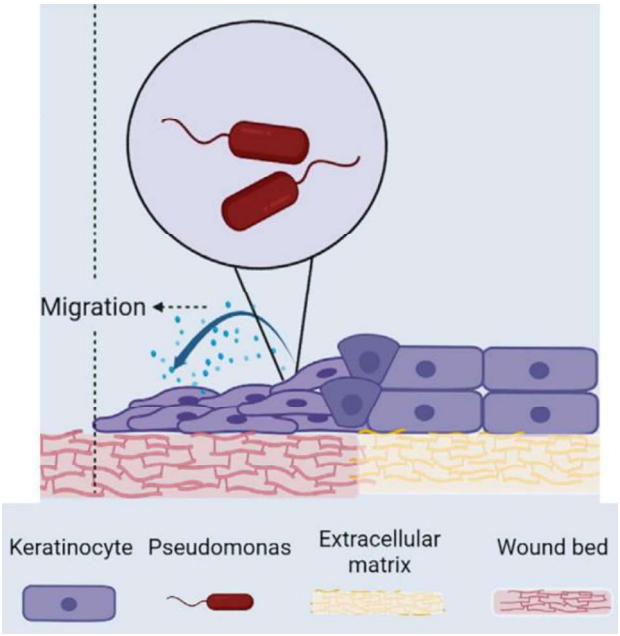

Fig. 1: The virulence factors delay healing of *P. aeruginosa*-infected wounds.

Chronic wounds infected with *P. aeruginosa* exhibit hindered healing and disease progression. The virulence factor produced by *P. aeruginosa* directly interferes with keratinocyte chemokine expression and migration, leading to impaired wound re-epithelization. As a consequence, the healing process is compromised, contributing to the persistent nature of the infection [18].

1. 1.2. *P. aeruginosa* and immune response

The immune system displays a remarkable capacity to adapt to environmental changes, providing the best response to a given immune challenge [19]. During an immune response, dendritic cells (DCs) play an essential role in initiating an adaptive and primary immune response through their ability to capture antigens and migrate T cells [20]. There is good evidence that bacteria cause a severe immune response in human bodies. For example, in HIV-infected patients, *S. aureus* infection leads to functional defects in $CD4^+$ T cell responses [21]. In detail, HIV-infected participants with methicillin-resistant *S. aureus* (MRSA) skin and soft tissue infections (SSTIs) have deficient MRSA-specific $IFN\gamma^+$ memory CD4 T cell responses with *S. aureus* infection [22]. Salmonella lipopolysaccharide (LPS) and flagellin induce DC maturation, enhancing antigen presentation and inducing their migration to T cell areas of various lymphoid tissues to imitate the adaptive phase of the immune response [23].

Mammalian hosts provide a number of niches that can be colonized by microorganisms, including the skin, intestine, upper and lower respiratory tract, urogenital tract, and internal organs [7]. With these infections, *P. aeruginosa* secretes many extracellular proteases as virulence factors, and among them, protease IV (PIV), elastase A (staphylolysin, LasA), and elastase B (pseudolysin, LasB) play a crucial role in pathogenesis by causing proteolytic damage to host tissues (Fig. 2), disrupting tight junctions, and subverting host innate immunity [24]. Meanwhile, microbes attain the highest levels of resistance to our present assortment of antibiotics and the immune system [25], suggesting that therapies for bacterial infection are difficult. It has been reported that *P. aeruginosa* infection can alter immune response, such as natural killer (NK) cells [26] and T lymphocytes with T cell receptors [27]. In detail, *P. aeruginosa* infection significantly impairs NK cell cytotoxic response to a human B lymphoma cell line, resulting in the alteration of antitumor immunity [26]. Meanwhile, T lymphocytes produce the proinflammatory cytokine IL-17, whose level is substantially increased after *P. aeruginosa* infection compared to healthy human skin [27]. *P. aeruginosa* infection could increase significantly $CD4^+$ $CD25^+$ regulatory T cells (Tregs)[26]. There are additional important virulence factors that have an impact on host cell physiology, such as the lectins.

1. 2. Lectins

Lectins, glycoproteins with a unique capability to reversibly bind to monomeric or oligomeric carbohydrates, play a crucial role in binding to the viral surface. By crosslinking with glycans, they can disrupt the interaction with co-receptors [28]. Meanwhile, lectins specifically target glycoproteins because they consist of proteins that are covalently linked to glycans. These glycans serve as recognition sites for lectins, allowing them to bind selectively to the glycoproteins on the surface of host cells. Thus, these multivalent proteins form reversible linkages upon interaction with sugars/glycoproteins linked to the host cell membrane or in solution [29], suggesting that lectins facilitate the binding to the host cell by interacting with specific glycoproteins. They have been isolated from various sources, including bacteria, algae, plants, fungi, body fluids of invertebrates, lower vertebrates, and mammalian cell membranes [29]. The percentile distribution of lectins is from various microbial groups [29], depicting that the majority of

lectins are from mushrooms. Depending on their biological function, lectins are also known as hemagglutinins, adhesins, selectins, galectins, or siglecs [30]. Lectins play many key roles in the control of various physiological and pathological processes in living organisms, including fertilization, embryogenesis, cell adhesion, cell migration, organ formation, inflammation, immune defense, microbial infection, and cancer formation [31, 32]. Here, in my project, I will focus on the function of *P. aeruginosa* lectin LecB on cell adhesion, cell migration, and immune response.

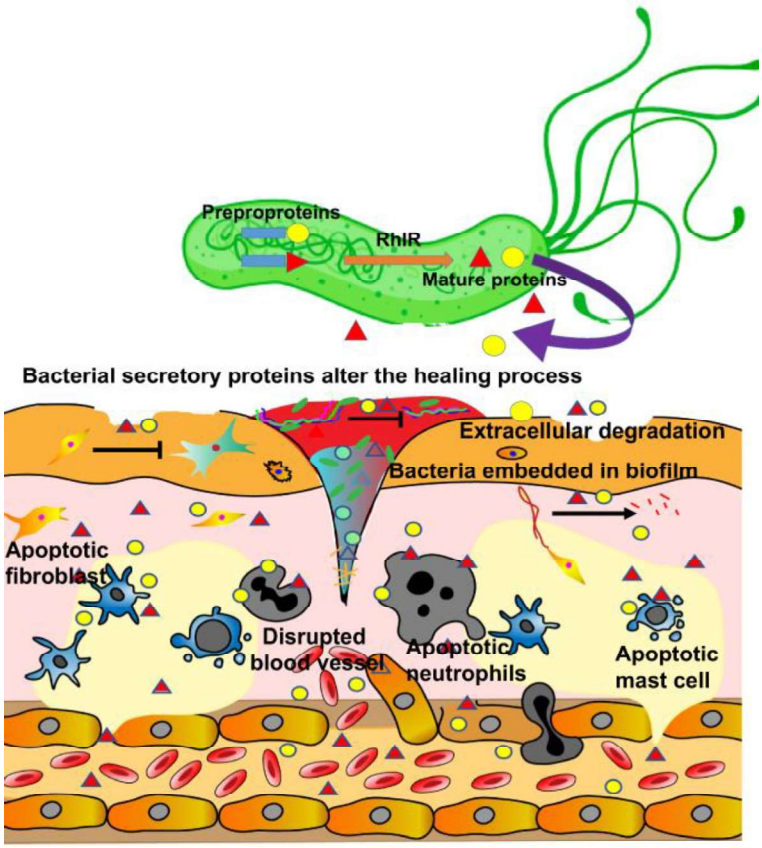

Fig. 2: *P. aeruginosa* delayes cutaneous wound healing through multiple mechanism.

The process of normal wound healing is a well-coordinated sequence involving various cell populations, mediators such as cytokines and growth factors, and the extracellular matrix. However, when *P. aeruginosa* is present, it triggers apoptosis in neutrophils, macrophages, and mast cells, resulting in impaired phagocytosis. This leads to a prolonged inflammatory phase, as the infection elevates pro-inflammatory cytokine levels, hindering the proliferation and remodeling phases of wound healing. The virulence factors of *P. aeruginosa* exacerbate the situation by degrading the extracellular matrix (ECM), which inhibits the proliferation of crucial cells like fibroblasts, keratinocytes, and endothelial cells (ECs). Moreover, these factors also cause the inactivation of complement proteins and hinder the conversion of plasminogen to plasmin and fibrinogen to fibrin, culminating in chronic wound healing [11].

1. 2.1. Structure and impact of *P. aeruginosa* lectins

P. aeruginosa produces two soluble lectins, the D-galactose (D-Gal)-specific lectin PA-IL (LecA) and the L-fucose-specific lectin PA-IIL (LecB), amongst many other virulence factors [33]. They are expressed and released by *P. aeruginosa* as a result of a regulatory cascade initiated by quorum-sensing [34]. LecA and LecB are produced in the cytoplasm of *P. aeruginosa* but has been shown to be located in the outer membrane and involved in biofilm formation [35]. LecA and LecB are tetrameric lectins, which play crucial roles in diverse infection steps, going from the adhesion to host cells to the biofilm formation [36]. LecA consists of four 12.8 kDa monomers (Fig. 3.A) with a medium-range affinity for D-Gal (Fig. 3.B). However, this is still 10-fold higher than average affinities of C-type lectins for their ligands, and this interaction is very selective. LecA contains a single Ca^{2+} within its carbohydrate-binding site, where it coordinates with specific amino acids and galactosides [37]. LecB consists of four 11.7 kDa monomers (Fig. 3.C) with a high affinity for fucoside-terminated glycans (Fig. 3.D, Fig. 4.A) and also recognizes D-mannose (Fig. 4.B) and D-arabinose [34][38]. Biochemical and structural studies reveal that LecB is characterized by unusual micromolar affinity of LecB for fucose, which is attributed to the participation of two bridging Ca^{2+} in the binding pocket and large enthalpy contribution [36]. Besides, these two Ca^{2+} ions are directly involved in carbohydrate coordination [35]. Each monomer includes 114 amino acids where cysteine, methionine, and histidine are lacking [35]. The overall fold of LecB is that of a nine-stranded antiparallel ß-sandwich. In each subunit, strands 1-5 form a key structural motif, extended by strands 6-8, which associate with strands 1 and 4 to form a 5-stranded curved ß-sheet. Tetramerization occurs mainly by the antiparallel association of ß-strands comprising amino acides 79-85 from each dimer with their counterparts in the other dimer. Besides, some amino acids are involved in binding of L-fucose [39].

Due to the strong binding affinity of LecB for L-fucose, L-fucose is widely acknowledged as a potent inhibitor of LecB. For example, L-fucose recuses the inhibited collective cell migration and wound healing in Madin-Darby canine kidney strain cell line (MDCK) monolayers induced by LecB [10], and it inhibits apical invasion of *P. aeruginosa* in polarized MDCK cells [40]. In addition, derivatives of L-fucose (Fig. 4.C) are used as antagonists of LecB in several studies. The derivatives of L-fucose inhibit LecB carbohydrate-binding function [41]. Here, I will introduce some details about DH445. DH445 is a type of monovalent glycomimetic LecB inhibitor. On a structural level, LecB forms noncovalent homotetramers, and each monomer contains two Ca^{2+}-ions, which mediate the binding to its carbohydrate ligands, such as L-fucose and D-mannose (Fig. 4.C)[42]. DH445 is an artificially synthesized methyl-mannose derivative with a thiophene residue and LecB ligand and inhibitor. It has been reported that the IC_{50} of L-fucose for $LecB_{PAO1}$ is 149 µM compared with the IC_{50} of D-mannose for $LecB_{PAO1}$ is 157 µM using established competitive binding assays [41]. Due to higher affinities toward fucosides over mannosides, research focused on fucose-based inhibitors with multivalent presentation to further increase avidity [43]. However, the IC_{50} value of L-fucose is quite high. I utilized DH445 as antagonists of LecB in my second part of project to figure out a fucose-based inhibitor which has higher affinity toward LecB.

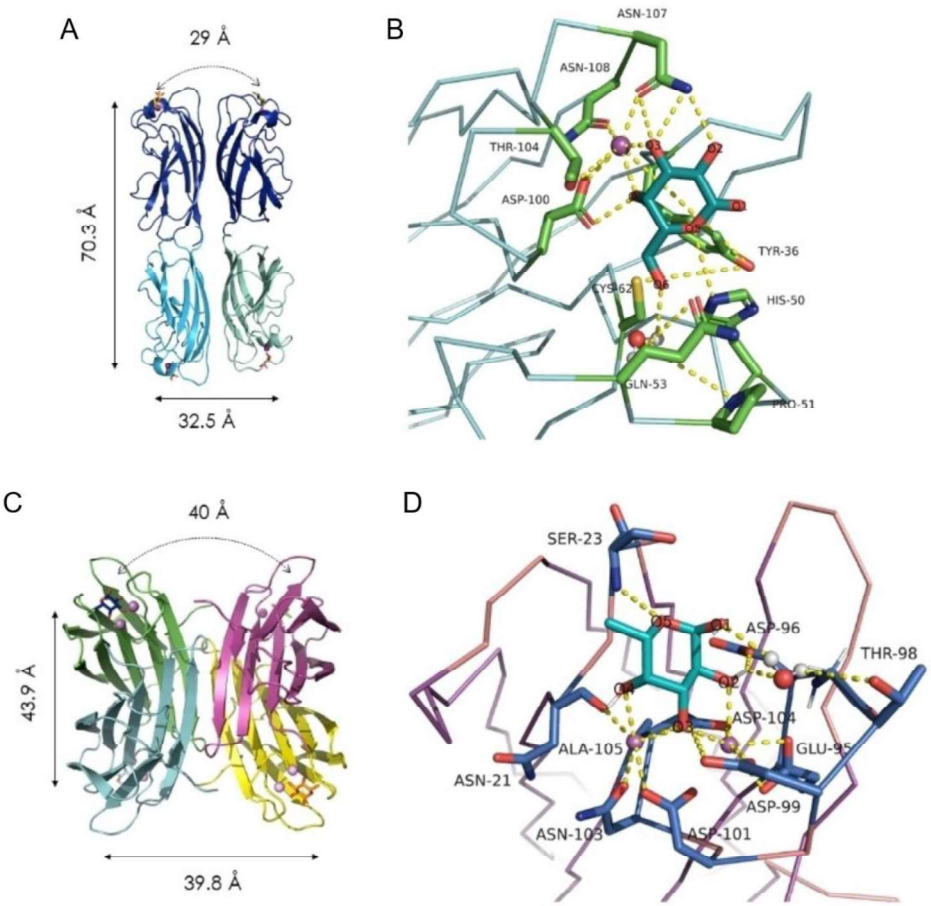

Fig. 3: Structure of *P. aeruginosa* lectins.

(A) LecA tetramer structure, with distances between Ca^{2+} (magenta spheres), and shortest distance between galactose-binding sites (curved arrow) indicated. (B) LecA binding-site interactions with D-Gal. (C) LecB tetramer structure, with distances between Ca^{2+} (magenta spheres), and shortest distance between fucose-binding sites (curved arrow) indicated. (D) LecB binding-site interactions with L-Fucose [38].

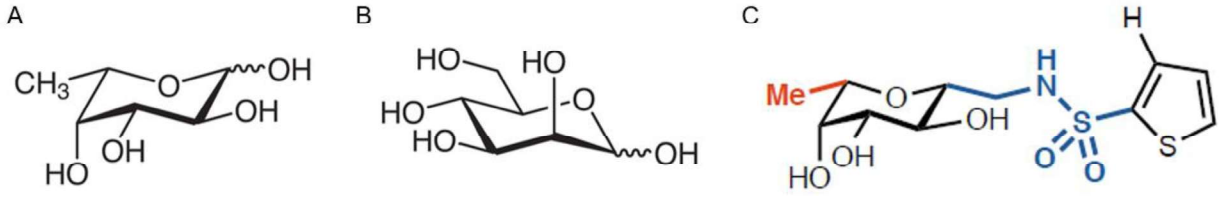

Fig. 4: Structure of LecB inhibitors.

(A) L-fucose. (B) D-mannose. (C) DH445 is an artificially synthesized methyl-α-L-fucoside derivative with a thiophene residue. The orange colored methyl group originating from L-fucosides enhances the binding to LecB through a lipophilic interaction [42][44].

LecB has been implicated in several cellular processes, such as cellular migration and wound healing [5][10], cell proliferation [5], immune response [45], and cell cycle [9]. Regarding cell migration, LecB alone is sufficient to attenuate cell migration and proliferation of human lung cancer cell and induce the reduction of nuclear factor kappa-light-chain-enhancer of activated B cells (NF-κB) and ß-catenin [5]. LecB can specifically clear integrins from the wound edge of cells and block cell migration and wound healing in epithelial cells [10]. In addition to the impact of LecB on cell migration and wound healing, LecB triggers B cell receptor (BCR)-dependent activation *in vitro*, ultimately resulting in the activation-induced death of B cells [45]. With regards to cell cycle, LecB associates with insulin-like growth factor-1 receptor (IGF1R) and dampens its signaling, resulting in the arrest of the cell cycle [9], and it induces differentiation and apoptosis of acute monocytic leukemia cells with the reduction of β-catenin level [46]. There is also some evidence of LecB regarding cytotoxicity *in vivo* model, that LecB induces alveolar-capillary barrier injury *in vivo*, leading to higher bacterial dissemination into the bloodstream [47]. Overall, these observations indicate that LecB, as an important virulence factor, is associated with the pathogenicity of *P. aeruginosa*. I have known that LecB can block epithelial cell wound healing, and lung cancer cell migration with the reduction of β-catenin level, however, the molecular mechanisms induced by LecB are unclear.

1. 2.2. Cellular function of LecB in cell adhesion

A typical role of lectins LecA and LecB is involved in the recognition and adhesion between a *P. aeruginosa* and the host cell, which is a crucial process in the development of bacterial infections [33]. For example, LecB can bind the oligosaccharides of many humans and mammalian glycoproteins, after that, the adhesion of *P. aeruginosa* to the epithelial tissue surface precedes colonization [34]. LecB has the ability to bind to some glycoproteins secreted by epithelial cells, and it can bind to the immobilized fibronectin [34], which is a glycoprotein binding to cell surface receptors called integrins and other ECM components, like collagen and proteoglycans [48]. It indicates that LecB may induce immobilized epithelial cells after the binding of LecB under the microenvironment [34]. Integrin-mediated cell adhesion is important for development, immune responses, hemostasis, and wound healing [49]. Interestingly, LecB induces patches with basolateral characteristics at the apical membrane [40], and LecB can strongly bind to the glycosylated moieties of ß1-integrin on the basolateral plasma membrane, which causes the inhibition of epithelial wound healing [10]. Consequently, there exists a hypothesis suggesting that LecB might induce cell immobilization by binding to host cells via glycoproteins, based on the crystal structure of LecB. Here, I will show some research regarding LecB affecting cell adhesion and its signaling cascades *in vitro* in the first part of the project.

Besides, LecB is involved not only in adhesion but also in the formation of *P. aeruginosa* biofilms. Biofilms are complex communities of microorganisms embedded in a self-produced matrix of extracellular polymeric substances (EPS)[50]. LecB is believed to play a role in the accumulation of EPS in the biofilm, further strengthening the structural integrity of the biofilm [51]. In the case of *P. aeruginosa*, biofilm formation is a significant factor contributing to its virulence and resistance to antimicrobial agents [50]. It

is needed for the proper assembly of type IV pili, which, in turn, are required for biofilm formation, indicating that LecB is required for *P. aeruginosa* adhesion form biofilms as well. Besides lectins, *P. aeruginosa* utilizes other virulence factors, including flagella and type IV pili, to ensure adhesion to host cells. These additional factors play a vital role in facilitating the attachment of bacterium and interaction with the cells of the host organism, contributing to its pathogenicity and the establishment of infections [34].

1. 2.3. Cellular function of LecB in cell migration

Lectins are proteins that can recognize and bind to specific carbohydrate structures on the cell surface. In the context of cell migration, LecB has the ability to interact with glycoproteins on the cell membrane can influence cell movement and motility [47]. *P. aeruginosa* contributes to the remodeling of the ECM by affecting the production or degradation of certain matrix components [52]. This can create pathways for cell migration or alter the cell's microenvironment, affecting its ability to move. While, LecB is located in the outer membrane of *P. aeruginosa*, indicating that LecB may remodel the ECM to influence cell motility. LecB binding to glycoproteins might interfere with the interactions between cell surface receptors and their ligands, affecting cell migration-related receptor signaling. For example, basolaterally applied LecB interacts with ß1-integrin and causes its pronounced internalization, which can explain why MDCK cells cannot migrate anymore [10]. With the treatment of LecB on the scratched wounds, no lamellipodia form and no cells migrate, which indicate that LecB strongly inhibits collective cell migration and wound healing in MDCK monolayers. In human lung cancer cells, LecB is sufficient to attenuate cell migration via the reduction of β-catenin level [5]. However, only the conclusion of the expression of downstream ß-catenin on cell migration induced by LecB, the molecular mechanism after the binding of LecB on the host cells is not solved. Here, I will show some research regarding LecB affecting cell migration and its signaling cascades *in vitro* in the first part of the project.

1. 2.4. Cellular function of LecB in immune system

According to our previous literature, we have found that LecB can bind to murine B cells and induce an intracellular signaling cascade that changes the flux of Ca^{2+} [45]. 10 µg/ml LecB induces a Ca^{2+} release similar to that induced by BCR stimulation with anti-κ antibodies in mature follicular B cells. Saturating the LecB carbohydrate binding sites with soluble L-fucose (25 mg/ml) prevents LecB binding to B cells Ca^{2+} flux, indicating that this activation process is fucose specific [45]. Strong intracellular signaling can drive B cells into activation-induced cell death. LecB triggers BCR-dependent activation *in vitro*, ultimately resulting in activation-induced death of B cells with a strong burst of Ca^{2+} release [45]. However, the impact of LecB on the immune system remains incompletely understood. To date, only one paper is shown to report the effect of LecB on immune system suppression [53]. It reported that LecB suppresses immune responses

inhibiting DC migration and T cell proliferation *in vivo* [33], which I will introduce in detail in my second part of the project. Here, I will present examples of some other lectins.

Our immune system can discriminate between self and non-self by sensing pathogen-associated molecular patterns (PAMPs). Lectins from bacteria or microfungi are distinguished as pathogens from immune systems to induce the immune response. For example, the C-type lectin receptor family functions as immune sensors for adjuvant lipids derived from pathogens and damaged tissues, thereby promoting innate/acquired immunity [54]. In particular, another C-type lectin in shrimp promotes cellular immunity in the form of phagocytosis [55]. Immune recognition via mannan-binding lectin (MBL) triggers the activation of the complement system. Based on structural similarities between the complement component 1q and MBL, as well as structural and genetic similarities between MBL-associated serine proteases and the classical complement pathway components C1r/C1s, it has been suggested that the MBL pathway of complement activation resembles the classical pathway [56]. It is an elegant demonstration of the remarkable ability of innate immunity to detect molecular patterns that specifically characterize microorganisms [56]. These results from the literature indicate that some lectins can induce the immune response.

2. Part A. The crucial role of host cell flotillins in aggravating the impact of *Pseudomonas aeruginosa* lectin LecB on cell adhesion and migration

Yubing Guo[1,2,3], Anna-Sophia Kittel[1,2], Taras Sych[1,2], Ramin Omidvar[1,2], Celine Enderle[1,2], Christopher G. Mueller[3,*], Winfried Römer[1,2*]

[1] Faculty of Biology, Albert-Ludwigs-University Freiburg, 79104 Freiburg, Germany

[2] Signalling Research Centres BIOSS and CIBSS, Albert-Ludwigs-University Freiburg, 79104 Freiburg, Germany

[3] CNRS UPR 3572, IBMC, University of Strasbourg, 67000 Strasbourg, France

[*] Correspondence to

Winfried Römer (winfried.roemer@bioss.uni-freiburg.de), Schänzlestraße 18, Albert-Ludwigs-University Freiburg, 79104 Freiburg, Germany

Christopher G. Mueller (c.mueller@unistra.fr), 2 All. Konrad Roentgen, Strasbourg University, 67000, France

Manuscript in preparation

Abstract

Plenty of bacteria use lectins to efficiently adhere to the host tissue and induce severe infections, such as pneumonia and wound infections caused by the opportunistic bacterium *P. aeruginosa*. Under this condition, bacterium enhances the adhesive ability of the tissue and diminishes tissue repair mechanisms, resulting in constant infections and delayed wound healing. Here, we discover the effect of the fucose-specific *P. aeruginosa* lectin LecB on cell adhesion and cell migration mediated by flotillins. LecB alone is sufficient to enhance the adhesive ability and attenuate the ability to migrate of human H1299 non-small cell lung cancer cell line. We unravel that LecB has less capability to increase cell adhesion and decrease cell migration with the knockout of flotillin-1 or the knockdown of flotillin-2 alone expression in H1299 cells. Moreover, we find that LecB can trigger ß1-integrin/FAK signaling and its downstream signal ß-catenin, which is mediated by fotillin-1. We successfully show that L-fucose inhibits the process of cell adhesion and cell migration and affect the nuclear translocation of ß-catenin induced by LecB, providing more evidence that L-fucose could heal the wound infected by *P. aeruginosa* LecB. We identify that flotillins interacted not only with *P. aeruginosa* lectin LecA from our previous work but also with lectin LecB, flotillin-1 thereby aggravating the processes of cell adhesion and migration.

Keywords: Bacteria, lectin LecB, cell adhesion, cell migration, flotillin-1, ß1-integrin/FAK-Src/ß-catenin signaling

A. 1. Introduction

A. 1.1. Cell adhesion

Cell adhesion is essential in cell communication and regulation, and is of fundamental importance in the development and maintenance of tissues [57]. The complex interactions of cells with ECM play crucial roles in mediating and regulating many processes, including cell adhesion, migration, and signaling during morphogenesis, tissue homeostasis, wound healing, and tumorigenesis [58]. For most cells in most environments, the movement begins with protrusion of the cell membrane followed by the formation of new adhesions at the cell front that links the actin cytoskeleton to the substratum, generation of traction forces that move the cell forwards, and disassembly of adhesions at the cell rear [59]. The process of cell adhesion involves a multitude of factors present, both intrinsic and extrinsic, to cell membranes, such as the cytoskeleton, membrane-bound adhesion proteins, and glycocalyx elements [60]. After determining its direction of motion, the cell extends a protusion in this direction by actin polymerization at the leading edge. It then adheres its leading edge to the surface on which it is moving and de-adheres at the cell body and rear. Finally, it pulls the whole cell body forward by contracile forces generated at the cell body and rear of the cell (Fig. A1)[61]. For example, the transmembrane protein, integrin, forms adhesion sites to anchor between the cell and matrix or the other cell's adhesion molecule. These adhesion molecules are attached to the cytoskeleton, the actin filament through the focal adhesion (FA) complex [62]. Meanwhile, some signaling pathways are involved in the process of cell adhesion. The transfection of rodent fibroblast cells with Src and Ras oncogenes reduces the adhesiveness to fibronectin by impairing α5ß1-integrins, the activation of oncogene ErbB2 in breast cancer up-regulates α5ß1-integrin and enhances adhesion [63]. The Rho GTPases (RAS homologue) Rac, Rho, and Cdc42 together regulate adhesion by directly controlling the balance between the actin-mediated protrusion and myosin II-mediated contraction [64]. The activation of WNT signaling and epithelial-mesenchymal transition (EMT)-associated changes in cell adhesion involve the displacement of β-catenin from adherens junctions (AJs), where it links E-cadherin to the actin cytoskeleton [65].

A. 1.1.1. The phases of cell adhesion

The passive cell adhesion process is an *in vitro* process in static medium culture, where cells undergo morphological alterations driven by passive deformation and dynamic reorganization of the cytoskeleton. *In vitro* settings facilitate cell adhesion through passive surface adsorption. The cell glycocalyx coat initiates the initial contact, leading to subsequent attachment, cell spreading, and the formation of FAs [60].

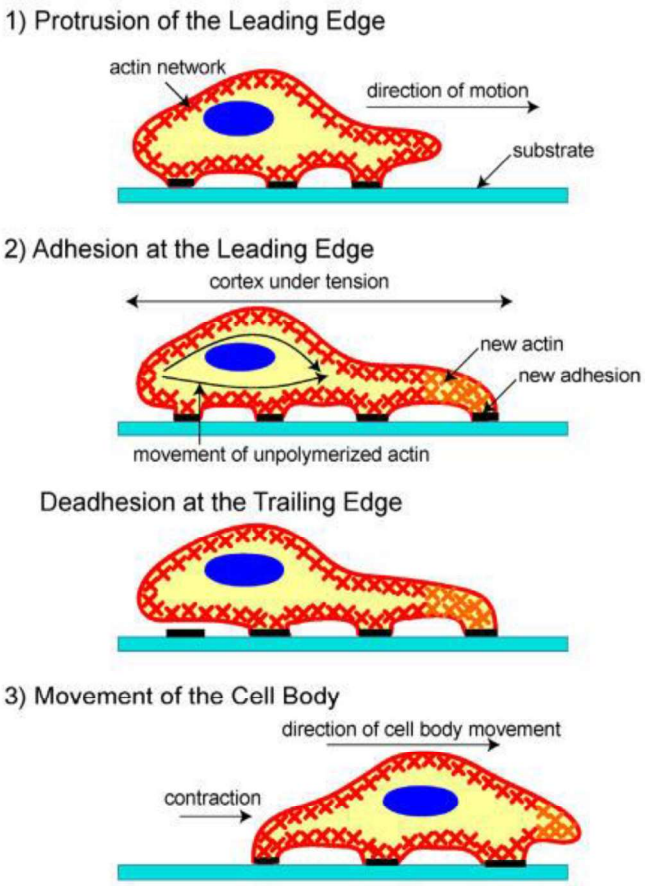

Fig. A1: The schematic of the three stages of cell movement.

First, a cell propels the membrane forward by orienting and reorganizing (growing) the actin network at its leading edge. Second, it adheres to the substrate at the leading edge and deadheres (releases) at the cell body and rear of the cell. Finally, contractile forces, generated largely by the action of the actin-myosin network, pull the cell forward [61].

In detail, the process of static *in vitro* cell adhesion is characterized by three stages (Fig. A2): attachment of the cell body to its substrate (initial stage), flattening and spreading of the cell body, and the organization of the actin skeleton with the formation of FA between the cell and its substrate, like ECM [66]. Following the initial attachment, cells start flattening and spreading on the substrate ECM, resulting in the decrement of cell height (the cell flattens) and increment of contact area (Phase I in Fig. A2)[67]. Next, cells spread beyond the projected area of the unspread spherical cell (Phase II in Fig. A2)[68]. The spreading process is the combination of continuing adhesion with the reorganization and distribution of the actin skeleton around the edge of the cell's body [67]. Cells will reach their maximum spread area through expansion, and adhesion strength will become stronger (Phase III in Fig. A2). Cell spreading appears to be accompanied by actin organization into microfilament bundles. The strength of adhesion

becomes stronger with the length of time a cell is allowed to adhere to a substrate or another cell. The initial adhesive interaction between the cells and the substrates is driven by the specific integrin-mediated adhesion and starts with the binding of single receptor-ligand pairs [68]. This will initiate the subsequent receptor-ligand bonds and quickly enhance in number, thus increasing the total adhesion strength [69].

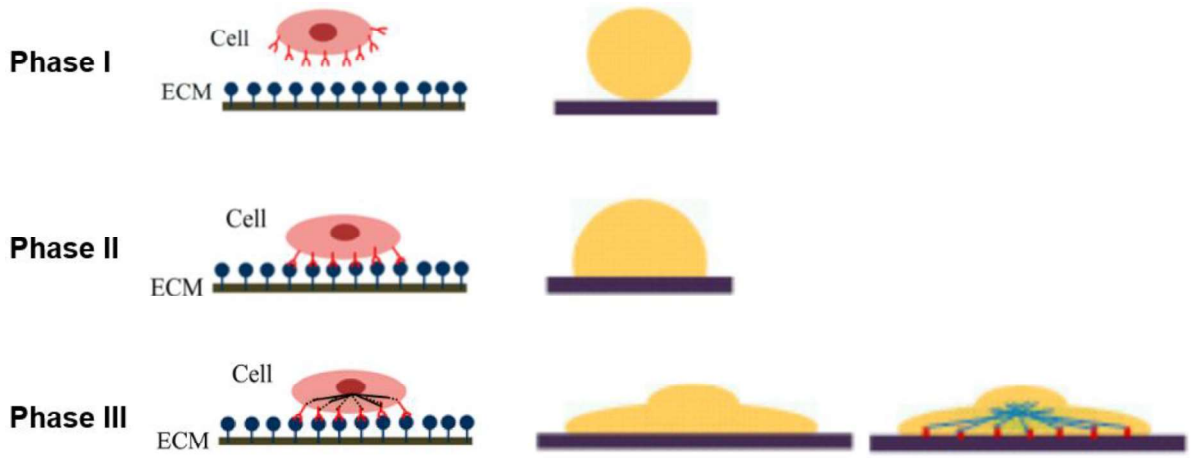

Fig. A2: Evaluation of passive *in vitro* cell adhesion stages.

The attachment of the cell body to its substrate (initial stage), flattening and spreading of the cell body, and the organization of the actin skeleton with the formation of FA between the cell and its substrate (Phase I). Cell spreading appears to be accompanied by the organization of actin into microfilament bundles (Phase II). The strength of adhesion becomes stronger with the length of time a cell is allowed to adhere to a substrate or another cell. The initial adhesive interaction between the cells and the substrate are driven by the specific integrin-mediated adhesion and starts with the binding of single receptor-ligand pairs (Phase III) [57].

A well-known technique, atomic force microscopy (AFM)-based single-cell force spectroscopy (SCFS), is utilized in cell adhesion studies. SCFS measurement methods are developed to measure the strength of cell adhesion down to single cell level [57]. In SCFS, the force required to separate a living cell from its substrate is measured using controlled parameters [70]. In SCFS adhesion measurements, a single cell is attached to a coated cantilever, such as collagen-coated [70] and Cell-tak-coated cantilever [71]. Cell-tak, a biocompatible glue, is a specially formulated protein solution extracted from marine mussel [72]. It technique aids in immobilizing poorly adherent cells, promoting their attachment to the Petri dish [72]. During the measurement of the cantilever, the cantilever deflection is determined using a laser beam reflected by the back of the cantilever onto a multi-segment photodiode (PD). The cantilever-bound cell is lowered towards the substrate (I in Fig. A3.A) until a preset force is reached (II in Fig. A3.A). After a given dwell time, the cantilever is retracted from the substrate (III in Fig. A3.A) until the cantilever-bound cell and substrate are entirely separated (IV in Fig. A3.A). During both approach and retraction, detachment

force (F_d) curves are recorded [70]. The de-adhesion of a cell from a substrate described by the F_d curve can be broken into three phases (Fig. A3.B). During the initial phase (a in Fig. A3.B), the retraction of the cantilever inverts the force that is acting on the single cell from pushing to pulling. After that, the cell starts to detach from the substrate, and individual force steps can be observed during the second phase (b in Fig. A3.B). During this phase, the receptor(s) either detaches from the substrate surface or is pulled away from the cell cortex at the tip of a membrane tether. While parts of the cell cortex are in contact with the substrate, either of these processes can occur. Finally, during the phase of detachment (c in Fig. A3.B), the cell body is no longer in contact with the substrate, thus, attachment is mediated exclusively by tethers [73]. Here, in my project, I utilized the SCFS system to measure the F_d curves. In my case, the cantilever was coated by Cell-tak to stick a single H1299 cell. During the test, the probe slowly approached the fibronectin-coating surface, contacted it, and retracted it, and the force-distance curves were obtained by recording the cantilever deflection (Fig. A3.C). The difference in F_d between untreated and LecB treatment groups was depicted in the parts of the results.

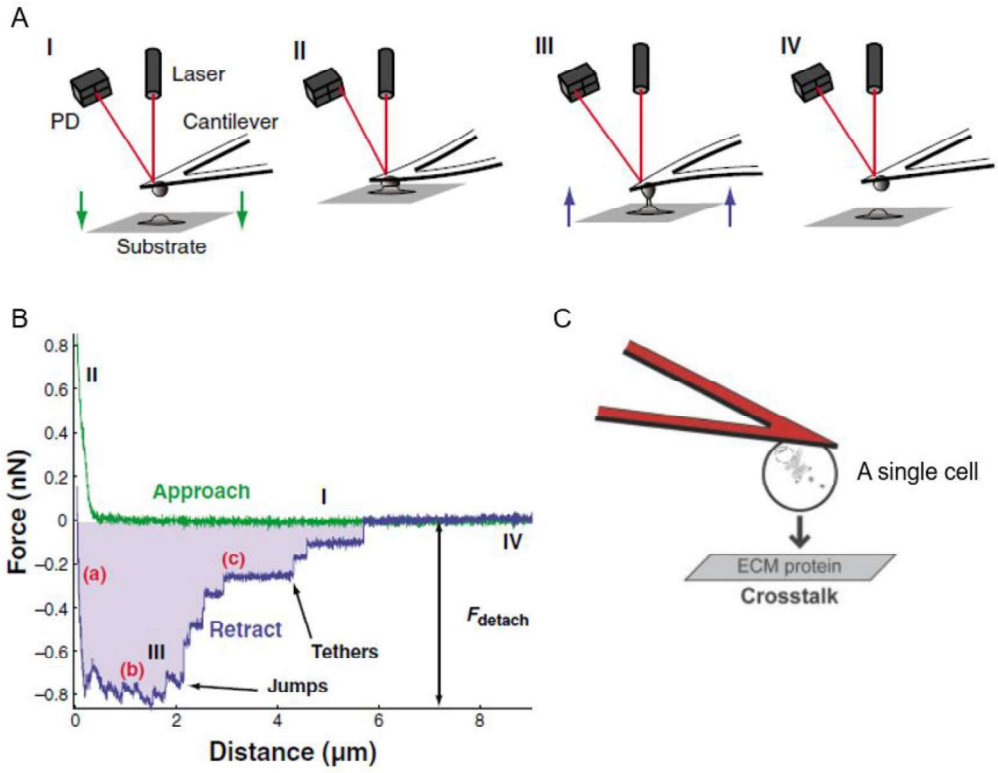

Fig. A3: Single-cell force spectroscopy setup.

Depiction of a cell-adhesion measurement (A) for which characteristic approach (green) and retraction (blue) traces are shown (B). (A) In this technique, the cell and the substrate are brought into contact (AI). The substrate that is probed can be another cell, a functionalized surface or an organic matrix. The position on a PD of a laser beam (red line) that is reflected off the back of the cantilever measures the deflection of the cantilever and thus the force that

acts on the cantilever. During the approach (denoted by green arrows), the cell (probe) is pressed onto the substrate until a pre-set force (usually <1 nN) is reached (AII). After a contact time ranging from 0 to 20 minutes, the cell is retracted from the substrate (marked by blue arrows), and a force-distance curve is recorded (B). This curve corresponds to a cell-adhesion signature. As the strain on the cell increases, bonds that have been formed between the substrate and the cell break sequentially (AIII) until the cell has completely separated from the surface (AIV). During the separation of the cell from the surface, two types of molecular unbinding events can occur. In the first event, the receptor remains anchored in the cell cortex and unbinds as the force increases (denoted as jumps). The second type of unbinding event occurs when receptor anchoring is lost and membrane tethers are pulled out of the cell. In the unbinding-force–distance curve, long plateaus of constant force characterize tethers. The shaded area in B represents the measured work of cell detachment from the substrate [73]. (C) SCFS setup for detecting integrin crosstalk. AFM cantilevers are coated either with ECM proteins as primary substrates. ECM proteins enable the specific attachment of a single cell to the functionalized cantilever [70].

A. 1.1.2. Dynamic cell adhesion

Cell-ECM, flow circulation, and the signalization process under blood flow *in vivo* are known to be dynamic processes. Cell attachment is a crucial parameter which influences the whole process as a low attachment efficiency will lead to a low expansion yield [74]. Cell attachment involves interaction between several cell adhesion molecules (CAMs) and substrates on the surface of the microcarrier [74]. The integrin family is the main surface receptor family regulating cell adherence (Fig. A4)[75], which is introduced in detail in a next chapter. Various cells adhere to their surrounding surfaces, a crucial mechanism for their survival. This adhesion process plays a pivotal role in essential cellular processes, including embryogenesis, cell orientation, morphogenesis, cell motility, immune responses, development, and reorganization [60]. The process is influenced by a diverse range of factors, both intrinsic and extrinsic to the cell membrane. These factors include the cytoskeleton, membrane-bound adhesion proteins, and glycocalyx elements [60][76]. A wide range of receptors is expressed on the surface of the cells, which helps to bind different ligands with varying affinity. The longer the cell adhesion time to the substrate, the stronger the adhesion strength, which is directly proportional to the number of integrin-ligands pairs, thus increasing the overall contact time [60]. The *in vivo* dynamic cell adhesion is mediated through molecular bonding along with the non-covalent cascade and signaling pathways [60]. The *in vivo* cell adhesion cascade and signaling events involve two main phases: the docking phase occurring between the rolling of cells to ECs and to cell arrest, and the locking phase consisting of firm adhesion to the transmigration of the cell [77]. The adhesive bond is defined as the sum of non-covalent interactions, such as hydrogen bonds, electrostatic interactions, van der Waals forces, and dipole-dipole interactions between two macromolecules [57]. Moreover, cell adhesion cascade and signaling *events in vivo* involve three basic steps: selectin-mediated rolling, chemokine-triggered activation, and integrin-dependent arrest [57][78]. Here, in my project, I focused more on integrin-mediated cell adhesion.

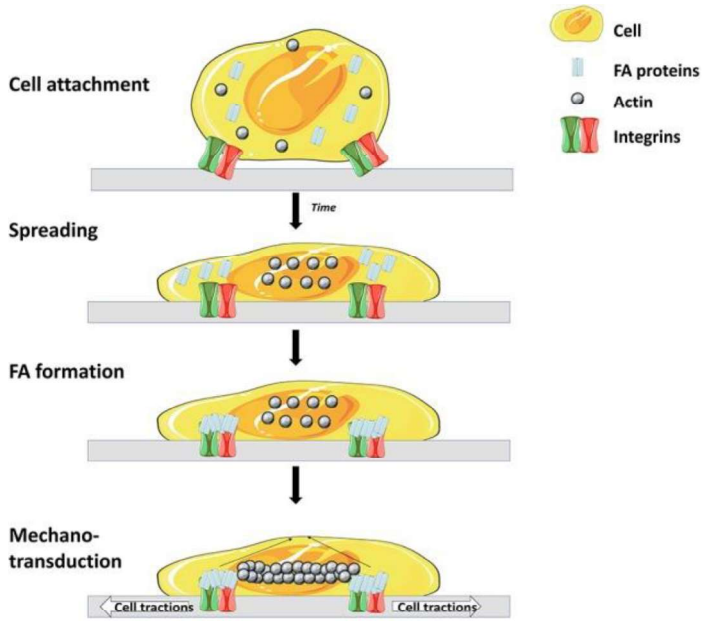

Fig. A4: Main steps and molecules involved in cell adhesion to matrix.

Cell surface receptors, primarily integrins, play a crucial role in the interaction with specific molecules within the extracellular matrix. This interaction facilitates the attachment and spreading of the cell. Further, the attachment process is reinforced through the interplay between focal adhesion proteins (FA proteins) and integrins. Ultimately, a cytoskeleton rearrangement takes place, resulting in the cell spreading over the surface, completing the process of cellular adhesion and migration. [74].

A. 1.1.3. Integrins: key receptors of cell adhesion

Cell adhesion serves two vital functions in cell migration. First, it generates traction by linking the extracellular substratum, like ECM, to the cellular cytoskeleton. Second, it organizes the signaling networks that regulate migration. Integrin-ECM engagement leads to integrin clustering and the formation of integrin adhesion complexes (IACs) that support cell adhesion [78]. The schematic representation of integrins at the plasma membrane in both bent (inactive) and extended (active) conformations (Fig. A5), where collagen fibers promote clustering and IACs formation. Changes in the conformation of integrin extracellular domains are responsible for the changes in integrin monomer affinity. Similarly, clustering of integrins can enchance the binding of multivalent ligands and kindlins have recently emerged as major players in clustering [79]. There are three distinct conformations observed in an inactive integrin: an inactive, bent conformation with a closed headpiece; a primed, extended conformation with a closed headpiece; an active, extended conformation with an open headpiece, bound to a ligand (Fig. A5)[80]. The capacity of intracellular signals to change the conformation of the extracellular domain requires a remarkable transmemebrane allosteric change, a change that must traverse the integrin transmembrane domain (TMD)[49]. Truncation of the integrins at the C-termini of extracellular domains results in constitutively active integrins [81], indicating that TMDs and cytoplasmic

tails limit the activation state of integrins [49]. Integrins are among the most abundant cell surface receptors and are expressed in all cell types apart from erythrocytes [82]. Integrins represent a sizable family of cell surface adhesion receptors comprising 24 non-covalently associated subunits, consisting of 18 α subunits and 8 β subunits. These subunits exhibit overlapping substrate binding capabilities, contributing to the versatility and functionality of integrins in cellular adhesion processes [80]. Both subunits are tightly bound to each other by interactions between the α-propeller and the ß-like domain in the extracellular "head" regions of both subunits. α subunit binds collagen ligands, while ß subunit binds fibronectin ligands [62]. For example, some integrins, such as α5β1, interact with a limited number of ECM ligands, while others, such as αvβ3 and α4β1, have multiple ECM binding partners [83]. α4β1-integrin can interact with fibronectin, vitronectin and fibrinogen [84]. αvβ3-integrin can interact with fibronectin and osteopontin [84]. Here, in my project, I investigated more on the function of ß1-integrin induced by LecB since ß1-integrin can interact with ECM, like fibronectin [80][85].

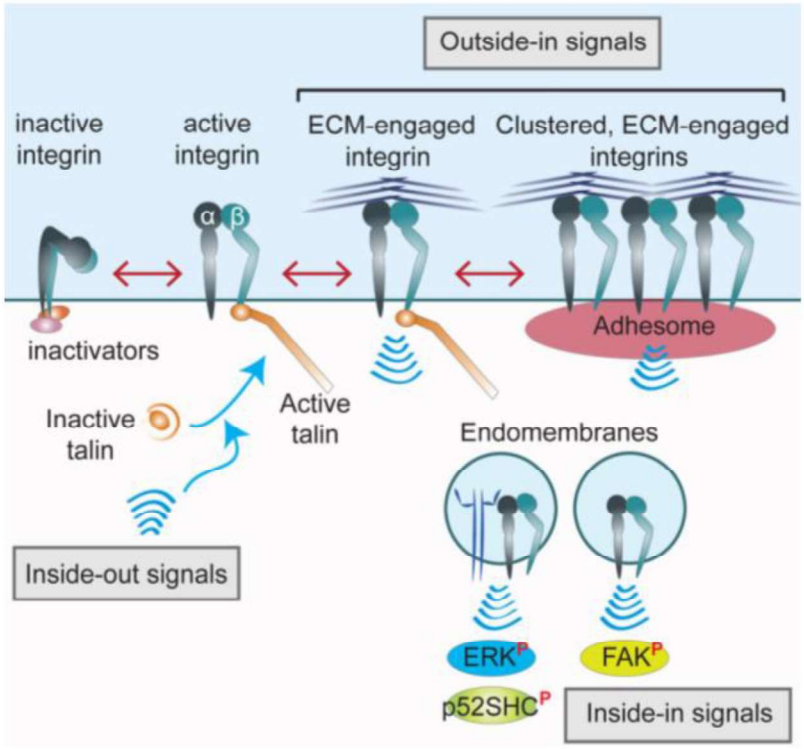

Fig. A5: Composition and signal of the integrin family.

Integrins serve as bidirectional signaling molecules, with "inside-out" signals regulating the binding of talin to integrin β-tails, thus precisely controlling the integrin's affinity for ECM ligands. Upon ECM binding, various protein complexes, such as scaffolding and adaptor proteins, kinases, and phosphatases, are recruited to the integrin cytoplasmic tails, facilitating integrin downstream signaling (outside-in signaling). Moreover, integrins can also signal from within endosomes (inside-in signaling), supporting FAK activity and suppressing anoikis, a process of

programmed cell death when cells detach from their ECM. Additionally, integrins play a role in promoting signaling downstream of co-trafficking mesenchymal-epithelial transition (MET), which supports anoikis resistance, tumor growth, and the dissemination of cancer cells to the lungs [83].

Integrins are activated through "inside-out" signals (Fig. A5): an intracellular signal promoting the binding of proteins such as talin and kindlin to the β-integrin tail switching the receptor into an extended conformation with high affinity for ECM ligands. Integrin binding to ECM ligands, in turn, triggers "outside-in" signals that recruit protein complexes, consisting of scaffolding/adaptor molecules, kinases, and phosphatases, to regulate cell behavior (Fig. A5). The network of proteins recruited to integrin adhesion sites, like talin and vinculin, varies in composition and size giving rise to multiple classes of integrin-ECM adhesions [83][86]. Moreover, integrins can also induce the signals from within endosomes, inside-in signaling, to support FAK activity and suppress anoikis to promote signaling downstream of co-trafficking MET to support anoikis resistance, tumor growth, and cancer cell dissemination to lungs [83][87]. Anoikis resistance refers to the ability of cell death that would typically occur when cells lose their normal anchorage to the ECM or neighboring cells. Anoikis is a critical mechanism that helps maintain tissue integrity and prevents the survival and growth of detached cells, which could otherwise lead to uncontrolled cell proliferation and metastasis [88]. Thus, I also focused on the phosphorylation of FAK and its activation mediated by ß1-integrin induced by LecB.

Within the cellular environment, the integrin tails serve as platforms to recruit regulatory elements. These IACs play a crucial role in reinforcing the cytoskeleton and initiating downstream signaling cascades that are essential for cell survival, proliferation, polarization, and migration [78](Fig. A6). Integrin heterodimers exhibit the ability to interact with multiple ligands, and some heterodimers can bind the same ligand, albeit with varying affinities or eliciting different intracellular responses. For example, both α5β1- and αvβ3-integrins can bind to fibronectin, but only αvβ3 is capable of binding to vitronectin [89]. Considering the diverse cell types and extracellular environments present in the body, IACs can adopt various forms in both migrating and non-migrating cells. Among these, the most extensively studied are FAs and FA-like structures, which will be discussed in more detail below. Furthermore, specialized cell types employ unique IACs, including hemidesmosomes, podosomes, invadopodia, and the immunological synapse. It is important to note that not all of these specialized IACs are directly involved in the migration process [90, 91]. IACs possess the capability to integrate both biochemical cues, such as ECM composition, and mechanical cues, like ECM stiffness. They transduce this information through a combination of biochemical signaling cascades and mechanical organization of the cytoskeleton. In the context of directed cell migration, IAC signaling plays a crucial role in mediating durotaxis (migration toward stiffer substrates), chemotaxis (migration toward regions of higher chemokine concentration), and haptotaxis (migration toward regions of higher ECM concentrations)[92]. IACs are phosphorylation platforms that are especially enriched for tyrosine phosphorylation, suggesting an important regulatory role of kinases and phosphatases at these signaling hubs [78]. For example, CDK1, acting as the central regulator of the cell

cycle, predominantly forms complexes with cyclins A2 (outside of mitosis) and B1 (during mitosis). It orchestrates intricate morphological processes by phosphorylating over a hundred target proteins. Among these targets are various cytoskeletal and adhesion proteins. Additionally, recent phosphoproteomic analysis of IACs has indicated the likelihood of many more targets being involved in this complex regulatory network [93]. Cell migration and proliferation, driven by FAK- and Src-dependent phosphorylation, are observed to proceed independently of IAC composition [94]. This finding suggests the potential existence of distinct functional modules for signaling and mechanosensing within IACs, indicating a possible segregation of these processes within the complex.

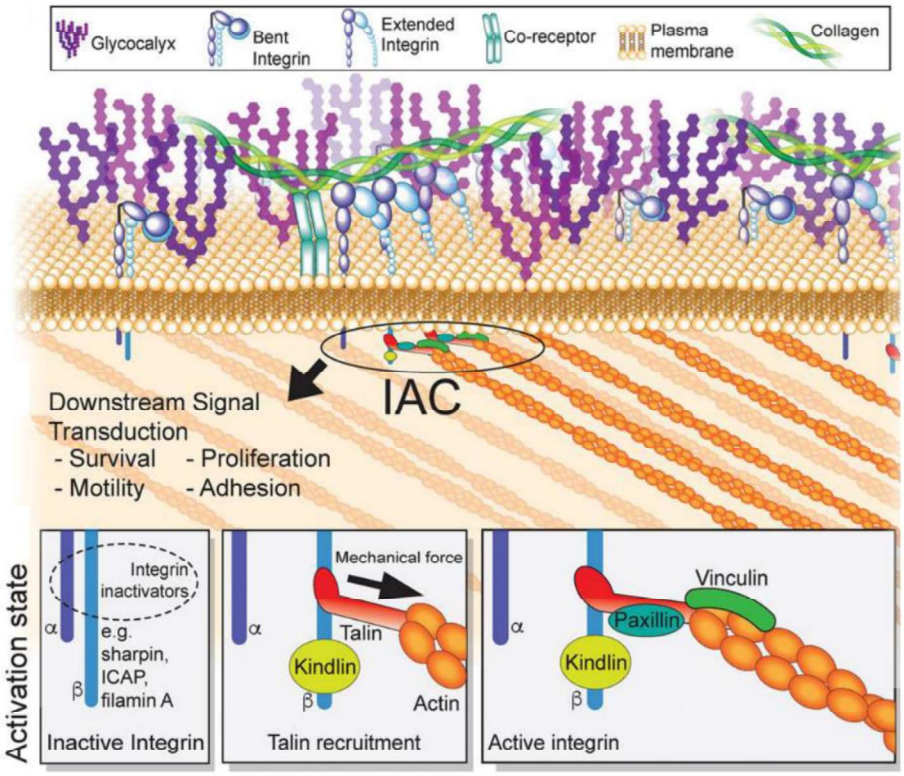

Fig. A6: Integrin signaling and activation.

The diagram illustrates integrins positioned on the plasma membrane, displaying both bent (inactive) and extended (active) conformations. Collagen fibers play a pivotal role in promoting clustering and the formation of IAC. Downstream signal transduction emanates from the IAC complex, reinforcing the actin cytoskeleton [78].

A. 1.1.4. Extracellular matrix: key attachments of cell adhesion

Cell-ECM interactions are essential for the regulation of cell behavior and fate in multiple developmental and homeostatic processes, among them tissue and organ formation, remodeling, and repair [95]. The crosstalk between cells and environments is further complicated by the physiological heterogeneity of the

ECM, with its wide variety of adhesion ligands that are recognized by multiple adhesion receptors, which might interact with each other, either positively or negatively [96]. For example, vav guanine nucleotide exchange factor 3 (Vav3) can regulate fibronectin-dependent cell adhesion in lung epithelial cells via the interaction between Vav3 and ß1-integrin [97], suggesting that fibronectin is essential for the process of cell adhesion. αv-class integrin governs fibroblast cell adhesion to fibronectin, and αv-class integrin mediating signaling acts together to orchestrate α5ß1-integrin mediating adhesion strengthening [85]. Meanwhile, fibronectin alters integrin clustering and FA stability with a concomitant enhancement in force-triggered integrin signaling along the FAK-Src complex in fibroblasts [98]. It indicates that the interaction between integrins and fibronectin can alter the activity of the cytoskeleton and induce the FAK-Src complex.

A. 1.2. Focal adhesion

The most well-characterized adhesive structures involved in the process of cell migration and cell adhesion are FAs and FA-like structures [78]. FAs are sites where integrins and proteoglycans mediated cell adhesion links to the actin cytoskeleton. The components of FAs are diverse and include scaffolding molecules, GTPases, and enzymes such as kinases, phosphatases, proteases, and lipases [99]. FA formation and maturation require the involvement of various proteins in different contexts [100]. For example, focal adhesion kinase (FAK) can regulate the cytoskeleton, structures of cell adhesion sites, and membrane protrusions to regulate cell movement [101]. Moreover, the intermediate proteins talin and vinculin are fundamental mechanosensors, as they can change conformation and signaling properties upon force-induced stretching, and they allow force transmission through ß subunit, inducing cell migration and detection of stiffness [86][102, 103]. The loss of talin and recruitment of tensin is linked to FAs, which in fibroblasts can lead to metabolic reprogramming at these more stable complexes [104, 105].

A. 1.2.1. The structure of focal adhesion

FA structures, called “apical plaques”, are localized on the apical side of ECs [106]. Numerous studies have indicated that ECs have some mechanism for responding to fluid flow [106]. When ECs line the interior of blood vessels, they form a continuous monolayer known as the endothelium. ECs interact with the underlying ECM through FAs, which serve as anchor points [107]. Spatially, adhesions physically interact with the ECM and neighboring cellular systems, which affect the developing structures and can be considered functional domains of the adhesion sites [95]. Meanwhile, for FAs, these are the lamellipodium, and the attached stress fiber, which passes directly through the upper surface of the cell, are connected to this apical plaque [95][108]. ECM, integrins, and cytoskeletal proteins, such as talin, paxillin, and vinculin, are localized in both the apical plaque and the FAs. FAK-Src complex is also localized in both the apical plaque and the FAs at the basal portion of the cell, which indicates that the complex acts as signal transduction machinery (Fig. A7). Meanwhile, ECM-bound integrins can link to the actin cytoskeleton or

intermediate filaments [93]. For example, both NPXF motifs, binding sites for talin and kindlin in β2-integrin, are required for force transmission through integrin [93]. The evidence suggests that integrins play a crucial role in binding to certain actin cytoskeletons. Small FA-like structures first form at the adhesion surface, and the cells eventually begin to elongate as spindles along the boundary between the adhesive micropattern and the nonadhesive region. For example, some small FA-like structures are formed at the distal end of the cell undergoing extension, and well-developed FAs are formed at the boundary of the micropattern [109].

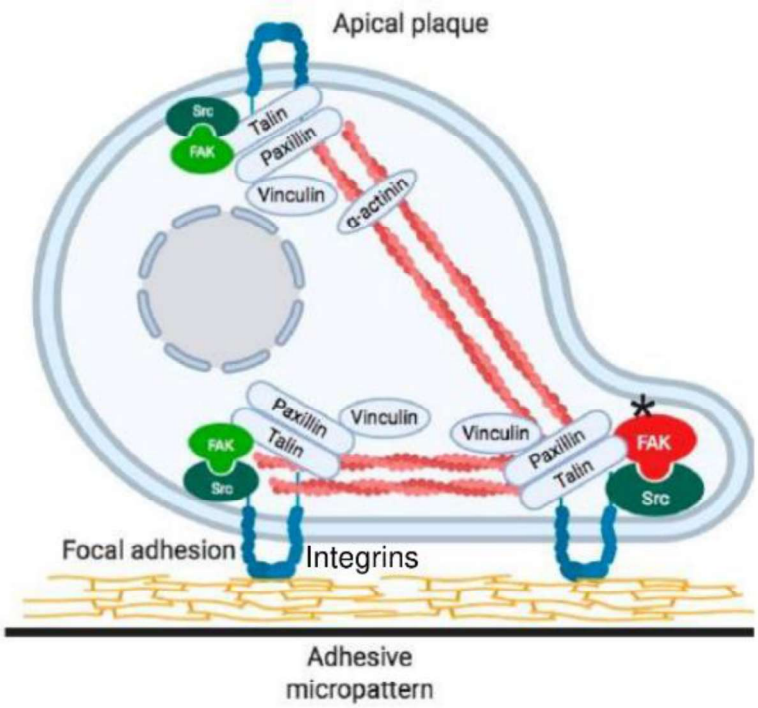

Fig. A7: The structure of focal adhesion.

Schematic illustration of a cell adherent on the border of the adhesive micropatterns. FAs at the bottom of the cells and the apical plaque are shown. FAK is highly accumulated at the border of the adhesive micropatterns, and the FAK seems to be tyrosine phosphorylated. The asterisk indicates tyrosine phosphorylated active FAK [109].

A. 1.2.2. Focal adhesion kinase

FAK is discovered as a kinase that is highly phosphorylated in response to cell adhesion and a key signaling component at the FA complex [99][110]. FAK is identified as a substrate of the viral Src oncogene and a highly tyrosine-phosphorylated protein that is localized to integrin-enriched cell adhesion sites that are known as focal contacts [101]. Focal contacts are formed at ECM-integrins junctions, which bring together cytoskeletal and signaling proteins during cell adhesion, cell migration, and cell spreading [101], indicating

that FAK is also a key player in the processes of cell adhesion and cell migration. The genomic designation of human FAK is protein-tyrosine kinase-2 (PTK2), located at human chromosome 8q24 term [101]. FAK is a 125 kDa tyrosine kinase that is composed of an N-terminal 4.1 protein, ezrin, radixin, moesin (FERM) and kinase domain in the middle, and a C-terminal focal adhesion targeting (FAT) domain (Fig. A8.A)[111]. Regarding the FERM domain, it serves as a major regulator of FAK activity through binding to the kinase domain, blocking the accessibility to tyrosine phosphorylation site Y397, and preventing autophosphorylation [112], which means that the FERM domain plays an important role in the cellular processes. Interestingly, the Src SH2 domain binds to FAK phosphorylated at Y397, and Src activity contributes to the activation of FAK at Y576, Y577, Y861, and Y925 [113]. In other signaling pathways involving the FERM domain, it can interact with vascular endothelial cadherin (VE-cadherin), resulting in the regulation of phosphorylation of ß-catenin in the cell-cell junctional complex [114]. Upregulation of the FERM domain blocks FAK activation and inhibits G-protein-stimulated cell migration [101]. Meanwhile, FERM can be localized to the nucleus and may directly bind to the transactivation region of p53 to block the transcriptional activity of p53 [113], suggesting that FAK is involved in the processes of cell proliferation and cell survival. The kinase domain contains two tyrosine phosphorylation sites, Y576 and Y577, in the activation loops (Fig. A8.A)[110][113]. With regards to the FAT domain, it promotes the colocalization of FAK with integrins at focal contacts, which shows that FAK can bind to the cytoplasmic tails of integrins through some integrin-associated proteins, like paxillin and talin (Fig. A8.A, B)[113]. Moreover, the FAT domain contains two proline-rich regions binding sites for the Src SH3 domain (Fig. A8.A, C). SH3 domain-mediated binding of the adaptor protein p130Cas to FAK is vital in promoting cell migration through the activation of Rac at membrane extensions [101][113]. The FAT region also contains two main tyrosine phosphorylation sites, Y861 and Y925, both of which are phosphorylated by the Src kinase (Fig. A8.A)[110].

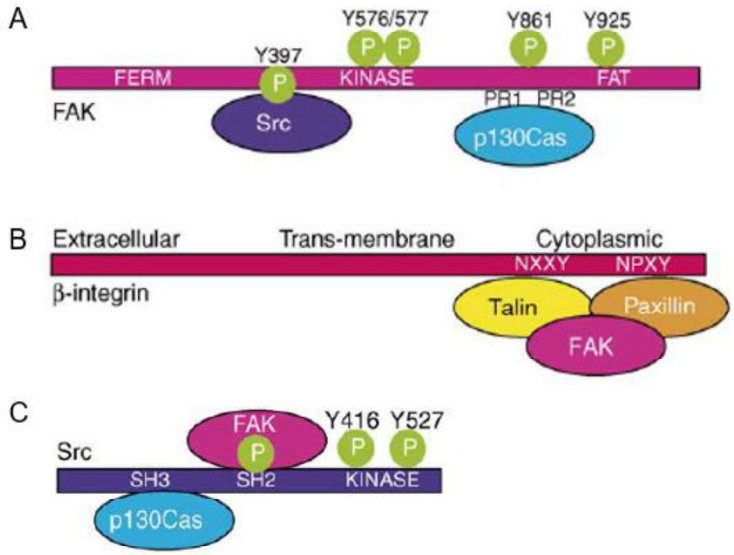

Fig. A8: Simplified binding interactions between ß-integrins, FAK and Src.

(A) Structural features and domains of FAK. Src and p130Cas contain interaction domains such as SH2 and SH3 domains that recognize phosphorylated tyrosines and proline-rich motifs (PR1 and PR2), respectively. Src SH2 domain binds to FAK phosphorylated at Y397 and Src activity contributes to maximal FAK activation by phosphorylation of FAK at Y576, Y577, Y861 and Y925. The p130Cas SH3 domain binds to PR1 and PR2 domains in the FAK C-terminal domain. (B) Structural features and domains of ß-integrin. FAK is recruited to the ß-integrin cytoplasmic domain in part by association with the integrin binding proteins talin and paxillin. (C) Structural features and domains of Src. The Src SH3 domain binds to p130Cas within a proline-rich motif termed the Src binding domain and both FAK and Src can phosphorylate p130Cas within the substrate domain at multiple sites to promote Crk binding to p130Cas [113].

FAK can mediate the regulation of Rho-family GTPases, which control the formation and disassembly of actin cytoskeletal structures, like stress fibers, lamellipodia, and filopodia in the cells [101]. In particular, the FAK-Src complex can regulate the transient suppression of integrin mediating RhoA-GTP levels [115] and the activation of Rac1 and Cdc42 [116]. It indicates that FAK signaling and FAK-Src complex can also be involved in cell motility. For example, the activation of integrin/Src/FAK signaling and suppression of AMP-activated protein kinase (AMPK) signaling induce the process of cell adhesion in fibroblasts [117]. FAK signaling is required in the promotion of cell migration in fibroblasts [118], and the activated FAK/phosphoinositide 3-kinase (PI3K)/protein kinase B (AKT) signaling can mediate cell invasion induced by galectin-1 [119]. In addition, FAK signaling is involved in cell survival [111], cancer progression, and metastasis [120]. For example, tubulointerstitial nephritis antigen-like 1 (Tinagl1) can reduce tumor growth and metastasis via α5ß1-integrin/FAK signaling [120]. Integrin-mediated adhesion induces the autophosphorylation of FAK at Y397, creating a binding site of Src (Fig. A9)[121]. Meanwhile, ß-catenin Y142 is a direct FAK substrate promoting ß-catenin activation in ECs facilitating cell-cell adhesion

breakdown [114]. Upon FAK activation, the FAK-Src complex phosphorylates and recruits several downstream signaling targets, including PI3K/AKT. These hints indicate that the FAK-Src complex can regulate the signaling of ß-catenin. Glycogen synthase kinase 3 (GSK3) generally acts as a downstream signaling protein molecule of AKT [122]. Growth factor receptor-bound protein 2 (Grb2) coordinates signaling downstream of integrin/FAK to activate c-Jun N-terminal kinase (JNK). Grb2 also interacts directly with dishevelled (Dvl)[123]. Dvl can stimulate c-Jun-dependent transcription activity and the kinase activity of JNK [124]. Loss of phosphatase and tensin homolog (PTEN) function causes the activation of PI3K/AKT and JNK pathways [125]. PTEN also controls FAK. FAK promotes Wnt/β-catenin pathway activation by phosphorylating GSK3β [126]. This phosphorylation inhibits the activity of GSK3β which otherwise would drive rapid degradation of β-catenin. In addition, FAK is shown to trigger the β-catenin signaling pathway through nuclear translocation of β-catenin and transcriptional activation of β-catenin target genes (Fig. A9)[127]. I have known that LecB can also induce proteasomal β-catenin degradation in lung cancer cells [5], but FAK signaling mediating the degradation of ß-catenin is unclear. Thus, a hypothesis that LecB can trigger the degradation of ß-catenin via FAK signaling has risen.

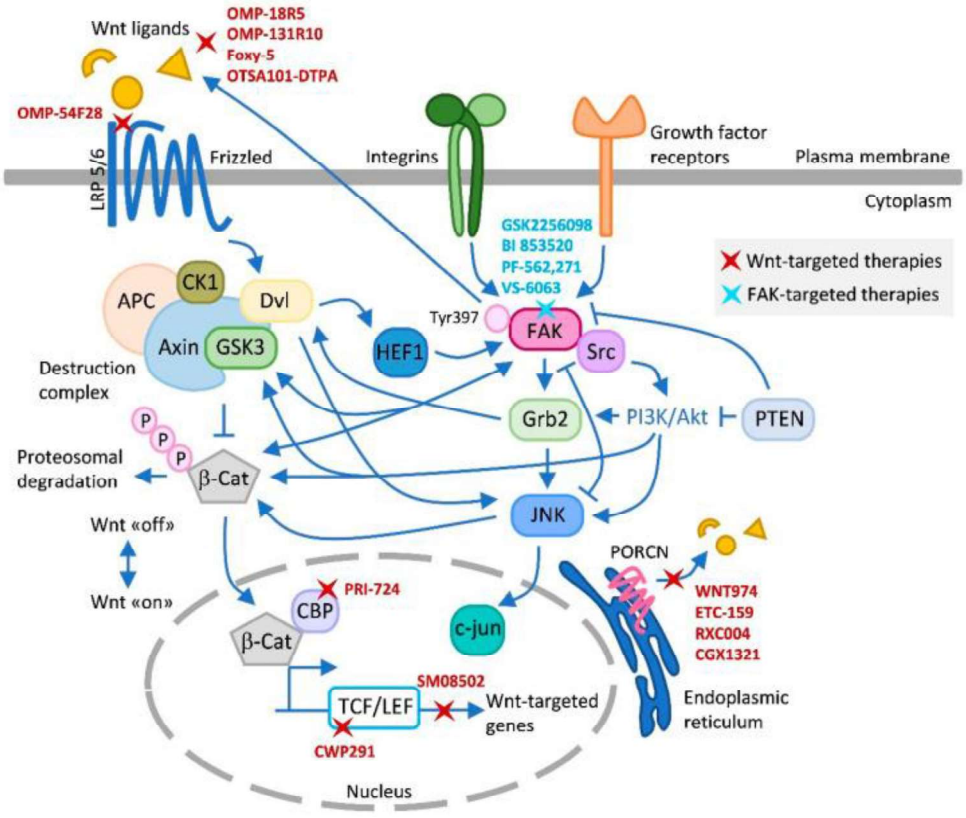

Fig. A9: The scheme of FAK signaling crosstalks.

This figure summarizes the main known crosstalks existing between Wnt and FAK that have been described in the text and in the literature, and the different Wnt and FAK inhibitors tested in clinical trials. FAK appears to be an important regulator of the Wnt signaling pathway. However, a wide range of FAK-Wnt interactions at different levels that are context- and cell-type dependent. Thus, a better understanding of the nature and physiological relevance of this interaction is necessary, before devising combinatorial therapeutic strategies. Arrows indicate activation/induction [127].

A. 1.2.3. Regulation of integrins through focal adhesions

As I mentioned previously, integrins are the vital players that link to ECM, the FAK-Src complex, and the cytoskeleton. Thus, integrins can mediate the structures of FAs, resulting in some cellular processes, like cell adhesion and cell migration. For example, in the case of fibroblasts cultured on fibronectin, translocating α5ß1-integrin transmits cytoskeleton-generated tension to extracellular fibronectin molecules to form the process of cell adhesion [128]. Meanwhile, FAs of ECs assembled on α5β1-integrin-selective substrates rapidly recruit αvβ3-integrins, causing the maturation of FA and cell spreading [129]. Besides, integrins can regulate the FAK-Src complex in FAs. Integrin-mediated activation of the FAK-Src complex stimulates the activity of Cdc42 and Rac1, leading to the formation of filopodia and membrane-ruffling lamellipodia [121]. It means that integrins can mediate FAK-Src complex in FAs. It has been established that LecB can interact with ß1-integrin in MDCK cells [10], and in lung cancer cells, LecB is capable of inducing proteasomal degradation of β-catenin [5]. According to the other introduction and hypothesis mentioned before, I suspect that if LecB can alter the processes of cell adhesion and cell migration via ß1-integrin/FAK-Src/ß-catenin signaling in the cells.

A. 1.3. Flotillins

A. 1.3.1. The structure and cellular function of flotillins

Flotillin-1 and flotillin-2 (also called reggie-2 and reggie-1) are discovered as neuronal proteins upregulated in retinal ganglion cells during the regeneration of axons after lesions of the optic nerve, implying that they contribute to regeneration [130]. Flotillin-1 and flotillin-2 are widely distributed and highly conserved proteins, showing approximately 50% amino acid sequence identity. They are monotopic integral membrane proteins, with molecular weights of 49 kDa and 47 kDa, respectively [131]. Flotillins have three domains, an N-terminal stomatin/prohibitin/flotillin/HflC/K (SPFH) domain, also known as prohibitin homology domain (PHB) or “band 7 domain,” a central linear α-helical region, and a C-terminal flotillin domain (Fig. A10.A)[132, 133]. The SPFH domains of flotillins present with six antiparallel β sheets and four partially exposed α helices, forming an ellipsoidal-like globular domain, which is associated with the cytoplasmic face of the bilayer [133, 134]. The SPFH domain contains two hydrophobic stretches that could mediate its interaction with the inner leaflet of the plasma membrane (Fig. A10.B)[131]. Meanwhile, the SPFH domain also contains putative cholesterol recognition amino acid consensus (CRAC) motifs outside of the hydrophobic stretches, and these might participate in mediating the interaction of flotillins

with membranes, and more specifically, with lipid rafts [131][135]. For example, flotillins can interact with CRAC domains, and the translocation of flotillin-2 from the plasma membrane to the endocytic compartments depends on at least one of these protein CRAC domains [136]. Meanwhile, the SPFH domain allows the association of flotillins with cholesterol-rich membrane domains via interaction with the hydrophobic amino acid stretches or with putative CRAC motifs and through posttranslational modifications [137]. The SPFH domain of flotillins is involved in some cellular processes. For example, the trafficking of flotillin-1 to the plasma membrane has been suggested to take place via a Golgi-independent pathway and to depend on the SPFH domain [138]. The SPFH domain of flotillin-2 can bind to F-actin, and this interaction regulates the lateral motility of flotillin microdomains [139]. It indicates that flotillin-2 is involved in cell motility, which is the reason why I included flotillins in my project. With regards to C-terminus, it includes the so-called flotillin domain that has been suggested to be involved in oligomerization [131][140]. Heterooligomerization of flotillin-1 with flotillin-2 has been reported to be mediated by the C-terminal part of the proteins [140]. Interestingly, the SPFH domain might also contain some determinants that regulate flotillins heterooligomerization [131].

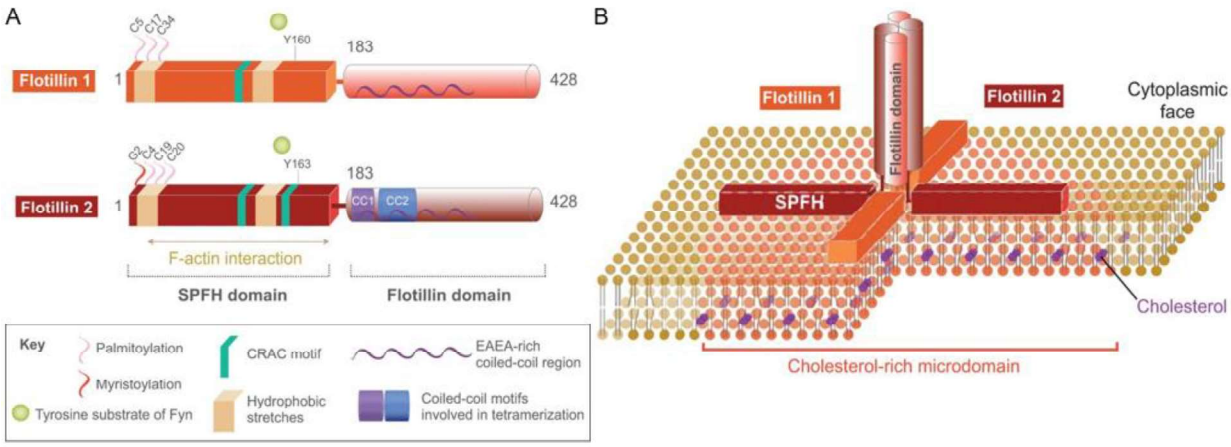

Fig. A10: Structural features of flotillins.

(A) This figure depicts the linear representation of flotillin-1 and flotillin-2, highlighting the main functional motifs and identified residues. It shows the coiled-coil (CC) motifs that have been experimentally proven to be involved in the association between flotillin monomers. Specifically, the CC1 (amino acids 184-238) and CC2 (amino acids 239-321) in flotillin-2 are represented. (B) The schematic representation illustrates a flotillin tetramer formed through coiled-coil interactions between the flotillin domains. It also shows the association of the flotillin tetramer with the plasma membrane in cholesterol-rich micro-domains through the SPFH domains [131].

Flotillins are shown to be involved in various cellular processes such as cell adhesion, cell migration, signal transduction through receptor tyrosine kinases, as well as in cellular trafficking pathways [141]. The functions of cell adhesion and cell migration are introduced in a next chapter. Here, in this paragraph, I

focus on the functions of signal transduction and cellular trafficking. On the one hand, it has been reported that flotillins are regulators of epidermal growth factor receptor (EGFR)/mitogen activated protein kinases (MAPK) signaling upon direct stimulation of the EGFR in keratinocytes [142]. Meanwhile, flotillins are identified as downstream targets of the mitogen activated kinases ERK1/2, leading to the activation of growth factor receptors and transcription factors [143]. There are also many signaling pathways mediated by flotillins [137], but I will only introduce two examples. Flotillin-1 can induce GTPase HRas and HRas/AKT activation, inducing HRas-mediated invasion/migration in breast cancer cells [144]. Upregulating flotillin-2 expression enhances the activity of PI3K/AKT3 and NF-κB, promoting malignancy of nasopharyngeal carcinoma cells [145]. On the other hand, flotillins are the components of lipid rafts and are involved in clathrin-independent endocytosis (CIE)[146]. Flotillins may mediate the transfer of a ligand to the invagination rather than contribute to the endocytic process [146]. For example, flotillin-1 can colocalize with early endosome (EE) marker, early endosome antigen 1 (EEA1), mediating protein kinase C (PKC)-triggered endocytosis [147]. Meanwhile, flotillin-2 is a regulator of the Rab11a/SNX4-controlled sorting and recycling pathway in HeLa cells [148]. Flotillins not only interact with EE and recycling endosome (RE), but also localize to some other endosomal structures, like late endosome (LE) and lysosome [149]. It suggests that flotillins display a dynamic cellular localization and assist in endocytic trafficking cargo [141].

A. 1.3.2. The role of flotillins in cell adhesion

The membrane domains have crucial roles in the regulation of cell adhesion and signaling cascades [137]. As we know, flotillins are lipid raft-associated proteins that are present in nearly every type of vertebrate cell and are highly conserved among organisms [133]. Thus, flotillins can play an important role in the process of cell adhesion. It has been reported that flotillins are regulators of integrin-ECM adhesions [150], and flotillin-2 can regulate α5ß1-integrin trafficking and FA [151]. Indeed, flotillins play a role in modulating integrin signaling and function, which are crucial for cell-ECM interactions, cell adhesion, migration, and other cellular processes that depend on integrin-ECM adhesions. They are involved in the dynamic regulation of integrin clustering and focal adhesion turnover, contributing to the overall coordination of cell-ECM interactions and cellular responses to the extracellular environment [152]. Specifically, the knockdown (KD) of flotillin-2 leads to the increased number of FAs upon the stimulation of fibronectin, and FAs are disorganized, as seen with paxillin and α5ß1-integrin in the absence of flotillin-2 [151]. Moreover, the flotillin-2 deletion mutant can enhance the activity of FAK and regulate cytoskeletal remodeling [153]. Flotillins can colocalize with γ-catenin and E-cadherin, and interaction domains in γ-catenin contain 12 ARM protein domains which is implicated in mediating protein-protein interactions [154], resulting in epithelial cell-cell adhesion [155, 156]. Interestingly, flotillin-2 interacts with ß-subunit integrin via α-actinin, activating FAK phosphorylation which may affect FA and cell migration *in vitro* [152]. However, most research is about the function of flotillin-2 in cell adhesion, and the impact of flotillin-1 is less understood. Here, in my project, I focused more research on the role of flotillin-1 in cell adhesion and cell migration induced by LecB.

A. 1.3.3. The role of flotillins in cell migration

In addition to the role of flotillins in cell adhesion and endocytosis, flotillins are a vital player in the process of cell migration. For example, flotillins can bind to the insulin receptor CAP *in vitro*, resulting in the activation of Rho GTPases, which contribute to cell migration through tissues and tissue-like environments [157–159]. Specifically, the migration rate of ECs is upregulated by flotillin-1 and mediated by phosphorylated flotillin-1 [160]. Meanwhile, Flotillin-1 is involved in the EMT process of several solid tumors to promote metastasis, cell migration, and cell invasion [161]. The KD of flotillin-2 blocks wound healing in A549 cells [162], suggesting that not only flotillin-1 but also flotillin-2 can mediate the process of cell migration. Interestingly, the downregulation of flotillin-2 cells showed an overall reduced level in activated Src kinases, which can positively regulate the ß-catenin/Wnt signaling pathway [156][163, 164]. It indicates that a small panel of molecules relevant to Wnt/β-catenin pathway activity is devised, like flotillins and Src, which arouses my interest regarding if flotillins mediate FAK-Src complex and Wnt/β-catenin signaling induced by LecB.

A. 1.4. ß-catenin signaling

A. 1.4.1. The structure of ß-catenin

ß-catenin is an oncogenic protein that plays an important role in the Wnt signaling pathway and is an important component of the cadherin cell adhesion complex [165, 166]. ß-catenin has three domains, a central domain, an N-terminal domain, and a C-terminal domain (Fig. A11.A). The central armadillo repeat domain (residues 141-664) is composed of 12 armadillo repeats, and an N-terminal domain harbors the binding site for ß-catenin as well as the GSK3 and CK1 phosphorylation sites that are recognized by the ß-TrCP ubiquitin ligase [167]. Specifically, the central domain is the most conserved region of ß-catenin, which is consistent with its role as the binding site for most ß-catenin binding partners. The N-terminal and C-terminal domains are sensitive to trypsin digestion and thus may be structurally flexible, whereas the central domain forms a relatively rigid scaffold [167, 168]. The N-terminal and C-terminal domains can interact with the armadillo repeat domain by a fold-back mechanism, which could regulate the partner-binding properties of the armadillo repeat domain [167][169]. With regards to the N-terminal GSK3 phosphorylation sites (Fig. A11.B, C), ß-catenin can phosphorylate at serine S33 and S37, which is an essential tool in defining the interactions, distribution, regulation, and deregulation of ß-catenin and its role in signal transduction [165][167]. Besides, there are lots of phosphorylation sites of ß-catenin reported in the research. For example, Src can stimulate the phosphorylation of ß-catenin at Y654, resulting in the decreased affinity of E-cadherin for ß-catenin [167].

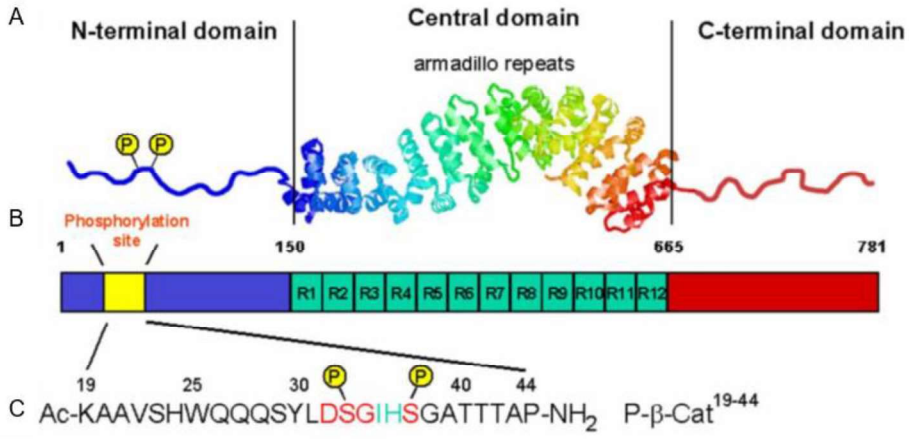

Fig. A11: Schematic representation of the ß-Catenin.

(A) The protease-resistant fragment of β-Catenin, containing the armadillo repeat region, adopts a three-dimensional structure. The core region of β-Catenin consists of 12 repeats of a 42-amino acid sequence motif known as the armadillo repeat. These 12 repeats form a super helix of helices, resulting in a long, positively charged groove in the proteolytically resistant fragment. However, the structure of the N and C terminal domains of β-Catenin remains unresolved. (B) The full primary structure sequence of β-Catenin is depicted, with the 12 armadillo repeats shown in green. The phosphorylation site containing the consensus motif DpSGXXpS is highlighted in yellow. (C) The sequence of the phosphorylated β-Catenin fragment is provided for reference [165].

A. 1.4.2. The role of cadherin-catenin complex in cell adhesion

The cadherin-catenin complex plays a crucial role in epithelial cell-cell adhesion and the maintenance of tissue architecture [170]. Cadherins extracellular domains join with the cytoplasmic tail to form signaling hubs called AJs [171]. The catenins bind the intracellular domain of the cadherin to the actin cytoskeleton through AJs [170]. This interaction between the transmembrane cadherin and actin filaments of the cytoskeleton is necessary for strong cell-cell adhesion (Fig. A12 right panel)[170][172]. Any dysfunction of the cadherin-catenin complex reduces cell adhesion. For example, the dysfunction of the cadherin-catenin complex has been reported in the neoplastic process leading to ß-catenin accumulation in the cytoplasm and nucleus of the tumor cells [171][173]. Interestingly, my target proteins, flotillins, can be involved in the cadherin-catenin complex in cell adhesion. For example, flotillin-1 can interact with ß-catenin and E-cadherin and is required to build a cadherin-catenin complex containing membrane microdomains [174], suggesting that flotillin-1 is a major regulator of the cadherin-catenin complex mediating cell adhesion in both mesenchymal and epithelial cells. Meanwhile, the downregulation of flotillin-2 can induce the disruption of the cadherin-catenin complex at AJs in A431 cells [156], indicating that flotillin-2 also is involved in the cadherin-catenin complex. Thus, I linked flotillins to ß-catenin signaling induced by LecB.

E-cadherin, a transmembrane glycoprotein of five repeats and a cytoplasmic domain, is expressed primarily in epithelial cells [175]. It has been reported that α5ß1-integrin increases the transactivation of

ß-catenin, resulting in cell migration in glioma cells [176]. Meanwhile, the ß1-integrin receptor can activate GSK3β phosphorylation and result in the nuclear translocation of β-catenin under the matrix stiffness signal [177]. In addition, the nuclear accumulation of β-catenin can be triggered by integrins via FAK signaling [123], and I have known that LecB can interact with ß1-integrin [10]. It indicates that integrins can be involved in the activation of ß-catenin, which arouses my hypothesis that ß1-integrin can mediate the nuclear translocation of β-catenin via FAK signaling induced by LecB in the cells.

A. 1.4.3. The regulation of ß-catenin signaling

Wnt signaling is a well-known potent pathway that activates nuclear ß-catenin [178]. The highly branched Wnt pathway includes a β-catenin-dependent transcriptional cascade and other branches that signal through cytoskeleton, calcium, or planar cell polarity [179]. The Wnt/β-catenin signaling pathway is built in such a manner that the activation of the signal at the membrane via the Frizzled receptors [180]. In the absence of a Wnt signal, free cytoplasmic ß-catenin is phosphorylated by serine/threonine kinases, casein Kinase Iα (CKIα) and GSK3ß in a large APC/axin scaffolding 'β-catenin destruction complex' that targets ß-catenin for degradation (Fig A12 left panel)[167][178]. In the presence of Wnt signaling, this destruction complex is disrupted, and dissociation of GSK3ß prevents phosphorylation of ß-catenin. This increased stability of ß-catenin leads to its translocation in the nucleus and induces transcriptional activation of target genes by ß-catenin interaction with T cell factor/lymphoid enhancer factor (TCF/LEF) DNA-binding proteins (Fig. A12 left panel)[167][178]. Besides, integrin-mediated adhesion induces the autophosphorylation of FAK at Y397, creating a binding site of Src [121]. FAK is probably responsible for Src-dependent phosphorylation, resulting in the nuclear translocation of ß-catenin in migration-induced epithelial cells [181].

ß-catenin locates at three positions, plasma membrane, cytoplasm, and nucleus, which have different functions. ß-catenin at the cell membrane balances adhesion and signaling [182], which have been introduced previously regarding the cadherin-catenin complex in cell adhesion. In the cytoplasm, free ß-catenin is recognized by the destruction complex and rapidly targeted for degradation. The phosphorylated ß-catenin is mediated by GSK3ß, undergoing degradation [182]. From our previous research, I have verified that LecB can induce proteasomal ß-catenin degradation depending on GSK3ß activity in H 1299 cells [5]. The inhibition or bypassing of ß-catenin destruction leads to increased levels of ß-catenin, which accumulates in the cytoplasm and then translocates into the nucleus [182]. Nuclear ß-catenin signals are involved in many cellular functions, such as cell proliferation [183] and cell migration [166][184]. Specifically, the wound healing process can promote the accumulation of ß-catenin in the nucleus [184], which arouses my interest regarding the effect of nuclear ß-catenin on cell migration and cell adhesion induced by LecB.

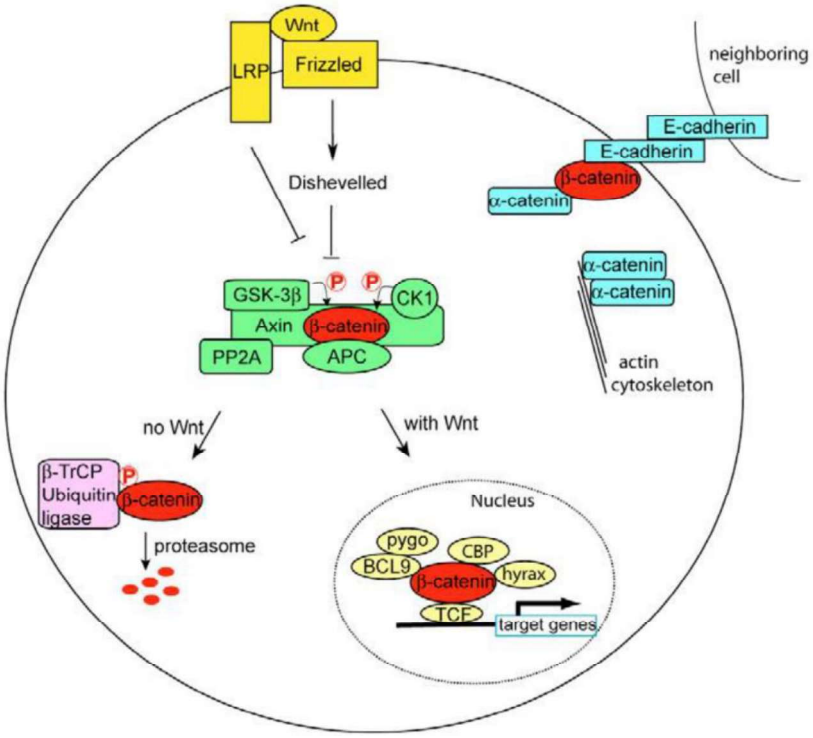

Fig. A12: Roles of ß-catenin in the cells.

Roles of β-catenin in the cell. β-catenin binds to E-cadherin and α-catenin at AJs. In the vicinity of these juctions, α-catenin binds to actin as a homodimer. In the absence of Wnt signaling, β-catenin joins the destruction complex (green, left panel), where it is phosphorylated by CK1α and GSK-3β, which causes it to be ubiquitylated by the β-TrCP ubiquitin ligase and subsequently degraded by the proteasome. This results in the activation of Wnt-target genes. Mutations in APC, axin or β-catenin lead to stabilization of β-catenin in the absence of a Wnt signal and consequent upregulation of Wnt-target genes. ß-catenin binds to E-cadherin and ß-catenin at AJs (right panel) [167].

A. 2. Project objectives

P. aeruginosa, an opportunistic pathogen, poses a significant threat to humanity as it continues to develop increasing resistance against current treatment options. The virulence factors of *P. aeruginosa*, including the fucose-specific lectin LecB, can cause severe infections in the host cells. According to the study of Dr. Roland Thuenauer and Catherine Cott, LecB can block epithelial cell migration by triggering ß-catenin degradation. However, the molecular mechanisms of ß-catenin degradation induced by LecB are unclear. My hypothesis suggests that LecB enhances cell adhesion, leading to a larger number of cells adhering to each other or the culture plate, ultimately resulting in a majority of immobilized cells. During my investigation, I explored factors related to LecB, including flotillins and ß1-integrin, as they play crucial roles in cell adhesion and cell migration processes. The overall aims are to investigate the effect of *P. aeruginosa* lectin LecB on cell adhesion and cell migration and the molecular mechanisms after the binding of LecB on the host cells.

The three significant aims are:

Aim 1: To investigate the impact of flotillins on the process of cell adhesion and cell migration induced by LecB

Numerous studies showed that flotillins are involved in the process of cell adhesion and cell migration. In this project, the primary objective is to gain a deeper understanding of how flotillins mediate cell adhesion and cell migration induced by LecB.

Aim 2: To verify the colocalization and co-precipitation of LecB with molecular factors, such as flotillin1/2 and ß1-integrin

Based on our previous research, LecB can interact with ß1-integrin in MDCK cells, and LecA can interact with flotillin-1 in H1299 cells. This has led to a hypothesis that LecB may also interact with flotillins. Thus, the second goal of our project is to investigate the potential crosslink between flotillins and ß1-integrin induced by LecB.

Aim 3: To investigate the molecular mechanisms behind LecB-induced nuclear accumulation of ß-catenin.

LecB can induce a clear accumulation of β-catenin around centrosomes in H1299 cells in our previous studies, resulting in the blockage of cell migration. While the specific molecular mechanisms that occur after the binding of LecB to H1299 cells remained unclear. As the third aim of my project, I aimed to investigate the outcomes following the binding of LecB in H1299 cells.

A. 3. Materials and methods

A. 3.1. Cell culture and stimulation

The human non-small cell lung cancer cell H1299 (American Type Culture Collection, CRL-5803) control cells and corresponding *ΔFLOT1* cells (flotillin-1 knockout model) were cultured in Roswell Park Memorial Institute (RPMI) 1640 medium (Gibco) supplemented with 10% fetal calf serum (FCS) (Gibco) and 2 mM L-glutamine (Gibco) at 37°C and 5% CO_2. The *ΔFLOT1* cell line was created previously using the CRISPR/Cas9 system [185].

Recombinant LecB (UniProt ID: Q9HYN5_PSEAE) was transformed with the plasmid pET25pa21 and produced from *E.coli* BL21 (DE3). LecB was purified as previously described [9]. LecB was dissolved in PBS (with Ca/Mg) (Gibco) and used at a concentration of 50 µg/ml (1.06 µM). LecB was fluorescently labelled with Alexa Fluor488 (Thermo Fisher Scientific) monoreactive NHS ester and purified with Zeba Spin desalting columns (Thermo Fisher Scientific) according to the manufacturer's instructions. The fluorescent LecB was called LecB-A488. Biotinylated LecB was obtained using sulfo-SS-Biotin (Thermo Fisher Scientific) according to manufacturers' instructions and dialyzed twice for 1 h in water and once in PBS overnight at 4°C. The biotinylated LecB was called LecB-Biotin.

To block fucose-binding sites of LecB, L-fucose (Sigma-Aldrich) was dissolved in ultrapure water, sterile filtered, and used at a final concentration of 43 mM in the presence or absence of LecB according to our previous research [5][10].

A. 3.2. Transient siRNA transfection

H1299 control and *ΔFLOT1* cells were transfected with on-target SMART pools of control siRNA (Horizon Discovery, D-001810-01-20) and flotillin-2 (FLOT2) siRNA (Horizon Discovery, L-003666-01-0010). The silencing of flotillin-2 in H1299 control cells was called FLOT2 knockdown (KD) cells, while the silencing of flotillin-2 in *ΔFLOT1* cells was called *ΔFLOT1*/FLOT2 KD cells. During the incubation with a mixture of 100 nM siRNA and Lipofectamine 2000 (Thermo Fisher Scientific, 11668027), cells were kept in serum-free medium for 12 h incubation at 37°C and then in RPMI 1640 medium supplemented with 10% FCS and 2% L-glutamine at 37°C, according to the manufacturer's protocol. LecB stimulation was performed 48 h post-silencing.

A. 3.3. Wound healing assay

Cells were seeded in 6-well plates (Sigma-Aldrich) and allowed to form monolayers with 100% confluent for 2 days at 37°C. Then, the monolayers were scratched with a 200 µl tip to create a wound. Images were acquired at indicated time points using a 10X air objective (NA=0.25) under an optical microscope (EVOS XL Cell Imaging System). Distances between both cell fronts were measured by Image J. A dashed line was

drawn at the wound's edge, indicating the cell front. The distance between two dashed lines was measured at 0 h as the initial distance of the wound. At the indicated time points, the migration distance was described as the distance of the wound subtracted from the initial distance.

A. 3.4. Cell adhesion assay

24-well plates (Sigma-Aldrich) were coated with 0.5 mg/ml streptavidin or 1 µg/ml fibronectin (R&D Systems) overnight, and all procedures were conducted at 37°C. After that, plates were blocked with 1% (wt/vol) BSA (Sigma-Aldrich) or TBST buffer (LI-COR Biosciences) for 1 h. After washing with PBS twice, either 50 µg/ml LecB-Biotin for streptavidin-coated plates or 50 µg/ml LecB for fibronectin-coated plates was added into the wells for 1 h. Then, cells were seeded in the plate at a density of 1 x 10^5 cells per well. The non-adherent cells were washed away with PBS after the indicated time points. Cells were stained with Cell Mask deep red plasma membrane stain (Thermo Fisher Scientific, C10046), and images were acquired for indicated time points using 20X air objective (NA=0.45) with the EVOS microscope. The number of adherent cells in the images was counted by Image J.

A. 3.5. Single-cell force spectroscopy measurements and analysis

35 mm Petri dishes with a polymer coverslip bottom (ibidi) were coated with 1 µg/ml fibronectin (R&D Systems) overnight, and all procedures were conducted at 37°C. After blocking with TBST buffer (LI-COR Biosciences) and washing twice with PBS, 50 µg/ml LecB was added to the surface for 1 h incubation in LecB treatment groups. After that, Petri dishes were washed twice with PBS, and changed to Hanks' balanced salt solution (HBSS) (Gibco) supplemented with 1% (vol/vol) FBS, 1% (vol/vol) L-glutamine, 1% (vol/vol) non-essential amino acids solution (NEAA) (Pan Biotech), 0.55% (vol/vol) Glucose solution (Gibco), 10 mM (vol/vol) HEPES buffer solution (Gibco).

All force measurements were performed using a CellHesion 200 (JPK BioAFM, Bruker Nano GmbH) integrated with an inverted Nikon Ti microscope equipped with a 20X multi immersion objective (NA=0.45). The incubator chamber in which the AFM was housed was conditioned at 37°C. Silicon nitride probes (cantilever C, MLCT-O10, Bruker Nano GmbH) were first plasma-cleaned and coated with 3.5 µg Cell-tak (Corning, 354240)/cm^2 for 20 min. The redundant Cell-tak was washed away with Milli-Q H_2O. Using the AFM system, we caught a suspended H1299 cell with the Cell-tak-coated cantilever constants of 0.02±0.005 N/m. During the measurement, the cantilever slowly approached the fibronectin-coated surface, became in contacted, was retracted it, and the force-distance curves were obtained by recording the cantilever deflection. For the curve measurements, the approach and retract velocity was 1 µm/s, the contact force was 1 nN, the contact time was either 0 s or 5 s, and the pulling length was 50 µm. Each data set was generated using about 30-40 cells, and 1-5 force curves were recorded in each cell. The F_d curves were computed using JPK data processing software (version 6.1.163).

A. 3.6. Immunofluorescence, confocal microscopy and image analysis

Cells were grown on 12 mm glass coverslips in a 4-well Nunc plate (Thermo Fisher Scientific) to 70% confluence at 37°C. Cells were treated with either 50 µg/ml LecB or 50 µg/ml LecB-A488 for indicated time points. Then, cells were fixed with 4% (wt/vol) paraformaldehyde (PFA) for 10 min at RT, and quenched with 50 mM ammonium chloride for 5 min at room temperature (RT). For the staining of flotillin-1 antibody, the cells were subjected to ice-cold methanol for 8 min at -20°C after the quenching. The cells were incubated with 0.2% (vol/vol) Saponin (Thermo Fisher Scientific) in PBS at RT. After that, the cells were blocked with 3% BSA (vol/vol) (Carl Roth) in PBS and subsequently stained with primary and corresponding secondary antibodies at RT. The nucleus and F-actin were counterstained with DAPI (Sigma-Aldrich) and phalloidin ATTO 565 (Sigma-Aldrich), respectively. Cells were mounted using Mowiol medium (Carl Roth) containing DABCO (Carl Roth). Images were acquired with a Nikon microscope (Eclipse Ti-E A1R system) with a 60X oil immersion objective (NA=1.49). Co-localization was calculated by Fiji ImageJ 1.0 software using the Coloc2 plugin, and the accumulation of ß-catenin in the nuclei was measured using a home-made FIJI macro available here: https://github.com/taras-sych/Beta-catenin-quantification.

The following antibodies were used for immunofluorescence stainings in this study: anti-Flotillin-1 (Cell Signaling Technology, #18634), anti-EEA1 (BD Biosciences, 610457), anti-Rab9 (Cell Signaling Technology, #5118), anti-Rab11(Cell Signaling Technology, #5589), anti-ß-catenin (BD Biosciences, 610153), anti-FAK (Y397) (Thermo Fisher Scientific, 44-624G) followed by goat-anti-rabbit Alexa Fluor 647 (Thermo Fisher Scientific, A21245). Anti-Flotillin-2 (BD Biosciences, 610383) and anti-LAMP1 (Cell Signaling Technology, #9091) followed by goat anti-mouse Alexa Fluor 647 (Thermo Fisher Scientific, A21236). Anti-ß1-integrin (R&D Systems, AF1778) followed by donkey anti-goat Cy3 (Jackson ImmunoResearch, 705-165-147), and anti-FAK (Thermo Fisher Scientific, AHO1272) followed by donkey anti-mouse Alexa Fluor 488 (Thermo Fisher Scientific, A21202).

A. 3.7. SDS-PAGE and immunoblot analysis

Cells were seeded in a 6-well plate (Sigma-Aldrich) at a density of 3 x 10^5 cells per well at 37°C. After the LecB treatment, the cells were washed with cold PBS and lysed in RIPA buffer [20 mM Tris-HCl, pH 8, 0.1% (wt/vol) SDS, 10% (vol/vol) glycerol, 13.7 mM NaCl, 2 mM EDTA and 0.5% (wt/vol) sodium deoxycholate in water] supplemented with protease (Merck) and phosphatase inhibitors (Merck). The protein concentration was determined by using a BCA kit assay (Thermo Fisher Scientific) according to manufacturer's instructions. Then, the protein samples were separated via SDS-PAGE gel electrophoresis and subsequently transferred onto a nitrocellulose membrane. The membranes were blocked in either 5% (wt/vol) non-fat milk powder (Carl Roth) or 1% (wt/vol) BSA powder (Sigma-Aldrich) in TBS supplemented with 0.1% (vol/vol) Tween-20 (Bio-Rad) at RT for 1 h, and incubated with target primary antibodies

overnight at 4°C and corresponding secondary antibodies for 1 h at RT. For stripping membranes, the membranes were incubated in harsh stripping buffer [1 M Tris-HCl, pH 6.8, 10% (wt/vol) SDS in water] supplemented with 0.8% (vol/vol) ß-mercaptoethanol at 55°C for 30 min, then blocked in 5% non-fat milk blocking buffer for 1 h at RT, followed by the incubation of target primary antibodies overnight at 4°C and corresponding secondary antibodies for 1 h at RT. Finally, protein bands were visualized via ECL chemiluminescent substrate (Bio-Rad) using the Vilber Lourmat Fusion FX chemiluminescence imager (Peqlab Biotechnology).

Following antibodies were used for immunoblot analysis in this study: anti-flotillin-1 (Cell Signaling Technology, #18634), anti-FAK (Y397) (Thermo Fisher Scientific, 44-624G), anti-Src (Y416) (Cell Signaling Technology, #6943), anti-Src (Cell Signaling Technology, #2123), anti-GAPDH (Sigma-Aldrich, G9545) followed by anti-rabbit-HRP (Cell Signaling Technology, #7074). Anti-flotillin-2 (BD Bioscience, 610383) and anti-FAK (Thermo Fisher Scientific, AHO1272) followed by anti-mouse-HRP (Cell Signaling Technology, #7076). Anti-ß1-integrin (R&D Systems, AF1778) followed by donkey anti-goat-HRP (Jackson ImmunoResearch, 705-035-147).

A. 3.8. Immunoprecipitation

For immunoprecipitations, the Capturem IP & Co-IP kit (Takara, 635721) was used according to the manufacturer's instructions. Briefly, H1299 cells were treated with 50 µg/ml LecB for indicated time points at 37°C and lysed by the provided lysis buffer supplemented with a protease inhibitor cocktail. After the normalization of the protein concentrations based on the BCA assay, an aliquot of the protein lysates was set aside to serve as input protein. The remaining protein lysates were incubated with the target primary antibodies for 1 h at 4°C. The antibody/antigen complex was loaded on equilibrated spin columns. The unbound antibodies were washed away with the provided washing buffer. After that, the complex was eluted in the elution buffer. Input samples and eluate samples were mixed with 5X SDS loading buffer and subjected to SDS-PAGE gel electrophoresis for further analysis.

The following antibodies were used for immunoprecipitation in this study: anti-flotillin-1 (Cell Signaling Technology, #18634), anti-flotillin-2 (Sigma-Aldrich, F1680), anti-ß1-integrin (BioLegend, 303002).

A. 3.9. Pull-down assay

H1299 cells were seeded in a 6-well plate (Sigma-Aldrich) at a density of 3 x 10^5 cells per well at 37°C. Cells were stimulated with 50 µg/ml LecB-Biotin for indicated time points and lysed with a lysis buffer [25 mM Tris/HCl, 150 mM NaCl, 1 mM EDTA, 1% (wt/vol) NP-40 and 5% (vol/vol) glycerol in water] supplemented with protease (Merck) and phosphatase inhibitors (Merck). After the normalization of the protein concentrations based on the BCA assay, an aliquot of the protein lysates was set aside to serve as input protein. Input proteins were denatured with 5X SDS loading buffer and boiled at 95°C for 10 min. The

remaining protein lysates were incubated with magnetic streptavidin beads (Thermo Fisher Scientific) overnight, rotating at 4°C. Subsequently, beads were washed with lysis buffer three times at 4°C. Pulled-down (PD) proteins were eluted with 2X SDS loading buffer and boiled at 95°C for 10 min and subjected to SDS-PAGE gel electrophoresis for further analysis.

A. 3.10. Statistical analysis

All data were obtained from at least three independent experiments and are presented as the means ± standard error of the mean (SEM). Statistical analysis was performed using two-tailed unpaired t-test, one-way or two-way ANOVA, or Kruskal–Wallis test to determine the significance of the data. Tests with a P-value < 0.05 are considered statistically significant and marked by asterisks.

A. 4. Summary of results and discussion

A. 4.1. LecB enhances flotillins-mediated cell adhesion and attenuates cell migration

As an opportunistic pathogen, *P. aeruginosa* is one of the most common pathogens found in infected wounds [186]. It was reported that LecB attenuates epithelial cell migration significantly [5][9] and LecB was involved in cell adhesion which plays an integral role in cell communication and regulation, such as cell migration [57]. In order to assay if LecB is sufficient to promote cell adhesion to a substrate, I first conducted cell adhesion assays with LecB bound via biotin to streptavidin-coated plates. The presence of LecB increased cell adhesion in a time-dependent manner from 1.3- (1 h) to 3.5-fold (24 h) compared with the untreated groups. As L-fucose applied in higher concentrations (43 mM) saturates the carbohydrate-binding pockets of LecB, highly reduced binding of LecB to the cell membrane of MDCK cells [10] and H1299 cells [5] could be detected in former studies. In this study, L-fucose (applied in a concentration of 43 mM) blocked LecB-mediated cell adhesion for indicated time points (Fig. A13.A, Supplementary Fig. 1.A). Flotillins (flotillin-1 and 2) play a role in cell-matrix adhesion during cell spreading [152][187]. To investigate the impact of flotillin-1 in LecB-triggered cell adhesion and cell migration, I used an established stable CRISPR-Cas9 knockout model of *FLOT1* (*ΔFLOT1*) in H1299 cells [185], which was verified by SDS-PAGE and immunoblot analysis (Supplementary Fig. 2.A). I performed cell adhesion assays in *ΔFLOT1* cells, and found that the adhesion of *ΔFLOT1* cells on LecB-coated surfaces only increased significantly after 12 h with a rise from 1.2- to 1.4-fold, in comparison to H1299 control cells for which the LecB-triggered cell adhesion significantly increased after 30 min. The presence of L-fucose dampened the effect of LecB on cell adhesion to approximately the untreated level in *ΔFLOT1* cells (Fig. A13.B, Supplementary Fig. 1.B). Additionally, to figure out the effects of flotillin-2, I used RNA interference (RNAi) technique with flotillin-2 siRNA to silence the expression of flotillin-2 in H1299 control cells (FLOT2 KD cells), which was confirmed by SDS-PAGE and immunoblot analysis (Supplementary Fig. 2.B). From the immunoblot results, I observed more than 95% silencing of flotillin-2 expression in H1299 control cells after RNAi. In the following, I aimed at elucidating the role of flotillin-2 alone and together with flotillin-1 for cell adhesion. The adhesion of FLOT2 KD cells on LecB-coated surfaces only increased significantly after 12 h with a rise from 1.1- to 1.3-fold. The presence of L-fucose suppressed the increased LecB-triggered cell adhesion compared with the untreated groups (Fig. A13.C, Supplementary Fig. 1.C). Upon the depletion of both flotillin-1 and flotillin-2 (*ΔFLOT1*/FLOT2 KD cells), LecB did not further enhance cell adhesion at indicated time points (Fig. 13.D, Supplementary Fig. 1.D). Notably, the number of adherent *ΔFLOT1*/FLOT2 KD cells was significantly lower than the number in H1299 control, *ΔFLOT1*, and FLOT2 KD cells. Since flotillins are required for the formation of functional cell-cell junctions (CCJs) and cell-cell adhesions [131][174]. I speculated that the silencing of both flotillin-1 and flotillin-2 decreased the ability of cell adhesion to the Petri dish, indicating fewer *ΔFLOT1*/FLOT2 KD adherent cells. These findings clearly point to a functional link between the microbial virulence factor LecB and the host cell flotillins in cell adhesion processes.

The dynamic cell adhesion is mediated through molecular binding with the non-covalent interactions between cell surface receptors and their ligands of the ECM. Cell-ECM mechanical interactions can

influence lots of cell behaviors and functions [60]. For example, cells interact mechanically with the ECM by their internal actin-myosin machinery, mediating distant cell communication and essential cellular processes such as cell migration and orientation [188]. Thus, I conducted to mimic the ECM-coated plates to assess the ability of cell adhesion for the treatment of LecB. I coated the glass bottom of Petri dishes with fibronectin overnight, then blocked the surface with TBST blocking buffer, followed by an incubation either with or without 50 µg/ml LecB at 37°C for 1 h. After that, the AFM cantilever with a single, immobilized H1299 cell was slowly approach to the coated surfaces (i.e. fibronectin-only or fibronectin plus LecB), and force-distance curves with contact times of 0 s and 5 s, respectively, were recorded by SCFS. The maximum downward force exerted on the cantilever of the AFM is referred to as F_d [73], which was depicted as the strength of cell-fibronectin or cell-LecB-fibronectin binding in our study. For a contact time of 0 s, the average F_d value for fibronectin-coated surfaces (23.8±19.3 pN) was significantly lower than for fibronectin plus LecB-coated surfaces (224.1±174.5 pN) (Supplementary Fig. 3.A). Extending the contact time to 5 s, it depicted that the average F_d value for fibronectin-coated surfaces (53.8±18.2 pN) was significantly smaller than for fibronectin plus LecB-coated surfaces (419.6±211.6 pN) (Supplementary Fig. 3.A). Our data provided an additional shred of evidence that LecB incubation significantly increased the interaction forces with cells by binding to fibronectin for a contact time of 0 s and 5 s, respectively. It suggested that LecB increased fibronectin-dependent cell adhesion ability in H1299 cells. By analyzing typical retraction curves in untreated and LecB groups, I found that the majority of rupture events (or unbound events) occured in LecB groups (Supplementary Fig. 3.A). More incidences of adhesion on the LecB-fibronectin complexes at the cell membrane were detected, indicating the higher affinity when LecB was bound to fibronectin. Besides, I performed cell adhesion assay via fibronectin-coated plates with H1299 control and *ΔFLOT1* cells, and histograms showed similar trends compared with that in LecB-Biotin-streptavidin-coated surfaces. The adhesion of H1299 control cells on fibronectin-coated surfaces constantly increased after LecB treatment (Supplementary Fig. 3.B), compared with *ΔFLOT1* cells for which LecB only significantly increased cell adhesion forces on fibronectin-coated surfaces after 12 h (Supplementary Fig. 3.C). Nevertheless, L-fucose inhibited the rise of fibronectin-dependent cell adhesion mediated by LecB in H1299 control and *ΔFLOT1* cells.

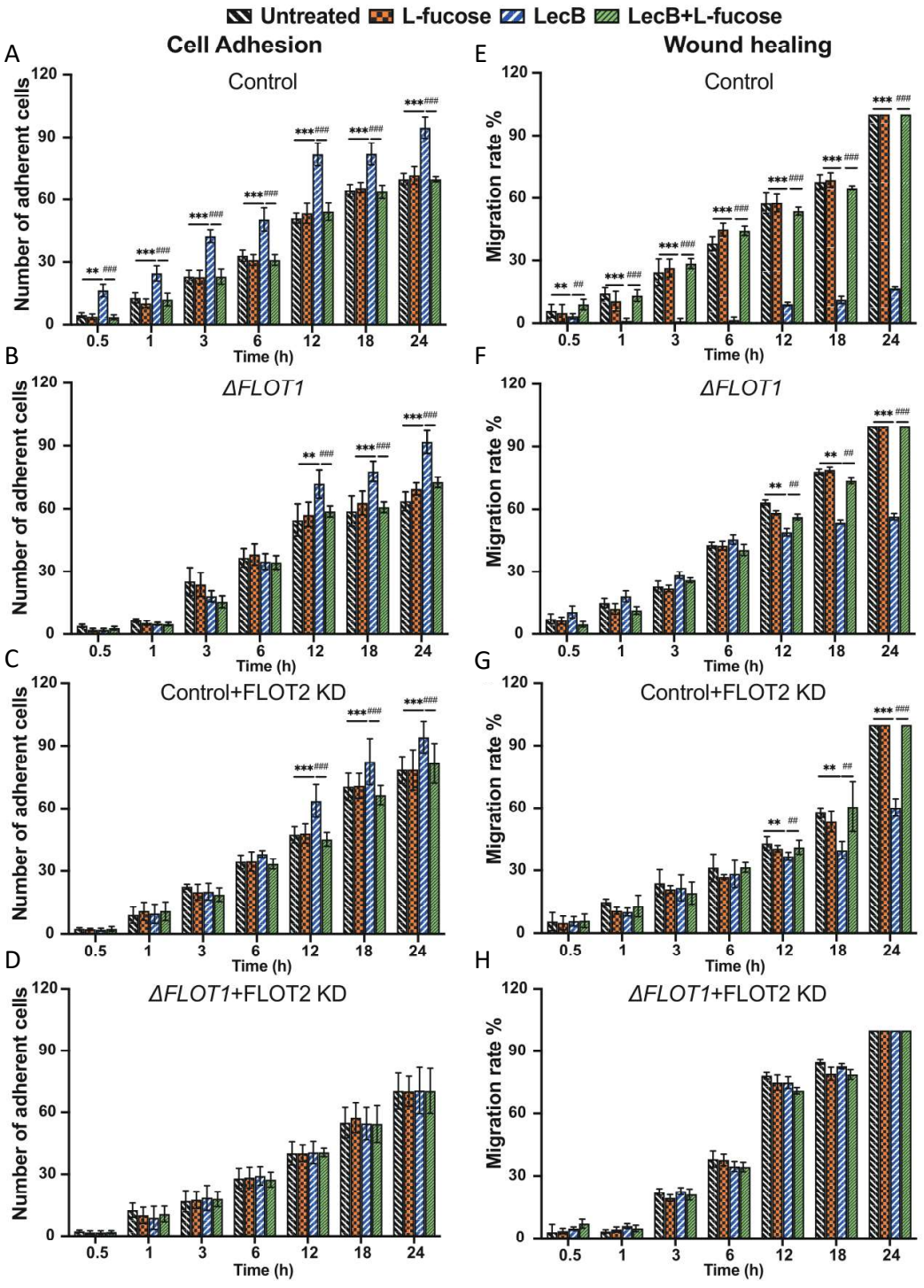

Fig. A13: LecB enhances cell adhesion and attenuates wound healing influenced by flotillins.

(A) H1299 control cells, (B) *ΔFLOT1* cells, (C) FLOT2 KD cells, and (D) *ΔFLOT1*/FLOT2 KD cells were seeded in 12-well plates which were coated with streptavidin and LecB-Biotin sandwich with or without L-fucose or only streptavidin (Untreated). Cells were stained at 0.5, 1, 3, 6, 12, 18 and 24 h with Cell Mask deep red plasma membrane stain (red)

and counted via ImageJ. Error bars indicate means ± SEM of N = 5 biological replicates. **p < 0.01 vs Untreated, ***p < 0.001 vs Untreated (two-way ANOVA). ###p < 0.001 vs LecB groups (two-way ANOVA). (E) H1299 control cells, (F) *ΔFLOT1* cells, (G) FLOT2 KD cells, and (H) *ΔFLOT1*/FLOT2 KD cells were grown to 100% confluent in 6-well plates, scratched by a pipette tip, and stimulated LecB with or without L-fucose as indicated. Distances between the cell fronts were acquired after 0.5, 1, 3, 6, 12, 18 and 24 h. Error bars indicate means ± SEM of N = 5 biological replicates. **p < 0.01 vs Untreated, ***p < 0.001 vs Untreated (two-way ANOVA). ##p < 0.01 vs LecB groups, ###p < 0.001 vs LecB groups (two-way ANOVA).

To investigate the migratory activity of cells, I performed scratch wound healing assays. The cell monolayers were scratched with a 200 µl pipette tip to create a wound either with or without the treatment of 50 µg/ml LecB and the presence of 43 mM L-fucose. LecB stimulation inhibited the wound healing process with a significant rise from 1.8- to 25.8-fold decrease compared with untreated groups from 0.5 h to 3 h, however, the presence of L-fucose neutralized to untreated level in H1299 cells. For longer stimulation periods from 6 h to 24 h, LecB stimulation significantly blocked the process of cell migration from 25.3- to 6.0-fold (Fig. 13.E, Supplementary Fig. 4.A). To investigate the impact of flotillins on LecB-mediated cell migration, I also performed scratch wound healing assays with *ΔFLOT1* cells, FLOT2 KD cells, and *ΔFLOT1*/FLOT2 KD cells. With the silencing of flotillin-1 and flotillin-2 alone in the cells, the collective cell migration and wound healing was dampened after 12 h LecB treatment. LecB significantly inhibited the *ΔFLOT1* cells migratory rate by 32% and 44% after 18 and 24 h, respectively (Fig. A13.F, Supplementary Fig. 4.B), and decreased the FLOT2 KD cells migratory rate from around 18% to 40% at 18 h and 24 h, respectively (Fig. A13.G, Supplementary Fig. 4.C). It indicated that the silencing of flotillin-1 and flotillin-2 alone postponed the wound healing process, which was blocked by LecB in H1299 control cells. Adding L-fucose restored flotillin-mediated cell migration induced by LecB. Notably, there was no blockage of cell migration for the condition of LecB in *ΔFLOT1*/FLOT2 KD cells (Fig. A13.H, Supplementary Fig. 4.D), suggesting that the silencing of both flotillin-1 and flotillin-2 suppressed the blockage of LecB on wound healing.

In summary, LecB had the ability to enhance cell adhesion and attenuate cell migration, which was neutralized by L-fucose in H1299 control cells. Meanwhile, LecB had less capability to increase cell adhesion and decrease cell migration with the situation of silencing of flotillin-1 or flotillin-2 alone expression in the cells. Nevertheless, LecB could not mediate the cell adhesion and cell migration with the silencing of both flotillin-1 and flotillin-2.

A. 4.2. LecB colocalizes and co-precipitates with flotillin-1 and flotillin-2 and is involved in the cellular trafficking pathway

Since the absence of host flotillins somehow dampens the effects of the bacterial lectin LecB, I were curious about if and where LecB and flotillins could interact. First, we investigated by immunofluorescence whether LecB colocalizes with flotillin-1 and/or flotillin-2. H1299 control cells were incubated with LecB-

A488 for indicated time points, fixed and stained with antibodies towards flotillin-1 or flotillin-2. The immunofluorescence results demonstrated that the recruitment of flotillin-1 and flotillin-2 to the plasma membrane and cytoplasm was mediated by LecB in a time-dependent manner (white asterisks in Fig. 14.A, B). The fluorescence signals overlapped between flotillin-1 and LecB at the plasma membrane at 1 h, with the Manders' colocalization coefficient (M1=0.090±0.040) (Fig. A14.C, Supplementary Fig. 5.A). After that, I found that LecB was observed in puncta-like structures that colocalized with the signal of flotillin-1 in perinuclear regions at 3 h of stimulation with the Manders' colocalization coefficient (M1=0.317±0.022) (Fig. A14.A, C). During longer stimulation periods, the Manders' colocalization coefficient (M1) between LecB and flotillin-1 increased from 0.394±0.012 (12 h) to 0.464±0.014 (24 h) (Fig. A14.C). For the recruitment of flotillin-2, flotillin-2 was detected almost exclusively in the perinuclear region in the untreated cells but re-localized to the plasma membrane upon LecB treatment at 1 h, with the Manders' colocalization coefficient (M1=0.102±0.004) (Supplementary Fig. 5.B). Then, LecB was observed in punctuated structures that colocalized with flotillin-2 in perinuclear areas at 3 h, with the Manders' colocalization coefficient (M1=0.105±0.005) (Fig. A14.B, C). For the longer stimulation periods, the Manders' colocalization coefficient (M1) between LecB and flotillin-2 increased from 0.344±0.013 (12 h) to 0.457±0.017 (24 h) (Fig. A14.C). Besides, I performed immunoprecipitation of LecB to assess potential interactions between LecB and flotillins. The normalized protein lysates were incubated with flotillin-1 or flotillin-2 antibodies on ice for 1 h, and the unbound antibodies were washed away. The protein lysate/antibody complexes were loaded to the spin column for further SDS-PAGE and immunoblot analysis. On the one hand, in a time-course immunoprecipitation assay, I found an increase of the co-precipitated levels of flotillin-1 and flotillin-2 in the eluted fractions with LecB (Fig. A15.A, B), which indicated that LecB interacted with both flotillin-1 and flotillin-2 in H1299 control cells. On the other hand, I screened for potential LecB-interacting proteins via a pull-down assay in control cells. Lectin-bound membrane fragments were isolated using streptavidin beads together with biotinylated LecB and were assessed by SDS-PAGE and immunoblot analysis. I detected the recruitments of flotillin-1 and flotillin-2 in the eluted fractions, suggesting that LecB interacted with flotillin-1 and flotillin-2 (Fig. A15.C).

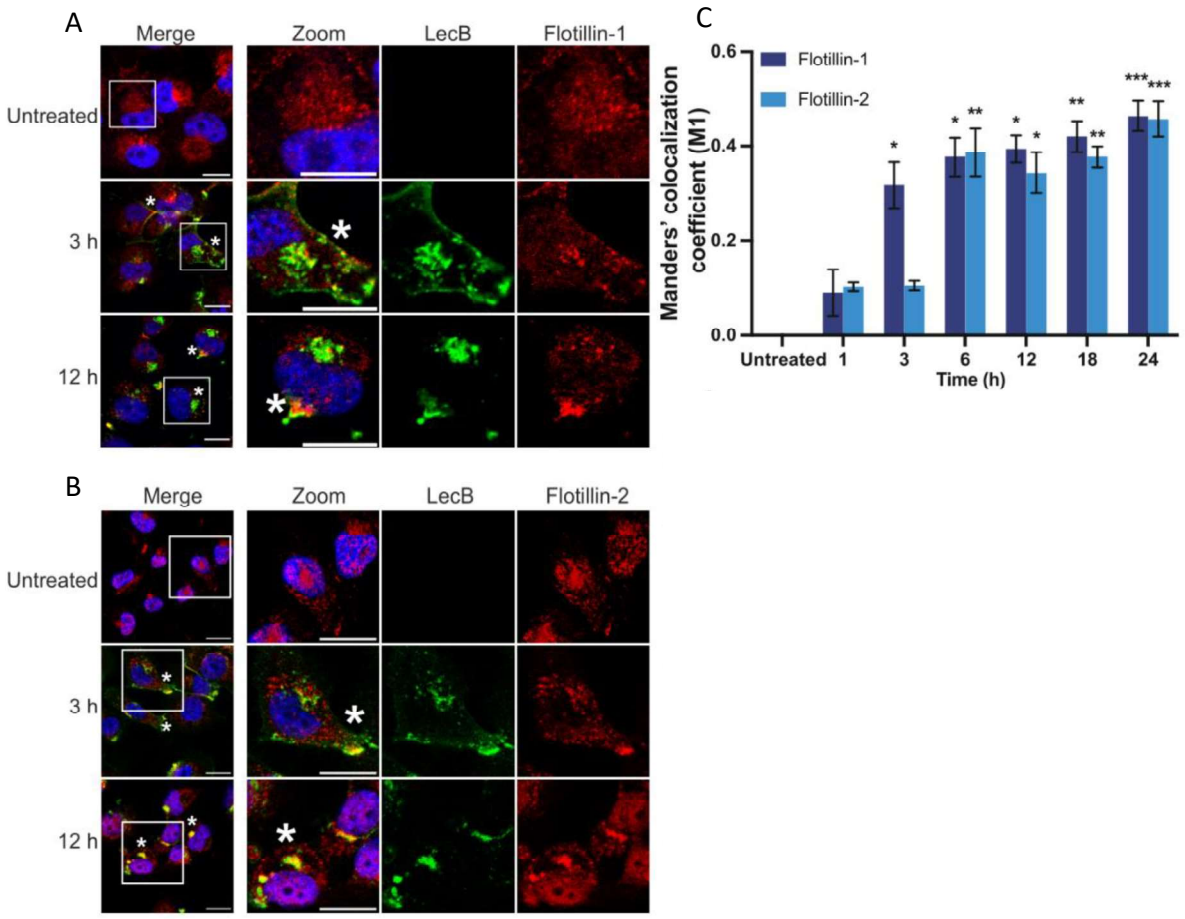

Fig. A14: Flotillins are recruited to the plasma membrane with LecB treatment.

(A) H1299 control cells were treated with LecB-A488 (green) as indicated and analyzed by a confocal fluorescence microscope with immunostaining for flotillin-1 (red) and counterstained for DNA (DAPI, blue). White asterisks pointed at colocalizations. Scale bar, 20 µm. (B) H1299 control cells were treated with LecB-A488 (green) as indicated and analyzed by a confocal fluorescence microscope with immunostaining for flotillin-2 (red) and counterstaining for DNA (DAPI, blue). White asterisks pointed at colocalizations. Scale bar, 20 µm. (C) Manders' colocalization coefficient (M1) quantified between the fluorescence signals of LecB and flotillin-1 were statistically compared to untreated groups. Error bars indicate means ± SEM of N = 3 biological replicates. *$p < 0.05$ vs Untreated, **$p < 0.01$ vs Untreated, ***$p < 0.001$ vs Untreated (Kruskal–Wallis test).

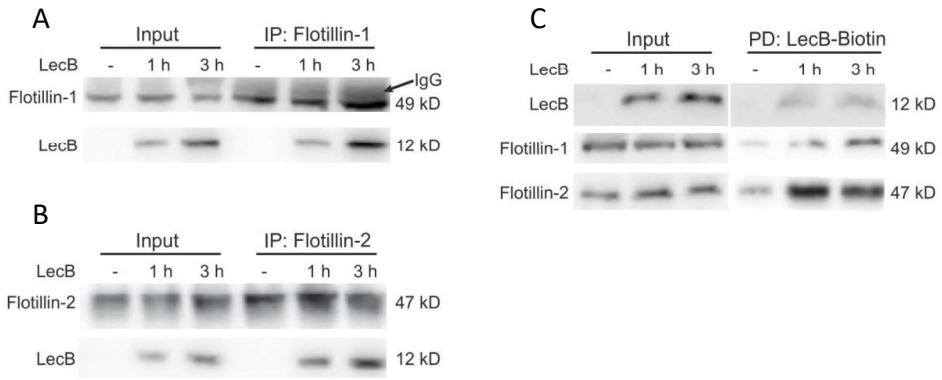

Fig. A15: Flotillins can interact with LecB.

(A) H1299 control cells were stimulated as indicated, and immunoprecipitation of flotillin-1 co-precipitated LecB after 1 h and 3 h stimulation. (B) Immunoprecipitation of flotillin-2 co-precipitated LecB after 1 h and 3 h stimulation. (C) Pull-down assay verified that flotillins interacted with LecB.

Intracellular trafficking plays a vital role in the delivery of proteins in various eukaryotic cells [189]. From the literature, the intracellular trafficking of LecB has for so long been ill defined, but the trafficking of other lectins has been revealed. For example, endogenous lectin, galectin-3, is a β-galactoside binding lectin that mediates many physiological functions, including the binding of cells to the ECM for which the glycoprotein α5β1-integrin [190], and the intracellular trafficking pathways between the plasma membrane and endosomal organelles [191]. It was reported that galectin-3 was sorted into the EE. Consequently, galectin-3 converged with newly synthesized cargo from the trans-Golgi network (TGN) in EE to the RE [191]. Therefore, I hypothesized that LecB could be trafficked to different endocytic compartments in the cells, like galectin-3. To uncover the trafficking pathway of LecB, I focused on the different endocytic compartments, such as EE marker EEA1, LE marker Rab9, RE marker Rab11 and lysosome marker LAMP1 via immunofluorescence assay. H1299 cells were incubated with LecB-A488 for indicated time points. To determine the intracellular trafficking of LecB, the fixed cell were stained for EEA1, Rab9, Rab11, and LAMP1, respectively. The EE is the initial destination for protein internalized from the plasma membrane [191]. Here, LecB was observed in puncta-like structures that colocalized with the signal of EEA1 in a time-dependent manner (Supplementary Fig. 6.A) with the Manders' colocalization coefficient (M1) between 0.100±0.005 and 0.510±0.026 from 3 h to 24 h stimulation, respectively (Fig. A16). Then, the EE compartment is a major cellular sorting station from which cargo molecules can either be trafficked to the LE [192]. The co-localizations between LecB and Rab9 were observed in perinuclear regions after 6 h stimulation (Supplementary Fig. 6.A). However, the Manders' colocalization coefficient (M1) between LecB and Rab9 was at the peak with the value of 0.437±0.023 at 18 h, which was lower than the Manders' colocalization coefficient (M1) of LecB and EEA1 (Fig. A16). After that, the LE travels to the lysosome for degradation or is transported to the RE for recycling to the plasma membrane [192]. On the one hand, the fluorescence signal of LecB and LAMP1, which was represented by Manders'

colocalization coefficient (M1), overlapped predominantly in perinuclear regions from 0.197±0.020 (6 h) to 0.213±0.015 (24 h) (Fig. A16, Supplementary Fig. 6.C), with a maximum Manders' colocalization coefficient (M1=0.280±0.020) at 12 h (Fig. A16). On the other hand, in addition to the trafficking of lysosome, LecB revealed considerable co-staining on Rab11 after 3 h stimulation (Supplementary Fig. 6.D), with a maximum Manders' colocalization coefficient (M1=0.434±0.013) at 6 h (Fig. A16). Interestingly, the values calculated for the Manders' colocalization coefficient (M1) of LecB with Rab9, LAMP1, and Rab11 were lower than that for LecB with EEA1. Especially, the decreasing colocalizations of LecB with Rab9 and LAMP1 were reported after 12 h treatment of LecB. While the colocalizations of LecB with EEA1 went up continually with the treatment of LecB, which indicated that degradation of LecB was later than the accumulation of LecB with EE, the majority of cargo occurred in EEA1-positive EE and was recycled back to the plasma membrane partly. Based on our results, we clearly observed that LecB bound on the cell membrane at 1 h and 3 h of stimulation, then LecB was endocytosed to cytoplasmic and perinuclear regions after 6 h stimulation.

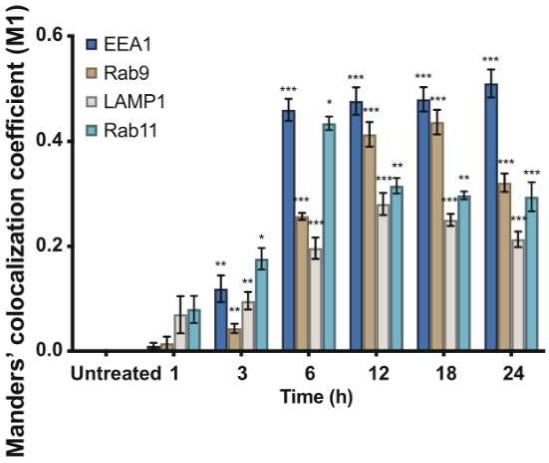

Fig. A16: The Manders' colocalization coefficient (M1) between LecB and endosome markers.

Manders' colocalization coefficient (M1) quantified between the fluorescence signals of LecB with different endosome markers were statistically compared to untreated groups. Error bars indicate means ± SEM of N = 3 biological replicates. *p < 0.05 vs Untreated, **p < 0.01 vs Untreated, ***p < 0.001 vs Untreated (two-tailed unpaired t-test).

In summary, flotillins were recruited to the plasma membrane in the course of LecB stimulation. Flotillin-1 and flotillin-2 colocalized with LecB in H1299 cells. In the time-course of LecB stimulation, LecB was transported to EE, LE, lysosomes and RE, and the trafficking pathway of LecB was interfered by the expression of flotillins in the cells.

A. 4.3. Flotillin-1 co-precipitates with ß1-integrin and attenuates the internalization and expression of ß1-integrin in the cells

Integrins are a family of transmembrane molecules which constitute the principal cell adhesion receptors for the ECM [82], and the establishment of solid cell adhesion inhibits cell migration [193]. From our previous results, LecB interacted directly with the carbohydrate of ß1-integrin, verified by lectin blot assay, and caused its internalization, which had a potential role in the blockage in cell migration in MDCK cells [10]. A supposition arose if there is a link between flotillins and ß1-integrin, since it was demonstrated that LecB interacted with both, flotillins and ß1-integrin.

To elucidate potential interactions between flotillins and ß1-integrin already before or as a result of LecB treatment, I first verified if LecB interacts with ß1-integrin in H1299 cells. I performed an immunoprecipitation assay, the normalized protein lysates were incubated with ß1-integrin antibodies, and the unbound antibodies were washed away. The protein lysate/antibody complexes were loaded to the spin column for further SDS-PAGE gel electrophoresis and immunoblot analysis. The result demonstrated that ß1-integrin could be detected with LecB in the eluates of the corresponding immunoprecipitation of LecB-treated H1299 cell lysates (Fig. A17.A). Interestingly, I also noticed a decrease in co-precipitated ß1-integrin, while an increase in co-precipitated LecB from 1 h to 3 h in comparison with the untreated condition (Fig. A17.A). In addition, I investigated the interactions between flotillins and ß1-integrin via immunoprecipitation assay, the normalized protein lysates were incubated with flotillin-1 antibodies. The results confirmed that flotillin-1 and ß1-integrin could be detected together in the corresponding eluates of the immunoprecipitation as a result of LecB treatment (Fig. A17.B), but not flotillin-2 and ß1-integrin (Supplementary Fig. 7.A). In detail, I observed a faint band of co-precipitated flotillin-1 and a strong band of co-precipitated ß1-integrin in the untreated condition, suggesting that flotillin-1 slightly interacted with ß1-integrin without LecB treatment (Fig. A17.B). To the contrary, a much stronger band of co-precipitated flotillin-1 was shown upon LecB stimulation at 1 h compared with the untreated conditions, and a strong band of co-precipitated ß1-integrin was observed upon LecB treatment at 1 h as well (Fig. A17.B). Furthermore, the co-precipitated ß1-integrin at 3 h decreased compared with the untreated conditions (Fig. A17.B). It indicated that LecB promoted the interaction between ß1-integrin and flotillin-1 at 1 h stimulation, while the interaction started dissociating at 3 h stimulation. Thus, I focused more on the interaction between ß1-integrin and flotillin-1 afterwards. I further investigated the colocalization between flotillin-1 and ß1-integrin via immunofluorescence assay, where I stained H1299 control cells with antibodies directed towards ß1-integrin and flotillin-1, respectively. From the results, I found a time-dependent colocalization between flotillin-1 and ß1-integrin for the condition of LecB in cells (colocalization marked by white asterisks in Fig. A17.C, Supplementary Fig. 7.B). From 1 h to 3 h incubation of LecB, ß1-integrin and flotillin-1 partially colocalized at the cell membrane, and other parts of the colocalizations were nearby the nuclei in puncta-like structures. From 6 h to 24 h incubation of LecB, the colocalizations between ß1-integrin and flotillin-1 concentrated only in perinuclear regions (A17.C, Supplementary Fig. 7.B). I quantified the Manders' colocalization coefficient (M1) of flotillin-1 and ß1-integrin with or without LecB treatment of H1299 cells via Image J, the histogram depicted that the

Manders' colocalization coefficient (M1) increased by 1.3- to 1.7-fold from 1 h to 24 h stimulation of LecB (A17.D).

Next, to uncover if flotillins influence ß1-integrin internalization triggered by LecB treatment, I incubated H1299 control cells, *ΔFLOT1* cells, FLOT2 KD cells, and *ΔFLOT1*/FLOT2 KD cells with LecB in a time-course. The fixed cells were stained for ß1-integrin. Immunofluorescence results showed that ß1-integrin started to concentrate in perinuclear regions already after 1 h LecB treatment, and more than 90% of internalized ß1-integrin were observed nearby nuclei from 6 h to 24 h LecB treatment in H1299 control cells (Fig. A18.A). Similarly, in *ΔFLOT1* and FLOT2 KD cells, the fluorescence signal of ß1-integrin was also in vesicular structures and perinuclear regions after 6 h of LecB treatment (Fig. A18.B, Supplementary Fig. 7.C). Strikingly, in *ΔFLOT1*/FLOT2 KD cells, the majority of the fluorescence signal of ß1-integrin was detected at the cell membrane, while the minority of ß1-integrin was internalized into the cytoplasm from 1 h to 24 h LecB incubation compared with the untreated conditions (Supplementary Fig. 7.D). Moreover, I used SDS-PAGE gel electrophoresis and immunoblot analysis to detect the expression of ß1-integrin in H1299 control and *ΔFLOT1* cells. The results demonstrated that the expression of ß1-integrin increased around 1.3- to 1.7-fold from 1 h to 6 h of incubation with LecB, but decreased by 1.2- to 2.0-fold from 12 h to 24 h LecB treatment compared with untreated conditions in H1299 control cells (Fig. A18.C). In comparison, the expression of ß1-integrin raised around 1.1- (6 h) to 2.1-fold (24 h) in *ΔFLOT1* cells (Fig. A18.D). This indicated that the expression and internalization of ß1-integrin were affected by flotillins, especially by flotillin-1 triggered by LecB incubation.

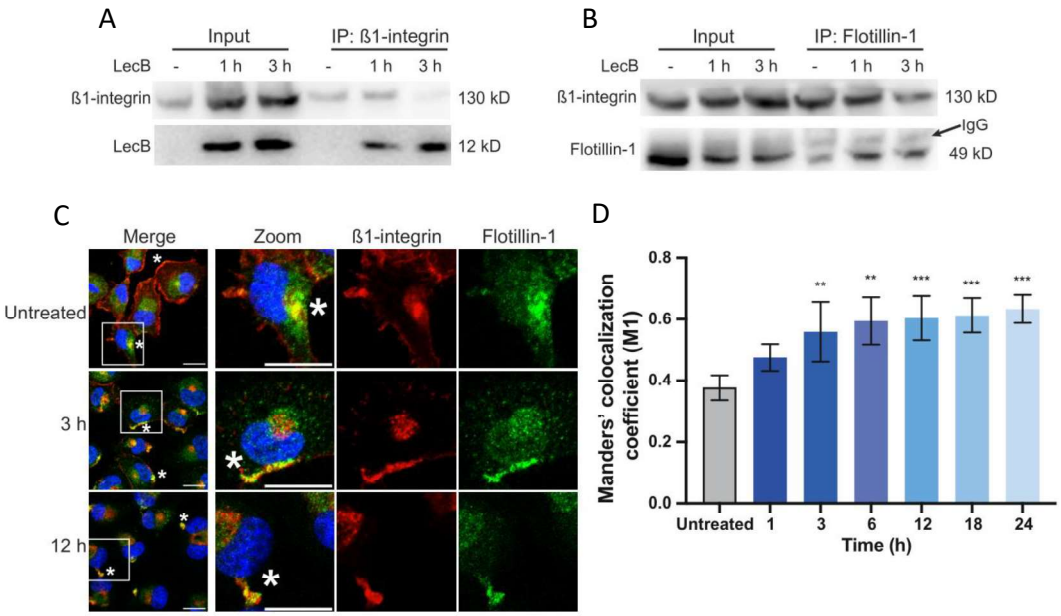

Fig. A17: Flotillin-1 can interact with ß1-integrin induced by LecB.

(A) H1299 control cells were stimulated as indicated, and immunoprecipitation of ß1-integrin co-precipitated LecB after 1 h and 3 h stimulation. (B) H1299 control cells were stimulated as indicated, and immunoprecipitation of ß1-integrin co-precipitated with flotillin-1, after 1 h and 3 h LecB stimulation. (C) H1299 control cells were treated with LecB as indicated and analyzed by a confocal fluorescence microscope with immunostaining for ß1-integrin (red), flotillin-1 (green), and counterstained for DNA (DAPI, blue). White asterisks pointed at colocalizations. Scale bar, 20 µm. (D) Manders' colocalization coefficient (M1) quantified between the fluorescence signals of flotillin-1 and ß1-integrin were statistically compared to untreated groups. Error bars indicate means ± SEM of N = 3 biological replicates. *p < 0.05 vs Untreated, **p < 0.01 vs Untreated, ***p < 0.001 vs Untreated (one-way ANOVA).

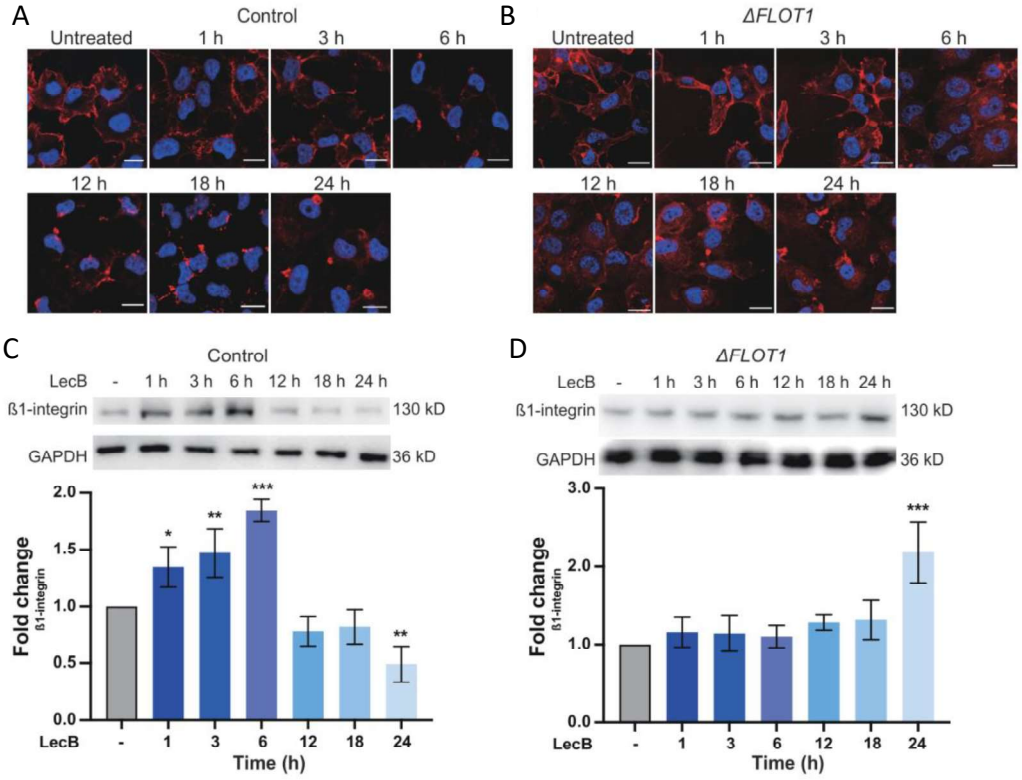

Fig. A18: Flotillin-1 interferes the expression of ß1-integrin induced by LecB.

(A) H1299 control cells and (B) *ΔFLOT1* cells were treated with LecB as indicated and analyzed by a confocal fluorescence microscope with immunostaining for ß1-integrin (red), and counterstained for DNA (DAPI, blue). Scale bar, 20 µm. (C) H1299 control cells and (D) *ΔFLOT1* cells were treated with LecB as indicated and ß1-integrin protein level was expressed by SDS-PAGE and immunoblot analysis. Histograms depict ß1-integrin protein level. Error bars indicate means ± SEM of N = 3 biological replicates. **p < 0.01 vs Untreated, ***p < 0.001 vs Untreated (one-way ANOVA).

Taken together, ß1-integrin interacted with flotillin-1 but not with flotillin-2 in H1299 cells. LecB triggered the cellular internalization of ß1-integrin in the cells, while host cell flotillins attenuated the internalization and expression of ß1-integrin with LecB treatment.

A. 4.4. Flotillin-1 mediates FAK signaling induced by LecB

Cell adhesion and cell migration suggest cytoskeletal remodeling, which is led by the crosstalk between FAK and Wnt/ß-catenin signaling pathway [127]. Flotillin-deficient A431 cells migrated faster in a wound healing assay. In addition, increased membrane motility in flotillin-deficient Hela cells correlated with high FAK expression [151]. Thus, I sought to characterize the flotillin-1 and FAK/ß-catenin expression axis induced by LecB.

First, to determine the interaction between flotillins and FAK, I utilized immunoprecipitation assays. The normalized protein lysates were incubated with flotillin-1 and flotillin-2 antibodies individually, the unbound antibodies were washed away. The results confirmed a time-dependent recruitment of FAK to flotillin-1 in H1299 cells, which is only induced by LecB treatment (Fig. A19.A), but not flotillin-2 and FAK could be detected together in the corresponding eluates of the immunoprecipitation as a result of LecB treatment (Supplementary Fig. 8.A). This indicated that FAK interacted with flotillin-1 in a LecB-dependent manner. Meanwhile, I observed an IgG heavy chain band in the immunoprecipitation elutes (Fig. A19.A), slightly higher than the flotillin-1 band. According to the literature, the higher band was an unspecific band. It pointed towards IgG heavy chain around 50-55 kDa from the protein A sepharose incubated in anti-flotillin-1 in the absence of the eluted samples [194]. Integrin-mediated cell adhesion leads to the phosphorylation of FAK Y397 (pFAK), which serves as the major site of autophosphorylation, creating a binding site for Src kinase [121]. This active FAK-Src complex facilitated Rac activation, lamellipodia formation and cell migration in polarized cells [101]. Thus, I detected the level of pFAK in H1299 control and *ΔFLOT1* cells after LecB treatment via SDS-PAGE gel electrophoresis and immunoblot assay. From the analysis, I monitored a nearly 1.3-fold increase of pFAK from 1 h to 6 h LecB treatment and a decrease from 2.3-fold to 2.9-fold from 18 h to 24 h compared with the untreated conditions respectively, in H1299 control cells (Fig. A19.B). The amounts of pFAK did not change before 12 h LecB treatment, while significantly increased by 2.4-fold at 24 h LecB treatment in *ΔFLOT1* cells (Fig. A19.C). Moreover, I also observed the phosphorylation of Src at Y416 (pSrc) in H1299 control and *ΔFLOT1* cells, respectively. The results indicated that a burst from 1.4-fold to 1.7-fold from 1 h to 6 h of LecB stimulation in H1299 control cells, while a strong rise of approximately 1.8-fold from 18 h to 24 h in *ΔFLOT1* cells (Supplementary Fig. 8.B, C). FAK promotes normal and cancer cell migration by regulating focal adhesion formation and turnover through multiple signaling connections [113]. Thus, I further investigated in detail the distribution of FAK and pFAK in H1299 control and *ΔFLOT1* cells via immunofluorescence assay. H1299 cells were treated with LecB for indicated time points, fixed and stained with antibodies towards pFAK and FAK, and with phalloidin to stain F-actin in the cells. White boxes point to the cell periphery, where FAs are mostly located . From the insets, the puncta of FAK and pFAK were typically localized at the leading

edges, such as lamellipodia and filopodia in the untreated control cells (examples are indicated by white asterisks in Fig. 6d). In H1299 control cells, the FAK and pFAK staining rather concentrated in the cytoplasm and less at the leading edges at different time points from 1 h to 24 h LecB stimulation compared with untreated conditions (white asterisks in Fig. A19.D, Supplementary Fig. 8.D). Regarding F-actin, the formation of stress fibers was observed in the untreated groups in H1299 control cells, which contrasted with redistribution and dissociation of F-actin for the LecB-treated conditions after 12 h of LecB stimulation (Fig. A19.D, Supplementary Fig. 8.D). Strikingly, there were more protrusions of FAK and pFAK at the front of lamellipodia and filopodia *ΔFLOT1* cells in the untreated and 1 h to 6 h LecB-treated conditions, and the puncta of FAK and pFAK localized in the cytoplasm in the untreated and LecB-treated conditions (white asterisks in Fig. A19.E, Supplementary Fig. 8.E). Moreover, I counted the number of FAs, which showed a significant drop from 2.2- (1 h) to 116.6-fold (24 h) and a slighter decrease from 1.3- (1 h) to 6.4-fold (24 h) in H1299 control and *ΔFLOT1* cells, respectively (Fig. A19.D, E), suggesting that flotillin-1 mediated the number of FAs with the treatment of LecB.

To sum up, FAK interacted with flotillin-1, but not with flotillin-2 in H1299 cells. LecB induced the phosphorylation of FAK at Y397 and Src at Y416, and distributed the location of FAs. Furthermore, flotillin-1 mediated FAK-Src complex expression and the distribution of FAs induced by LecB in the cells.

A. 4.5. LecB induces flotillins-dependent nuclear translocation of ß-catenin

ß-catenin is localized in several intracellular pools, which indicates different functions. For instance, the membrane-bound pool of ß-catenin is involved in intercellular adhesion, whereas the cytoplasmic and nuclear pool of ß-catenin is a central component of the Wnt pathway [195]. The FAK-triggered ß-catenin signaling pathway through the nuclear translocation of ß-catenin and transcriptional activation of ß-catenin target gene *in vivo*, such as c-Myc [126]. Our results identified that flotillin-1 interacted with FAK and changed the expression and distribution of pFAK and FAK with the treatment of LecB. Thus, I speculated that flotillin-1 probably mediates the translocation of ß-catenin activated by LecB-induced phosphorylation of FAK.

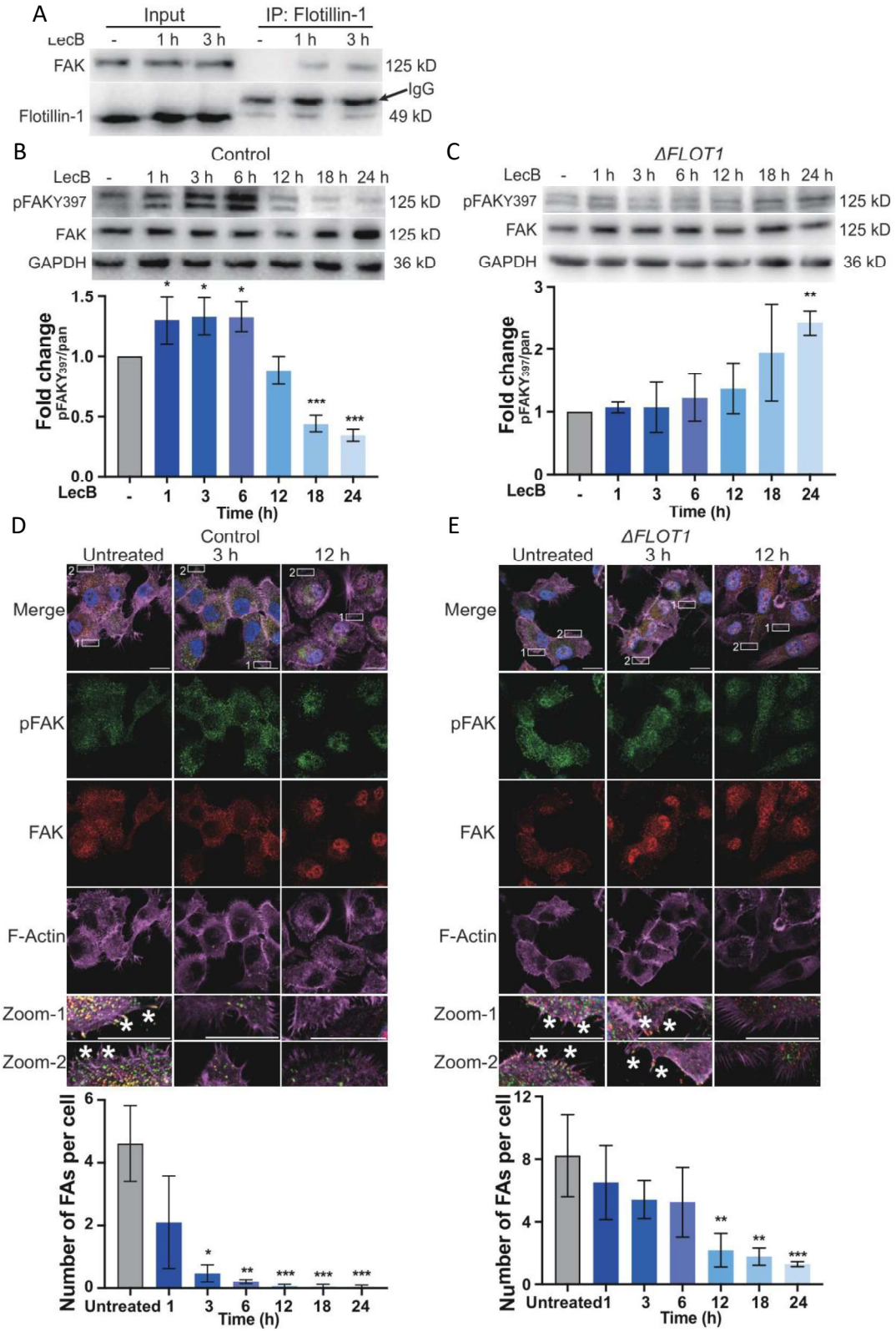

Fig. A19: Flotillin-1 triggers FAK signaling induced by LecB.

(A) H1299 control cells were stimulated as indicated, and immunoprecipitation of FAK co-precipitated with flotillin-1, after 1 h and 3 h LecB stimulation. (B) H1299 control cells and (C) *ΔFLOT1* cells were treated with LecB as indicated and FAK Y397 and FAK protein level was expressed by SDS-PAGE and immunoblot analysis. Histograms depict FAK Y397 protein level in H1299 control and *ΔFLOT1* cells, respectively. Error bars indicate means ± SEM of N = 3 biological replicates. **p < 0.01 vs Untreated, ***p < 0.001 vs Untreated (one-way ANOVA). (D) H1299 control cells and (E) *ΔFLOT1* cells were treated with LecB as indicated and analyzed by a confocal fluorescence microscope with immunostaining for FAK Y397 (green), FAK (red), F-actin (magenta) and counterstained for DNA (DAPI, blue). White boxes show the cell periphery of FAs, and white asterisks point at FAs which are counted for analysis. Histograms depict the number of FAs per cell. Error bars indicate means ± SEM of N ≥ 50 cells. *p < 0.05 vs Untreated, **p < 0.01 vs Untreated, ***p < 0.001 vs Untreated (one-way ANOVA). Scale bar, 20 µm.

To investigate if LecB has an impact on the membrane-bound pool of ß-catenin, I used the immunofluorescence technique for staining cells with a ß-catenin antibody to observe the localization of ß-catenin in LecB-treated cells. The results confirmed a reduction of ß-catenin fluorescence at the cell membrane in a time-dependent manner, and a significant accumulation of ß-catenin in nuclei from 3 h to 24 h LecB treatment in H1299 control cells (Fig. A20.A). It indicated that ß-catenin was located from the plasma membrane to nuclei, especially after 3 h stimulation there was less signal of ß-catenin at the plasma membrane compared with the untreated groups. I also quantified the fluorescence intensity of nuclear ß-catenin, the histogram depicted a significant increase from 1.5- (1 h) to 2.6-fold (24 h) with the treatment of LecB. Besides, the presence of 43 mM L-fucose blocked the accumulated intensity of nuclear ß-catenin at 24 h of LecB stimulation in H1299 control cells, while incubation with L-fucose alone did not influence the membrane-bound pool of ß-catenin (Fig. A20.A, Supplementary Fig. 9). To understand the effect of flotillins on the LecB-induced nuclear translocation of ß-catenin, I stained with an antibody towards ß-catenin in *ΔFLOT1* cells, FLOT2 KD cells, and *ΔFLOT1*/FLOT2 KD cells. I monitored a reduction of ß-catenin at the plasma membrane of *ΔFLOT1* cells, and an accumulation of ß-catenin in the perinuclear regions but not in the nuclei from 1 h to 24 h stimulation of LecB. Meanwhile, the perinuclear areas of ß-catenin were normalized to the untreated level (i.e. without LecB) in presence of L-fucose (Fig. A20.B). The distribution of ß-catenin in FLOT2 KD cells was similar to that of *ΔFLOT1* cells, where more signals of ß-catenin were located in the cytoplasm compared to less accumulation of ß-catenin in the nuclei (Fig. A20.C). In addition, LecB stimulation did not change the nuclear translocation of ß-catenin in *ΔFLOT1*/FLOT2 KD cells, where less fluorescent ß-catenin was accumulated in the nuclei in the untreated and LecB-treated groups (Fig. A20.D).

In summary, LecB induced the nuclear translocation of ß-catenin, which was blocked by L-fucose. Moreover, the silencing of flotillins interrupted the accumulation of ß-catenin in LecB-treated cells.

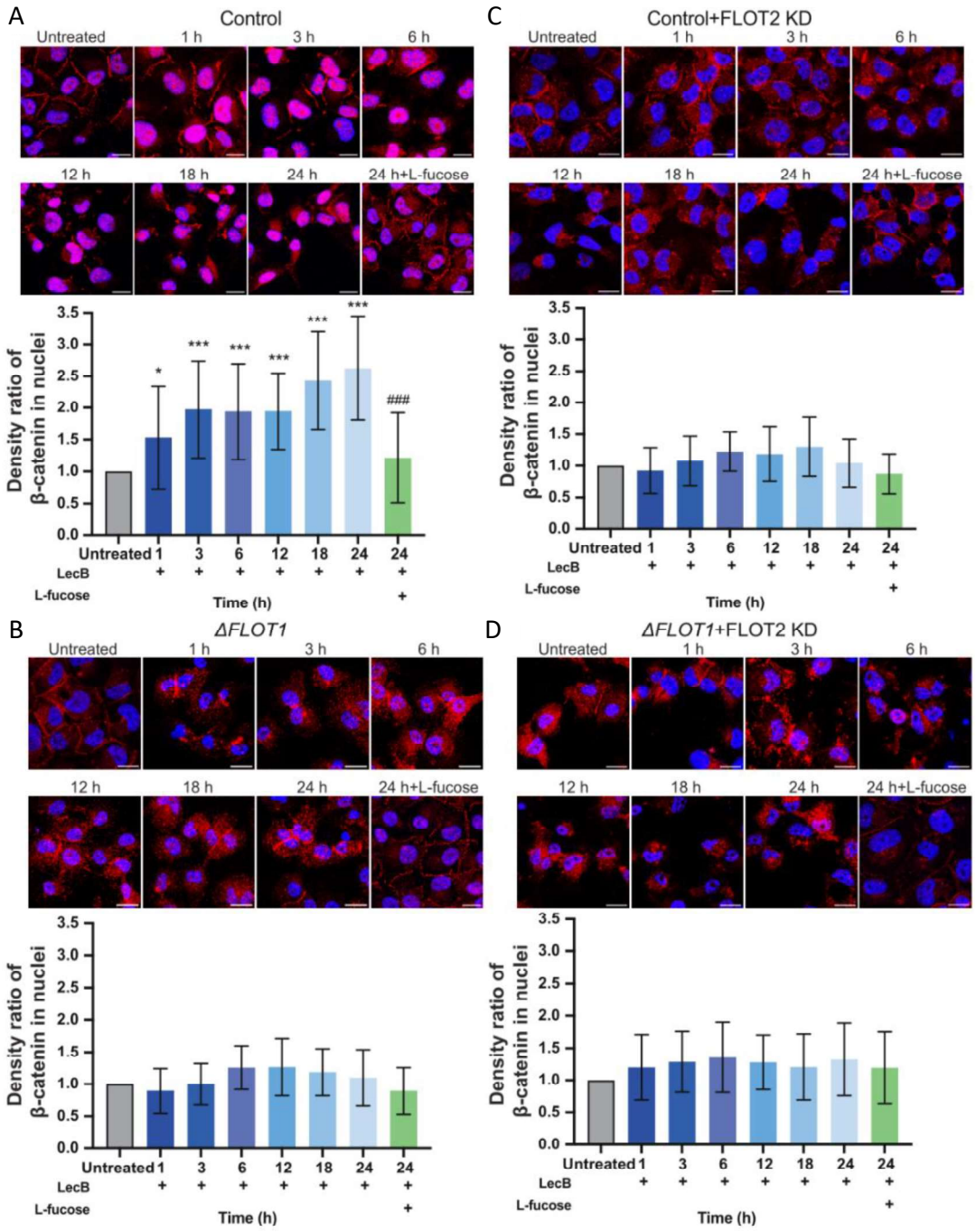

Fig. A20: LecB triggers the accumulation of ß-catenin to nuclei depending on flotillins.

(A) H1299 control cells, (B) *ΔFLOT1* cells, (C) FLOT2 KD cells, and (D) *ΔFLOT1*/FLOT2 KD cells were treated with LecB or without LecB (Untreated) and analyzed by a confocal fluorescence microscope with immunostaining for ß-catenin (red) and counterstained for DNA (DAPI, blue). Scale bar, 20 µm. Histograms depict the density ratio of ß-catenin in nuclear. Error bars indicate means ± SEM of N ≥ 150 cells. **p < 0.01 vs Untreated, ***p < 0.001 vs Untreated (Kruskal–Wallis test). ###p < 0.001 vs LecB groups (Kruskal–Wallis test).

A. 4.6. Discussion

In this study, I reveal that LecB can trigger flotillin-1-mediated ß1-integrin/FAK-Src signaling and downstream signal ß-catenin, which leads to the promotion of cell adhesion and attenuation of cell migration in H1299 cells. In accordance with previous studies, LecB reduces the level of cytoplasmic ß-catenin depending on GSK3ß-dependent phosphorylation, resulting in the inhibition of tissue repair processes in H1299 cells [5]. Meanwhile, LecB significantly inhibits collective cell migration and wound healing, which is blockable with L-fucose in MDCK monolayers [10]. Here, our findings provide more evidence of the molecular mechanisms of the LecB-induced suppressed cell migration and elevated cell adhesion, which is blocked by L-fucose in H1299 cells.

I demonstrate that LecB can enhance flotillins-mediated cell adhesion and attenuate cell migration in H1299 cells. Flotillins form a family of two ubiquitously expressed and highly conserved proteins with particularly high expression levels in heart, brain and lungs [196]. However, the molecular mechanism of flotillins still need to be understood, especially in the aspect of cell adhesion and cell migration. On the one hand, flotillins are involved in the process of cell-cell adhesion, whereas they can stabilize adherens junctions on the plasma membrane [131]. Meanwhile, flotillin-1 from lamprey shares is highly homologous with the sequence from humans, and the overexpression of flotillin-1 can upregulate the adhesion molecules mRNA levels, such as intercellular cell adhesion molecule 1 (ICAM1) and vascular cell adhesion molecule 1 (VCAM1) in human carcinoma cells, indicating that flotillin-1 plays an essential role in cell adhesion [197]. On the other hand, flotillin-1/2 are reported to colocalize and interact with E-cadherin and ß-catenin at CCJs in myoblasts [174]. Flotillins are required to build E-cadherin-containing lipid microdomains and allow E-cadherin stabilization at CCJs, triggering cell-cell adhesion integrity and for the formation of functional CCJs [131][174]. These are in agreement with our results that flotillins have an impact on lung cancer cell adhesion. However, in microenvironments, ECM is essential for cell adhesion and cell migration. Thus, I mimic a fibronectin circumstance instead of a streptavidin-coated Petri dish to measure the flotillin-1-mediated cell adhesion via cell adhesion assay and SCFS. There is not much literature regarding the research on flotillins and fibronectin. One example is that the overexpression of flotillin-2 accelerates, and its depletion inhibits cell spreading on fibronectin [187]. A similar phenotype is described in that significantly fewer flotillin-1 and FLOT2 KD cells have migrated towards fibronectin as compared to control siRNA-transfected HeLa cells [152]. Furthermore, FLOT2 KD affects the distribution of FAs and increases the number of FAs in HeLa cells on fibronectin [151]. These examples suggest that flotillins are essential for cell-matrix adhesion structures. Our data provide an additional line of evidence that LecB increased fibronectin-dependent cell adhesion ability with a significantly high value of F_d in H1299 cells with the contact times of 0 s and 5 s, which means that LecB can promote more cells adherent to fibronectin. Besides, cell adhesion histograms show that LecB increases the ability of cell adhesion in H1299 control cells in a fibronectin environment, but the risen ability of cell adhesion is postponed in *ΔFLOT1* cells after 12 h LecB treatment. Our new insight that LecB enhances the fibronectin-dependent cell adhesion mediated by flotillin-1 in human lung cancer cells, which favors that flotillins KD can increase FAs formation on fibronectin, inducing a stable adhesion [57][187].

Regarding cell migration, I have known a shred of evidence of the blockage of LecB-induced cell migration but less understanding of flotillins-mediated cell migration. Cott et al. found that LecB can block wound healing and cell proliferation with the reduced level of cytoplasmic ß-catenin in H1299 cells [5]. Thuenauer et al. found the inhibition of epithelial cell and polarized cell migration caused by LecB with the internalization of α3ß1-integrin and the activation of PI3K and Rac, respectively [10][40]. In comparison with these results, I first introduce the research on LecB-induced cell adhesion and cell migration with the interactions between LecB and flotillins in H1299 cells. Whereas the same results of the migration rate via scratch assay perform on endothelial cells and endothelial cells overexpressing flotillin-1, indicating that flotillin-1 does not affect cell migration [160]. To the contrary, the overexpression of flotillin-1 not only promotes the gastric cancer cell migration and invasion, but also increases the wound healing ability of gastric cancer cells [161]. Various studies describe the different cellular functions of flotillin-1 on different cell types regarding the process of cell migration. Considering this diversity of flotillin-1-mediated cell migration, it arouses our interest in the impact of host cell flotillins on LecB-suppressed cell migration. Thus, I first find that LecB can enhance flotillins-mediated cell adhesion and attenuate cell migration in H1299 cells. Moreover, I observe that the silencings of flotillin-1 or flotillin-2 and both flotillin-1/2 do not significantly influence the wound healing rate in H1299 cells. Those findings are strongly supported by the overexpression of flotillin-1 does not affect cell migration [160].

Interestingly, the intracellular trafficking of LecB is first observed via EE, LE, lysosome, and RE in H1299 cells in our findings. From our previous paper, Landi et al. have demonstrated a similar intracellular trafficking of LecB in keratinocytes, where LecB is transported to autophagosomes, LEs, and lysosomes [9]. Nevertheless, LecB is not detected in REs in keratinocytes [9], which is quite different to the intracellular trafficking of LecB in H1299 cells. Because LecB is endocytosed together with IGF1R and subsequent transports towards autophagosomes without receptor activation, inducing the suppression of keratinocyte survival and cell cycle arrest [9]. The internalized structures of LecB in keratinocytes [9] are similar to puncta-like structures of LecB in the perinuclear regions in H1299 cells. In addition, galectin-3 can be transported to EE, LE and RE for recycling to the cell membrane in polarized MDCK cells [191][198], which is similar to the trafficking of LecB in H1299 cells. Furthermore, galectin-3 is reported to colocalize with N-cadherin and ß-catenin at CCJs, decreasing the stability of CCJs and the integrity of cell-cell adhesion in human carcinoma cells [199]. Galectin-3 can bind cells to the ECM via ß1-integrin in mouse embryonic fibroblasts, driving cell membrane bending and the glycosphingolipid-dependent formation of plasma membrane invaginations [198]. Besides, it also binds to ß1-integrin in breast cancer cells, organizing the redistribution of integrins on the cell surface thereby enhancing cellular spreading or motility [200]. These results favor that galectin-3 can bind to integrins and change the cellular morphology to enhance cell migration, which is the opposite of our results. Here, I find that LecB can bind to host cell ß1-integrin and distribute the FA structures to block the process of cell migration in H1299 cells. In polarized MDCK cells, basolateral LecB application leads to marked clustering of endogenous galectin-3, suggesting that LecB outcompetes galectin-3-integrin interaction [10]. Thus, ß1-integrin could bind to more LecB than endogenous galectin-3 to block lung cancer cell migration.

Which signaling cascades are LecB able to trigger during the process of cell adhesion and cell migration? Here, I pay more attention on ß1-integrin/FAK-Src/ß-catenin signaling cascades in H1299 cells. The first line of evidence can be deduced from our experiments regarding the interactions between LecB and flotillins, LecB and ß1-integrin and flotillins and ß1-integrin. I have known that LecB interacts with ß1-integrin in MDCK cells [10], and lectin LecA interacts with flotillin-1 and internalizes into H1299 cells together [185]. Thus, I hypothesize that LecB may cross-link different molecular factors, like flotillin-1 and ß1-integrin, due to its character as a tetramer [35], then it generally activates signaling pathways, like FAK-Src complex and ß-catenin signaling intracellularly. Here, I find the colocalization between LecB and flotillins on the cell membrane, the co-precipitation of LecB and flotillins, and the co-precipitation of LecB and ß1-integrin in H1299 cells. These findings indicate the fact that LecB regulates flotillins and ß1-integrin interacting together, which triggers the downstream signaling, leading to the process of cell adhesion. Besides, results depict the co-precipitation between flotillin-1 and ß1-integrin, but not with flotillin-2 in H1299 cells. After LecB stimulation, there is less ß1-integrin interacting with flotillin-1 in H1299 control cells, indicating that ß1-integrin potentially degrades with the LecB treatment, which is also shown in the ß1-integrin protein expression starting to decrease after 12 h LecB treatment. This is in agreement with the finding by others that degradation of internalized ß1-integrin induced by LecB in polarized cells with the inhibition of epithelial wound healing [10]. Without the expression of flotillin-1, ß1-integrin endocytoses into cells partly in comparison with ß1-integrin internalizing into H1299 control cells after 6 h LecB treatment, and the protein expression of ß1-integrin goes up constantly. Based on these results, I demonstrate that flotillin-1 mediates the expression of ß1-integrin induced by LecB. The second derives from our previous mass spectrometry data. By mass spectrometry analysis of LecB pull-down fractions in keratinocytes, I determine that LecB may interact with flotillins and FAK capable of cell migration and cell adhesion [9]. This makes it on one hand more hints for us to investigate FAK signaling cascade. On the other hand, there has been speculation in the literature about flotillins involved in FAK signaling in the process of cell adhesion and migration. It has been reported that flotillin-2 co-traffics with α5ß1-integrin and affects the turnover of FAs in HeLa cells [151], but the co-trafficking between flotillin-1 and ß1-integrin remains still unclear. Flotillin-1 is capable of binding α-actinin [152], where the cytoplasmic integrin ß-subunit tail can bind in HeLa cells. These results point out that flotillin-1 activates FAK and colocalizes with α-actinin in lamellipodia-like structure upon integrin stimulation, inducing enhanced cell migration, especially the increased metastasis formation [152]. These examples are in agreement with our finding that LecB triggers flotillin-1-mediated FAK signaling pathway and reorganizes the localizations of FAs in H1299 cells.

The nuclear accumulation of ß-catenin through the LecB-triggered cascade I describe here will need further clarification. It has been depicted that integrin mediates the FAK-Src complex [113], and its engagement results in elevated levels of nuclear ß-catenin, increasing ß-catenin-regulated promoter activation, and transcriptional activation of Wnt/ß-catenin target genes, like GSK3ß in ovarian carcinoma cells [201]. Interestingly, the N-terminal SPFH domain of flotillins can bind to F-actin, which regulates the lateral motility of flotillin microdomains and influences the formation of flotillin platforms [131]. In

addition, FAK is connected to alterations in the polymerization or stabilization of F-actin and microtubule [101], which is supported by our observations that the scaffolding protein flotillin-1 assembles with FAK triggered by LecB in H1299 cells. LecB activates the ß1-integrin downstream FAK-Src complex at early time points and inactivates FAK-Src complex after 12 h LecB stimulation, followed by the nuclear translocation of ß-catenin in H1299 cells. These signaling cascades are also mediated by flotillin-1 that FAK-Src complex is activated constantly with LecB treatment after 12 h, followed by more ß-catenin concentrating perinuclear areas and cytoplasm in *ΔFLOT1* cells. Interestingly, flotillin-1 assists ß-catenin export via exosomes to regulate the Wnt signaling pathway through the exosomal discharge of ß-catenin in HEK 293T cells [202], and flotillins can interact with ß-catenin and E-cadherin at CCJs as mentioned above [174]. Meanwhile, membrane-cytoskeletal protein 4.1 N interacts with flotillin-1 in non-small cell lung cancer cells [163]. 4.1 N KD can enhance the protein expression of flotillin-1 and cytosolic ß-catenin, resulting in the suppression of cell proliferation and migration [163]. These samples highly favor our observations that flotillins mediate the intracellular expression of ß-catenin induced by LecB in H1299 cells. FAK-Src complex can activate the Rac1-GTP level, resulting in membrane ruffling lamellipodia which is the formation of the motile cell surface [121].In particular, Src can interact with flotillin-1, and cytoskeleton remodeling precedes flotillin re-ordering related to spectrin remodeling during capacitation *in vivo* [203]. This evidence substantially agrees with our hypothesis that LecB can bind with ß1-integrin and triggers the following FAK-Src complex and ß-catenin signaling mediated by flotillin-1 in H1299 cells. Khalili et al. has depicted an evaluation of cell adhesion stages in the literature. Phase I is initial attachment, Phase II is flattening, which is intervened by integrins bonding, and Phase III is fully spreading and the structural organization decided by FA structures [57]. Our results favor the steps of cell adhesion in that LecB has its tetrameric crystal structure to attach the host cells and promote the majority of cells adhere together. After that, LecB can regulate the interaction of flotillins and ß1-integrin, and activate the expression of ß1-integrin bond to ECM. Then, LecB can trigger FAK-Src complex and its downstream ß-catenin signaling and distribute the localizations of FAs, lamellipodia- and filopodia-like structures mediated by flotillin-1 in H1299 cells.

In addition, evidence has accumulated recently regarding FAK-Src complex and ß-catenin signaling triggered by bacteria and lectins. Foodborne pathogen *Campylobacter jejuni* activates the phosphorylation of FAK at Y397 and Src via the fibronectin-binding protein CadF, which is a well-known bacterial outer membrane protein, inducing filopodia formation and enhancing bacterial invasion in fibroblasts [204]. I have known that LecA, which has a similar function to LecB since their similar quaternary structures [34], has the ability to block H1299 cell migration [205] and LecA-mediated increase in phosphorylation of Src kinases at Y416 from 1 h to 3 h stimulation in H1299 cells [185]. Besides, galectin-1 can induce FAK hyperactivation by selectively amplifying the αvβ3-integrin signal, leading to hepatocellular carcinoma cell invasion and lung metastasis [119]. Our findings that LecB inhibits H1299 cell migration with increased phosphorylation of FAK at Y397 and Src at Y416 from 1 h to 6 h stimulation provide more insight into bacterial lectins trigger Src signaling cascade. Regarding ß-catenin signaling, *P. aeruginosa* infection reduces the cytosolic ß-catenin level and increases the nuclear ß-catenin level in

murine macrophages, inducing macrophage autophagy [206]. It suggests that ß-catenin is translocated to the nucleus following *P. aeruginosa* infection, which favors our previous results regarding the degradation of cytosolic ß-catenin induced by LecB [5], resulting in the nuclear accumulation of ß-catenin induced by LecB in H1299 cells.

A. 4.7. My contributions

With support from Prof. Dr. Winfried Römer (principal supervisor), DR1-CNRS Dr. Christopher G. Mueller and helps from Dr. Taras Sych and Dr. Ramin Omidvar, I conceptualized and conducted the study. During this time, I co-mentored two thesis students whose contributions were partly incorporated into the publication manuscript:

- Celine Enderle: internship and B.Sc. thesis, manuscript co-author
- Anna-Sophia Kittel: internship and M.Sc. thesis, manuscript co-author

My contributions to the publication manuscript, all publication figures, and all the experiments include these points:

1) Identify the increased cell adhesion and decreased cell migration induced by LecB, flotillins mediating in the process of cell adhesion and cell migration (with Celine Enderle for the cell adhesion part, Anna-Sophia Kittel for the cell migration part, Dr. Ramin Omidvar for the AFM part).
2) Investigate the interactions between LecB and flotillin-1/2 with imaging by confocal microscopy and immunoprecipitation assay.
3) Investigate the interaction between flotillin-1 and ß1-integrin and the internalization of ß1-integrin mediated by flotillin-1/2 with the treatment of LecB with imaging by confocal microscopy and immunoprecipitation assay.
4) Identify LecB triggering ß1-integrin/FAK-Src/ß-catenin signaling cascade mediated by flotillin-1 with imaging by confocal microscopy and immunoprecipitation assay (with Dr. Taras Sych for the quantification of ß-catenin signal).

A. 5. Conclusions

With more and more cases of socioeconomic infections of *P. aeruginosa*, I should pay more attention to the interplay between the bacterial virulence factor LecB and the process of cell adhesion and cell migration. *P. aeruginosa* is an opportunistic pathogen that has the ability to adhere to host cells, which is critical for initiating infections. Bacterial lectins are recognized as adhesins which are a specific target for host cell surface glycoconjugates [47], followed by some cellular processes, such as the blockage of wound healing [5][10], the arrest of the cell cycle [9] and the attenuation of cell proliferation [5].

Here, in my first part of the project, I introduce a scaffold protein, flotillin, which is involved in cell adhesion, cell migration, and cellular trafficking [141]. Notably, flotillin-1/2 is reported to interact with LecA, assisting *P. aeruginosa* invasion into host cells [185]. The findings revealed that LecB, as a bacterial adhesin, severely enhances the process of cell adhesion and attenuates the process of cell migration in human non-small cell lung cancer cell H1299. I unraveled that LecB had less capability to increase streptavidin-dependent cell adhesion and decrease cell migration with the knockout of flotillin-1 or the KD of flotillin-2 alone expression in H1299 cells. It indicated that LecB enhanced flotillin-mediated cell adhesion and attenuated cell migration in H1299 cells. I used fibronectin instead of streptavidin and LecB-Biotin to mimic the common microenvironment. I found that LecB increased fibronectin-dependent cell adhesion ability, which was mediated by flotillin-1. Moreover, I found the colocalization and interaction between LecB and flotillin-1/2. Furthermore, I introduced ß1-integrin as another interactor of LecB. I found that ß1-integrin could interact with flotillin-1 but not with flotillin-2 induced by LecB. Meanwhile, the silencing of flotillin-1/2 could postpone the intracellular trafficking of ß1-integrin triggered by LecB. Consequently, I identified that LecB triggered the recruitment of flotillins, especially flotillin-1, as an essential interactor of LecB. LecB also induced the FAK-Src complex, and LecB changed the position of FAK from the leading edge of cells to the cytoplasm. The knockout of flotillin-1 recused the decreased FA number induced by LecB. Moreover, LecB induced the nuclear accumulation of ß-catenin, which was blocked by the silencing of flotillin-1/2. In *ΔFLOT1*/FLOT2 KD cells, there was no translocation of ß-catenin in nuclei, but most ß-catenin was in the cytoplasm nearby the nuclei. Thus, I revealed that LecB could trigger ß1-integrin/FAK-Src signaling and its downstream signal ß-catenin mediated by flotillin-1. Translocation of ß-catenin in the nucleus induces transcriptional activation of target genes by ß-catenin interaction with TCF/LEF DNA-binding proteins, leading to activate the expression of c-Myc and cyclin D1, which induce cell proliferation, migration, and invasion [207](Fig. A21). Nevertheless, I did not verify the interaction between of ß-catenin and TCF/LEF and the expression of c-Myc and cyclin D1 induced by LecB. I identified that L-fucose inhibited flotillins-mediated cell adhesion and cell migration and affected the nuclear translocation of ß-catenin induced by LecB, providing more evidence that L-fucose could heal the wound infected by *P. aeruginosa* LecB.

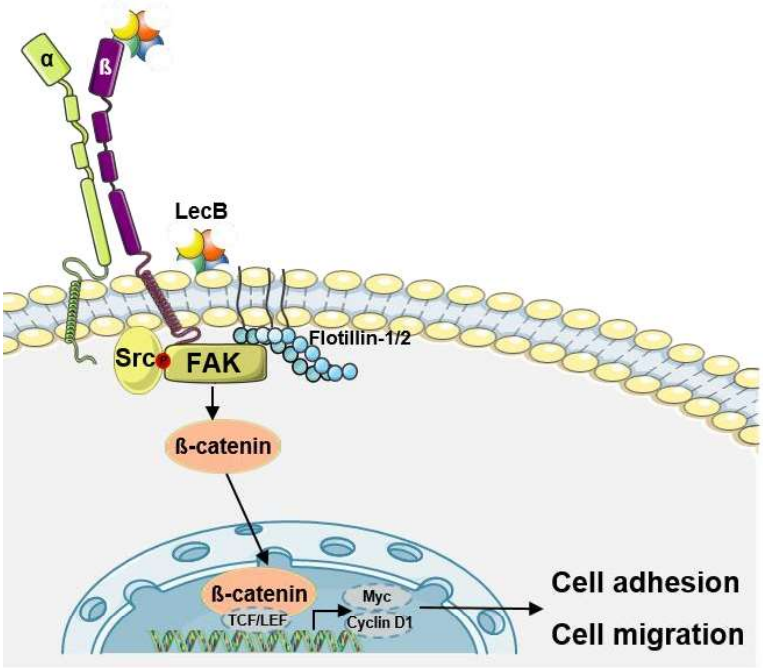

Fig. A21: The scheme of the crucial role of host cell flotillins in aggravating LecB-mediated cell migration and adhesion and signaling cascades.

Upon infecting human body surfaces, skin or lung, *P. aeruginosa*-produced LecB would bind host cells. This leads to dysfunction of cell adhesion and cell migration. As a consequence, LecB binds to host cell flotillins on the cell membrane, and triggers ß1-integrin/FAK/ß-catenin signaling cascades, resulting in the enhancement of cell adhesion and attenuation of cell migration. Dashed grey ovals point the undectcted results. Translocation of ß-catenin in the nucleus induces transcriptional activation of target genes by ß-catenin interaction with TCF/LEF DNA-binding proteins, leading to activate the expression of c-Myc and cyclin D1, which induce cell proliferation, migration, and invasion.

A. 6. Outlook

In the first part of the project, I demonstrated a novel interactor of LecB, flotillin-1, in H1299 cells. Moreover, LecB could trigger ß1-integrin/FAK-Src signaling and its downstream signal ß-catenin mediated by flotillin-1, resulting in promoted cell adhesion and suppressed cell migration. However, some open questions require further attention.

Flotillins have been implicated in plenty of cellular processes, such as cell adhesion and cell migration, cell-cell adhesion, cytoskeleton rearrangement, membrane trafficking as well as host cell invasion by *P. aeruginosa* infection [141][174][185]. Moreover, mass spectrometry analyses revealed the presence of receptors within the enriched proteins in the LecB pull-downs in keratinocytes [9]. The data showed the potential interaction between LecB and flotillin-1. Besides, I screened several interesting molecular factors, which are also involved in the process of cell adhesion and cell migration, like ICAM1, epithelial cell adhesion molecule (EPCAM), basal cell adhesion molecule (BCAM), and activated leukocyte cell adhesion molecule (ALCAM). For example, the loss of ICAM1 inhibits wound healing, keratinocyte migration from the edges of the wound toward the center, and granulation tissue formation [208]. Moreover, it has been reported that N-glycosylation of EPCAM enhances the ability of cell adhesion by regulating the expression of fibronectin and ß1-integrin, activating the FAK/PI3K/Akt signaling pathway in breast cancer cells [209]. Similarly, BCAM is reported to bind with other ECM components, such as laminin. The preferential binding of BCAM and α3ß1-integrin to laminin α5 promotes A549 cell migration [210]. The inhibition of ALCAM in endometrioid endometrial cancer cells decreases cell migration, invasion, and cell-cell adhesion [211]. These several shreds of evidence indicate that CAMs, including ICAM1, EPCAM, BCAM, and ALCAM, play an essential role in cell adhesion and cell migration. Meanwhile, I have verified the colocalization between CAMs and LecB in H1299 cells via immunofluorescence assy. The significant colocalization between LecB and CAMs can be observed in H1299 cells (data not shown). Thus, I have a superficial clue that LecB probably colocalizes with CAMs, resulting in promoted cell adhesion and suppressed cell migration. Meanwhile, I can utilize the Pull-down assay and immunoprecipitation assay to verify the interaction between LecB and CAMs again. I can also investigate if the binding of LecB to CAMs triggers FAK/ß-catenin signaling cascade. In addition to CAMs, the integrin family contains α subunits and ß subunits, enhancing the ability of cell adhesion. Here, in my first part of the project, I only concentrated on the research between LecB and ß1-integrin. Besides, not only ß1-integrin can be involved in cell adhesion and cell migration, but also many other integrins, such as α5-integrin and ß2-integrin. For example, ubiquitination of α5-integrin is required for proper fibroblast migration [212], and the activated ß2-integrin reduces macrophage cell migration and wound healing [213]. I can characterize the function of other integrins, like ß1-integrin, in cell adhesion and cell migration induced by LecB. The molecular mechanism of nuclear ß-catenin-mediated cell migration and adhesion is unclear. As I mentioned above, translocation of ß-catenin in the nucleus induces transcriptional activation of target genes by ß-catenin interaction with TCF/LEF DNA-binding proteins, leading to activate the expression of c-Myc and cyclin D1, which induces cell proliferation, migration, and invasion [207]. However, this is only my hypothesis. In the next steps, the protein expression of c-Myc and cyclin D1 induced by LecB can be investigated by western blot assays.

Then, the interaction of ß-catenin and c-Myc and cyclin D1 can be shown with the incubation of LecB. Moreover, I can also verify the interaction of ß-catenin and c-Myc and cyclin D1 with the presence of Wnt/β-catenin signaling inhibitor, such as FzM1 [214].

Here, I utilized L-fucose as an antagonist of LecB to block the function of LecB in the research. I found that L-fucose inhibited the increased cell adhesion and decreased cell migration induced by LecB, and it restored the nuclear accumulation of ß-catenin induced by LecB. Nevertheless, I did not investigate if L-fucose mediates the ß1-integrin/FAK signaling cascade induced by LecB. Our collaborator, Prof. Dr. Alexander Titz, works on the chemical structures of L-fucose and D-mannose. They successfully investigated some derivatives from mannoside to block LecB [41][215]. I verified one L-fucose derivative, DH445, to inhibit the decreased DC migration and T cell activation triggered by LecB *in vivo* in my second part of the project, but I did not use DH445 *in vitro*. I can compare the inhibition efficiency of DH445 with L-fucose regarding cell adhesion and the signaling cascade induced by LecB.

A. 7. Supplementary figures

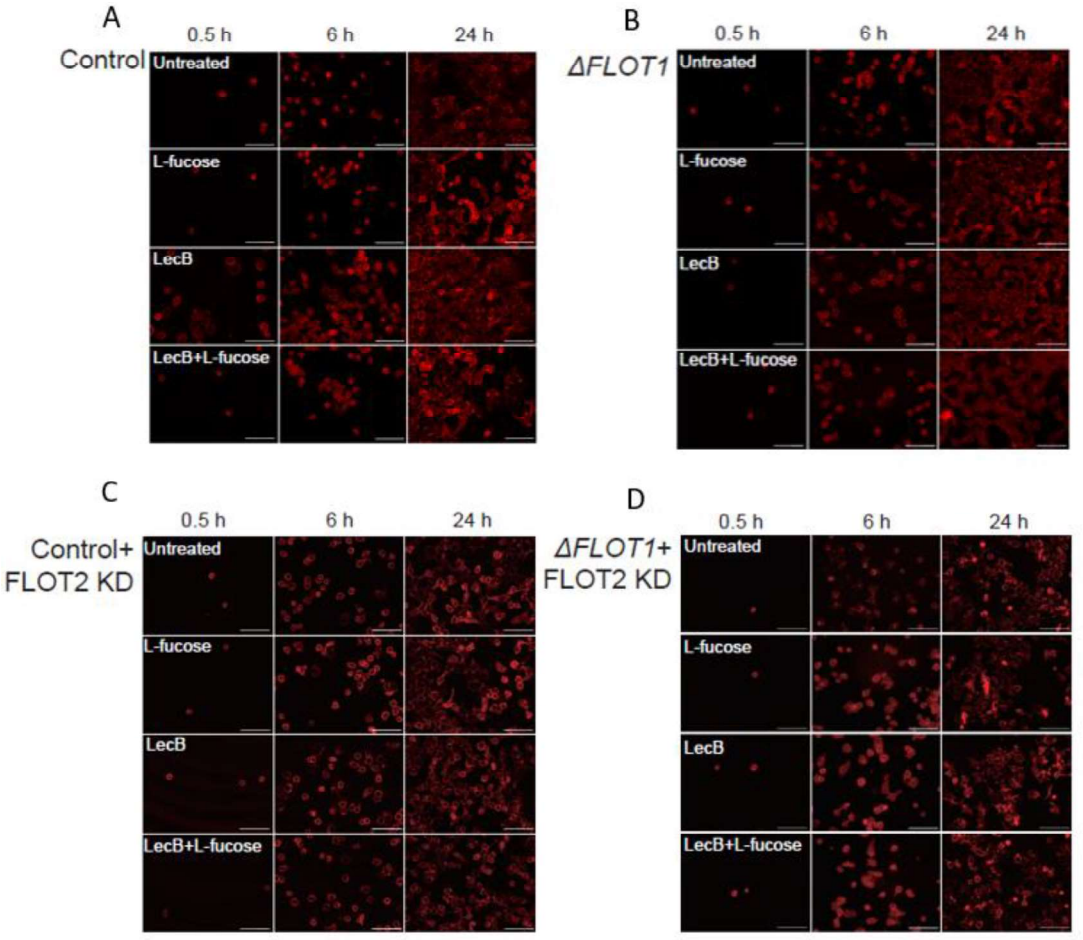

Supplementary Fig. 1: LecB enhances cell adhesion mediated by flotillins.

The representative figures of streptavidin-coated cell adhesion assays in (A) H1299 cells, (B) *ΔFLOT1* cells, (C) FLOT2 KD cells, and (D) *ΔFLOT1*/FLOT2 KD cells at 0.5 h, 6 h, and 24 h treatment of LecB. Scale bar, 100 µm. The representative figures of scratch wound healing assays in (B) H1299 cells, (D) *ΔFLOT1* cells, (F) FLOT2 KD cells, and (H) *ΔFLOT1*/FLOT2 KD cells at 0 h, 6 h, and 24 h treatment of LecB. Scale bar, 100 µm.

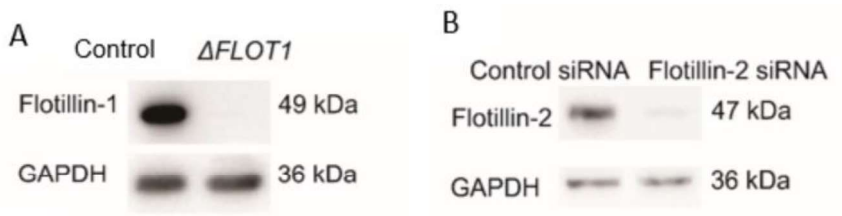

Supplementary Fig. 2: The verification of *ΔFLOT1* cells and the knockdown of flotillin-2.

(A) H1299 and *ΔFLOT1* cells were lysed and flotillin-1 protein level was depicted. (B) H1299 cells were transfected with control and flotillin-2 siRNA and lysed, and flotillin-2 protein level was depicted.

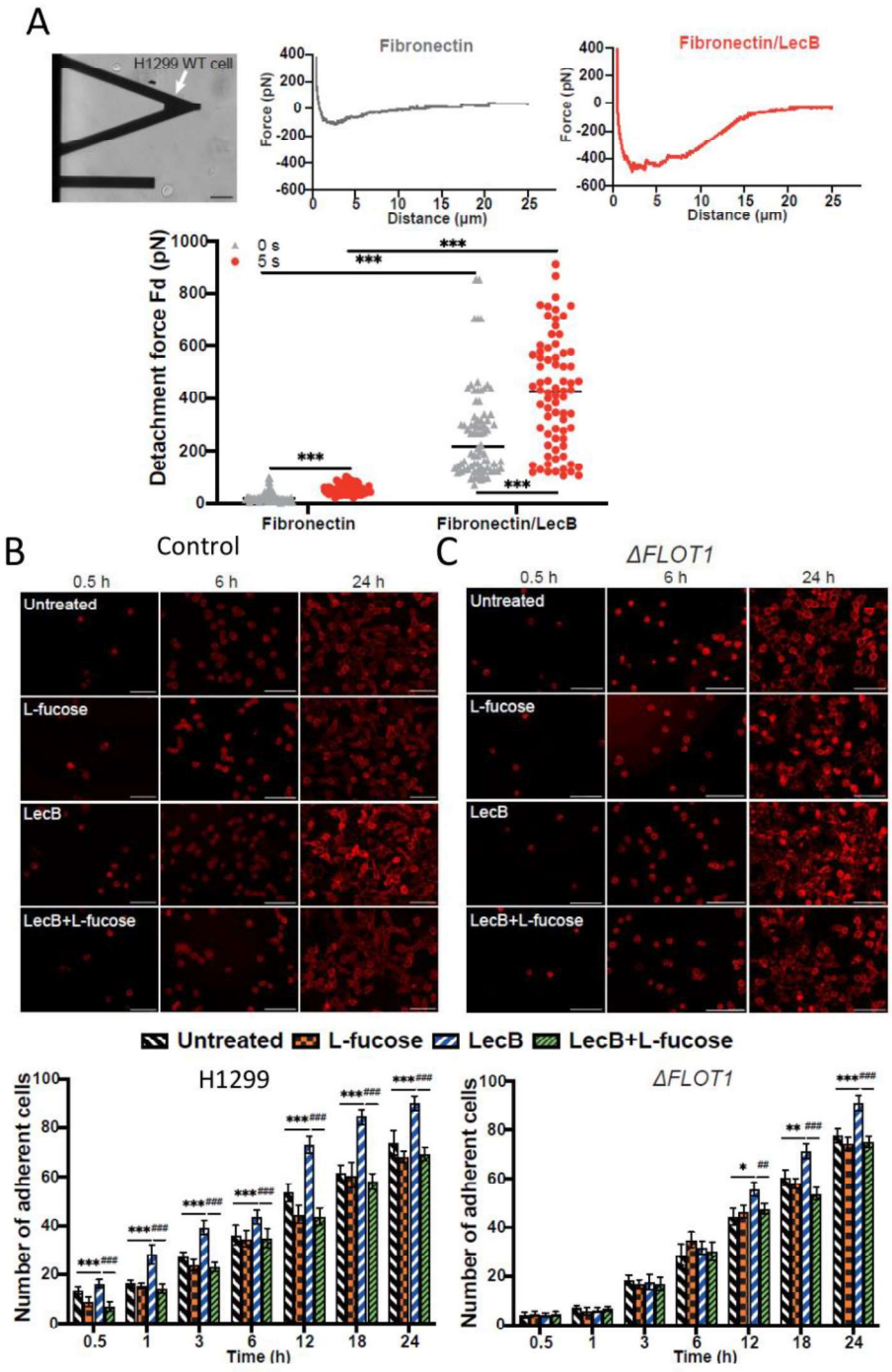

Supplementary Fig. 3: LecB enhances fibronectin-dependent cell adhesion mediated by flotillin-1.

(A) A single H1299 cell was attached to the cantilever (upper panel, left), and representative force-distance curves depicted untreated and LecB groups at dwell 0 s (upper panel, right). The F_d between untreated and LecB for 0 s and 5 s of dwell time (lower panel). Scale bar, 50 µm. Error bars indicate means ± standard error mean of N ≥ 100 cells. ***p < 0.001 vs Untreated (two-way ANOVA). The representative figures of fibronectin-coated cell adhesion assay in (B) H1299 cells, (C) *ΔFLOT1* cells from 0.5 h to 24 h. Histograms depicted the number of adherent cells, *p < 0.05 vs Untreated, **p < 0.01 vs Untreated, ***p < 0.001 vs Untreated (two-tailed unpaired t-test). ##p < 0.01 vs LecB groups, ###p < 0.001 vs LecB groups (two-way ANOVA). Scale bar, 50 µm.

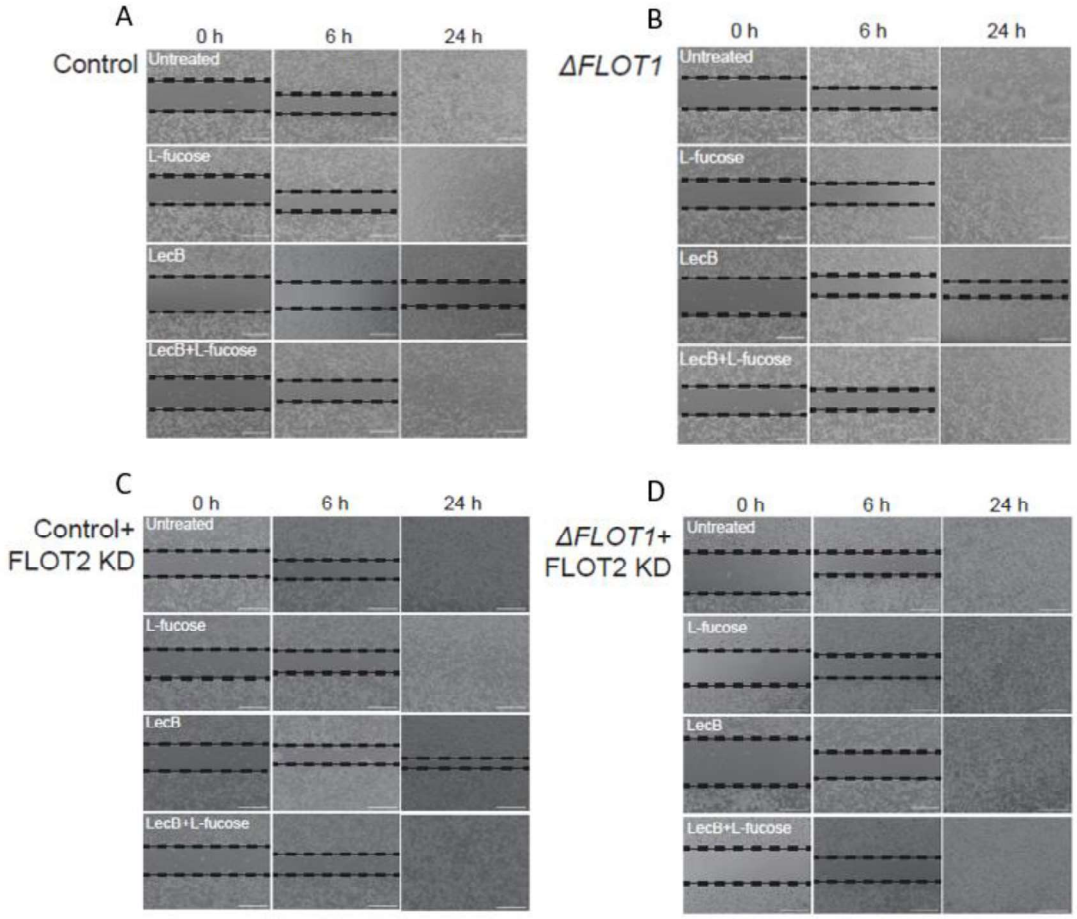

Supplementary Fig. 4: LecB attenuates wound healing mediated by flotillins.

The representative figures of scratch wound healing assays in (A) H1299 cells, (B) *ΔFLOT1* cells, (C) FLOT2 KD cells, and (D) *ΔFLOT1*/FLOT2 KD cells at 0 h, 6 h, and 24 h treatment of LecB. Scale bar, 100 µm.

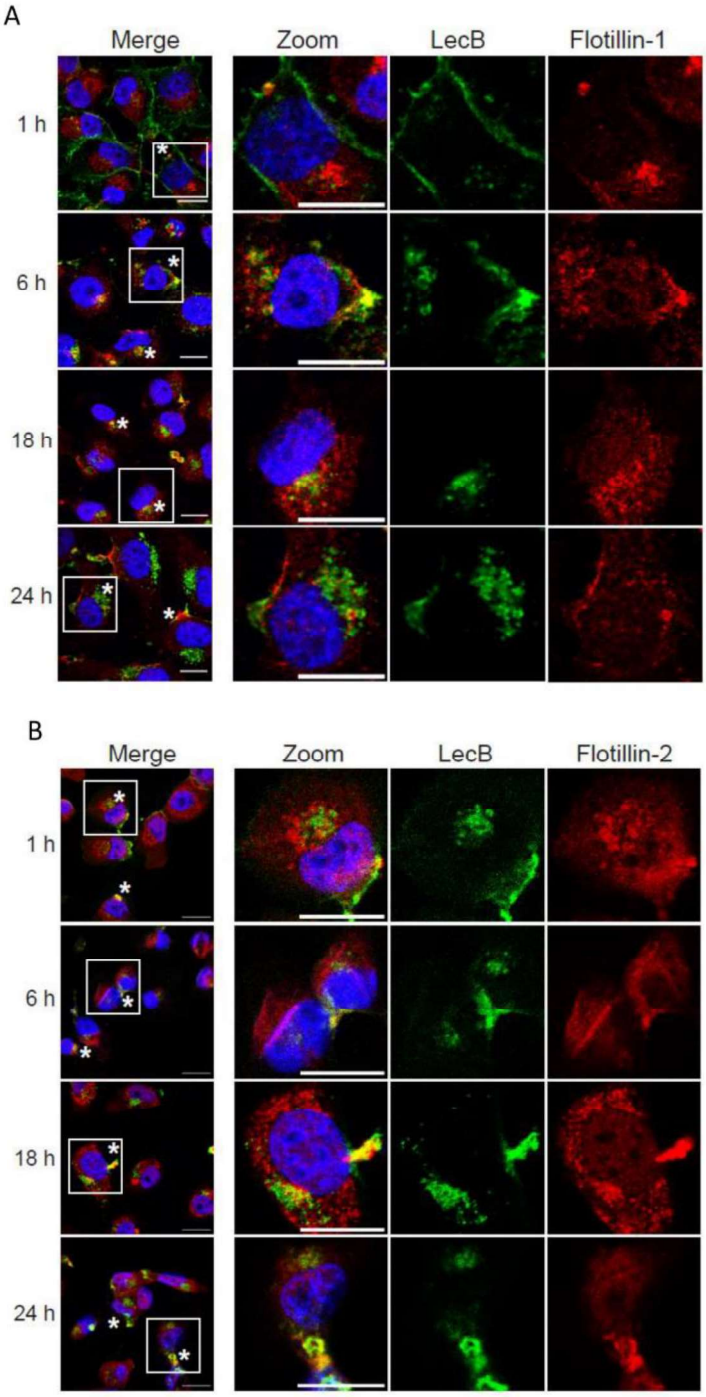

Supplementary Fig. 5: Flotillins colocalize with LecB.

(A) H1299 control cells were treated with LecB-A488 (green) as indicated and analyzed by a confocal fluorescence microscope with immunostaining for flotillin-1 (red) and counterstained for DNA (DAPI, blue). White asterisks pointed at colocalizations. Scale bar, 20 µm. (B) H1299 control cells were treated with LecB-A488 (green) as indicated and analyzed by a confocal fluorescence microscope with immunostaining for flotillin-2 (red) and counterstaining for DNA (DAPI, blue). White asterisks pointed at colocalizations. Scale bar, 20 µm.

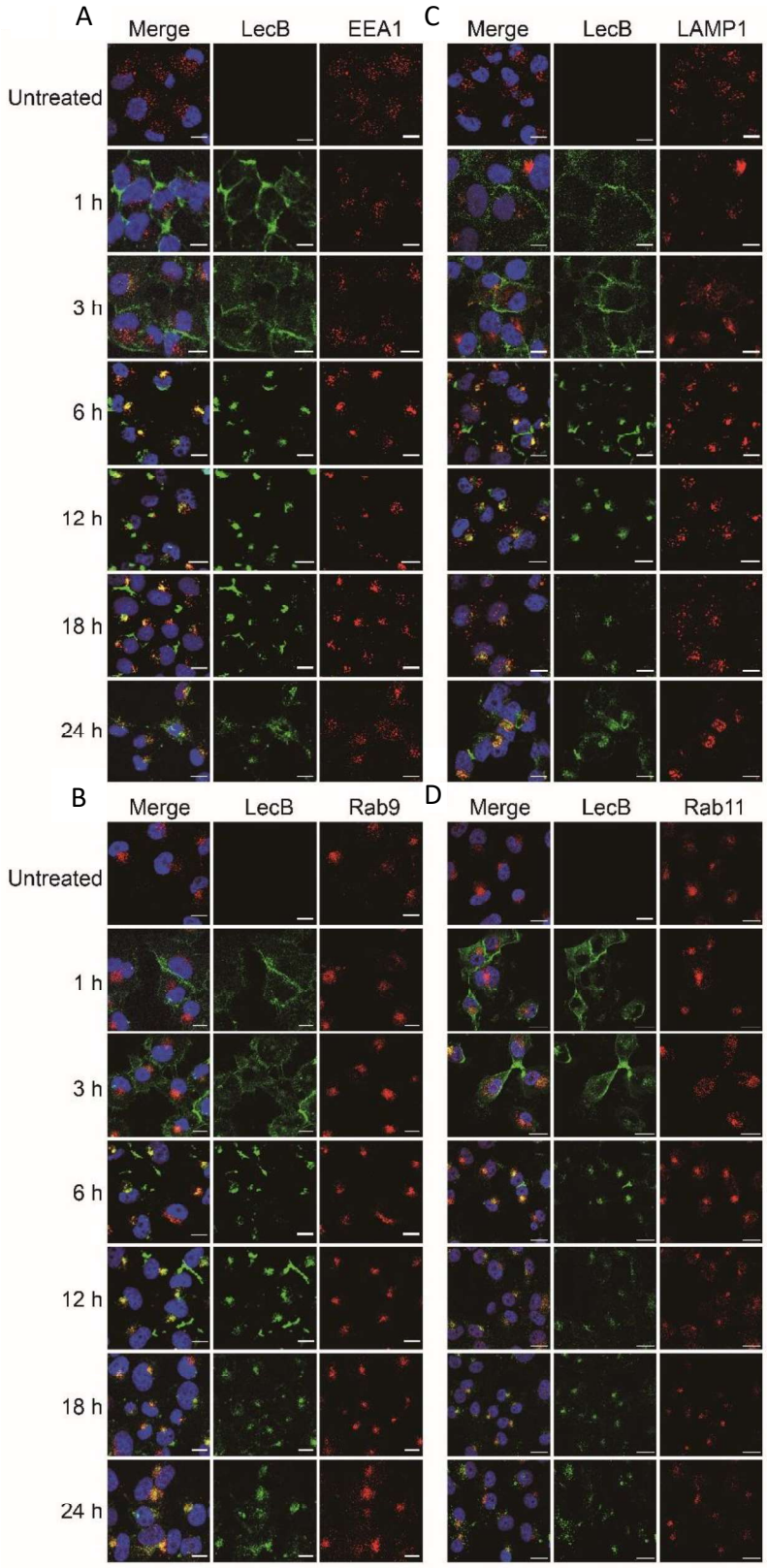

Supplementary Fig. 6: The trafficking pathway of LecB in H1299 cells.

H1299 control cells were treated with LecB-A488 (green) and analyzed by a confocal fluorescence microscope with immunostaining for (A) EEA1 (red), (B) Rab9 (red), (C) LAMP1 (red), and (D) Rab11 (red) and counterstained for DNA (DAPI, blue). Scale bar, 20 µm.

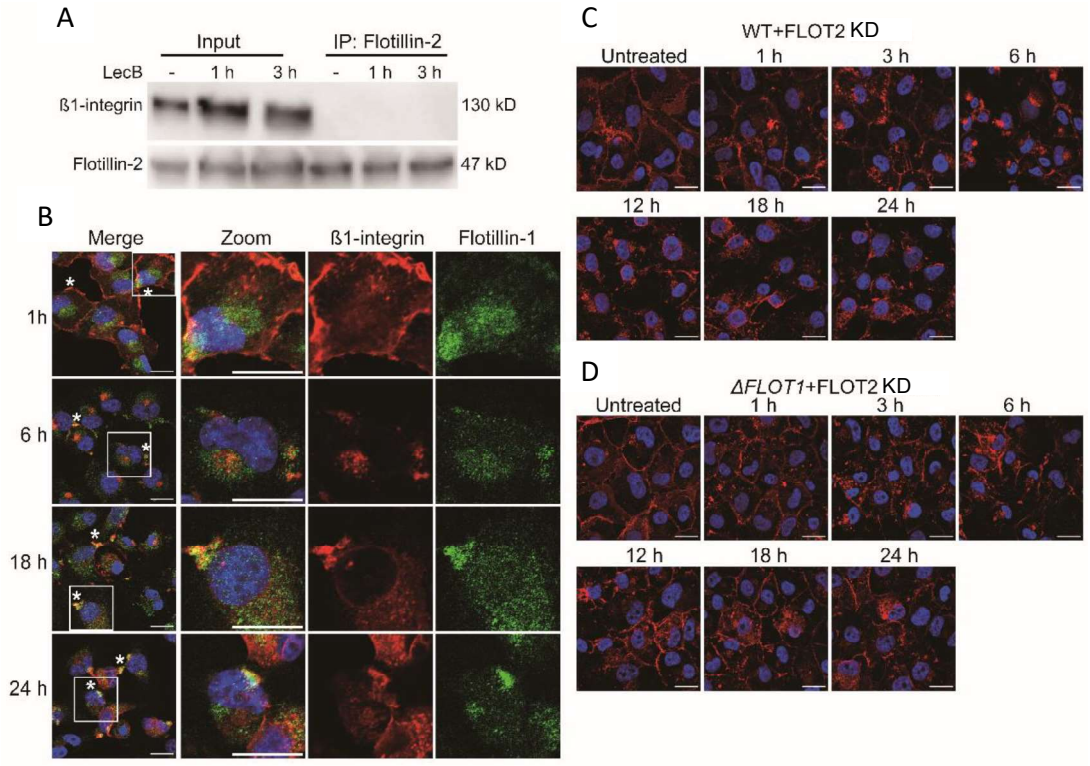

Supplementary Fig. 7: ß1-integrin is interfered by flotillins with the treatment of LecB.

(A) H1299 cells were stimulated as indicated, but there was no immunoprecipitation of ß1-integrin co-precipitated with flotillin-2, after 1 h and 3 h LecB stimulation. (B) H1299 control cells were treated with LecB as indicated and analyzed by a confocal fluorescence microscope with immunostaining for ß1-integrin (red), flotillin-1 (green), and counterstained for DNA (DAPI, blue). White asterisks pointed at colocalizations. Scale bar, 20 µm. (C) FLOT2 KD cells and (D) *ΔFLOT1*/FLOT2 KD cells were treated with LecB as indicated and analyzed by confocal fluorescence microscopy with immunostaining for ß1-integrin (red), and counterstained for DNA (DAPI, blue). Scale bar, 20 µm.

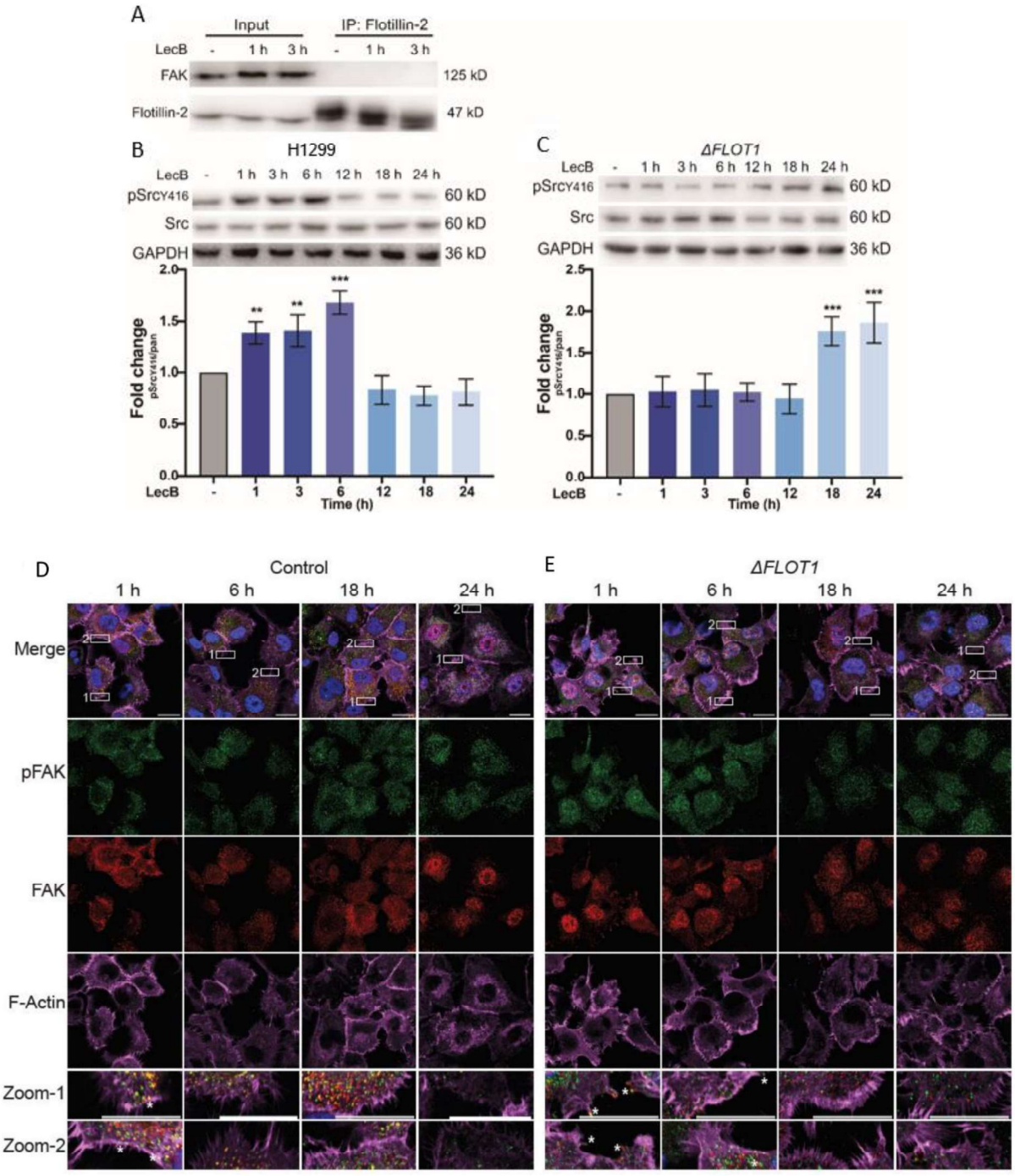

Supplementary Fig. 8: Flotillin-1 mediated FAK-Src complex induced by LecB.

(A) *ΔFLOT1* cells were stimulated as indicated, but there was no immunoprecipitation of FAK co-precipitated with flotillin-2, after 1 h and 3 h LecB stimulation. (B) H1299 cells, (C) *ΔFLOT1* cells were stimulated as indicated and Src Y416 and Src protein level was expressed by western blot analysis. Histograms depict Src Y416 protein level. Error bars indicate means ± standard error mean of N = 3 biological replicates. *p < 0.05 vs Untreated, ***p < 0.001 vs Untreated (one-way ANOVA). (D) H1299 control cells and (E) ΔFLOT1 cells were treated with LecB as indicated and

analyzed by a confocal fluorescence microscope with immunostaining for FAK Y397 (green), FAK (red), F-actin (magenta) and counterstained for DNA (DAPI, blue). White boxes show the zoomed figures of FAs. Scale bar, 20 µm.

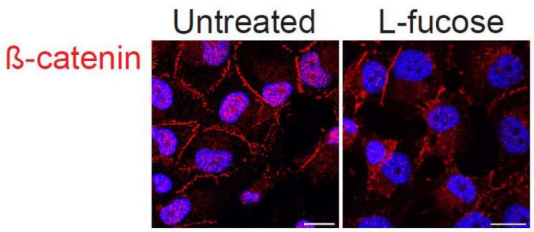

Supplementary Fig. 9: The influence of L-fucose on the expression of ß-catenin.

The influence of L-fucose on the expression of ß-catenin was shown via immunofluorescence assay in H1299 cells. ß-catenin (red), and DNA (DAPI, blue). Scale bar, 20 µm.

3. Part B. The *Pseudomonas aeruginosa* lectin LecB suppresses the immune response by inhibiting transendothelial migration of dendritic cells

B. 1. Introduction

B. 1.1. Lymphatic system

The mammalian circulatory system comprises both the cardiovascular system and the lymphatic system [216]. The lymphatic system is an open, low-pressure, and unidirectional transit network from the extracellular space to the venous system. It plays a crucial role in regulating tissue fluid homeostasis, absorption of gastrointestinal lipids, and immune surveillance throughout the body [217]. Moreover, lymphatic vessels (LVs) are an extensive drainage network in the lymphatic system, including lymphatic capillaries, pre-collecting LVs, and collecting LVs [217]. The fluid surrounding the body's cells is termed interstitial fluid. When this fluid enters the lymphatic system, it is referred to as 'lymph'. It goes through the lymphatic capillaries, which are also called initial lymphatics. From there, lymph drains into the collecting vessels, which passes through at least one, but usually several lymph nodes (LNs) distributed throughout the body. Collecting vessels merge into grander trunks which empty into the ducts. Finally, the ducts return the lymph into the venous circulation via the right lymphatic duct and the thoracic ducts, completing the circuit of fluid transport (Fig. B1)[218].

B. 1.1.1. The structure of lymphatic system

The lymphatic system is composed of a network of vessels, including LVs, LNs, and other lymphoid organs [219]. Their sizes range from 10 µm to 2 mm in diameter [220]. In this chapter, I will introduce more on LVs and other lymphoid organs, and the characterized LNs are presented in detail in a next chapter.

Blood and LV networks form two arms of the vertebrate cardiovascular system that play complementary roles in body homeostasis maintenance [221]. Lymphatic capillaries are comprised of a single thin layer of oak leaf-shaped lymphatic endothelial cells (LECs) forming discontinuous button-like cell-cell junctions, typically made up of one or two closed-ended tubes, highly attenuated cells in cross-section [217][220][222]. The characterized markers of LECs are introduced in the chapter afterwards. The ECs in the lymphatic capillaries are mural cells coverage and have little or no basement membranes [217][223]. Therefore, lymphatic capillaries are highly permeable to interstitial fluid and solutes, allowing the entry of macromolecules, such as lipids, and even permitting the trafficking of immune cells [217]. The interstitial fluid enters through the small lymphatic capillaries that gradually combine to form larger diameter vessels, namely the pre-collectors, collectors, trunks, and ducts [219].

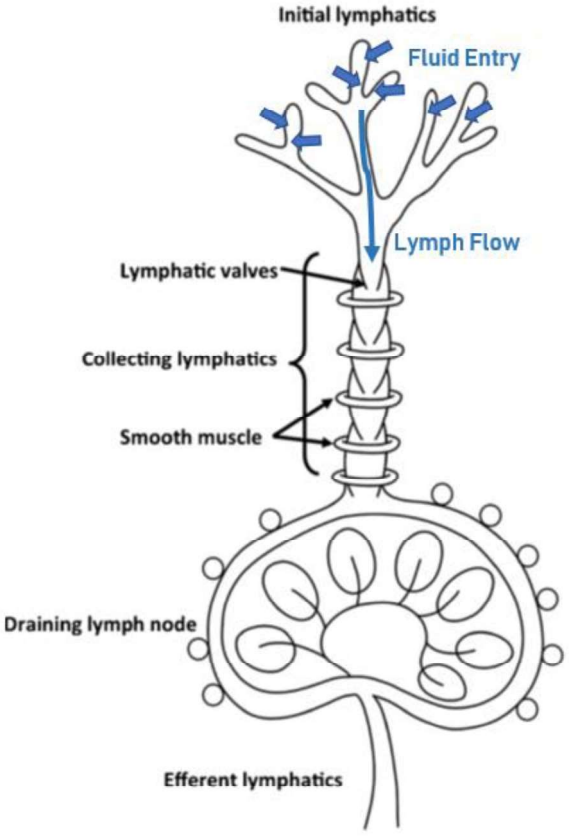

Fig. B1: Schematic of the lymphatic system.

Initial LVs comprised of closed-end lymphatic capillaries branch into the tissue and then come together to form larger LVs, with smooth muscle cells surrounding the endothelium for smooth peristaltic-like contraction toward the LN. Besides, the lymphatic system includes the draining LN (dLN) and efferent lymphatics. The vessels maintain flow to regulate fluid drainage away from tissues and back into circulation. First, fluid moves into the collecting LVs. Once the vessels have sufficiently swelled with fluid, the change in stress pressures causes activation of the muscle cells, which contract the affected segment of collecting LVs, perpetuating fluid movement, and the lymphatics valves preventing subsequent backflow. Then, fluid and small molecules (<70 kDa) are permitted to enter into the LN [224].

Many molecules and proteins play an integral role in lymphatic function. On the one hand, the button-like junctions display an alternating pattern of the adhesion proteins VE-cadherin and platelet endothelial cell adhesion molecule (PECAM-1), forming overlapping flaps between adjacent ECs and providing the foundational function of regulating vessel permeability [217][225, 226]. The characterized function of VE-cadherin in LECs will be introduced in a next chapter. On the other hand, interstitial fluid pressure and the strain of the ECM, which can be affected by skeletal motion, can determine the elasticity, strength, and hydration of the lymphatics [220]. The collecting LVs have a continuous basement membrane composed of collagen IV, fibronectin, and laminins [227]. Besides, ECM can directly guide lymphatic vascular growth

by providing adhesive gradients for the directional migration of cells [228]. Thus, ECM is a complex but highly organized network of the regulation of the lymphatic system.

The immune organs are grouped as primary and secondary based on their functional roles. The primary lymphoid organs are the sites of lymphocyte formation and acquisition of immunocompetency and include the red bone marrow and the thymus [218]. The secondary lymphoid organs are where immune responses occur, including LNs, spleen, and lymphoid follicles or nodules [223]. The spleen is the largest single mass of an immune tissue in the body. The spleen provides a source of lymphocytes for the bloodstream and is thought to assist in fighting infection because it becomes enlarged in certain diseases where the blood is infected [223]. B cells and T cells carry out immune functions in the spleen, while spleen macrophages destroy blood-borne pathogens by phagocytosis [223]. The spleen is also an organ were B cell mature. Regarding the lymphoid follicles or nodules, they are spherical or ovoid structures composed of aggregated lymphocytes and a meshwork of reticular cells [229]. They are found in the mucous membranes, so are called mucosa-associated lymphoid tissue [230]. There are two types of lymphoid nodules, including primary and secondary nodules [218]. The former consists of B cells surrounded by a loose network of DCs. Upon encountering an antigen, the DCs stimulates the development of the secondary nodules by the activation of the B cells, which are bounded by cortical dendritic cells, and macrophages form what is termed a germinal center [218]. Surrounding this center, there is a condensation of B cells, forming the outer part of the secondary nodule [231]. The gut-associated lymphoid tissue (GALT) of mice includes two additional types of smaller organized lymphoid tissues, cryptopatches (CPs) and isolated lymphoid follicles (ILFs)[232]. 90% of the cells in ILFs are lymphocytes comprising a slightly higher proportion of T cells than B cells [233]. $CD57^{hi}PD\text{-}1^{hi}$ follicular T cells and $CD4^{+}CD25^{+}CD127^{-}IL\text{-}2^{-}$ Tregs are mostly found in ILFs, whereas cytokine-producing T-cell subsets are mainly located in the GALT-free lamina propria [233, 234]. LNs are presented in detail in a next chapter.

B. 1.1.2. The function of lymphatic system

The principal function of the lymphatic system is to maintain tissue fluid homeostasis by removing the protein-rich lymph from the extracellular space and returning it to the blood circulation [235]. In addition to the regulation of tissue fluid, the lymphatic vasculature is important for the transport of immune cells and soluble antigens to LNs, management of peripheral immune tolerance, and absorption of dietary fats in the gastrointestinal organs [217]. On the one hand, the intestinal lymphatic system plays key roles in fluid transport, lipid absorption, and immune function [236]. Part of the gut membrane in the small intestine contains tiny finger-like protrusions called villi. Lymph flows from the small intestine via a unidirectional process that originates at single lacteals that are contained within each small intestinal villi [237]. Meanwhile, lymph flows directly from the small intestine via a series of LVs and nodes that converge at the superior mesenteric lymph duct [236]. On the other hand, LVs are essential for the trafficking of leukocytes and soluble antigens from peripheral tissues to dLNs [238]. Another critical function of the

lymphatic system is to defend the body from exposure to potentially hazardous microorganisms via LNs. The function of LNs and the trafficking of lymphocytes are introduced in a next chapter.

B. 1.1.3. Markers of lymphatic vessels

The lymphatic-specific markers help us to understand the study of LVs in healthy and diseased tissue. They include lymphatic vessel endothelial hyaluronan receptor-1 (LYVE-1), vascular endothelial growth factor receptor-3 (VEGFR-3), integral membrane glycoprotein podoplanin (PDPN), common lymphatic endothelial and vascular receptor 1 (CLEVER1), junctional adhesion molecule 1 (JAM1) and prospero homeobox 1 (PROX1)[217]. Here, I introduce more on the characters of PROX1 since I also utilized PROX1 as a lymphatic marker in the project.

Oliver et al. identified PROX1 in mice due to its homology to the Drosophila homeobox protein prospero [239]. PROX1 is a nuclear transcription factor for the early steps of LEC differentiations from the embryonic veins and remains required for lymphatic identity [217]. Beginning at embryonic day 9.5 (E9.5), a few scattered cells around the developing forelimb begin to express PROX1, and at E10.5, this expression is obvious in more cells [240]. Whereas ECs lining one side of the anterior cardinal vein start to express PROX1, ECs position on the other side remain PROX1-negative [240]. At E12.5, the number of PROX1-positive cells, which also express LYVE-1 and VEGFR-3, is substantially increased, whereas LYVE-1 and VEGFR-3 expression is no longer apparent in ECs of the veins [241]. These findings strongly suggest that the expression of PROX1 in the subset of cardinal vein ECs directs the initiation of a program leading to the genesis of the lymphatic vascular system [240]. The lack of PROX1 can block the development of LVs and lymphatic networks in mice [240].

Concerning other markers, LYVE-1 is an integral membrane glycoprotein and a useful marker for identifying lymphatic capillaries [217][242]. It is an important component of ECM and a key molecule in cell migration during inflammation, wound healing, and tumorigenesis [217]. For example, LYVE-1 deletion impairs DC migration to skin-draining LNs [243]. VEGFR-3 plays a critical role in embryonic cardiovascular development and is thought to be expressed exclusively on the lymphatic endothelium, high endothelial venules (HEVs), and rarely on adult vascular endothelium [244]. It is the quintessential lymphatic receptor tyrosine kinase binding VEGFC and VEGFD, which is crucial for LEC proliferation and migration in embryos and adults [217]. In embryos, VEGFR-3 is initially expressed in all vasculature, but during development, its expression in blood vessels decreases and becomes restricted to the developing LVs. Therefore, it is thought to be expressed almost exclusively by the lymphatic endothelium and is thus considered a major regulator in lymphangiogenesis [244]. CLEVER1 is expressed in alternatively activated macrophages and in sinusoidal ECs in various tissues such as liver, spleen and LN [245]. CLEVER1 has been shown to function as a scavenger receptor for acetylated low density lipoprotein (ac-LDL) and its derivatives [246]. It plays a role in angiogenesis and, most recently, and has been hypothesized to function

as an adhesion molecule for leukocyte and tumor cell trafficking in the lymphatic system [245][247]. JAM is an intercellular adhesion molecule that belongs to the Ig superfamily [248].

B. 1.2. Lymph node

B. 1.2.1. The structure of lymph node

LNs are found in groups that follow the routes of LVs [223]. They generate highly specialized microenvironments for mounting effective immune responses [249]. The function of LNs is to filter the lymph coming from the draining area and to scan the lymph for antigens [250]. There are many immune responses initiated in LNs in mammals. In brief, antigen-loaded DCs from the draining area via the afferent lymphatics present their antigens to T lymphocytes in the T cell zone (in the paracortex in the LN). T cells, which are T cell receptor-specific for the presented antigens, are activated, and after that, they differentiate and proliferate. Activated T helper cells migrate into the B cell zone (in the cortex in the LN) to assist B cells. These antigen-specific B cells differentiate into plasma cells for effective antibody production. Activated $CD4^+$ helpers or $CD8^+$ T cytotoxic cells, migrate to the medulla, from where they leave the LN through efferent lymphatics and travel via the blood system to the inflamed or endangered area of their specific draining area (Fig. B2)[250]. In the LNs, the majority of cells are leukocytes; and the other cells are the non-leukocytic stromal cell types, which include blood vessel endothelial cells (BECs), LECs, and fibroblastic reticular cells (FRCs). All cells are essential for the function of the organ [249]. The afferent LVs with circular cross-sectional profiles transform into several branched sinus systems lined by a layer of LECs. At the efferent side of the LN, lymphocytes use specialized lymphatic sinuses to enter the efferent lymphatic vasculature, which finally drains these cells back into the blood circulation. Many lymphocytes enter the LN from the blood via HEV, which are lined by unique BECs that are specialized for supporting the multistep leukocyte extravasation cascade [249][251]. FRCs wrap paracortical collagen conduits and provide a responsive scaffold that supports leukocyte survival, migration, and LN expansion [252]. Along these FRCs linking conduits, the migratory path of mature antigen-presenting DCs intersects naïve and memory-circulating T lymphocytes that enter LNs via HEV [252]. Our previous results show that LecB can block epithelial cell migration [5][10]. In the previous Ph.D. project of Dr. Janina Sponsel, she has found that LecB can bind to LECs in the LN *in vivo*, which rasies my hypothesis that if LecB blocks DCs migration to the LN, this would result in the fewer activated T cells in the LNs. In my second part of the project, I focus on the DCs migration and T cell activation in the LNs exposed to LecB.

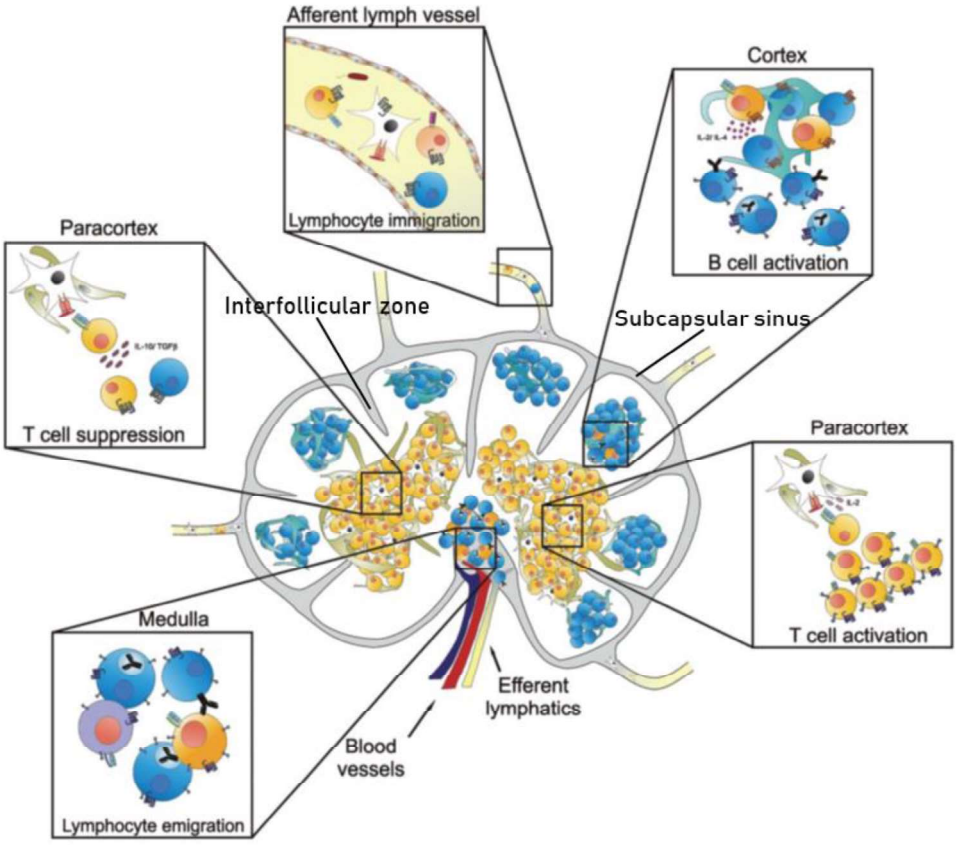

Fig. B2: Schematic of the lymph node.

LNs are the sites where immune activation or suppression takes place. Within the paracortex of the LN, DC present antigens to T cells which proliferate and differentiate into effector or memory T cells after recognizing the specific antigen whereby an immune response is initiated. B cell activation occurs in the B cell follicles (in the cortex). Activated B cells and T cells migrate to the medulla to leave the LN through the efferent lymphatics [250].

LN lymphangiogenesis, the proliferation of LECs within the subcapsular sinus (SCS), interfollicular zone, and medulla, is a common feature of non-malignant, immune-reactive LNs and is hypothesized to improve DC migration through changes in lymph flow [252–254]. In detail, the CC chemokine receptor (CCR) 7 and its ligands C-C linked chemokine (CCL) 19 and CCL21 control a diverse array of migratory events in adaptive immune function [255]. These chemokines are generally considered 'homeostatic' as they are constitutively produced and are not normally induced by inflammation [255]. The primary sources of CCL19 and CCL21 are a variety of stromal cells within primary and secondary lymphoid organs, while CCL21 is also expressed in LECs in peripheral tissues [255]. LECs form the boundaries of the SCS and create and maintain chemokine gradients, like CCL21, that direct DC migration toward the paracortex for antigen presentation to T cells [252]. The ECs within HEVs express peripheral node addressins (PNAd) and transmembrane glycoproteins required for $CCR7^{+}$ naïve and central memory T lymphocyte adhesion,

rolling, and transmigration [252]. Moreover, the absence of CCR7 on DCs is shown to abolish DC transmigration across the SCS into the LN parenchyma [256, 257]. In terms of CCL19, it is produced by activated DCs, FRCs, and HEVs in secondary lymphoid organs [256]. It has been reported that CCL19$^{-/-}$ mice reveal no defect in DC migration through dermal LVs, and induce T cell activation [258]. To sum up, the primary function of the CCR7/CCL19/CCL21 axis is to establish and propagate anatomical microenvironments conducive to cognate interactions between antigen-presenting cells (APCs) and antigen-specific lymphocytes, an important process in effective adaptive immune system function [255]. In addition, VEGF family members are homodimeric glycoproteins that are mitogenic for ECs and are angiogenic factors that act via the endothelial-specific receptor tyrosine kinases [259]. They include VEGFB, VEGFC, and VEGFD, which are all sufficient to activate lymphangiogenic responses in LNs (Fig. B3)[252]. VEGFB recognizes VEGFR1, VEGF is the ligand of both VEGFR1 and VEGFR2 [260], while VEGFC and VEGFD were first identified as ligands of the tyrosine kinase receptors VEGFR2 and VEGFR3 [259]. In detail, both VEGFR1 and VEGFR2 act early during endothelial differentiation although with different functions [259]. It has been reported that VEGFR1$^{-/-}$ embryos die because of excessive endothelial proliferation [261] and VEGFR2$^{-/-}$ embryos die with no endothelial or hematopoietic cells [262]. VEGFC binds to its receptor VEGFR3 that is mainly expressed in LECs after embryogenesis [263], which results in the transduction signals that promote LEC survival, proliferation, and migration [260]. Other mediators include VEGFD, which also binds to VEGFR3, fibroblast growth factors, ephrin-B2, and hyaluronic acid [263, 264]. VEGFR2 is crucial for the development of blood vasculature, while VEGFR3 plays vital roles in the growth and remodeling of blood vessels [265]. To sum up, VEGFR signaling is essential for lymphangiogenic responses.

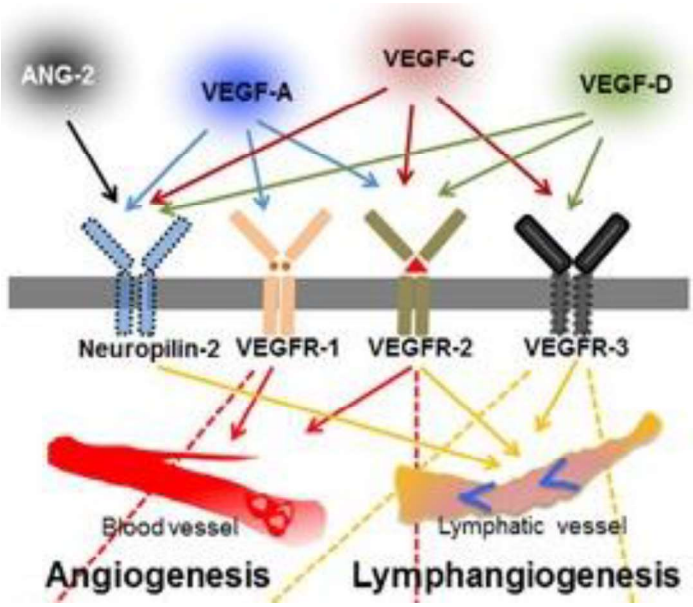

Fig. B3: Schematic illustration showing the interaction of specific cytokines and their receptors.

Postnatally, blood vessels express VEGFR1 and VEGFR2, while the lymphatic endothelium expresses VEGFR2, VEGFR3, and Neuropilin-2. These receptors play a significant role in tumor vessels, as their binding induces specific phosphorylation events. Consequently, VEGFA, VEGFC, VEGFD, and ANG-2 emerge as crucial cytokines that promote lymphangiogenesis in both blood vessels and LVs [266].

B. 1.2.2. Lymphocytes entering into the lymph node via afferent lymphatic vessels

A hallmark of lymphocytes is their ability to recirculate between the bloodstream and secondary lymphoid organs [267]. Lymphocytes enter the LN via afferent LVs (Fig. B4) or from the blood through the HEVs [249]. It has been observed that T lymphocytes are the most common cell type in afferent lymph, 80%--90% [256]. From a model of a LN in a sheep, it has been known that naïve T cells home to LNs via HEVs, which led to a model that effector and/or memory T cells, but not naïve T cells, home to LNs via afferent lymphatics [268, 269]. Nevertheless, it is different in the mouse model of LNs. Naïve T cells enter into the afferent LV draining towards a popliteal LN, the cells not only home to the T cell zone of the popliteal LN but also to the T cell areas of LNs that are located further downstream, such as the medial iliac LN [257][269]. Interestingly, Tomura et al. have found that T lymphocytes can migrate from one LN to another LN via lymphatics [270]. In these T lymphocytes, the majority are $CD4^+$ T cells, while $CD8^+$ T cells are only found in small numbers [256]. On the one hand, $CD4^+$ T cells play critical roles in mediating adaptive immunity to a variety of pathogens [271]. On the other hand, they help B cells make antibodies, enhance and maintain responses of $CD8^+$ T cells, regulate macrophage function, orchestrate immune responses against a wide variety of pathogenic microorganisms, and regulate immune responses [271]. As for $CD8^+$ T cells, they are vital effectors of the adaptive immune system and play a crucial role in combating intracellular pathogens and cancers [272]. Antigen-specific $CD8^+$ T cells are identified by $B220^+$ B cell follicles in the LN [272]. $CD4^+$ T cells and $CD8^+$ T cells both recognize their respective antigens on the same DC [273]. Antigen-specific contact with the $CD4^+$ T cell enables the DC to optimize antigen presentation and deliver specific cytokine and co-stimulatory signals to the $CD8^+$ T cell that promote its clonal expansion and differentiation into an effector or memory T cell [273]. There are some key molecules involved in the migration of DCs into the LN. CCR7 and its ligand CCL21 are well-known as the predominant pathway involved in T cell egress from peripheral tissue via afferent LVs in a steady state and inflammation [274]. For example, around 50% of skin-associated $CD4^+$ T cells express CCR7, and almost all migratory T cells are CCR7 positive [275]. In addition, T cells also use various adhesion molecules, like CLEVER1, for their migration through afferent lymphatics [274]. CLEVER1 is expressed by both efferent and afferent LVs and has been shown to be important for T cell entry into afferent LVs [276, 277]. It has been reported that the KD of CLEVER1 significantly decreases skin egress of $CD4^+$ and $CD8^+$ T cells to the dLN *in vivo* [276, 277]. Meanwhile, lymphatic-expressed ICAM1 and VCAM1 are vital for T cell migration to dLNs [274]. For example, VCAM1 antibody co-injection prevents Treg but not $CD4^+$ T cell migration from footpads to draining LN *in vivo* [278]. The blockage of ICAM1 can reduce T cell adhesion, crawling, and transmigration across lymphatic endothelium and decrease T cell advancement from capillaries into lymphatic collectors of skin explants [279].

DCs are also frequently found in afferent lymph; their proportion with other cells is estimated at 5--15% [256]. The trafficking of DCs to LNs through afferent LVs is crucial for the execution of their functions [280]. It has been demonstrated that both bone marrow and skin-derived DCs directly enter the LN parenchyma through the floor of the afferent side of the SCS, primarily via the interfollicular regions [269][281]. Besides, DCs that migrate via afferent lymphatics to dLNs, also resident DCs exist in secondary lymphoid organs [274]. For example, resident DCs can take up and present antigen that has arrived in dLNs in the absence of a 'cell-transporter' via afferent lymphatics [274][282]. Interestingly, resident and migratory DCs also display differences in the activation of the type of T cells. For example, migratory DCs are shown to activate $CD4^+$ but not $CD8^+$ T cells in dLNs [283]. In comparison, resident DCs prime $CD8^+$ T cells in a delayed manner, helped by the already activated $CD4^+$ T cells [274][283]. During the migration of DCs into the LN via afferent lymphatics, there are lots of factors involved. On the one hand, for example, DCs need to activate and upregulate the chemokine receptor CCR7, which guides their migration toward lymphatics [274]. CCR7 is upregulated on both DCs in response to a maturation-inducing stimulus and on semimature DCs migrating in steady-state conditions [274][284]. Moreover, CCL21 is involved in the trafficking of DCs as well. Both KDs of CCR7 and CCL21 have been shown to severely impair DC migration to dLNs [285]. On the other hand, some adhesion molecules mediate DC migration. For example, JAM1 is expressed by DCs and the lymphatic endothelium. JAM1 helps DC migration to the LN via afferent lymphatics [280], and the absence of JAM1 can increase the process of DC migration with the positive regulation of β1-integrin expression by JAM1 [286]. It has been reported that plasmacytoid DC migration to regional LNs is mediated by interactions between integrins on plasmacytoid DCs and JAM1 on HEVs of regional LNs [287]. Meanwhile, other integrin ligands, like ICAM1 and VCAM1, can influence DC migration. Blockage of VCAM1 and ICAM1 is shown to diminish DC migration to dLNs [274][288]. In my second part of the project, I will study lymphocyte entry via afferent LVs since Dr. Janina Sponsel has found that LecB can induce phenotypical changes in LECs and LecB is captured by dLNs.

B. 1.2.3. T cells activation by dendritic cells

DC subsets are exposed to the antigen, and after DCs enter from afferent lymph, migratory DCs join the network of the largely sessile LN resident DCs, which are embedded in the stromal network of the T cell zone [289]. DC migration is characterized by a pronounced CCR7-mediated directional movement towards the SCS of the LN, where they cross the SCS floor in a CCR7-independent manner [269][290]. After that, migratory DCs enter the interfollicular zone of the LN and enter the deep T cell zone [290]. Then, DCs interact with naïve T cells and prime the T cells [267].

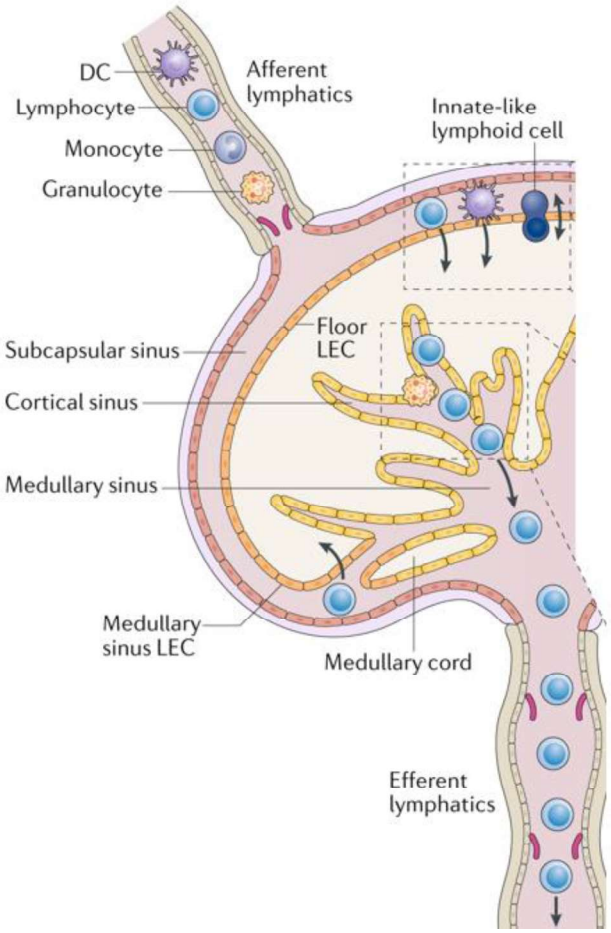

Fig. B4: Leukocyte entry and exit through lymphatics in the lymph node.

DCs and T cells enter the dLN through the floor LECs in the SCS. Lymphocytes migrate into the LN parenchyma via the medullary sinus LECs. In the subcapsular sinus, innate-like lymphoid cells undergo constant patrolling between the sinus lumen and parenchyma below the floor LECs. Granulocytes can adhere to the cortical and medullary sinuses. Lymphocyte egress from the LN takes place mainly via the cortical sinuses. The best-characterized adhesive and chemotactic signals involved in trans-sinusoidal leukocyte traffic [249].

DCs are the most potent APCs, for naïve T cell activation. The cellular contact between a T cell and a DC provides the opportunity for antigen recognition to occur through T cell receptor (TCR) interactions with peptide, and major histocompatibility complexes (MHC), which are present at the DC surface (Fig. B5)[291]. Individual TCRs are capable of recognizing different ligands, such as self-peptides and foreign peptides, with a broad range of affinities [292]. The TCR has one α-chain and one β-chain forming a heterodimer that confers ligand binding specificity to the TCR [293]. Most αβ TCRs recognize short peptides that are expressed on the APC surface bound to MHC class I molecules, which are recognized by $CD8^+$ T cells, or MHC class II molecules, which are recognized by $CD4^+$ T cells [293]. αβ heterodimers

associate with CD3 and its three polypeptides and expressed in all T cells, including CD3γ, CD3δ, and CD3ε [292, 293]. TheCD3γ, CD3δ, andCD3ε subunits are genetically related to each other, belonging to the C-type Ig superfamily [293]. TCR signaling plays a critical role in the lineage specification and development of T cells [292]. TCR-CD3 subunits undergo a finely regulated process of assembly and secretion via the endoplasmic reticulum (ER) and the Golgi apparatus. After the synthesis and assembly, TCR-CD3 subunits are expressed on the cell surface [293]. TCR-CD3 complexes are not stable but continuously traffic between the plasma membrane and endosomal compartments, undergoing constitutive rapid cycles of endocytosis and recycling before eventually being degraded in lysosomes [293, 294] TCR signal transduction is involved in several cellular processes. For example, TCR triggers Ca^{2+} calcineurin signaling, resulting in nuclear translocation of the nuclear factor of activated T cells [295]. TCR activates NF-κB signaling, resulting in nuclear translocation of the REL and NF-κB transcription factors [296]. TCR also induces MAPK signaling, resulting in actin polymerization and the activation of the transcription factors FOS, JUN, and activator protein 1 (AP-1)[292].

In my second part of the project, I utilized CD45.1 x OT-II TCR transgenic mice to generate transgenic $CD4^+$ recognizing an ovalbumin (OVA)-derived peptide. OT-II mice are frequently used as a transgenic strain-specific model to assess T cell help for responses to antigen presenting cells [297]. OT-II $CD4^+$ T-cells express transgenic OVA-specific αß-TCRs [297]. I also generated DCs from bone marrow precursors (BMDCs) matured by LPS. DCs can be devided into two subtypes: plasmacytoid DCs and myeloid DCs [298]. In mice, $CD8\alpha^+$ DCs present cytosolic chimeric antigens on the MHC class I, which induces $CD8^+$ T cell activation and differentiation into cytotoxic T cells [299]. While, $CD8\alpha^-$ DCs process extracellular chimeric antigens presenting them via MHC class II receptors to induce $CD4^+$ T cell activation to helper T cells [298]. As *in vitro*-differentiated DCs, BMDCs cannot be readily classified into DC subsets [300]. In my project, BMDCs were harvested, and 2×10^5 BMDCs were injected into ears and footpads of CD45.2 mice, which had received an intravenous injection of 10×10^6 $CD4^+$ T cells from CD45.1 x OT-II F1 mice. Allelic variants of the pan-haematopoietic cell marker CD45 (Ptprc), identified as CD45.1 and CD45.2, have been established as a marker system to track haematopoietic cells following congenic mouse bone marrow transfers [301]. Different isoforms of CD45 have been identified in mice, and the common form is CD45.2, which is expressed by C57BL/6 mice, and is encoded by the $Ptprc^b$ allele. An additional allelic variant, $Ptprc^a$, which translates to the CD45.1 form of the surface protein, has been identified in the SJL mouse strain [302]. This CD45.1 allele has been successfully backcrossed on to the BL/6 mouse background and has been widely used in immunological studies to track the contribution of specific genes to haematopoietic cell development [303]. CD45.1 and CD45.2 cells are widely used in transplant and adoptive transfer studies to track the donor and host cells. For example, CD45.1 bone marrow cells can be transferred into a CD45.2 host mouse and then identified with an antibody specific for CD45.1 at a later point in lymphoid tissues for infiltration and development into mature lymphocytes [304]. The CD45.1 specific antibody does not react with leukocytes expressing CD45.2, this is the reason why I generated BMDCs from CD45.1 xOT-II mice to inject into CD45.2 x OT-II mice.

In addition to the interaction between TCR and MHC complexes, DCs express important stimulators for T cell activation, such as the B7 family molecules: CD80 (B7-1) and CD86 (B7-2)(Fig. B5), playing an important role in either tolerogenic or immunogenic responses [305]. In detail, T cells express the CD28 receptor on their surface as the main responsible molecule for binding to the B7-1 and B7-2 molecules [305]. CD28 induces several intracellular processes, such as the production of cytokines and the transduction of signals triggering T cells to survive or to differentiate [306]. The interaction between CD28L/B7 induces the secretion of IL-2 and interferes with the tolerogenic property of immature DC [307]. This occurs primarily by decreasing the induction of Tregs and also by leveraging the differentiation of effector T cells [305][307]. The cytotoxic T lymphocyte antigen-4 (CTLA-4) molecule, also known as CD152, acts as an inhibitory receptor of the immune response [308]. Moreover, CTLA-4 shares homology with CD28, competing for binding their ligands, CD80 and CD86 [306]. The binding affinity of CTLA-4 for these ligands is stronger than its affinity for CD28, which indicates that CTLA-4 blocks the interaction between CD28 and B7, providing a negative signal to T lymphocytes, thus inhibiting the immune response [305, 306]. Under this competition, CD80 preferentially binds to CTLA-4, and this interaction during antigen presentation can result in IL-10-dependent TGF-$\beta 1^{+}$ regulatory T cell induction [309].

In addition, the interaction between CD40 and CD40 ligand (CD40L), expressed on DCs and T cells, respectively (Fig. B5), is strictly related to immune response [305]. CD40, initially characterized in B cells, is expressed by DCs, monocytes, platelets, and macrophages, as well as by non-hematopoietic cells such as myofibroblasts, fibroblasts, epithelial, and ECs [310]. CD40L, also known as CD154, is a member of the TNF superfamily and is expressed primarily by activated T cells, as well as some activated B cells and platelets [310]. The engagement of CD40 by CD40L promotes the clustering of CD40 and induces the recruitment of adapter proteins, TNFR-associated factors (TRAFs), to the cytoplasmic domain of CD40. The TRAFs activate different signaling pathways, including NF-κB signaling, MAPK signaling, and PI3K signaling [310].

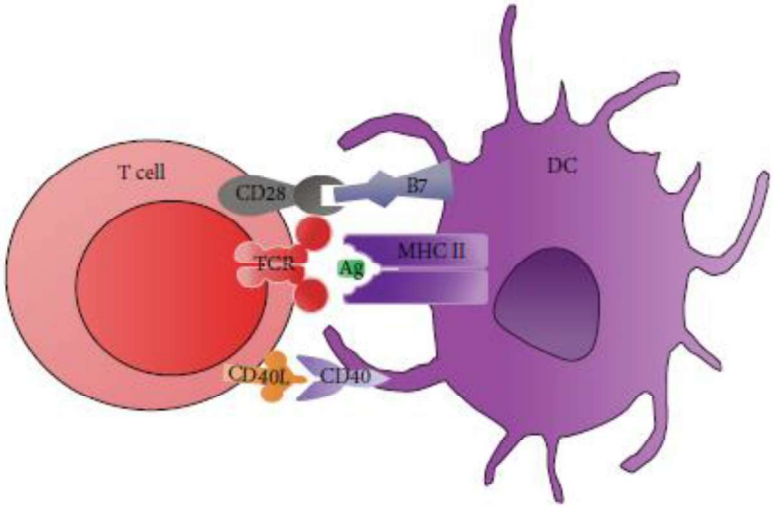

Fig. B5: Schematic representation of the dendritic cell and T cell interaction.

Activation of T cell involves both interactions between the TCRs, CD28 with their cognate ligands, CD80, and CD86 as well as the CD40L/CD40 pathway. Other costimulatory molecules, such as OX40/OX40-L and TIM-1 and PD-1/PD-L1, are not represented here [305].

B. 1.3. Endothelial cells

B. 1.3.1. Lymphatic endothelial cells

The majority of LN cells are leukocytes, but the organ also comprises different non-leukocytic stromal cell types, including BECs, LECs, and FRCs [249]. Within the LN, the SCS spans the whole LN cortex, which includes both B cell follicles and interfollicular areas, and is lined by LECs on both sides [249]. The LECs facing the capsule are called ceiling LECs, and those overlaying the lymphocyte-containing LN parenchyma are called floor LECs [269]. On the opposite side, the medullary sinus LECs form the sinus-facing surface of the medullary cords, which primarily contain lymphocytes and macrophages [249]. The afferent and efferent LVs with circular cross-sectional profiles transform into several branched sinus systems lined by a layer of LECs [249]. These hints indicate that LECs are essential in the LNs and LVs. I utilize a 10.1.1 antibody, which recognizes murine LEC surface protein calcium-activated chloride channel regulator 1 (CLCA1)[311]. Moreover, murine CLCA1 is also expressed on collecting and initial lymphatic vessels [312] as well as on splenic red pulp stromal cells and thymic medullary stromal epithelial cells [313]. Furuya M et al. have found that the role of murine CLCA1 is as an interacting partner for LFA1 to mediate lymphocyte adhesion to LECs, as treatment of LECs with the 10.1.1 antibody significantly reduced lymphocyte adhesion *in vitro* [314]. The 10.1.1 antibody activates lymphatic endothelium *in vitro*, and also rapidly induces LN lymphangiogenesis *in vivo*, suggesting a role for murine CLCA1 in regulation of LN lymphatic sinus growth [311].

The LEC layer is likely continuous without any open gaps, allowing direct material exchange between the sinus lumen and LN parenchyma [249][315]. Inter-LEC junctions in LNs contain both components of AJs and tight junctions, and the cells are underlined by a basement membrane [316]. ECs lining the vessel wall are connected by adherens, tight and gap junctions, and endothelial junctional proteins that play vital roles in tissue integrity but also vascular permeability, leukocyte extravasation, and angiogenesis [317]. For example, VE-cadherin is specific to ECs [318]. This is why I included VE-cadherin in the research on the influence of LecB on ECs. VE-cadherin is the transmembrane component of endothelial AJs [319]. VE-cadherin plays a multitude of roles in ECs, including the function of cell-cell adhesion and interaction, as well as transmembrane signal transduction [226]. It has been demonstrated that LV permeability increases significantly for both small and large solutes when vessels are exposed to VE-cadherin inhibition [320]. It suggests that vascular permeability is intimately linked with immune cell transportation, which is also the reason why I focus on VE-cadherin in my second part of the project. In addition, the VE-cadherin cytoplasmic tail is regulated by phosphatases and kinases, which modify protein function, signaling, and junctional permeability, resulting in the activation of vascular signaling pathways and ECs transmigration [321]. For example, VE-cadherin binds to kinase Csk at Y645, leading to the inactivation of Src [322]. The

three structural determinants of EC barrier integrity include: (1) actin stress fibers, (2) the submembranous cytoskeleton, and (3) the cortical actin ring (Fig. B6)[323]. The cortical actin ring provides centrifugal force to support and stabilize the EC membrane outwardly to allow contact with neighboring cells and the basement membrane [324]. Furthermore, the cortical actin ring facilitates the formation of lamellipodia, sheet-like lateral protrusions of the cell membrane, induced by rapid, branched actin polymerization and filament network formation [325]. With regards to other cytoskeleton proteins, the binding of the FAK FERM domain to the VE-cadherin cytoplasmic tail and the direct FAK phosphorylation of β-catenin at Y142 facilitates VE-cadherin-β-catenin dissociation and EC junctional breakdown [114]. As opposed to β-catenin, plakoglobin binds to either α-catenin or desmoplakin and vimentin [317]. It indicates that the VE-cadherin complex interacts more strongly with the vimentin cytoskeleton in this context [317]. In the previous Ph.D. project of Dr. Janina Sponsel, she has found that LecB can reduce VE-cadherin protein level and causes cortical actin ring formation in HUVECs. However, it remains unknown if LecB affects other cytoskeletons, like F-actin and FAK.

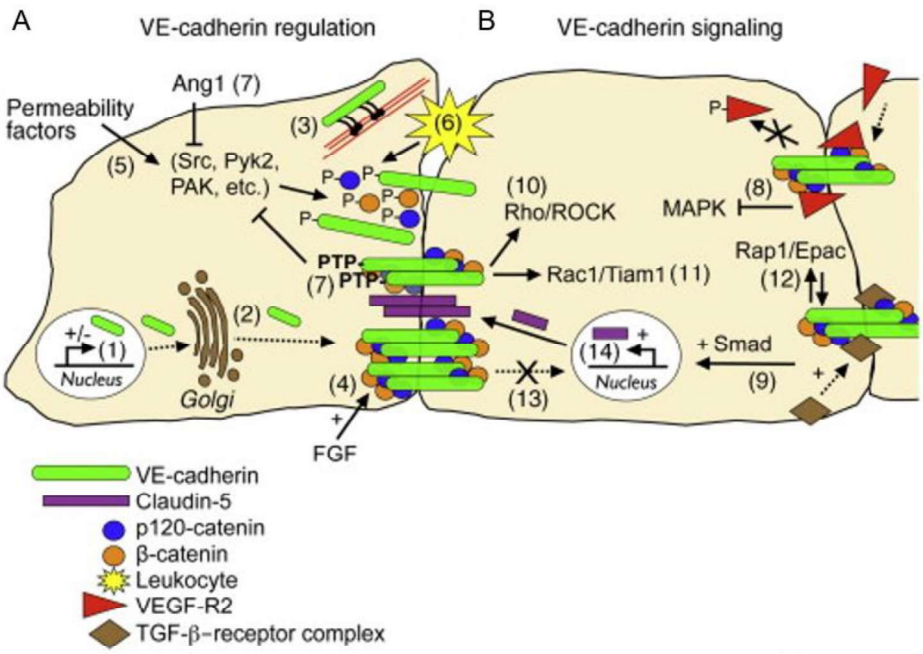

Fig. B6: Schematic of VE-cadherin regulation and signaling.

For simplicity, only p120-catenin and β-catenin are shown bound to VE-cadherin, excluding plakoglobin and α-catenin. (A) The mechanisms modulating VE-cadherin activity are as follows: (1) Changes in VE-cadherin gene expression through the activity of transcription factors Erg/Ets-1, TAL-1/SCL, and Twist/Slug/Snail. (2) Trafficking via Golgi-associated protein cPLA2α. (3) Transport along actin filaments facilitated by myosin-X. (4) Stabilization at the plasma membrane by p120-catenin, enhanced by FGF. (5) Phosphorylation induced by permeability factors, signaling through various kinases to promote adherens junction complex disassembly and/or VE-cadherin internalization. (6) Phosphorylation induced by leukocytes, promoting adherens junction complex disassembly. (7) Inhibition of

phosphorylation by protein tyrosine phosphatases or Ang1. (B) Regarding intracellular signaling through VE-cadherin, the following mechanisms are implicated: (8) Indirect binding to VEGF-R2, preventing its phosphorylation, internalization, and signaling to MAPK. (9) Binding to and assembly of the TGF-β receptor complex, enhancing Smad-dependent transcription. Signaling through small GTPases includes: (10) Rho/ROCK, promoting actomyosin contraction. (11) Rac1/Tiam1. (12) Rap1/Epac. Indirect regulation of gene transcription occurs by: (13) Limiting the amount of p120-catenin and β-catenin that can translocate to the nucleus. (14) Inhibiting FoxO1, leading to an increase in claudin-5 mRNA [326].

B. 1.3.2. Human umbilical vein endothelial cells

Many BECs in the laboratory use are from venous ECs [327]. Thus, I utilized HUVECs to verify the effect of LecB on ECs *in vitro*. EC monolayer forms a selective semipermeable barrier regulating the trafficking of macromolecules and blood cells across the vessel wall [328]. Important regulators of EC barrier function are the actin-myosin-based EC contractile machinery and actin cytoskeleton-anchored AJs consisting of VE-cadherin and catenins linked to the actin cytoskeleton [329, 330]. For example, a modified cAMP analogue 8-pCPT-20-O-Me-cAMP is an exchange protein directly activated by cAMP (EPAC) agonist. It simultaneously activates diverse signaling pathways in HUVECs, which has differential effects on endothelial barrier function, including the reorganization of the actin cytoskeleton to the cell periphery, the enhanced VE-cadherin localization at cell-cell junctions, and dephosphorylation of myosin light chains [329]. Intriguingly, the phosphorylation of VE-cadherin is involved in the endothelial adhesive mechanism [331]. For example, the overexpression of tyrosine/phenylalanine replacement mutants of VE-cadherin for either Y731 or Y658 in HUVECs inhibited transendothelial migration of leukocytes, indicating that phosphorylation of specific residues is involved in leukocyte extravasation [332]. Besides, small GTPases and other molecules can affect VE-cadherin adhesiveness in ECs. Rac has been described as blocking as well as promoting thrombin-induced permeability in HUVECs [331]. Meanwhile, Cdc42 was suggested to stimulate the interaction between α-catenin and ß-catenin, thereby preventing the increase of permeability in lung endothelium caused by a dominant negative form of VE-cadherin [333]. It suggests that the linkage of VE-cadherin to the actin cytoskeleton is the mechanism by which cadherin-mediated adhesion occurs in ECs. Therefore, some cytoskeleton proteins, like F-actin and FAK, were included in investigating VE-cadherin-mediated endothelial AJs induced by LecB.

B. 1.3.3. The endothelial adherens junctions

The endothelium is located at the inner side of all vessel types and is constituted by a monolayer of ECs. Interendothelial junctions contain complex junctional structures, namely AJ, tight junctions (TJ), and gap junctions (GJ), playing pivotal roles in tissue integrity, barrier function, and cell-cell communication, respectively [317]. AJ, TJ, and GJ are often intermingled and form a complex zonular system with variations in depth and thickness of the submembrane plaque associated with the junctional structure [317][334].

Lots of proteins exhibiting homophilic adhesive activities are located at interendothelial contacts, such as VE-cadherin in AJ, claudins and occluding in TJ, or connexins in GJ [317].

AJs are cell-cell adhesion structures pivotal to morphogenetic processes, lineage specification, and proliferation [335]. Endothelial AJs are essential for maintaining vascular integrity. Disruption of AJs leads to vascular leakage, tissue edema, hemorrhage, and other vascular complications (Fig. B7)[336, 337]. The cytoplasmic domain of VE-cadherin is highly homologous to that of classic cadherins, such as N-cadherin or E-cadherin, and shares with them some intracellular partners such as p120-catenin or ß-catenin [338]. VE-cadherin downregulates the expression of N-cadherin and junctional localization in ECs through the PI3K-AKT signaling pathway [339]. It suggests that the cytoplasmic tail of VE-cadherin is responsible for N-cadherin exclusion from the AJs. In addition, the anchorage of junctional proteins to the cytoskeleton has a crucial role in the control of EC shape, movement, and permeability [338]. The relationship between VE-cadherin and actin cytoskeleton has been introduced before.

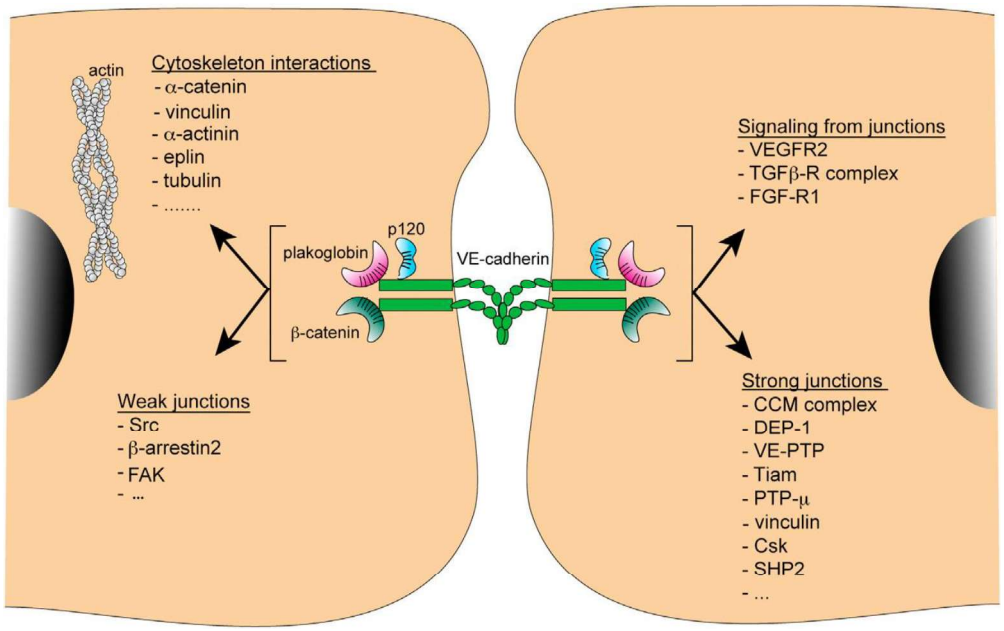

Fig. B7: Multiple Functions of adherens junctions in endothelial cells.

The organization of AJs is provided by VE-cadherin, which is linked through its cytoplasmic domain to p120-catenin, ß-catenin, and plakoglobin. These proteins assemble in diverse complexes and have different functions. The interactions of VE-cadherin with the growth factor receptors VEGFR2, FGFR1, and the TGFß-R complex modulate their downstream signaling. The cytoskeletal remodeling controlled by VE-cadherin is through its indirect interaction with various actin-binding proteins, such as α-catenin, vinculin, α-actinin, eplin, and others. In addition, the stability of the AJs is regulated by the clustering of VE-cadherin and its indirect association with different partners, such as Tiam, the CCM complex, and vinculin. Conversely, phosphorylation of VE-cadherin by Src or FAK, as well as the VE-cadherin interaction with ß-arrestin, induces junction weakening [338].

B. 2. Project objectives

The opportunistic pathogen *P. aeruginosa* is an important health problem. It increasingly develops resistance against existing treatment options. The virulence factors of *P. aeruginosa*, including the fucose-specific lectin LecB, can cause severe infections and immune responses in the host organism. According to the previous project of Dr. Janina Sponsel, she has found that LecB can bind to LECs in the LN *in vivo*, and LecB can reduce VE-cadherin protein level and causes cortical actin ring formation in HUVECs. However, the physiological consequence of LecB on the immune response is not well understood. Therefore, the overall aim is to investigate the effect of *P. aeruginosa* lectin LecB on immune response *in vivo* by focusing on the LN as the center for immune activation against infectious organisms.

The three significant aims are:

Aim 1: To investigate the interaction between LecB and LVs

LecB was shown to bind to LECs in the LN, indicating that LecB can be transported into the LN. However, the visualization of LecB entering or binding to the tissue capillary lymphatics at the site of injection was lacking. Therefore, I injected LecB-A488 into the mouse ear pinnae to check if LecB-A488 can drain into LVs and enter into the LNs.

Aim 2: To investigate the impact of LecB on immune cells, like T cells and DCs

I have known that LecB can block epithelial cell migration, and LecB can enter into the LNs after the injection. Therefore, I suspected that LecB would block immune cell migration in the LN as well. I analyzed DC migration into the T cell zone of LNs required for the activation of T cells.

Aim 3: To identify the underlying mechanism of the decreased VE-cadherin induced by LecB

To gain more insights into whether LecB alters ECs function, I utilized HUVECs. I have known that LecB can bind to HUVECs *in vitro*, and LecB reduces the expression of VE-cadherin in HUVECs. The underlying mechanism of the decreased VE-cadherin was unclear. I investigated cytoskeleton proteins, such as FAK and myosin.

B. 3. Summary of results and discussion

The results of my investigations were published in EMBO Reports, that I sign as second but equal contributing author. It is reprinted in chapter B.6., where I also discuss the data further. the data is discussed in full detail. Here, the major discoveries will be summarized, followed by an outline of my particular contributions.

B. 3.1. LecB binds to lymphatic vessels in skin *in vivo*

Since Dr. Janina Sponsel has observed that LecB binds to LECs in the LN, I wanted to uncover if LecB can bind to LVs in the skin from where LecB is probably transported into the LN. LecB-A488 was injected into the ear pinnae of *Prox1*^{CreERT2} *tdTomato*$^{Stop\text{-}flox}$ (*iProx-1tdT*) mice that express the red fluorescent tdTomato protein under the *Prox1* promoter active in LECs [340]. 4 h later, the ears were split and imaged by confocal microscopy. The results demonstrated that LecB colocalized with LVs and other cutaneous structures resembling blood vessels (publ. Fig 3A), indicating that the injected LecB in the skin drained into the LN via lymphatics. Therefore, the association of LecB with lymphatics raised the question of its physiological relevance in the context of a bacterial infection, which I present in a next chapter.

B. 3.2. LecB interferes with migration of dendritic cells and subsequent T cell activation *in vivo*

With regards to physiological relevance mediated by LecB, I investigate the DCs migration and T cell activation. First, I generated DCs from BMDCs, matured by LPS, fluorescently labeled, and injected into ears and footpads of mice treated twice with LecB on one side, while the other side was mock-injected with saline. For the culture of BMDCs, I co-cultured 10x10^6 bone marrow cells with 25 ng/ml of human fms-related tyrosine kinase 3 ligand (hFlt3L). Then, 1µg/ml OVA peptide was co-cultured with DCs for 18 h and 100 ng/ml LPS for 16 h before harvesting BMDCs after 8 days. I checked the BMDC generation from bone marrow progenitor cells by flow cytometry (Fig. B8). I could observe MHC-II$^+$ CD11c$^+$ B220$^-$ DCs, and during activation of BMDCs, BMDCs were seen as a CD86^{Hi} CD11c$^+$ cell population, which was between 20-40% in every experiment. The results showed that mature BMDCs could be generated *in vitro* from bone marrow cells.

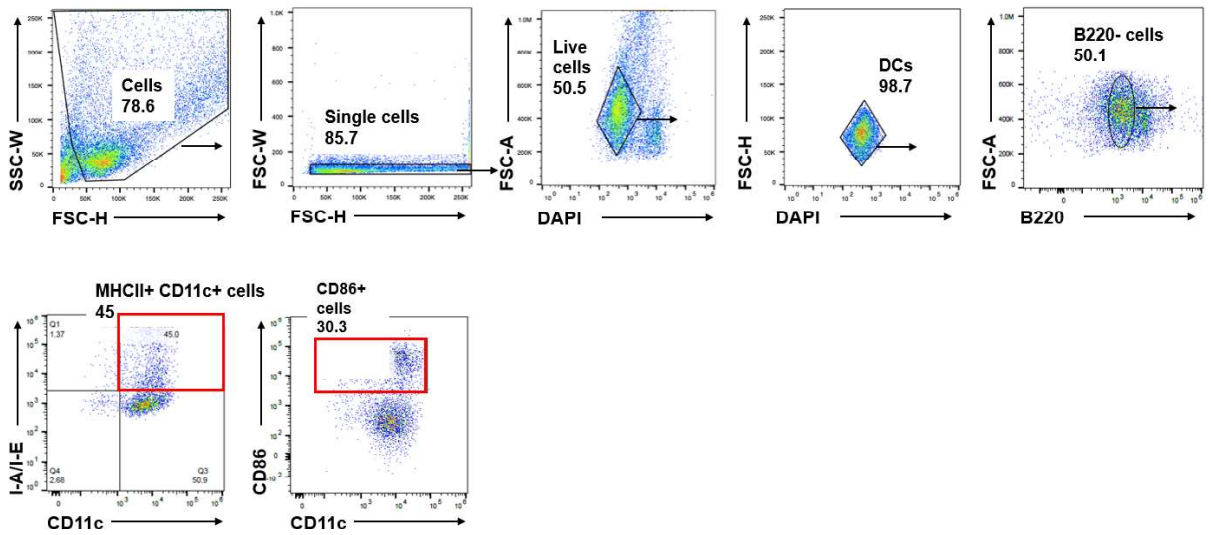

Fig. B8: Gating strategy verifying dendritic cells from bone marrow precursors.

Cells were stained with I-A/I-E-FITC, CD11c-PE, B220-PerCp-Cy5.5, CD86-APC, and DAPI. First DAPI$^-$ live cells were gated from single cells. Then, B220$^-$ cells were gated from live DCs. MHC II$^+$ CD11c$^+$ cells and CD86$^+$ cells were both gated from B220$^-$ cells.

Meanwhile, CD4$^+$ T cells from the CD45.1 x OT-II mouse were purified by the MACS system and stained by carboxyfluorescein succinimidyl ester (CFSE). CFSE was used to study cell proliferation in my project. This versatile dye is membrane permeant, so it enters into the cytoplasm where its acetate groups are removed by cellular esterases. Then, CFSE stably binds to the abundant amine groups present in cytoplasmic molecules, conferring a stable fluorescence intensity to cells which is equally divided between daughter cells after each division [341, 342]. Thus, I use a simple protocol to CFSE-labelled mouse T cells and analyze their proliferation *in vivo* by flow cytometry. CFSE$^+$ CD4$^+$ T cells were injected intravenously into a CD45.2 mouse. LecB was injected intradermally into the ear pinna and subcutaneously into the hind footpad on the right side of mice, and 5-6 h later, BMDCs were harvested and injected at the left and right side of mice. LecB was injected again at the same position after 24 h. Finally, after 4 days, auricular, popliteal, inguinal, and para aortic LNs were taken for further analysis as described in publ. Fig, 4B. Firstly, I used flow cytometric analysis to verify CD4$^+$ T cells labeled with CFSE staining. By staining for CD3e and CD4, I could distinguish CD45.1$^+$ CD4$^+$ T cells (data not shown).

In addition to the comparison between the control groups and LecB groups, some mice received an intraperitoneal injection of LecB inhibitor DH445, which was provided by Prof. Dr. Alexander Titz, Helmholtz Centre for Infection Research, Germany. After 4 days, the draining auricular and popliteal LNs were recovered, stained for CLCA1$^+$ lymphatics and B220$^+$ B cells. The number of BMDCs associated with lymphatics or localized within the central paracortical T cell zone, devoid of the peripheral B220$^+$ B cell

follicles, was assessed (publ. Fig 4C and D). In detail, I counted the number of BMDCs in the central paracortical T cell zone and the number in lymphatics via Image J software and did statics analysis. In the absence of LecB, the majority of BMDCs were found within the paracortex, which was not influenced by DH445. However, in the presence of LecB, many BMDCs failed to enter the T cell zone and were retained within the subcapsular lymphatics. Strikingly, DH445 reversed LecB-mediated inhibition of BMDC migration into the T cell zone.

To determine whether this abnormal migration alters T cell activation, I modified the above experiment as described in publ. Fig 4E. First, I checked the T cells population. Among live CD45.1$^+$ cells, T cells were distinguished as CD11c$^-$ CD3e$^+$ CD4$^+$ cell population (Fig. B9). The LNs were recovered, and the proliferation of CD45.1$^+$ T cells was assessed by measuring the CFSE label by flow cytometry (publ. Fig 4F). CFSE negative or low cells would indicate T cells having reduced the fluorescence intensity by cell division. The data, expressed as T cell proliferation, was normalized in each experiment to control mice or mice whose contralateral LN was not exposed to LecB (publ. Fig 4G). I found that LecB significantly reduced T cell proliferation and that this effect was reversed by the LecB inhibitor DH445. Taken together, the data uncovered the ability of LecB to inhibit the generation of adaptive immune response by restricting DC migration across lymphatics from the periphery to the LN T cell zone.

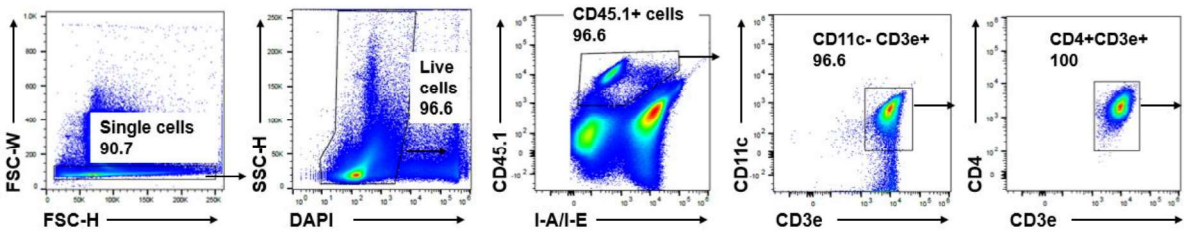

Fig. B9: Gating strategy showing isolation of T cells.

Cells were stained with I-A/I-E-APC, CD45.1-APC-Cy7, CD3e-PerCP-Cy5.5, CD4-AF700, and DAPI. First, DAPI$^-$ live cells were gated from single cells. Then, CD45.1$^+$ cells were gated from live cells, and CD11c$^-$ CD3e$^+$ cells were gated from them. Finally, CD4$^+$ CD3e$^+$ cells were selected for next injections into mice.

B. 3.3. LecB rearranges endothelial cell membrane and cytoskeleton *in vitro*

To investigate the effect of LecB on ECs on a molecular level, I utilized HUVECs as the experimental model. Since Dr. Janina Sponsel found that LecB reduced the protein expression of VE-cadherin, but the molecular mechanism behind it was unclear. As I introduce above, endothelial adhesion molecule VE-cadherin can bind to FAK FERM domain, resulting in EC junctional breakdown [114]. Thus, I wanted to investigate the localization and expression of VE-cadherin and the cytoskeleton proteins, such as F-actin, FAK, and myosin.

First, to determine the localization of VE-cadherin, FAK and F-actin, I performed immunofluorescence assay. HUVECs were untreated or exposed to LecB for 1 h or 3 h, stained for VE-cadherin, filamentous F-actin, FAK, and nuclei were colored with DAPI. The figures depicted that LecB perturbed the perimembranous area of VE-cadherin, F-actin, and FAK (publ. Fig 2E). In untreated cells, VE-cadherin was primarily distributed on the cell surface, forming AJs. However, in the presence of LecB, the location of VE-cadherin shifted into the cytoplasm and was often found in perinuclear positions. I analyzed VE-cadherin protein levels by western blot and found a time-dependent decrease (publ. Fig 2F). Concerning cytoskeleton proteins, visualizing F-actin with fluorescent phalloidin uncovered that LecB provoked the reduction in cellular stress fibers and the formation of a cortical actin rim. FAK was frequently displaced from a predominantly perimembranous location to an intracellular position after LecB (publ. Fig 2E). To get more information from the figures, I quantified the pixels and areas in each image of perimembranous and intracellular areas via Image J (Fig. B10). However, it was quite different in the quantification of VE-cadherin. The pixels and areas of VE-cadherin were subtracted by the counterpart of DAPI (white circle represented DAPI in Fig. B10). The histogram results showed that LecB significantly decrease the perimembranous expression of VE-cadherin, F-actin and FAK in HUVECs. Given the reduction of actin stress fibers that are central to cell mobility, I performed live imaging of HUVECs with Sir-actin exposed to LecB or left untreated. While untreated cells exhibited actin dynamics concomitant with cell motility, the 3 h LecB exposure left the cells sessile with low levels of polymerized actin (publ. videos EV1,2). To further explore the reduced cell contractility, I determined phosphorylation of the myosin regulatory light chain 2 that stabilizes myosin [288]. Western blot showed diminished myosin light chain2 phosphorylation at Ser19, and quantification of immunofluorescence revealed a loss in the perimembranous area after 3h of LecB exposure (Fig. B11).

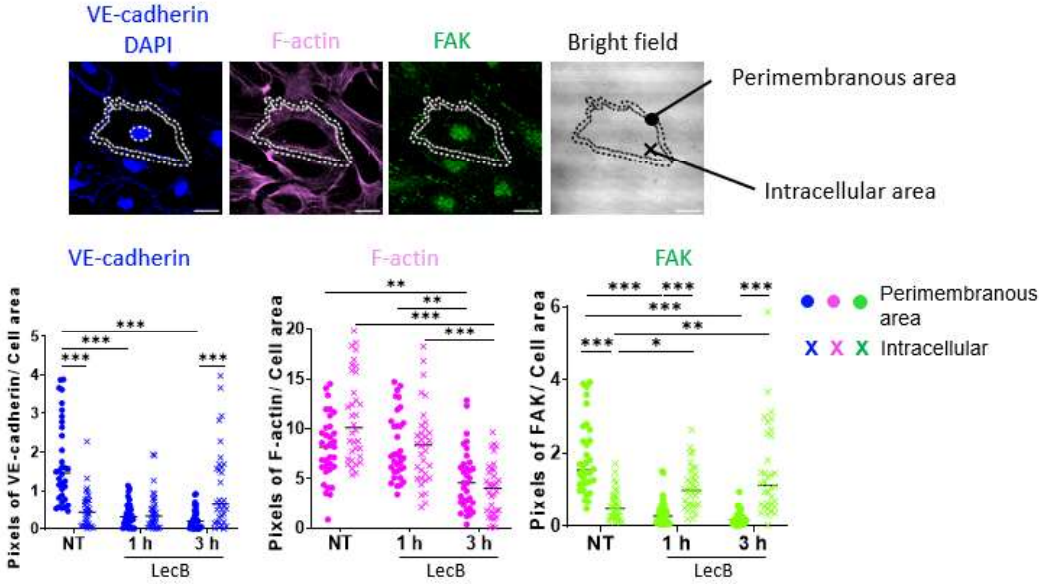

Fig. B10: Quantification of changes in adherens and cytoskelatal protein expression and subcellular localization in endothelial cells induced by LecB.

Top: HUVECs were stained with VE-cadherin, DAPI, F-actin and FAK, and the cell perimembranous and intracellular areas were identified on bright-field images. Bottom: The pixels of fluorescence of VE-cadherin, F-actin, FAK in these subcellular areas were determined for each cell using Fiji (ImageJ software) and normalized for cell surface area. For the intracellular VE-cadherin measures, the DAPI^{+} nuclear area was subtracted. The graphs depict these measures for each imaged cell. The data is expressed as ± SEM with each data point representing one cell. *P < 0.05, **P < 0.01, ***P < 0.001 as assessed by Kruskall-Wallis test. Scale bars, 20 µm.

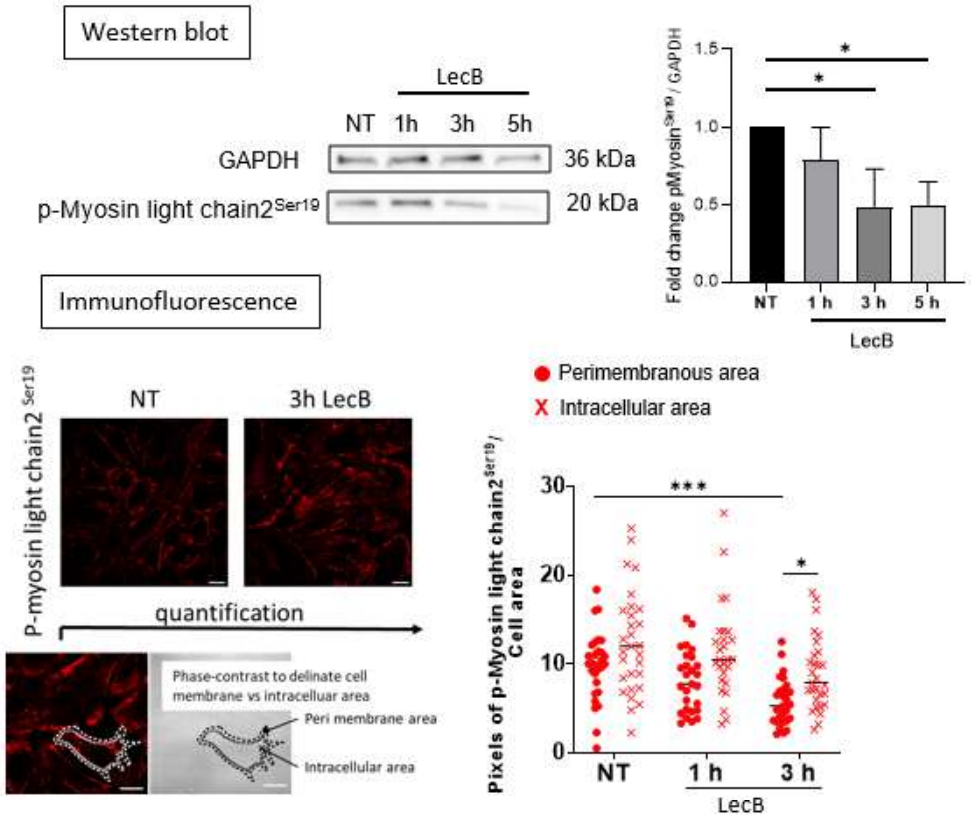

Fig. B11: LecB reduces myosin light chain phosphorylation.

Western blot analysis of p-Myosin light chain2 Ser19 and GAPDH in HUVEC lysates treated with LecB for the indicated times. Densitometric quantification of the western blot of p-Myosin light chain2 Ser19 relative to GAPDH. Below: Imaging and quantification of p-Myosin light chain2 Ser19 immunofluorescence of HUVECs NT or treated for 3h with LecB. The data is expressed as ± SEM. *P < 0.05, ***P < 0.001 as determined by the Kruskall-Wallis test with the NT condition.

Dr. Alessia Landi found that a strong cyclin D1 degradation, which led to the arrest of cell cycle and, thus, to the reduction of cell viability after 12 h LecB treatment in keratinocytes [9]. Thus, the reason for the reduction of perimembranous expression of VE-cadherin, F-actin, and FAK in HUVECs was unclear. One reason might be associated with the LecB treatment, while another reason might be related to the cytotoxicity of LecB, resulting in apoptosis in HUVESc. To determine the reason, I performed MTT and caspase-3 staining assays to assess the LecB toxicity. The results depicted that neither 1 h nor 3 h LecB treatment influenced cell viability of HUVECs, in comparison with positive controls, such as staurosporine and serum-free (Fig. B12.A). It has been reported that staurosporine can induce cell death and induces caspases-3/7 activity, and reduces the level of ATP in rat astrocytes [343]. Thus, I utilized caspase-3/7 green detection reagent to verify the cytotoxicity of LecB again. The results showed that, in positive control staurosporine groups, cells were stained with caspase-3 in green (Fig. B12.B). In contrast, cells were not stained with caspase-3 in green under the treatment of 3 h LecB (Fig. B12.C), indicating that LecB had no toxicity to HUVECs. In conclusion, LecB reorganizes the VE-cadherin positive adherens junction and the associated FAK and F-actin cytoskeleton with reduced myosin regulatory light chain phosphorylation, which would have a negative impact on cell contractility and therefore on leukocyte diapedesis. Moreover, it was not because of LecB toxicity perturbing perimembranous area of VE-cadherin, F-actin, and FAK in HUVECs.

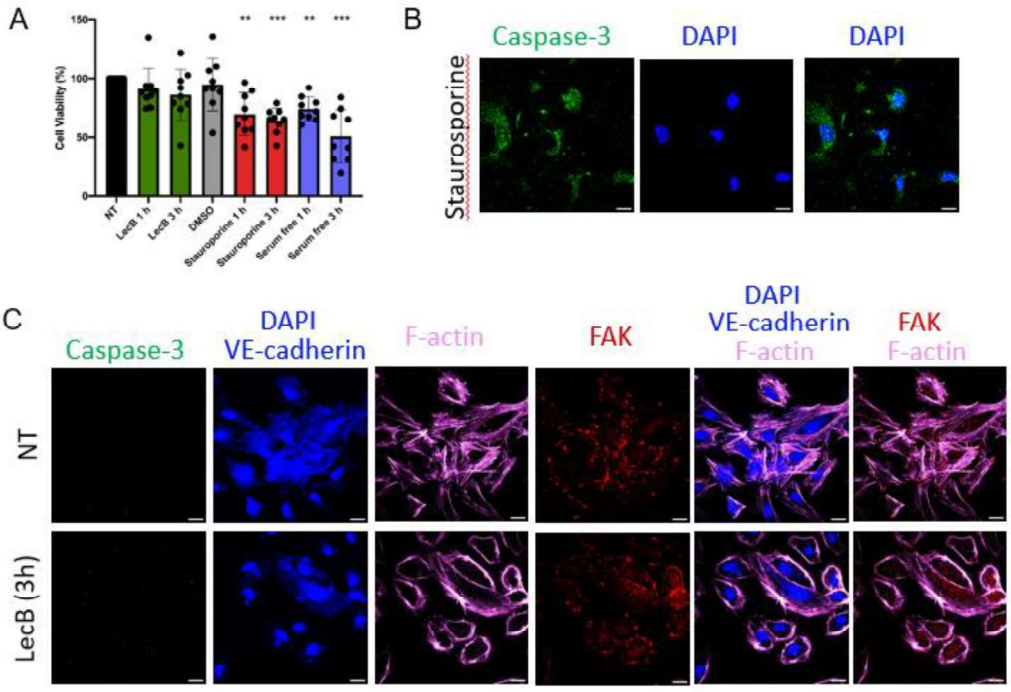

Fig. B12: LecB does not trigger apoptosis and leads to reduced myosin light chain phosphorylation.

(A) HUVECs were left untreated (NT), or incubated with LecB, DMSO, Staurosporine in DMSO and in serum-free medium for the indicated times, and cell viability assessed using the MTT assay. The data is expressed as ± SEM. (A) It is normalized to the NT conditions with each data point representing biological replica. *P < 0.05, **P < 0.01 ***P < 0.001 as determined by the Student's t-test in comparison with the NT condition. (B) HUVECs undergoing apoptosis with Staurosporine were imaged for caspase-3, and nuclei stained with DAPI. Scale bars, 20 µm. (C) NT or LecB-treated HUVECs were stained for the indicated proteins and caspase-3 to exclude imaging apoptotic cells. Scale bars, 20 µm. The cell perimembranous and intracellular areas were identified on the bright field cell images. The pixels in the subcellular areas for each cell image was determined using Fiji (ImageJ software) and normalized for cell surface area. The data is expressed as ± SEM. (A) It is normalized to the NT conditions with each data point representing biological replica. *P < 0.05, **P < 0.01, ***P < 0.001 as determined by the Kruskall-Wallis test with the NT condition.

B. 3.4. My contributions

With support from DR1-CNRS Dr. Christopher G. Mueller (principal supervisor) and Prof. Dr. Winfried Römer, and helps from Lutfir Hamzam and DH445 reagent provided by Prof. Dr. Alexander Titz, I conceptualized and performed the study. My contributions to some publication figures and some experiments include these points:

1) Colocalization between LecB and LVs in mouse skin *in vivo* with imaging by confocal microscopy.
2) Inhibition of DC migration and T cell activation by LecB *in vivo* with imaging by epifluorescence microscopy and flow cytometry (with Lutfir Hamzam for the T cell activation parts, DH445 inhibitor from Prof. Dr. Alexander Titz).
3) Investigate the rearrange of the EC membrane and cytoskeleton induced by LecB *in vitro* through imaging by confocal microscopy.
4) Assess the toxicity of LecB on ECs with MTT assay and imaging by confocal microscopy.

B. 4. Conclusions

My study sheds new light on the function of LecB, a lectin produced by *P. aeruginosa*. It has been reported that the second *P. aeruginosa* lectin, LecA, also interacts with ECs. For example, in the mink airways, ECs are marked by both LecA and LecB lining the vascular surface of the large vessel [344]. Lectins that have protein homology with *P. aeruginosa* are produced by other bacteria, such as *Burkholderia*, which causes morbidity and mortality among cystic fibrosis patients [345]. With regards to leukocyte migration, lectin obtained from *Lonchocarpus sericeus* seeds attenuates the leukocyte-endothelium interaction, such as rolling and adhesion, neutrophil transmigration and also the inflammatory hypernociception in response to injection of inflammatory stimuli [346]. However, co-author found that LecA did not inhibit human DC skin emigration, indicating that obstructing leukocyte migration is not a general property of bacterial lectins. On the one hand, from our previous results, LecB induces differentiation and apoptosis of acute monocytic leukemia cells with the reduction of β-catenin level [46], and causes BCR-dependent activation-induced death of B cells *in vitro* [45]. It suggests that LecB is associated with immune cells, resulting in the cellular processes, which supports my observations that LecB perturbs DC migration and the subsequent T cell activation. On the other hand, the major difference between LecA and LecB is that LecA specifically binds to galactose, while LecB specifically binds to fucose [47]. It has been reported that D-Gal-treated mice exhibit changes in T cell function, redistributing $CD4^+$ T cell subsets [347]. Besides, galactose induces the differentiation of tolerogenic DCs, supporting naïve T cell differentiation toward the Treg phenotype [348]. This evidence indicates that galactose has a cellular function on the immune cells, suggesting that galactose-binding LecA might have the same effect on the immune cells. However, there is less literature on the fucosylation and immune cells. My results will provide some hints regarding the physiological consequence of fucose-binding LecB on immune cells.

Here, in my second part of the project, I found that LecB-triggered restriction of cell migration in mice could be reproduced in an *in vitro* endothelial transmigration assay. The finding was that LecB could colocalize with LVs in mice. After entry of the tissue-draining LecB into LN, LecB interfered with migration of DCs and subsequent T cell activation *in vivo* (Fig. B13). Meanwhile, I also employed DH445, a LecB inhibitor, to investigate if DH445 can block LecB regarding immune responses. The results depicted that DH445 could rescue the reduced DC migration and T cell activation induced by LecB. Thus, DH445 may find an application to *P. aeruginosa* infections. By studying HUVECs in more detail, I found that LecB triggered the endocytic degradation of VE-cadherin, changes in FAK subcellular location, the formation of a cortical F-actin rim, and reduced phosphorylation of myosin light chain. Importantly, the degradation of VE-cadherin was not due to LecB toxicity-induced cell apoptosis. From the results of MTT and caspase-3 assay, LecB did not affect the cell viability of HUVECs, compared with positive controls, such as staurosporine and serum-free. Moreover, untreated cells exhibited actin dynamics concomitant with cell motility, the 3 h LecB treatment left the cells sessile with low levels of polymerized actin.

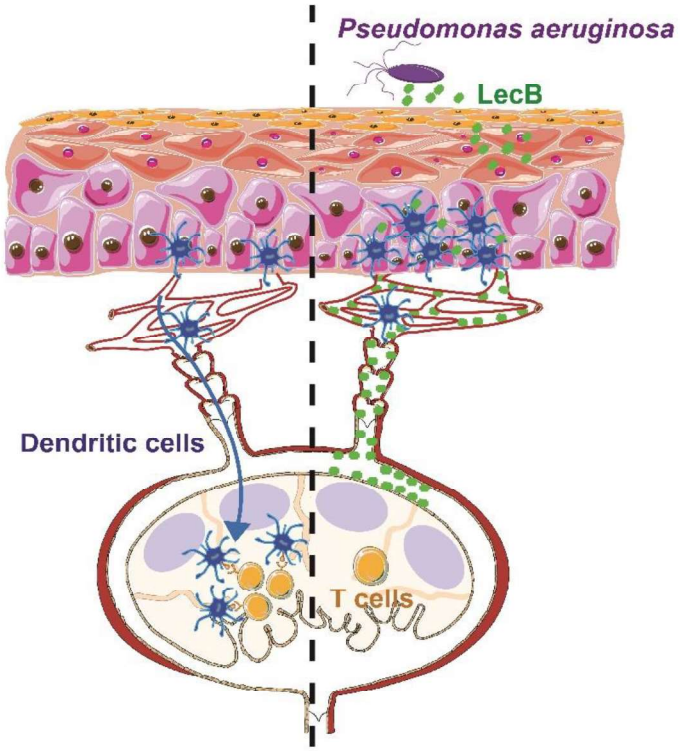

Fig. B13: The scheme of the LecB-induced immune responses *in vivo*.

Upon infecting human body surfaces, skin or lung, *P. aeruginosa*-produced LecB would bind to ECs in the tissue. This leads to dysfunction of intercellular adherence and cell mobility impeding the transendothelial passage of leukocytes. As a consequence, LecB impairs the migration of dendritic cells through the draining lymphatics into the paracortex of lymph nodes resulting in a reduced antigen-specific T cell response directed to fight the invading pathogen.

B. 5. Outlook

In the second part of the project, I demonstrated that LecB could also inhibit immune cell migration, such as DC migration, *in vivo*. Subsequently, LecB suppressed T cell activation in the LN *in vivo*, which was rescued by DH445. LecB triggered the endocytic degradation of VE-cadherin, changes in FAK subcellular location, the formation of a cortical F-actin rim, and reduced phosphorylation of the myosin light chain *in vitro*.

T cell activation can initiate the cell-based functions of the immune system, where they support their local defense mechanisms. Here, I found that LecB suppressed T cell activation in the LN in mice, which indicates that exogenous antigen LecB induces a cytotoxic T cell response. Besides, there are lots of researches about the effect of pathogen on T cell response. For example, SARS-CoV-2 virus results in the delayed or insufficient activation of T cell responses, which can contribute to severe lung damage or systemic inflammation [349]. Myeloid arginase-1 deletion mice lead to greater T cell recruitment and activation in response to *P. aeruginosa* pneumonia [350]. This evidence suggests that T cell response is an essential defense mechanism in the immune system after the pathogenic infection. However, the reduction of T cell response against LecB would allow other pathogens to infect the organs. With the intraperitoneal injection of LecB inhibitor DH445, I hope that it may be a novel method to cure the dysfunctional immune responses after the infection of LecB. It will also be of great interest to take this study further by injecting the PAO1 strain and the PAO1 ΔLecB strain (LecB deletion) into mice, investigating the effect of LecB on the immune response in mice with the infection of *P. aeruginosa*.

DH445 is an artificially synthesized derivative from methyl-α-L-fucoside, which is kindly provided by Prof. Dr. Alexander Titz. It is the first time that the function of DH445 in the blockage of LecB was analyzed *in vivo*. However, there are some other artificial derivatives that have a similar structure deriving from methyl-α-L-fucoside. For example, Alexander Titz et al. have designed C-glycosides fucoside-based compounds, which can bind to human Langerin protein in the millimolar range [42]. No toxicity is detected for the same compound tested up to a concentration of 100 μM using an immortalized human hepatocyte cell line [42]. It means that the safety window of the synthesized compound is quite high for humans.

In a further study, I tested the impact of LecB on the capacity to suppress the production of antibodies directly against LecB in mice. Therefore, I performed an ELISA assay based on streptavidin and LecB-Biotin (data not shown). In detail, the commercial streptavidin-coated 96-well plate was blocked with blocking buffer [4% (wt/vol) non-fat milk in TBS-T buffer] and coated with LecB-Biotin. Then, the mouse sera extracted after the 7-day and 14-day injection of LecB +/-DH445 were incubated at 37°C for 1 h. After washing, anti-mouse antibodies (IgG γ Fc and IgM F) were diluted and incubated at 37°C for 0.5 h. After washing, the TMB substrate is added to each well and incubated at 37°C for 15 min. The absorbance value at 450 nm was acquired with a microplate reader. The purpose of this test was to check the levels of certain antibodies in the serum. However, the data did not show a difference between mice injected with LecB in the absence or presence of DH445. A further study used ovalbumin as antigen injected in the absence or presence of LecB and in the absence or presence of alum as adjuvant. This experimental set

up was also unsuccessful to find a difference between with and without LecB. Thus I was unable to show that LecB had a repressive effect on the humoral immune response towards LecB that would be released by DH445. It is likely that the regimen of injecting LecB twice was not sufficient to efficiently block the humoral response. Moreover, owing to time, I did not carefully assess the generation of a germinal center response implicating DC-T cell crosstalk. Further work is therefore required to assess the physiological consequences of inhibition of DC migration by LecB on the immune response.

Integrins are essential for cell migration, and the cell surface expressions of CD18/ß2-integrin, CD11c/αX-integrin, and CD11b/αM-integrin induced by LecB in DC were investigated by collaborators. A reduction in the CD18/ß2-integrin-CD11c/ß2-integrin heterodimer on dermal DCs triggered by LecB was found, indicating that LecB negatively affects DC migration from human skin by binding to a cellular glycoligand [53]. In microenvironments, ECM is essential for cell migration, and the binding of integrins to ECM is introduced in detail in the previous charter. Therefore, it is important to investigate the effect of ECM during the process of cell migration. I mimicked fibronectin-coated plates to characterize the function of LecB in cell adhesion. It will be more meaningful to introduce ECM-integrin research in the mouse model by injecting LecB. Adhesive interactions with the ECM are dynamically engaged during the development and homeostatic turnover of tissues [351]. For example, ß1-integrin activity is required for laminin-induced cellular position sensing to pattern the early mouse embryo [352]. It suggests that ECM is critical to the research of integrins under the microenvironment.

In addition, flotillins were described as involved in various cellular processes such as cell adhesion, cell migration, signal transduction through receptor tyrosine kinases, as well as in cellular trafficking pathways [141]. Regarding cell migration, flotillins can also affect immune cell cytoskeletons. For example, following stimulation with chemoattractants, flotillin microdomains become rapidly redistributed to the uropod, a contractile structure at the back of migrating white blood cells [158]. Meanwhile, there is a connection between flotillin microdomains and actin-associated proteins, such as myosin IIA and spectrin [158]. Primary neutrophils isolated from flotillin-1-knockout mice show defects in myosin IIA activity, uropod formation, and migration through a resistive environment *in vitro* [353]. It indicates that flotillin can also mediate immune cell motility, inducing myosin IIA activity. In my first part of the project, I found that LecB can suppress the flotillin-mediated cell migration *in vitro*. Therefore, it is interesting to investigate if flotillin mediate immune cell migration induced by LecB *in vivo*.

Report

TRANSPARENT PROCESS OPEN ACCESS

EMBO reports

Pseudomonas aeruginosa LecB suppresses immune responses by inhibiting transendothelial migration

Janina Sponsel[1,2,3,†], Yubing Guo[1,2,3,†], Lutfir Hamzam[1], Alice C Lavanant[1], Annia Pérez-Riverón[1], Emma Partiot[4,5], Quentin Muller[1,6], Julien Rottura[1], Raphael Gaudin[4,5], Dirk Hauck[7,8,9], Alexander Titz[7,8,9], Vincent Flacher[1], Winfried Römer[2,3,10,*] & Christopher G Mueller[1,**]

Abstract

***Pseudomonas aeruginosa* is a Gram-negative bacterium causing morbidity and mortality in immuno-compromised humans. It produces a lectin, LecB, that is considered a major virulence factor, however, its impact on the immune system remains incompletely understood. Here we show that LecB binds to endothelial cells in human skin and mice and disrupts the transendothelial passage of leukocytes *in vitro*. It impairs the migration of dendritic cells into the paracortex of lymph nodes leading to a reduced antigen-specific T cell response. Under the effect of the lectin, endothelial cells undergo profound cellular changes resulting in endocytosis and degradation of the junctional protein VE-cadherin, formation of an actin rim, and arrested cell motility. This likely negatively impacts the capacity of endothelial cells to respond to extracellular stimuli and to generate the intercellular gaps for allowing leukocyte diapedesis. A LecB inhibitor can restore dendritic cell migration and T cell activation, underlining the importance of LecB antagonism to reactivate the immune response against *P. aeruginosa* infection.**

Keywords bacterial lectin; dendritic cells; lymphatics; migration; skin
Subject Categories Cell Adhesion, Polarity & Cytoskeleton; Immunology; Microbiology, Virology & Host Pathogen Interaction
DOI 10.15252/embr.202255971 | Received 15 August 2022 | Revised 5 February 2023 | Accepted 10 February 2023
EMBO Reports (2023) e55971

Introduction

Lectins, widespread among animals, plants, bacteria, and viruses, are proteins with carbohydrate binding properties (Meiers *et al*, 2019). Microbial lectins play a role in pathogenesis, such as the fimbria lectins FimH and FmlH for *E. coli* infection of the urinary tract (Rosen *et al*, 2008) or the influenza virus hemagglutinin that binds sialic acids of pulmonary epithelial cells (Lewis *et al*, 2022). *P. aeruginosa* is a widespread, Gram-negative bacterium that causes chronic cutaneous wound and airway infections. It belongs to the ESKAPE pathogens and is listed by the World Health Organization as one of the most critical bacterial pathogens. *P. aeruginosa* produces two lectins, LecA and LecB (formerly named PA-IL and PA-IIL) that form homotetramers and have high affinity for galactose and L-fucose, respectively (Gilboa-Garber, 1972). LecB is noncovalently linked to carbohydrate ligands of the outer bacterial cell surface and can be liberated by interference with soluble sugars or glycans (Tielker *et al*, 2005). It increases bacterial adherence to and infection of epithelial cells of the skin (Landi *et al*, 2019; Thuenauer *et al*, 2020) and the lung and contributes to pathogenicity in mouse models of lung infections (Mewe *et al*, 2005; Chemani *et al*, 2009). In addition, the lectin also contributes to the formation of biofilms (Tielker *et al*, 2005; Diggle *et al*, 2006). Therefore, LecB has been identified as a potential drug target in infections with *P. aeruginosa* (Wagner *et al*, 2016).

During an adaptive immune response against microbial infections, the B cell-driven humoral effector arm generates high-affinity and long-lived immunoglobulins for antibody and complement-mediated cytotoxicity and to block infections of host cells. In parallel, the T cell-mediated effector arm kills infected host cells. The

1 CNRS UPR 3572, IBMC, University of Strasbourg, Strasbourg, France
2 Signalling Research Centers BIOSS and CIBSS, University of Freiburg, Freiburg, Germany
3 Faculty of Biology, University of Freiburg, Freiburg, Germany
4 CNRS, Institut de Recherche en Infectiologie de Montpellier (IRIM), Montpellier, France
5 Université de Montpellier, Montpellier, France
6 Laboratoire BIOTIS, Inserm U1026, Université de Bordeaux, Bordeaux, France
7 Chemical Biology of Carbohydrates (CBCH), Helmholtz Institute for Pharmaceutical Research Saarland (HIPS), Helmholtz Centre for Infection Research, Saarbrücken, Germany
8 Deutsches Zentrum für Infektionsforschung (DZIF), Standort Hannover-Braunschweig, Germany
9 Department of Chemistry, Saarland University, Saarbrücken, Germany
10 Freiburg Institute for Advanced Studies (FRIAS), University of Freiburg, Freiburg, Germany
*Corresponding author. Tel: +33 3 88 41 70 27; E-mail: winfried.roemer@bioss.uni-freiburg.de
**Corresponding author. Tel: +49 761 203 67500; E-mail: c.mueller@unistra.fr
†These authors contributed equally to this work

dendritic cells (DCs) are key in initiating an efficacious immune response against bacterial infections. They are professional antigen-presenting cells, migrating from infected tissue via the lymphatic vessels to the draining lymph nodes (LNs), where they present pathogen-derived antigens to activate naïve and memory T cells. Under the influence of environmental cues, DCs direct the polarization of T helper cells supporting the humoral or cell-cytotoxic effector arms.

Microbial lectins, such as LecB, can modulate the immune response through their potent mitogenic potential on immune cells leading to uncontrolled cell proliferation, exhaustion, and cell death (Avichezer & Gilboa-Garber, 1987; Singh & Walia, 2014). LecB and BambL, a L-fucose-binding lectin from *Burkholderia ambifaria*, induce B cell activation and subsequent cell death *in vitro*. Injection of BambL into mice leads to polyclonal activation of B cells (Wilhelm *et al*, 2019; Frensch *et al*, 2021), which could thwart an efficient humoral immune response. However, on the whole, the impact of microbial lectins on the immune system has remained poorly studied.

Here, we investigated the effect of *P. aeruginosa* LecB on the vascular and the immune systems using human skin explants and mouse models. We found that LecB bound to blood and lymphatic endothelial cells *in vitro* and *in vivo* and caused profound cell junctional and cytoskeletal changes, impairing transendothelial migration of leukocytes. LecB inhibits the migration of DCs from skin via the lymphatics into the LN leading to a diminished T cell response, which is restored by a synthetic LecB inhibitor. These findings illustrate how a microbial lectin can curtail an immune response by inhibiting immune cell migration across endothelial barriers.

Results and Discussion

LecB disrupts migration of human skin DCs and binds to endothelial cells

To investigate the impact of the *P. aeruginosa* lectins on the immune system, we exposed human skin explants to recombinant LecA and LecB purified from *E. coli* (Chemani *et al*, 2009; Landi *et al*, 2019) for 3 days in culture medium and assessed the spontaneous migration of leukocytes. The cells accumulating in the medium were identified as HLA-DR$^-$ lymphocytes (mostly memory T cells), epidermal Langerhans cells, dermal CD14$^+$, and CD14$^-$ (CD1a$^+$) DCs (Fig 1A). While T cells were not significantly affected by either lectins, there was a significant reduction in dermal CD14$^+$ and CD14$^-$ DCs as well as in epidermal Langerhans cells with LecB but not LecA (Fig 1B). Adding the LecB glycomimetic inhibitor DH445 (Sommer *et al*, 2018) restored cell migration (Fig 1C). In light of the role of integrins (ITGs) in leukocyte migration and the loss of ITGb1 from epithelial cells by LecB (Thuenauer *et al*, 2020), we assessed the cell surface expression of CD18/ITGb2, CD11c/ITGaX, and CD11b/ITGaM. There was a reduction in the CD18/ITGb2-CD11c/ITGb2 heterodimer on dermal DCs but not Langerhans cells (Fig EV1). Thus, LecB negatively affects DC migration from human skin by binding to a cellular glycoligand. Given that DCs and Langerhans cells leave tissue via the lymphatic vessels, we next assessed interaction of LecB with the skin lymphatics. To this end, we cultured skin explants for 3 days with LecB conjugated to the fluorochrome AlexaFluor 488. The skin was then sectioned and stained for CD31 and HLA-DR, expressed by endothelial cells and the dermal DCs/epidermal Langerhans cells, respectively (Fig 1D). There was a noticeable overlap between LecB-A488 and CD31$^+$ endothelial cells. To confirm the LecB affinity for endothelial cells, the cells were isolated from human skin, expanded and exposed to LecB-A488 in the absence or presence of graded concentrations of the inhibitor DH445. The cells were stained for CD31, CD146, and glycoprotein 38 (podoplanin) and analyzed by flow cytometry (Fig 1E). Both blood and lymphatic endothelial cells bound LecB and the interaction was antagonized with increasing concentrations of DH445. These findings show that treatment with *P. aeruginosa* lectin LecB inhibits the emigration of DCs and binds to human lymphatic and blood endothelial cells.

The lectin inhibits human leukocyte transmigration *in vitro* and rearranges endothelial cell membrane and cytoskeleton

In light of these findings, we next asked whether LecB inhibits transendothelial passage of immune cells. To this end, human CMEC/D3 blood endothelial cells, which form tight cell junctions, were grown as a monolayer on the filter of Transwell plates, and then peripheral blood mononuclear cells (PBMCs), blood-isolated lymphocytes or monocyte were added to the top chamber. The cells were exposed to LecB and migration of the leukocytes across the endothelial cells into the lower chamber was assessed 24 h later (Fig 2A). We found that in the presence of LecB, significantly fewer cells migrated across the endothelial barrier into the lower chamber (Fig 2B). PBMCs and monocytes were most strongly impaired, although CD14$^-$ lymphocyte transmigration was also significantly decreased. Next, we counted the number of cells remaining on the CMEC/D3 cell monolayer, and, inversely to cell passage, there were more adherent leukocytes in the upper chamber in the presence of LecB (Fig 2C). These findings demonstrate that LecB impairs leukocyte passage across an endothelial monolayer. When staining CMEC/D3 cells for the adherens junctional protein VE-cadherin, we observed that while in untreated conditions, the VE-cadherin was clearly localized at the cell membranes, surprisingly, LecB disrupted this distribution (Fig 2D). We, therefore, analyzed more closely the changes inflicted by LecB on junctional proteins and the cytoskeleton of endothelial cells. First, we determined the binding of LecB-A488 to different endothelial cell lines *in vitro*. The lectin bound to the cell membrane of the human brain microvascular endothelial cell line hCMEC/D3, human umbilical vein endothelial cells (HUVECs), and skin lymphatic cells and was internalized in perinuclear vesicles (Fig EV2A). HUVECs were then left untreated or exposed to LecB for 1 h or 3 h, stained for VE-cadherin, filamentous (F)-actin, focal adhesion kinase (FAK), nuclei were colored with DAPI (Fig 2E), and images quantified for subcellular localization (Fig EV2B). In untreated cells, VE-cadherin was primarily distributed on the cell surface forming adherens junctions, however, in the presence of LecB, location of VE-cadherin shifted into the cytoplasm and was often found in peri-nuclear vesicles. We analyzed VE-cadherin protein levels by western blot and found a time-dependent decrease (Fig 2F). Visualizing F-actin with fluorescent phalloidin uncovered that LecB provoked the reduction in cellular stress fibers and the formation of a cortical actin rim. FAK, which plays a central role in initiating and integrating various signaling pathways with

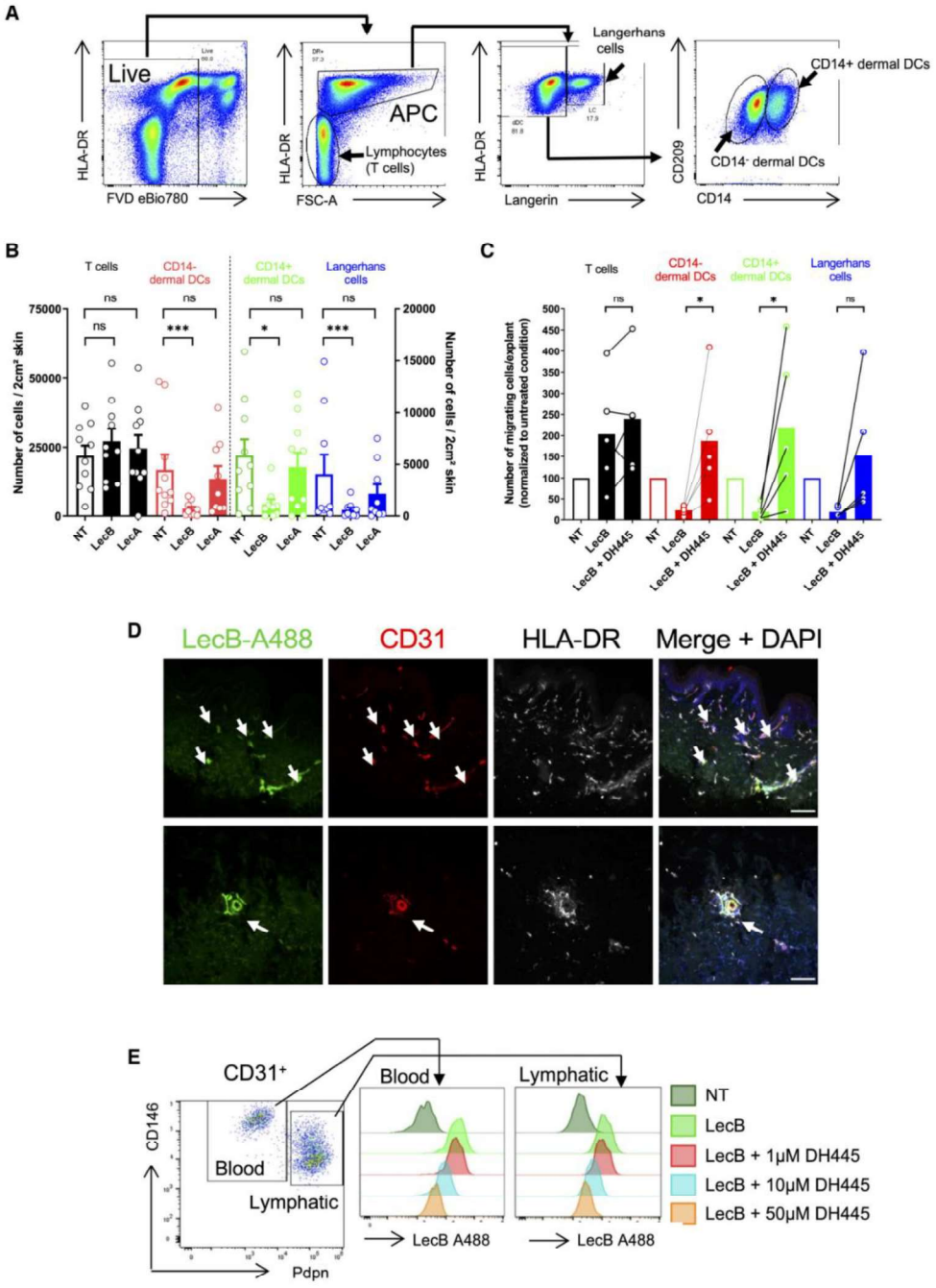

Figure 1.

Figure 1. LecB binds to endothelial cells in the skin and obstructs cell emigration.

A Flow cytometry gating strategy to identify the leukocytes emigrating from human skin explants into cell culture medium.

B Human skin explants were cultured in complete medium for 3 days in the absence (nontreated, NT) or presence of LecB or LecA, emigrated cells counted and identified by flow cytometry (panel A).

C As for panel (B) with DH445 and/or LecB added to the culture medium, normalized to the untreated condition.

D Epifluorescence imaging of human skin cross-sections after incubation of skin explant in culture with LecB-A488 and then stained for CD31, HLA-DR and cell nuclei (DAPI). Arrows point to $CD31^+$ endothelial cells bound by LecB-A488.

E Flow cytometry of LecB-A488 binding to ex vivo isolated $CD31^+$ $CD146^+$ podoplanin $(Pdpn)^-$ blood and $CD31^+$ $CD146^-$ $Pdpn^+$ lymphatic endothelial cells in the absence or presence of different concentrations of the LecB inhibitor DH445.

Data information: data are expressed as mean ± SEM of individual skin donors, that are linked in (C). The data in (C) are normalized to the untreated (NT) condition. ns, not significant, $*P < 0.05$, $***P < 0.001$, as assessed by the Kruskall–Wallis test (B) and Friedman test (C). The scale bars represent 100 μm (D).

effect on cytoskeleton (Quadri, 2012), is frequently displaced from a predominantly perimembranous location to an intracellular position after LecB. The alterations in protein expression and localizations were not due to LecB toxicity as assessed by cell viability by MTT and caspase-3 staining (Fig EV3A–C). Given the reduction of actin stress fibers that are central to cell mobility, we performed live imaging of HUVECs with Sir-actin exposed to LecB or left untreated. While untreated cells exhibited actin dynamics concomitant with cell motility, the 3 h LecB treatment left the cells sessile with low levels of polymerized actin (Movies EV1 and EV2). To further explore reduced cell contractility, we determined phosphorylation of the myosin regulatory light chain 2 that stabilizes myosin (Vicente-Manzanares *et al*, 2009). Western blot showed diminished myosin light chain2 phosphorylation at Ser19, and quantification of immunofluorescence revealed a loss in the perimembranous area after 3 h of LecB exposure (Fig EV3D). In conclusion, LecB reorganizes the VE-$cadherin^+$ adherens junction and the associated FAK and F-actin cytoskeleton with reduced myosin regulatory light chain phosphorylation, which would have a negative impact on cell contractility and, therefore, on leukocyte diapedesis.

LecB binds to lymphatic endothelial cells in skin and LN *in vivo*

We next turned to mouse models to explore the functional consequences for the immune system of LecB interaction with endothelial cells. First, LecB-A488 was injected into the ear pinnae of $Prox1^{CreERT2}$ $tdTomato^{Stop\text{-}flox}$ (*iProx-1tdT*) mice that express the red fluorescent tdTomato protein under the *Prox1* promoter active in lymphatic endothelial cells (Bazigou *et al*, 2011). 4 h later, the ears were split and imaged by confocal microscopy (Fig 3A). LecB-A488 co-localized with the $tdTomato^+$ lymphatic vessels in addition to binding to other cutaneous structures resembling blood vessels. As lymphatics drain into LNs, we next injected LecB-A488 into the ear pinnae or into the footpad and 4 h later visualized its localization within the auricular and popliteal LNs that respectively drain these injection sites (Fig 3B). LecB bound not only vascular structures, mostly lymphatics expressing both CD31 and CLCA1 and lining the subcapsular and medullary sinuses, but also $CD31^+$ $CLCA1^-$ blood vessels. A higher magnification revealed that LecB-A488 labeled structures extending from the subcapsular sinus across the cortex to blood endothelial cells, which are likely conduits transporting lymph-borne material from the lymphatic sinus to high endothelial venules (HEVs) (Gretz *et al*, 2000). Indeed, in HEVs stained with peripheral node addressins (PNAd), LecB-A488 labeling was apparent on the subluminal side (Fig EV4A). We next examined LecB binding to different cell populations by flow cytometry (Fig 3C). Lymphatic endothelial cells (LECs), blood endothelial cells (BECs), and fibroblastic reticular cells (FRCs) were identified based on CD31 and gp38 expression, and the HEVs as a $PNAd^+$ BEC subset. The remaining population that comprises pericytes was noted as double negative (DN). LecB-A488 binding was assessed for each stromal cell population by measuring its mean fluorescence intensity (Fig 3D). We found that LecB primarily targeted LECs, followed by BECs, HEVs, and FRCs. This finding confirms the microscopic assessment of LecB-target cells and supports the conclusion that LecB travels from the skin via the lymphatics to the LNs where it reaches BECs and HEVs via the FRC-formed conduits. We also assessed the mean fluorescence intensity of LecB-A488 in the different hematopoietic cell populations (Fig EV4B–D). The lymphatic sinus-associated macrophages (subcapsular and medullary sinus macrophages, SSM and MSM) displayed the strongest fluorescence followed by other macrophage subsets, whereas DCs showed a much lower binding to LecB. T and B lymphocytes were hardly targeted by the lectin. These data further support the lymphatic draining of subcutaneously injected LecB into the LN, where it is sampled by the lymphatic sinusoidal macrophages.

LecB interferes with migration of DCs from peripheral tissues and subsequent T cell activation *in vivo*

We next assessed the functional consequences of LecB binding to the lymphatics by assessing DC migration from skin to the LN paracortex, where they prime T cells. First, we determined whether DCs were inhibited by LecB in their migration to LNs by exposing mouse ear skin to the TLR-7 agonist imiquimod (Aldara cream) in the absence or presence of two intradermal injections of LecB. In spite of a strong increase in LN cellularity owing to the inflammatory stimulus, LecB prevented the entry of the migratory skin DC subsets and Langerhans cells into the draining LN (Fig 4A). Similar observations were made when targeting the DEC-205^+ skin DCs (Fig EV5A and B). We then generated DCs from bone marrow precursors (BMDCs), matured by LPS, fluorescently labeled, and injected into ears and footpads of mice treated twice with LecB on one side, while the other side was mock-injected with saline (Fig 4B). In addition, some mice received an intraperitoneal injection of LecB inhibitor DH445. Four days later, the draining auricular and popliteal LNs were recovered, stained for $CLCA1^+$ lymphatics and $B220^+$ B cells, and the number of BMDCs associated with lymphatics or localized within the central paracortical T cell zone, devoid of the peripheral $B220^+$ B cell follicles, was assessed (Fig 4C and D). In the absence of LecB, the majority of BMDCs was found within the paracortex, which was not influenced by DH445. However, in the presence of

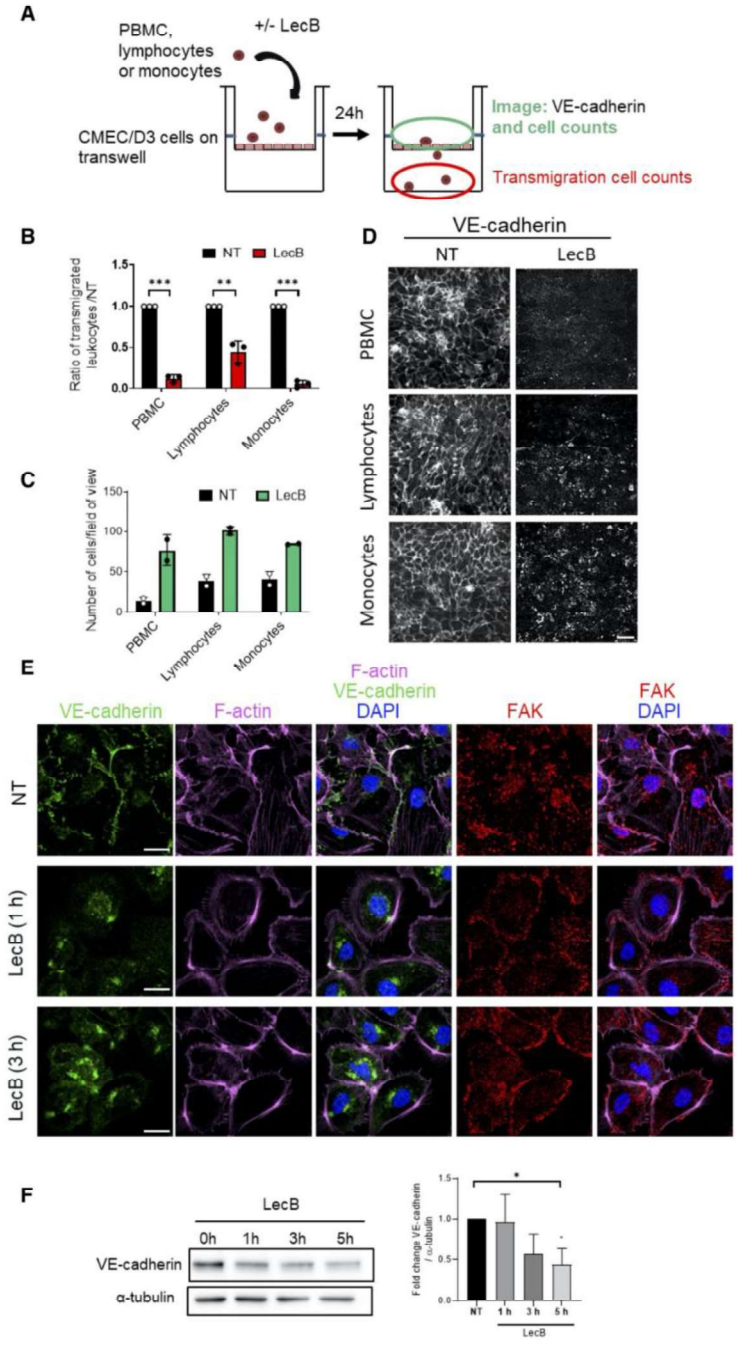

Figure 2.

Figure 2. LecB restricts leukocyte migration across endothelial cells and inflicts changes to cell membrane and cytoskeleton-associated proteins.

A Schematic illustration of the endothelial transmigration assay and its analysis.

B The graph shows the number of human peripheral blood mononuclear cells (PBMC), blood-isolated lymphocytes or monocytes transmigrated across the human CMEC/D3 endothelial cell barrier in the presence of LecB, relative to the nontreated (NT) condition.

C The graph shows the number of the indicated leukocytes remaining on the endothelial monolayer.

D Confocal images of the CMEC/D3 cells stained for VE-cadherin for the indicated experimental conditions.

E Confocal images of monolayers of HUVECs, nontreated (NT) or exposed to LecB for 1 or 3 h, were fixed and stained for VE-cadherin, F-actin, focal adhesion kinase (FAK), and nuclei with DAPI.

F Left: Western blot analysis of VE-cadherin and α-tubulin in HUVEC lysates treated with LecB for the indicated times. Right: Densitometric quantification of the western blot of VE-cadherin relative to α-tubulin.

Data information: (B, F) Data are expressed as mean ± SEM, $n = 3$ biological replicates. $^{*}P < 0.05$, $^{**}P < 0.01$, $^{***}P < 0.001$ as assessed by the Student's *t*-test (B) Kruskal–Wallis test (F). (C) Data are expressed as mean ± SEM, $n = 2$ biological replicates. The scale bars represent 40 μm (D) and 25 μm (E).

LecB, BMDCs failed to enter the T cell zone and were associated with the subcapsular lymphatics. Strikingly, DH445 reversed LecB-mediated inhibition of BMDC migration into the T cell zone. To determine whether this abnormal migration alters T cell activation, we modified the above experiment by injecting mature BMDCs loaded with ovalbumin into mice having received CFSE-labeled transgenic $CD4^+$ recognizing an ovalbumin-derived peptide (from OT-II x $CD45.1^+$ mice) (Fig 4E). The LNs were recovered and the proliferation of $CD45.1^+$ T cells assessed by dilution of the CFSE label by flow cytometry (Fig 4F). The data, expressed as T cell proliferation, was normalized in each experiment to control mice or mice whose contralateral LN was not exposed to LecB (Fig 4G). We found that LecB significantly reduced T cell proliferation and that this effect was reversed by the LecB inhibitor DH445. Taken together, the data uncovered the ability of LecB to inhibit the generation of an adaptive immune response by restricting DC migration across lymphatics from the periphery to the LN T cell zone.

LecB, produced by the opportunistic bacterium *P. aeruginosa*, is considered a virulence factor, however, its role on the immune system has not been studied. Here, we assessed the consequences of LecB administrated to human skin explants and to mice with respect to immune cell migration and initiation of a T cell immune response. We found that LecB targeted blood and lymphatic endothelial cells in human skin and in mouse skin and LNs. It disrupted the migration of the antigen-presenting cells from the skin via the lymphatics into the LN T cell zone and thereby inhibited the antigen-specific activation of T cells. The lectin restricted transendothelial migration of leukocytes *in vitro* and caused endothelial cell junctional and cytoskeletal changes. These findings support the conclusion that LecB is a potent virulence factor by restraining immune cell trafficking across endothelial barriers and thus preventing the immune system to mount an efficient response.

Immune cell migration is a prerequisite for an efficient immune response by activating T and B cells in the LNs against infections in peripheral tissue. Hereby, DCs play an important role through their capacity to traffic from tissue to LNs linking the innate and the adaptive immune effector arms. After exposing fluorescently tagged LecB intradermally to human skin and the mouse ear, we observed a strong association with blood and lymphatic endothelial cells. Likewise, in the LNs, the lymphatics sinuses were predominantly targeted. Other cells that efficiently bound LecB were the lymphatic sinusoidal macrophages, specialized in sampling and scavenging lymph-borne antigens, blood vessels, and fibroblastic reticular cells that formed the conduits between the LN lymphatic sinus and the HEVs. A molecular basis for the strong interaction of LecB with endothelial cells may be the glycocalyx, a thick layer of proteoglycans (e.g., syndecans, glypican), glycosaminoglycans, glycoproteins (e.g., selectins, integrins), and glycolipids (Moore *et al*, 2021).

The association of LecB with lymphatics raised the question of its physiological relevance in the context of a bacterial infection. We addressed this by studying leukocyte migration. In humans, Langerhans cells and dermal DC were restricted in their ability to exit the skin into the culture medium. T cells were less affected, indicative of taking a nonlymphatic route. In mice, our data showed that endogenous DCs or injected BMDCs were restrained in entering the LN, which consequently resulted in a lower T cell response. By providing two doses of LecB, we tried to optimize the experimental conditions to anticipate rapid and late BMDC arrival. Yet, because the half-life of LecB interaction with endothelial cells is not known, a more frequent regimen may have been required to observe a complete absence of BMDC migration into the T cell zone and subsequent abrogation of T cell proliferation. Alternatively, the high BMDC numbers may have contributed to overcome LecB-blockage of trans-endothelial migration. The glycomimetic DH445 proved effective in inhibiting LecB effects in skin explants and *in vivo*. DH445, which was administrated intraperitoneally, revealed high potency of inhibition, confirming its advantageous pharmacological properties (Sommer *et al*, 2018). These findings underline DH445 as a promising therapeutic option against *P. aeruginosa*.

We found that LecB-imposed restriction of cell migration from human skin or in mice could be reproduced in an *in vitro* endothelial transmigration assay. The finding that LecB strongly diminished the passage of different types of leukocytes is in line with the notion of general cell alterations rather than modifications of specific receptors or chemotactic signals. By studying HUVECs in more detail, we found that LecB triggered the endocytic degradation of VE-cadherin, changes in FAK subcellular location and the formation of a cortical F-actin rim. How do these changes correlate with reduced leukocyte diapedesis? Leukocytes pass through endothelial barriers mainly via the paracellular route, which involves destabilized cell–cell junctions and active actin stress fibers to create intercellular gaps for cell passage. Endothelial cell barrier enhancement agents lead to the disappearance of central stress fibers to generate a cortical F-actin rim, however, the adherens junctional VE-cadherin is stabilized at the cell surface (Garcia *et al*, 2001; Liu *et al*, 2002; Birukov *et al*, 2004; Birukova *et al*, 2007). One possible explanation for diminished leukocyte transmigration is that LecB impairs leukocyte diapedesis by preventing the development of transcellular tension necessary to create the intercellular openings. This model is supported by loss of stress fibers and reduced myosin regulatory chain phosphorylation,

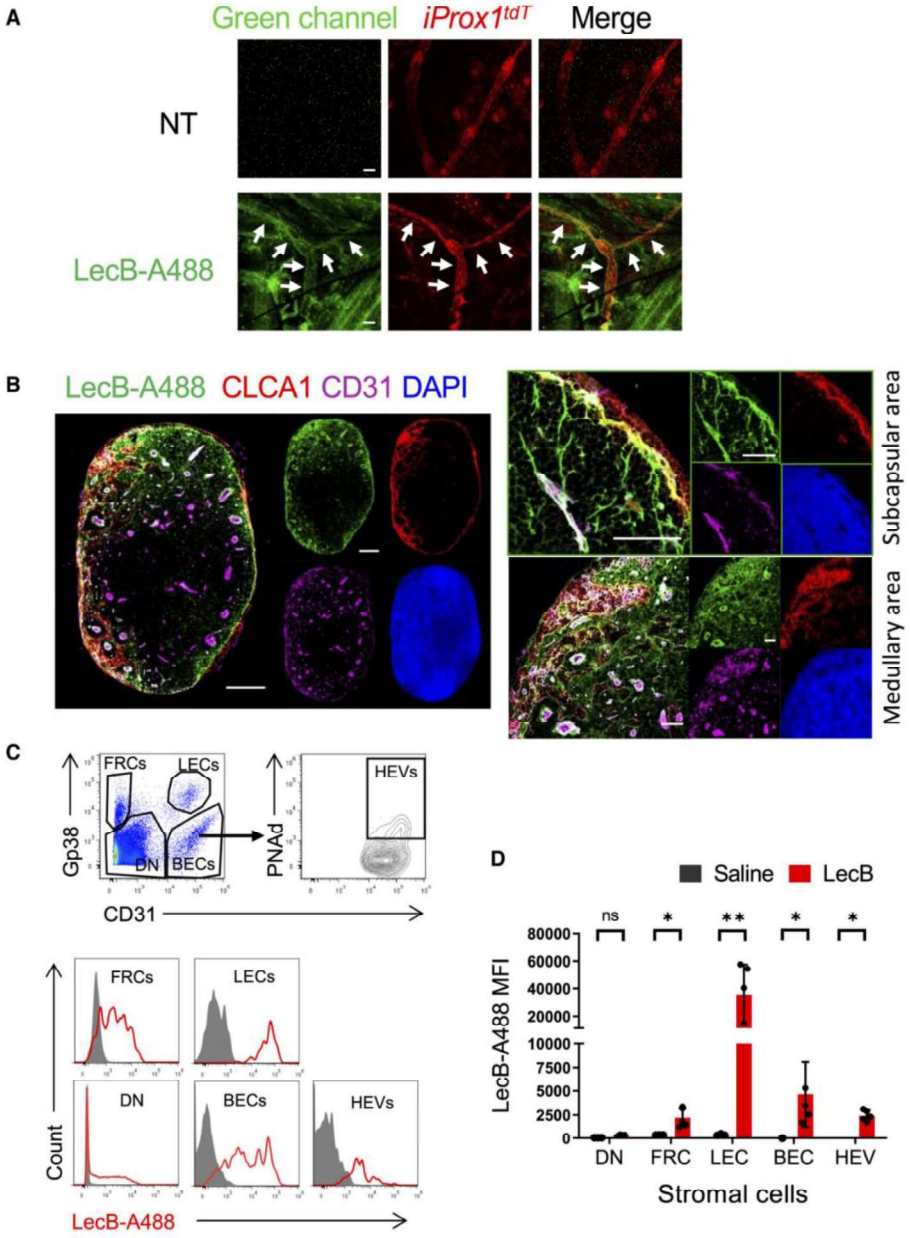

Figure 3.

Figure 3. Assessment of LecB drainage from the skin to LNs in the mouse.

A Whole mount confocal immunofluorescence of ear skin from Prox1-cre^{ERT2} tdTomato$^{stop\text{-}flox}$ (iProx1^{tdT}) after injection with LecB-A488 or saline (nontreated, NT). Arrows point to tdTomato+ lymphatic vessels bound by LecB-A488.

B Confocal imaging of LN sections after LecB-A488 injection and stained for chloride channel calcium-activated 1 (CLCA1), CD31 and cell nuclei (DAPI). Insets on the right show close-ups of the subcapsular and the medullary areas.

C Top: Flow cytometry gating strategy to identify LN stromal cell subsets among live CD45-TER-119 cells. Bottom: Flow cytometry histograms of green fluorescence for the identified stromal subsets after LecB-A488 (red line) or saline (gray curve) injection.

D The graph depicts the median fluorescence intensity (MFI) of green fluorescence of LecB-A488 versus saline of the cells analyzed in panel B.

Data information: The data are expressed as ± SEM with each data point represents one biological replicate (two LNs of one mouse). *$P < 0.05$, **$P < 0.01$ as determined by the Wilcoxon–Mann–Whitney test. The scale bars represent 50 μm (A), 200 μm (B left) and 50 μm (B right). BEC, blood endothelial cells; DN, double negative cells; FRC, fibroblastic reticular cells; HEV, high endothelial venules; LEC, lymphatic endothelial cells.

which would have a negative impact on cell contractility. However, reduction in integrin cell surface expression by LecB such as CD11c/ITGaX and CD18/ITGb2 may affect migration, although BMDC homing to LNs was not found to be dependent on integrins (Lämmermann *et al*, 2008). Further work is required to clarify the contribution of dysfunctional endothelial cells and compromised leukocyte–endothelial interaction in LecB-mediated inhibition of leukocyte migration.

It has been reported that the second *P. aeruginosa* lectin, LecA, also interacts with endothelial cells (von Bismarck *et al*, 2001; Kirkeby *et al*, 2007). Lectins that have protein homology with *P. aeruginosa* are produced by other bacteria, such as *Burkholderia*, which causes morbidity and mortality among cystic fibrosis patients (Lameignere *et al*, 2008). However, we found that LecA did not inhibit human DC skin emigration, indicating that obstructing leukocyte migration is not a general property of bacterial lectins. An important question is the dynamics of LecB production during an infection and whether it remains associated with the bacterium. Of consideration is also the role of LecB in biofilm formation that may —in the light of our results—protect the bacteria from immunological surveillance and attack. It is also reasonable to assume that the lectins might serve the bacterium to cross the blood or lymphatic endothelial barrier to spread systemically, as previously suggested (Plotkowski *et al*, 1994). In this context, it is interesting to note a case report of *Pseudomonas* in a mediastinal LN in the absence of bacterial counts in the blood, suggesting entry via the lymphatic drainage (Bansal *et al*, 2016). Our study employs purified LecB and calls for further studies using live *P. aeruginosa* expressing or lacking LecB. It also incites further investigation into the immunity-altering impact of other bacterial lectins. LecB inhibitors, similar to DH445, may find an application to bacterial infections beyond *Pseudomonas*.

Materials and Methods

Human skin

Fresh abdominal skin was obtained from patients undergoing abdominoplasty with written informed consent and institutional review board approval, in agreement with the Helsinki Declaration and French legislation. 2 cm^2 biopsies of ~ 1 mm thickness were placed at air–liquid interface onto 40-μm cell strainers in 6 ml complete medium (RPMI1640 supplemented with 10 μg/ml gentamycin, 100 units/ml penicillin, 100 μg/ml streptomycin, 10 mM HEPES [all from Lonza], and 10% fetal calf serum [FCS]). Lec B (5 μM) or Lec A (5 μM) was added to the skin explants. In some conditions, LecB was preincubated for 30 min with 100 μM of DH445 (Sommer *et al*, 2018). Human skin cells that had spontaneously emigrated into the culture medium after 3 days were recovered and stained for HLA-DR, Langerin/CD207, DC-SIGN/CD209 and CD14 (all from BD Pharmingen) to identify CD14$^+$ and CD14$^-$ dermal DCs as well as Langerhans cells and T cells. Cells were also stained for the integrin subunits CD18, CD11b, and CD11c (BD Pharmingen).

Mice

C57BL/6J, CD45.1 (B6.SJL-Ptprca Pepcb/BoyJ), OT-II (B6.Cg-Tg (TcraTcrb)425Cbn/J) (Charles River Laboratories, France), *Prox1-cre*^{ERT2} (Bazigou *et al*, 2011), B6;129S6-Gt(ROSA)26Sor$^{tm9(CAG\text{-}tdTomato)Hze}$ (Jackson Laboratories) mice were kept in pathogen-free conditions. The *Prox1*^{CreERT2} *tdTomato*$^{Stop\text{-}flox}$ (*iProx-1tdT*) mice received 50 mg/kg tamoxifen (Sigma-Aldrich) in sunflower oil/5% ethanol twice with a 24 h interval by gavage 2 weeks before experimentation. The mice then express the red fluorescent tdTomato protein in lymphatics under the specific *Prox1* promoter. All experiments were carried out in conformity with the animal bioethics legislation (APAFIS#16532-2018082814387618v4).

LecA and LecB preparation

The *P. aeruginosa* lectins were purified from *E. coli* (Chemani *et al*, 2009; Landi *et al*, 2019) using plasmid pET25pa2l (Mitchell *et al*, 2005). LecB was fluorescently labeled with Alexa Fluor488 (LecB-A488) monoreactive NHS ester (Thermo Fisher Scientific) and purified with Zeba Spin desalting columns (Thermo Fisher Scientific) according to manufacturer's instructions.

Chemical synthesis

The LecB inhibitor *N*-β-L-fucopyranosylmethyl 2-thiophenesulfonamide (named here DH445) was synthesized as previously described (Sommer *et al*, 2018).

Identification of LecB target cells by immunofluorescence of skin and LNs

Human skin (2 cm^2, 800 μm thick) was cultured in RPPMI medium supplemented with 10% fetal calf serum and antibiotics containing 5 μg/ml of LecB-A488. After 3 days, the skin was embedded in

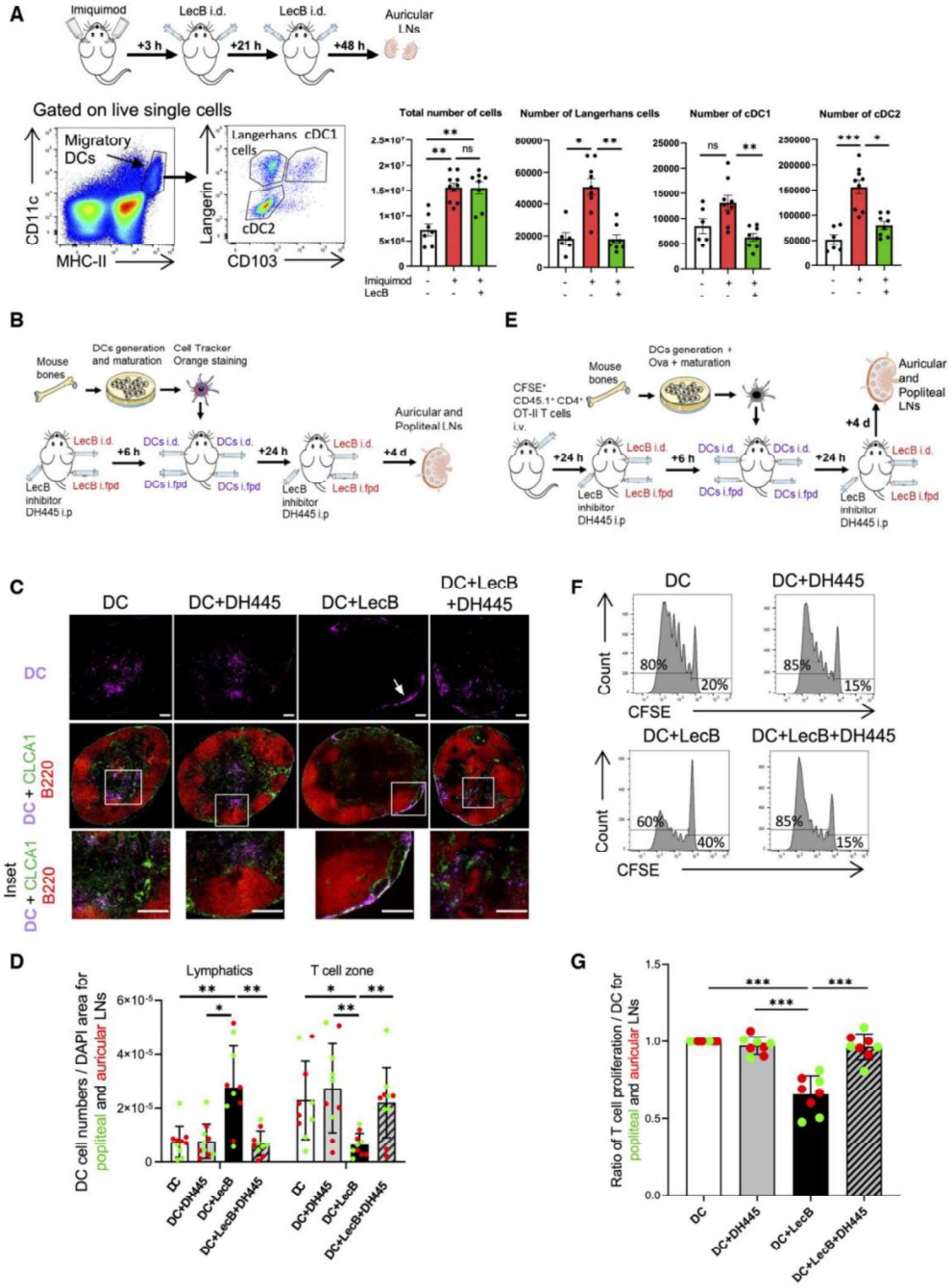

Figure 4.

Figure 4. Inhibition of DC migration and T cell activation.

A Schematic illustration of the experiment to assess inhibition of skin DCs migration to draining auricular LNs by intradermal LecB injection after mobilization by imiquimod (Aldara cream). Left: gating strategy to identify Langerhans cells, cDC1 and cDC2 subsets among the migratory DCs. Right: Graphs depict total auricular LN cell numbers, number of LCs, cDC1, and cDC2 without and with imiquimod application in the absence or presence of LecB.

B Schematic illustration of the experiment of panels (C, D).

C Epifluorescent imaging of LN sections stained for chloride channel calcium-activated 1 (CLCA1), expressed by the lymphatic endothelial cells, and B220$^+$ B cells residing in the LN cortex. DCs are visualized by their Cell Tracker Orange staining. Arrow points to DCs associated with a subcapsular lymphatic sinus. Insets show close-ups of DCs in the T cell paracortex (DC, DC+DH445, DC+LecB+DH445) or in the subcapsular lymphatic sinus (DC+LecB).

D The graph shows the DC numbers associated with CLCA1$^+$ lymphatics or the B220- T cell zone per LN section normalized for DAPI$^+$ area.

E Schematic illustration of the experiment of panels (F, G).

F Representative flow cytometry profiles of CFSE of donor CD45.1$^+$ CD3$^+$ CD4$^+$ ova-specific T cells in the different recipient mice. The proportion of proliferating versus CFSE$^+$ undivided T cells is noted.

G The graph depicts the proportion proliferating T cells of the different experimental condition relative to the DC-only control condition.

Data information: The data are expressed as ± SEM with each data point representing (A) two auricular LNs of one mouse, (D, G) a popliteal or an auricular LN of one mouse. *$P < 0.05$, **$P < 0.01$, ***$P < 0.001$ by (A) Kruskal–Wallis test, (D, G) one-way ANOVA test. Scale bars represent 200 μm. cDC1/2, conventional dendritic cells subset 1/2; i.d., intradermal; i.fp., intrafootpad; i.p., intraperitoneal; LCs, Langerhans cells.

freezing compound (Cell Path, Newton, Poys, UK) and cross-sectioned (7 μm thickness). Sections were stained for CD31 and HLA-DR (BD-Pharmingen) and nuclei visualized with DAPI (Sigma-Aldrich). Images were acquired on a Axio Observer.Z1 microscope (Carl Zeiss, Oberkochen, Germany) with a 20× air objective (Plan-Apochromat, NA 0.8, DIC, Zeiss) and the Metamorph software (Metamorph, Nashville, TN, USA). Images were processed with the open source software ImageJ. For mice, LecB-A488 (12.5 μg) was injected into mouse ear and into the hind footpads. 4 h later, ear pinnae were dissected and the dermal side fixed in 4% paraformaldehyde (PFA) (Sigma-Aldrich) and mounted with Fluoromount-G (Thermo Fisher Scientific). Images were acquired with a confocal microscope (Nikon, Eclipse Ti-E A1R system) and a 20× air objective (CFI Plan Fluor 20XC MI, 20×/0.75, OFN25 DIC). The auricular and popliteal LNs were harvested, embedded in freezing compound (Cell Path), and cryo-sectioned (8 μm thickness). Sections were acetone-fixed and stained for CD169 (BioLegend), chloride channel calcium-activated 1 (CLCA1, clone 10.1.1, a kind gift from Andy Farr, University of Washington, Seattle, USA), CD31 (eBioscience), and anti-PNAd (BioLegend). Nuclei were visualized with DAPI (Sigma-Aldrich).

Identification of LecB target cells by flow cytometry

Human skin cells that had spontaneously emigrated into the culture medium after 3 days were recovered and stained for HLA-DR, Langerin/CD207, DC-SIGN/CD209, and CD14 to identify CD14$^+$ and CD14$^-$ dermal DCs as well as Langerhans cells and T cells. To isolate blood and lymphatic endothelial cells, human skin was digested with 0.25% trypsin–EDTA (Gibco) to eliminate the epidermis, followed by digestion of the dermis with 1 mg/ml collagenase D (Roche, Switzerland) and 1 mg/ml DNase I (Roche) and for 18 h at 37°C. Endothelial cells were then positively selected using CD31-coupled magnetic beads (Miltenyi Biotec) and amplified in endothelial growth medium (EGM-2, PromoCell) on gelatin-coated flasks (Corning). LecB-A488 (1 μg/ml) was added to 5×10^4 cells in the absence or presence of the inhibitor DH445 (Sommer *et al*, 2018) (1–50 μM) for 2 h before staining cells for CD31 (BioLegend), CD146 (Miltenyi), and Podoplanin (BioLegend). LNs recovered from mice 4 h after injections of 12.5 μg LecB-A488 were minced and digested with 1 mg/ml collagenase D, 1 mg/ml Dispase (Roche) and 0.1 mg/ml DNAse I with frequent pipetting until full digestion. The cells were then filtered, red blood cells lysed in ammonium chloride buffer (BioLegend) and incubated with the different antibody cocktails. For stromal cells: anti-CD45-APC/Cy7 (BioLegend), TER-119-APC-eF780 (eBioscience), CD31-PE (BioLegend), anti-gp38/Podoplanin-PE/Cy7 (BioLegend), and anti-PNAd-biotin (BioLegend) followed by streptavidin-APC (eBioscience). DAPI (Sigma-Aldrich) was used to exclude dead cells. For myeloid cells: FcR were blocked with FcR Blocking Reagent (MACS Miltenyi Biotec) and cells stained with anti-CD45-APC/Cy7 (BioLegend), anti-CD11b-PerCP Cy5.5 (BioLegend), anti-Ly6C-PE (BD Pharmingen), and anti-Ly6G-APC (eBioscience). For sinusoidal macrophages: after FcR-blocking, cells were stained with anti-CD169-PE (BioLegend), anti-CD11c-PE-Cy7 (BD Pharmingen), anti-CD11b-PerCP-Cy5.5 (BioLegend), and anti-F4/80-APC (BioLegend). For DCs: after FcR blocking, cells were stained with anti-CD103-PE (BD Pharmingen), anti-CD11c-PE-Cy7 (BD Pharmingen), and anti-I-A/I-E-AF700 (BioLegend). Cells were washed with PBS and fixed in BD Cytofix™ Fixation Buffer (BD Biosciences) for 20 min and washed in BD Perm/Wash™ Buffer (BD Biosciences) for intracellular staining with Langerin-AF647 (Novus Biologicals). The Fixable Viability Dye eFluor 450 (eBioscience) was used as a dead cell marker. Flow cytometry was done on a Gallios (Beckman Coulter) and data analyzed with the FlowJo software (Tree Star, Inc.).

Endogenous DC migration

Mouse ears were treated with Aldara cream, containing 5% imiquimod, and 3 and 21 h later mice received into the ear pinna an injection of 12.5 μg LecB in 15 μl saline water. For DEC-205 targeting, 1 μg anti-DEC-205-A647 antibody diluted in 15 μl PBS was injected into ears pinna prior to Aldara cream application (Flacher *et al*, 2012). Auricular LNs were harvested 72 h afterwards. For single cell preparation, LNs were cut into small pieces and digested with 1 mg/ml collagenase D (Roche) and 0.1 mg/ml DNase I (Roche) in RPMI cell culture medium containing 2% FCS for 1 h at 37°C under agitation. For flow cytometry staining the antibodies were: CD11c-PE-Cy7, CD103-PE (BD Pharmingen), MHC-II-AF700, CD205-AF647 (BioLegend), and CD207 (Langerin)-AF488 (Eurobio).

BMDC generation, migration, and T cell stimulation

Bone marrows were flushed, red blood cells lysed in ammonium chloride buffer (BioLegend), cells filtered and cultured in complete medium containing 25 ng/ml FMS-like tyrosine kinase 3 ligand (hFlt3L, Peprotech). After 8 days, the BMDCs were activated with 100 ng/ml lipopolysaccharide (LPS) for 16 h, harvested and labeled with 15 μM Cell Tracker Orange (Thermo Fisher Scientific) for 30 min at 4°C. After washing in PBS, 2×10^5 BMDCs were injected subcutaneously into the ear pinna or into the hind footpad of C57BL/6 mice that had received 6 h before on one side 12.5 μg LecB into the ear and 12.5 μg LecB intra-footpad and contralaterally saline. Some mice concomitantly received a peritoneal injection of 50 mg/kg of LecB inhibitor DH445. After 4 days, the popliteal and auricular LNs were isolated, cryo-sectioned and stained for CLCA1 and B220. The number of Cell Tracker Orange$^+$ BMDCs trapped within the CLCA1$^+$ lymphatics or migrated into the B220$^-$ T cell zone was counted double blindly. For the *in vivo* T cell simulation assay, BMDCs were generated from C57BL/6 CD45.1$^+$ bone marrow, and 1 μg/ml chicken ovalbumin was added 2 h before addition of LPS. After 18 h, BMDCs were harvested and 2×10^5 cells injected into ears and footpads of CD45.2 mice, prepared as described above that had received an intravenous injection of 10×10^6 CD4$^+$ T cells from CD45.1xOT-II F1 mice. The T cells were isolated from spleens and LNs using negative magnetic bead selection (Miltenyi Biotec) and labeled with 500 nM carboxyfluorescein succinimidyl ester (CFSE, Thermo Fisher Scientific) for 15 min at RT. After 4 days, T cell proliferation in the draining LNs was determined by determining the proportion of the CFSE label, successively diluted with each cell division, among the live, CD3$^+$ CD45.1$^+$ T cells. Flow cytometry was done on a Gallios (Beckman Coulter) and data analyzed on FlowJo (Tree Star, Inc.).

Transmigration

Human CMEC/D3 cells (ATCC cell line collection) were grown in 24-well hanging cell culture inserts (PET, 5-μm pore, Millipore) at a density of 50,000 cells/cm^2. Cells were cultured for 7 days prior to transmigration to allow the establishment of a tight monolayer of cells. The tightness of the cell monolayer was verified by transendothelial electrical resistance. PBMCs were isolated from human healthy blood (local blood bank), and monocytes and lymphocytes selected as CD14-microbead-positive (Miltenyi Biotec) and -negative populations, respectively. After Cell Trace Yellow staining (Thermo Fisher Scientific), 250.000 cells were added into the top chamber of the hCMEC/D3 cell-containing inserts in RPMI GlutaMAX (Gibco), supplemented with 2% fetal bovine serum with or without 5 μg/ml LecB. The media of the bottom chamber was supplemented with 10% fetal bovine serum. Transwells were kept at 37°C and 5% CO_2 for 17 h and the cells from the bottom chamber were harvested and lysed with CellTiter-Glo Luminescent Cell Viability Assay (Promega). Luminescence was read in 96-well flat bottom white plates (Corning) using the Spark plate reader (Tecan). Cells in the top chamber were fixed with 4% PFA, permeabilized with 0.1% Triton X-100 and 0.5% BSA, and labeled with goat anti human VE-Cadherin (R&D Systems) and a secondary anti-goat antibody coupled with Alexa Fluor 488. Membranes were then detached from the inserts and mounted onto glass slides using Mowiol. Image acquisition was on an Axio Observer Z1 inverted microscope (Zeiss) equipped with a CSU-X1 spinning disk head (Yokogawa), a back-illuminated Electron-multiplying charge-coupled device (EMCCD) camera (Evolve, Photometrics), and 20× (0.75 numerical aperture) air objectives (Zeiss). Images were processed using FiJi (ImageJ software) with the plugin PureDenoise (École polytechnique fédérale de Lausanne, EPFL).

Endothelial cell–LecB interaction

Human CMEC/D3 cells were grown in EndoGRO-MV Complete Culture Media Kit (Millipore, Burlington, MA, USA), human umbilical vein endothelial cells (HUVECs), and human skin LECs (PromoCell GmbH, Heidelberg, Germany) in endothelial cell growth medium 2 (PromoCell GmbH, Heidelberg, Germany) at 37°C in a humidified incubator containing 5% CO_2 on gelatin-coated plates. Cells at passages 3–6 were used for the experiments. For immunofluorescence, HUVECs were grown on 12-mm glass cover slips in a 4-well Nunc plate (Thermo Fisher Scientific) to 70–100% confluence. Cells were treated with LecB or LecB-A488 (5 μg/ml) for 1 and 3 h. Then, cells were fixed with 4% (wt/vol) PFA for 10 min at RT, quenched with 50 mM ammonium chloride and incubated with 0.2% (vol/vol) saponin in PBS. After that, the cells were blocked with 3% BSA (vol/vol) in PBS and subsequently stained with anti-CD144/VE-cadherin (eBioscience) and anti-FAK (D Biosciences), followed by donkey anti-rabbit Alexa488 (Invitrogen) and goat anti-mouse Alexa647 (Invitrogen), respectively. Nuclei and F-actin were stained with DAPI (Sigma-Aldrich) and Phalloidin Alexa565 (Sigma-Aldrich), respectively. Samples were mounted on cover slips using Mowiol medium (Sigma-Aldrich), and images acquired with a Nikon microscopy (Eclipse Ti-E A1R system) with a 60× oil immersion objective. Images were processed using FiJi (ImageJ software). Subcellular protein distribution was measured as pixels using Fiji (ImageJ software), drawing the cell's perimembranous and the intracellular areas based on phase contrast images. For the quantification of VE-cadherin, the intercellular pixels/area were subtracted by DAPI pixels/area. For cell viability test, cells were treated with LecB or 1 μM Staurosporine (Sigma-Aldrich) for 1 h, followed by 8 μM CellEvent Caspase-3/7 Green Detection Reagent (Invitrogen). MTT (3-(4,5-dimethylthiazol-2-yl)-2,5-diphenyltetrazolium bromide) tetrazolium reduction assay kit (Roth, 11465007001) was additionally used.

Live imaging of HUVECs

HUVECs were seeded on 35-mm imaging dishes with a glass bottom (Ibidi) to 100% confluence. Cells were scratched and treated with or without LecB (5 μg/ml) for 3 h at 37°C. Then, cells were washed with PBS twice and incubated with 1 nM SiR-actin (CY-SC001, Spirochrome) for 1 h at 37°C, a fluorogenic, cell permeable dye with high specificity for F-actin. Live images were recorded with a Nikon microscopy (Eclipse Ti-E A1R system) with a 60x oil immersion objective for 30 min. Images were processed using FiJi (ImageJ software).

Western blot

To determine protein expression by western blot, HUVECs were washed, lysed in RIPA buffer containing phosphatase and protease

inhibitors (200 μM pefablock 0.8 μM aprotinin, 11 μM leupeptin, 1% [v/v] phosphatase inhibitor cocktail 3 [Sigma-Aldrich]) for 45 min on ice, and centrifuged to remove cell debris. The protein concentration of the cell lysates was determined using the Pierce BCA Protein Assay Kit (Thermo Scientific) according to the manufacturer's protocol. 25 μg of protein of each sample was separated on 8% SDS–polyacrylamide gels and transferred on nitrocellulose membranes by semi-dry blotting. The membranes were blocked in 3% BSA for 1 h at RT and incubated with VE-cadherin (eBioscience), anti-phospho-myosin light chain2 (Ser19) (Cell Signaling Technology), anti-α-tubulin (Cell Signaling), or anti-GAPDH (Sigma-Aldrich) overnight at 4°C. Membranes were then incubated with anti-rabbit IgG-HRP (Cell Signaling) or anti-mouse IgG-HRP (Cell Signaling) for 1 h at RT. The Clarity western ECL Blotting Substrate (BIO RAD) was used according to the manufacturer's protocol for signal development and chemiluminescence was detected using the Fusion FX chemiluminescence imager (Vilber Lourmat, Marne-la-Vallée, France). Densitometric quantification of blots was performed using ImageJ and protein levels were normalized to α-tubulin or GAPDH.

Statistical analysis

Statistical analysis was performed using GraphPad Prism (version 9.0.2) software and the indicated statistical analysis software.

Data availability

No large primary datasets have been generated and deposited.

Expanded View for this article is available online.

Acknowledgements

This project was supported by the Deutsche Forschungsgemeinschaft (DFG, German Research Foundation) under Germany's Excellence Strategy (EXC-294), by the Deutscher Akademischer Austauschdienst (DAAD, PPP Frankreich 2019 Phase I—project ID: 57445444), by the Ministry for Science, Research and Arts of the State of Baden-Württemberg (Az: 33-7532.20), by the Freiburg Institute for Advanced Studies (FRIAS), the Campus France-Germany Procope programme (42523VF). This work was supported by the Agence Nationale de la Recherche (ANR-20-CE15-0019-01) to RG. JS was supported by an international PhD fellowship from the French Ministry of National Higher Education and Research and a co-doctoral financial aid (No. CT-17-18) from the German-French University. YG acknowledges the China Scholarship Council and a co-doctoral financial aid (No. CT-07-20) from the German-French University. We would like to express our gratitude to the Life Imaging Center (LIC) of the University of Freiburg for support, Jean-Daniel Fauny for help in image data analysis, Delphine Lamon, and Fabien Lhericel for mouse handling and members of the teams for discussions. The funders had no role in study design, data collection and analysis, decision to publish, or preparation of the manuscript. Open Access funding enabled and organized by Projekt DEAL.

Author contributions

Janina Sponsel: Data curation; formal analysis; investigation; methodology; project administration. **Yubing Guo:** Data curation; formal analysis; investigation; methodology. **Lutfir Hamzam:** Investigation; methodology. **Alice C Lavanant:** Data curation; formal analysis; investigation; visualization; methodology. **Annia Pérez-Riverón:** Data curation; formal analysis; investigation; methodology. **Emma Partiot:** Data curation; investigation; methodology. **Quentin Muller:** Data curation; investigation; methodology. **Julien Rottura:** Investigation; methodology. **Raphael Gaudin:** Conceptualization; resources; supervision; funding acquisition; project administration. **Dirk Hauck:** Resources. **Alexander Titz:** Resources; methodology. **Vincent Flacher:** Conceptualization; data curation; formal analysis; investigation; methodology. **Winfried Römer:** Conceptualization; resources; supervision; funding acquisition; validation; investigation; methodology. **Christopher G Mueller:** Conceptualization; resources; data curation; formal analysis; supervision; funding acquisition; validation; investigation; visualization; methodology; writing – original draft; project administration; writing – review and editing.

Disclosure and competing interests statement

The authors declare that they have no conflict of interest.

References

Avichezer D, Gilboa-Garber N (1987) PA-II, the L-fucose and D-mannose binding lectin of *Pseudomonas aeruginosa* stimulates human peripheral lymphocytes and murine splenocytes. *FEBS Lett* 216: 62 – 66

Bansal A, Chand T, Kumar R (2016) *Pseudomonas* species as an uncommon culprit in transbronchial needle aspiration of mediastinal lymph node. *J Assoc Chest Physicians* 4: 91 – 93

Bazigou E, Lyons OT, Smith A, Venn GE, Cope C, Brown NA, Makinen T (2011) Genes regulating lymphangiogenesis control venous valve formation and maintenance in mice. *J Clin Invest* 121: 2984 – 2992

Birukov KG, Bochkov VN, Birukova AA, Kawkitinarong K, Rios A, Leitner A, Verin AD, Bokoch GM, Leitinger N, Garcia JG (2004) Epoxycyclopentenone-containing oxidized phospholipids restore endothelial barrier function via Cdc42 and Rac. *Circ Res* 95: 892 – 901

Birukova AA, Zagranichnaya T, Fu P, Alekseeva E, Chen W, Jacobson JR, Birukov KG (2007) Prostaglandins PGE(2) and PGI(2) promote endothelial barrier enhancement via PKA- and Epac1/Rap1-dependent Rac activation. *Exp Cell Res* 313: 2504 – 2520

von Bismarck P, Schneppenheim R, Schumacher U (2001) Successful treatment of *Pseudomonas aeruginosa* respiratory tract infection with a sugar solution – a case report on a lectin based therapeutic principle. *Klin Padiatr* 213: 285 – 287

Chemani C, Imberty A, de Bentzmann S, Pierre M, Wimmerová M, Guery BP, Faure K (2009) Role of LecA and LecB lectins in *Pseudomonas aeruginosa*-induced lung injury and effect of carbohydrate ligands. *Infect Immun* 77: 2065 – 2075

Diggle SP, Stacey RE, Dodd C, Cámara M, Williams P, Winzer K (2006) The galactophilic lectin, LecA, contributes to biofilm development in *Pseudomonas aeruginosa*. *Environ Microbiol* 8: 1095 – 1104

Flacher V, Tripp CH, Haid B, Kissenpfennig A, Malissen B, Stoitzner P, Idoyaga J, Romani N (2012) Skin langerin+ dendritic cells transport intradermally injected anti-DEC-205 antibodies but are not essential for subsequent cytotoxic $CD8^+$ T cell responses. *J Immunol* 188: 2146 – 2155

Frensch M, Jäger C, Müller PF, Tadić A, Wilhelm I, Wehrum S, Diedrich B, Fischer B, Meléndez AV, Dengjel J *et al* (2021) Bacterial lectin BambL acts as a B cell superantigen. *Cell Mol Life Sci* 78: 8165 – 8186

Garcia JG, Liu F, Verin AD, Birukova A, Dechert MA, Gerthoffer WT, Bamberg JR, English D (2001) Sphingosine 1-phosphate promotes endothelial cell barrier integrity by Edg-dependent cytoskeletal rearrangement. *J Clin Invest* 108: 689 – 701

Gilboa-Garber N (1972) Inhibition of broad spectrum hemagglutinin from *Pseudomonas aeruginosa* by D-galactose and its derivatives. *FEBS Lett* 20: 242 – 244

Gretz JE, Norbury CC, Anderson AO, Proudfoot AE, Shaw S (2000) Lymph-borne chemokines and other low molecular weight molecules reach high endothelial venules via specialized conduits while a functional barrier limits access to the lymphocyte microenvironments in lymph node cortex. *J Exp Med* 192: 1425 – 1440

Kirkeby S, Wimmerová M, Moe D, Hansen AK (2007) The mink as an animal model for *Pseudomonas aeruginosa* adhesion: binding of the bacterial lectins (PA-IL and PA-IIL) to neoglycoproteins and to sections of pancreas and lung tissues from healthy mink. *Microbes Infect* 9: 566 – 573

Lameignere E, Malinovská L, Sláviková M, Duchaud E, Mitchell EP, Varrot A, Sedo O, Imberty A, Wimmerová M (2008) Structural basis for mannose recognition by a lectin from opportunistic bacteria Burkholderia cenocepacia. *Biochem J* 411: 307 – 318

Lämmermann T, Bader BL, Monkley SJ, Worbs T, Wedlich-Söldner R, Hirsch K, Keller M, Förster R, Critchley DR, Fässler R *et al* (2008) Rapid leukocyte migration by integrin-independent flowing and squeezing. *Nature* 453: 51 – 55

Landi A, Mari M, Kleiser S, Wolf T, Gretzmeier C, Wilhelm I, Kiritsi D, Thünauer R, Geiger R, Nyström A *et al* (2019) *Pseudomonas aeruginosa* lectin LecB impairs keratinocyte fitness by abrogating growth factor signalling. *Life Sci Alliance* 2: e201900422

Lewis AL, Kohler JJ, Aebi M (2022) Microbial lectins: hemagglutinins, Adhesins, and toxins. In *Essentials of Glycobiology*, Varki A, Cummings RD, Esko JD, Stanley P, Hart GW, Aebi M, Mohnen D, Kinoshita T, Packer NH, Prestegard JH *et al* (eds), pp 505 – 516. Cold Spring Harbor, NY: Cold Spring Harbor Laboratory Press

Liu F, Schaphorst KL, Verin AD, Jacobs K, Birukova A, Day RM, Bogatcheva N, Bottaro DP, Garcia JG (2002) Hepatocyte growth factor enhances endothelial cell barrier function and cortical cytoskeletal rearrangement: potential role of glycogen synthase kinase-3beta. *FASEB J* 16: 950 – 962

Meiers J, Siebs E, Zahorska E, Titz A (2019) Lectin antagonists in infection, immunity, and inflammation. *Curr Opin Chem Biol* 53: 51 – 67

Mewe M, Tielker D, Schönberg R, Schachner M, Jaeger KE, Schumacher U (2005) *Pseudomonas aeruginosa* lectins I and II and their interaction with human airway cilia. *J Laryngol Otol* 119: 595 – 599

Mitchell EP, Sabin C, Snajdrová L, Pokorná M, Perret S, Gautier C, Hofr C, Gilboa-Garber N, Koca J, Wimmerová M *et al* (2005) High affinity fucose binding of *Pseudomonas aeruginosa* lectin PA-IIL: 1.0 a resolution crystal structure of the complex combined with thermodynamics and computational chemistry approaches. *Proteins* 58: 735 – 746

Moore KH, Murphy HA, George EM (2021) The glycocalyx: a central regulator of vascular function. *Am J Physiol Regul Integr Comp Physiol* 320: R508 – r518

Plotkowski MC, Saliba AM, Pereira SH, Cervante MP, Bajolet-Laudinat O (1994) *Pseudomonas aeruginosa* selective adherence to and entry into human endothelial cells. *Infect Immun* 62: 5456 – 5463

Quadri SK (2012) Cross talk between focal adhesion kinase and cadherins: role in regulating endothelial barrier function. *Microvasc Res* 83: 3 – 11

Rosen DA, Pinkner JS, Walker JN, Elam JS, Jones JM, Hultgren SJ (2008) Molecular variations in *Klebsiella pneumoniae* and *Escherichia coli* FimH affect function and pathogenesis in the urinary tract. *Infect Immun* 76: 3346 – 3356

Singh RS, Walia AK (2014) Microbial lectins and their prospective mitogenic potential. *Crit Rev Microbiol* 40: 329 – 347

Sommer R, Wagner S, Rox K, Varrot A, Hauck D, Wamhoff E-C, Schreiber J, Ryckmans T, Brunner T, Rademacher C *et al* (2018) Glycomimetic, orally bioavailable LecB inhibitors block biofilm formation of *Pseudomonas aeruginosa*. *J Am Chem Soc* 140: 2537 – 2545

Thuenauer R, Landi A, Trefzer A, Altmann S, Wehrum S, Eierhoff T, Diedrich B, Dengjel J, Nyström A, Imberty A *et al* (2020) The *Pseudomonas aeruginosa* lectin LecB causes integrin internalization and inhibits epithelial wound healing. *mBio* 11: e03260-19

Tielker D, Hacker S, Loris R, Strathmann M, Wingender J, Wilhelm S, Rosenau F, Jaeger KE (2005) *Pseudomonas aeruginosa* lectin LecB is located in the outer membrane and is involved in biofilm formation. *Microbiology* 151: 1313 – 1323

Vicente-Manzanares M, Ma X, Adelstein RS, Horwitz AR (2009) Non-muscle myosin II takes Centre stage in cell adhesion and migration. *Nat Rev Mol Cell Biol* 10: 778 – 790

Wagner S, Sommer R, Hinsberger S, Lu C, Hartmann RW, Empting M, Titz A (2016) Novel strategies for the treatment of *Pseudomonas aeruginosa* infections. *J Med Chem* 59: 5929 – 5969

Wilhelm I, Levit-Zerdoun E, Jakob J, Villringer S, Frensch M, Übelhart R, Landi A, Müller P, Imberty A, Thuenauer R *et al* (2019) Carbohydrate-dependent B cell activation by fucose-binding bacterial lectins. *Sci Signal* 12: eaao7194

4. The linkage between first project and second project

Overall, in my projects, I focused on the effect of *P. aeruginosa* lectin LecB on cell migration. Because we have known several shreds of evidence regarding that, LecB could block epithelial cell migration [10], lung cancer cell wound healing [5], and the tissue repair process of chronic human wounds [9]. One part concerns lung cancer cell migration *in vitro*, and another is about immune cell migration *in vivo*. Then, I can explain the molecular mechanism of LecB on cell migration not only in the cellular aspect but also in the immunological aspect.

Integrins are well known involved in the process of cell adhesion and cell migration. Of note, my previous results have demonstrated that LecB could interact with α3ß1-integrin in MDCK cells. The investigation between LecB and integrins was essential in my projects. I investigated the interaction between ß1-integrin and flotillin-1 and the protein expression of ß1-integrin triggered by LecB in H1299 cells. I found that ß1-integrin interacted with flotillin-1, and LecB increased the protein expression of ß1-integrin from 1 h to 6 h and decreased the counterpart from 12 h to 24 h. Collaborators investigated the cell surface expression of CD18/ß2-integrin, CD11c/αX-integrin, and CD11b/αM-integrin induced by LecB in DC. They found a reduction in the CD18/ß2-integrin-CD11c/ß2-integrin heterodimer on dermal DCs triggered by LecB, indicating that LecB negatively affects DC migration from human skin by binding to a cellular glycoligand [53]. Thus, the effect of integrins was involved in two parts of the project.

5. Additional Publications and contributions

Thuenauer R, Kühn K, **Guo Y**, Kotsis F, Xu M, Trefzer A, Altmann S, Wehrum S, Heshmatpour N, Faust B, Landi A, Diedrich B, Dengjel J, Kuehn EW, Imberty A, Römer W. The Lectin LecB Induces Patches with Basolateral Characteristics at the Apical Membrane to Promote Pseudomonas aeruginosa Host Cell Invasion. mBio. 2022 Jun 28; 13(3):e0081922. doi: 10.1128/mbio.00819-22. Epub 2022 May 2. PMID: 35491830; PMCID: PMC9239240.

Contributions:

I performed the experiments regarding the phosphorylation of PI3K and AKT induced by LecB and inhibitors in polarized MDCK cells (publ. Fig.1 F, H). I also performed the invasion assay to detect the invasive efficiency of *P. aeruginosa* WT and mutants in the host cells (publ. Fig. 2F). I analyzed the statistic and prepared the figures mentioned above.

AMERICAN SOCIETY FOR MICROBIOLOGY | mBio®

RESEARCH ARTICLE

The Lectin LecB Induces Patches with Basolateral Characteristics at the Apical Membrane to Promote *Pseudomonas aeruginosa* Host Cell Invasion

Roland Thuenauer,[a,b,c,d] Katja Kühn,[a,b] Yubing Guo,[a,b] Fruzsina Kotsis,[e] Maokai Xu,[a,b] Anne Trefzer,[a,b] Silke Altmann,[a,b] Sarah Wehrum,[a,b] Najmeh Heshmatpour,[a,b] Brian Faust,[a,b] Alessia Landi,[a,b] Britta Diedrich,[f,g] Jörn Dengjel,[f,g] E. Wolfgang Kuehn,[e] Anne Imberty,[h] Winfried Römer[a,b,i]

[a]Faculty of Biology, Albert-Ludwigs-University Freiburg, Freiburg, Germany
[b]Signalling Research Centres BIOSS and CIBSS, Albert-Ludwigs-University Freiburg, Freiburg, Germany
[c]Leibniz Institute for Experimental Virology (HPI), Hamburg, Germany
[d]Advanced Light and Fluorescence Microscopy Facility, Centre for Structural Systems Biology (CSSB), Hamburg, Germany
[e]Renal Division, Department of Medicine, Faculty of Medicine, Albert-Ludwigs-University Freiburg, Freiburg, Germany
[f]Department of Biology, University of Fribourg, Fribourg, Switzerland
[g]Department of Dermatology, Medical Center, Albert-Ludwigs-University Freiburg, Freiburg, Germany
[h]Université Grenoble Alpes, CNRS, CERMAV, Grenoble, France
[i]Freiburg Institute for Advanced Studies (FRIAS), Albert-Ludwigs-University Freiburg, Freiburg, Germany

Katja Kühn and Yubing Guo contributed equally.

ABSTRACT The opportunistic bacterium *Pseudomonas aeruginosa* can infect mucosal tissues of the human body. To persist at the mucosal barrier, this highly adaptable pathogen has evolved many strategies, including invasion of host cells. Here, we show that the *P. aeruginosa* lectin LecB binds and cross-links fucosylated receptors at the apical plasma membrane of epithelial cells. This triggers a signaling cascade via Src kinases and phosphoinositide 3-kinase (PI3K), leading to the formation of patches enriched with the basolateral marker phosphatidylinositol (3,4,5) trisphosphate (PIP_3) at the apical plasma membrane. This identifies LecB as a causative bacterial factor for activating this well-known host cell response that is elicited upon apical binding of *P. aeruginosa*. Downstream from PI3K, Rac1 is activated to cause actin rearrangement and the outgrowth of protrusions at the apical plasma membrane. LecB-triggered PI3K activation also results in aberrant recruitment of caveolin-1 to the apical domain. In addition, we reveal a positive feedback loop between PI3K activation and apical caveolin-1 recruitment, which provides a mechanistic explanation for the previously observed implication of caveolin-1 in *P. aeruginosa* host cell invasion. Interestingly, LecB treatment also reversibly removes primary cilia. To directly prove the role of LecB for bacterial uptake, we coated bacterium-sized beads with LecB, which drastically enhanced their endocytosis. Furthermore, LecB deletion and LecB inhibition with L-fucose diminished the invasion efficiency of *P. aeruginosa* bacteria. Taken together, the results of our study identify LecB as a missing link that can explain how PI3K signaling and caveolin-1 recruitment are triggered to facilitate invasion of epithelial cells from the apical side by *P. aeruginosa*.

IMPORTANCE An intriguing feature of the bacterium *P. aeruginosa* is its ability to colonize highly diverse niches. *P. aeruginosa* can, besides forming biofilms, also enter and proliferate within epithelial host cells. Moreover, research during recent years has shown that *P. aeruginosa* possesses many different mechanisms to invade host cells. In this study, we identify LecB as a novel invasion factor. In particular, we show that LecB activates PI3K signaling, which is connected via a positive feedback loop to apical caveolin-1 recruitment and leads to actin rearrangement at the apical

Invited Editor Suzanne M. J. Fleiszig, University of California, Berkeley

Editor Nina R. Salama, Fred Hutchinson Cancer Research Center

Address correspondence to Winfried Römer, winfried.roemer@bioss.uni-freiburg.de, or Roland Thuenauer, winfried.roemer@bioss.uni-freiburg.de.

The authors declare no conflict of interest.

Received 23 March 2022
Accepted 12 April 2022
Published 2 May 2022

plasma membrane. This provides a unifying explanation for the previously reported implication of PI3K and caveolin-1 in host cell invasion by *P. aeruginosa*. In addition, our study adds a further function to the remarkable repertoire of the lectin LecB, which is all brought about by the capability of LecB to recognize fucosylated glycans on many different niche-specific host cell receptors.

KEYWORDS actin, epithelial cells, fucose, host cell invasion, lectin, primary cilium

Pseudomonas aeruginosa is a ubiquitous environmental bacterium. Due to its intrinsic adaptability and the rise of multidrug-resistant strains, this bacterium poses a dangerous threat, especially in hospital settings. Accordingly, carbapenem-resistant *P. aeruginosa* strains were categorized by the World Health Organization (WHO) as priority 1 pathogens for which new antibiotics are critically required (1).

When infecting a human host, *P. aeruginosa* can switch between many lifestyles, including planktonic behavior and biofilm formation. In addition, evidence has accumulated during recent years that *P. aeruginosa* can also invade host cells. It has been demonstrated that *P. aeruginosa* is able to enter and survive (2, 3), move (4), and proliferate (5) in nonphagocytic cells. Moreover, after being taken up by macrophages, *P. aeruginosa* can escape phagosomes and eventually lyse the macrophages from the inside (6). The importance of the intracellular lifestyle for *P. aeruginosa* is supported by the observation that this bacterium has a whole arsenal of mechanisms to facilitate uptake by host cells. *P. aeruginosa* can invade by binding the remains of dead cells that are then taken up by surrounding cells through efferocytosis (7), by deploying the effector VgrG2b via its type VI secretion system (T6SS) to promote microtubule-dependent uptake (8), by utilizing cystic fibrosis transmembrane conductance regulator (CFTR) to stimulate caveolin-1-dependent endocytosis (9), and by interaction between the *P. aeruginosa* lectin LecA and the host cell glycosphingolipid globotriaosylceramide (Gb3) to facilitate invasion through a lipid zipper mechanism (10).

After incorporation by a human host, *P. aeruginosa* will typically interact with the apical plasma membranes of epithelial cells lining the mucosae. Interestingly, *P. aeruginosa* has developed mechanisms to manipulate the apical identity of these membranes. The hallmark of this process is the activation of phosphatidylinositol 3-kinase (PI3K), resulting in abnormal accumulation of phosphatidylinositol (3,4,5)-trisphosphate (PIP_3) at the apical plasma membrane, which eventually generates patches with basolateral characteristics at the apical plasma membrane (11). This inversion of polarity has been suggested to help in the binding of *P. aeruginosa* to cells, since this bacterium uses different mechanisms to bind apical and basolateral plasma membranes (12). It is also crucial for host cell invasion by *P. aeruginosa*, because inhibition of PI3K signaling markedly reduces bacterial uptake (13). However, the exact mechanism by which *P. aeruginosa* is able to convert apical to basolateral plasma membrane is not clear. The formation of patches with basolateral characteristics at the apical plasma membrane requires the type III secretion system (T3SS) but, strikingly, does not require any of the toxins that are secreted via the T3SS (14, 15). To explain these observations, two hypotheses were suggested: host cell membrane damage through bacteria might be the initial event leading to basolateral patch formation, or PI3K signaling might be triggered by a still-unknown factor from *P. aeruginosa* (11).

Here, we provide data showing that the tetrameric fucose-specific lectin LecB (16), which is exposed at the outer membrane of *P. aeruginosa* (17, 18), represents the missing link. We showed already in a previous publication that purified LecB is able to bind receptors at the apical and basolateral plasma membrane of polarized Madin-Darby canine kidney (MDCK) cells (19). On the basolateral side, LecB was able to bind integrins, which led to integrin internalization and loss of epithelial polarity. Since only minute amounts of integrins are found at the apical side of polarized MDCK cells (19, 20), LecB did not dissolve epithelial polarity when applied only to the apical side (19). Here, we reveal that binding of LecB to fucosylated apical receptors on epithelial host cells was sufficient to trigger a different signaling cascade in order to promote cellular uptake of

P. aeruginosa. Apical LecB binding led to Src signaling, followed by local PI3K activation, PIP_3 patch formation at the apical plasma membrane, Rac1 signaling, and actin rearrangement to trigger the formation of protrusions in order to enable host cell invasion of *P. aeruginosa*. In addition, we show that caveolin-1 is recruited abnormally to apical membranes after LecB stimulation and that PI3K activation requires caveolin-1. These data suggest LecB as a unifying factor that facilitates and modulates many of the invasion mechanisms that have been reported for *P. aeruginosa*.

RESULTS

Apical LecB treatment triggers Src-PI3K/Akt signaling. To more closely analyze the effects caused by the application of purified LecB to the apical side of polarized MDCK cells, we used MDCK cells stably expressing the green fluorescent protein (GFP)-tagged reporter PH-Akt-GFP, which indicates the localization of the lipid PIP_3 (Fig. 1A) (21). In unstimulated cells, PH-Akt-GFP localized mainly to the basolateral plasma membrane, as expected from the role of PIP_3 as a basolateral marker in polarized epithelial cells (21). In cells treated apically with LecB, PIP_3 accumulated at the apical side and protrusions formed that were positive for PH-Akt-GFP (Fig. 1A, white arrows). This replicates the effects that were previously observed after interaction of whole *P. aeruginosa* bacteria with the apical plasma membrane of MDCK cells (22).

Importantly, we demonstrated already that apical LecB application did not disturb the integrity of tight junctions (19). Thus, LecB-mediated apical PIP_3 accumulation cannot be explained by a loss of the barrier function of tight junctions. We therefore investigated whether activation of PI3K is the cause of apical PIP3 accumulation. Staining cells with antibodies recognizing active PI3K (pP85-Y458 and pP55-Y199) (23, 24) revealed a clearly visible recruitment and activation of PI3K to subapical regions in LecB-treated cells (Fig. 1B). In addition, incubating the cells with the broad-spectrum PI3K inhibitor LY294002 blocked the apical appearance of PH-Akt-GFP after LecB treatment (Fig. 1C and D). Activation of PI3K was also detectable by Western blotting (WB) and peaked at approximately 15 min after initiation of LecB stimulation (Fig. 1E). Upstream from PI3K, the activation of Src kinases was required, as demonstrated by the ability of the Src kinase inhibitors PP2 and SU6656 to block LecB-induced PI3K activation (Fig. 1F). LecB also activated Akt, for which phosphorylation at S473 was detectable after 30 min of LecB application and peaked at approximately 4 h (Fig. 1G). Akt signaling occurred downstream from PI3K, because the broad-spectrum PI3K inhibitor LY294002 blocked Akt activation (Fig. 1H). Further tests revealed that the PI3K subunit p110α was mainly responsible for LecB-mediated Akt activation, since the p110α-specific inhibitor PIK-75 blocked Akt activation (Fig. S1A in the supplemental material), whereas the p110β-specific inhibitor TGX-221 did not (Fig. S1B). Another fucose-binding lectin, *Ulex europaeus* agglutinin I (UEA-I), failed to replicate LecB-triggered Akt signaling (Fig. S1C), thus indicating that the observed effects are specific for LecB.

To demonstrate that LecB-mediated PI3K/Akt activation is not limited to MDCK cells, we carried out experiments in other cell lines. We chose H1975 lung epithelial cells because *P. aeruginosa* frequently infects lungs. Whereas MDCK cells are Gb3-negative, H1975 cells express Gb3 (Fig. S2). The glycosphingolipid Gb3 has been previously found to be required for LecA-mediated internalization of *P. aeruginosa* (10). In H1975 cells, LecB also triggered Akt activation, in a dose- and time-dependent manner (Fig. S3A to D) and dependent on PI3K (Fig. S3E and F, showing the results of experiments using the pan-PI3K inhibitors wortmannin and LY294002 and the Akt inhibitor triciribine). As a further control, we verified that soluble L-fucose, which prevents LecB from engaging with host cell receptors, is able to inhibit LecB-triggered Akt signaling (Fig. S3G and H). This demonstrates that LecB binding to fucosylated receptors is necessary to trigger PI3K/Akt signaling and also validates the purity of our LecB preparation.

To identify apical interaction partners of LecB, we applied LecB-biotin apically to polarized MDCK cells, lysed them, and precipitated LecB-receptor complexes with streptavidin beads. Mass spectrometry (MS) analysis revealed 12 profoundly enriched

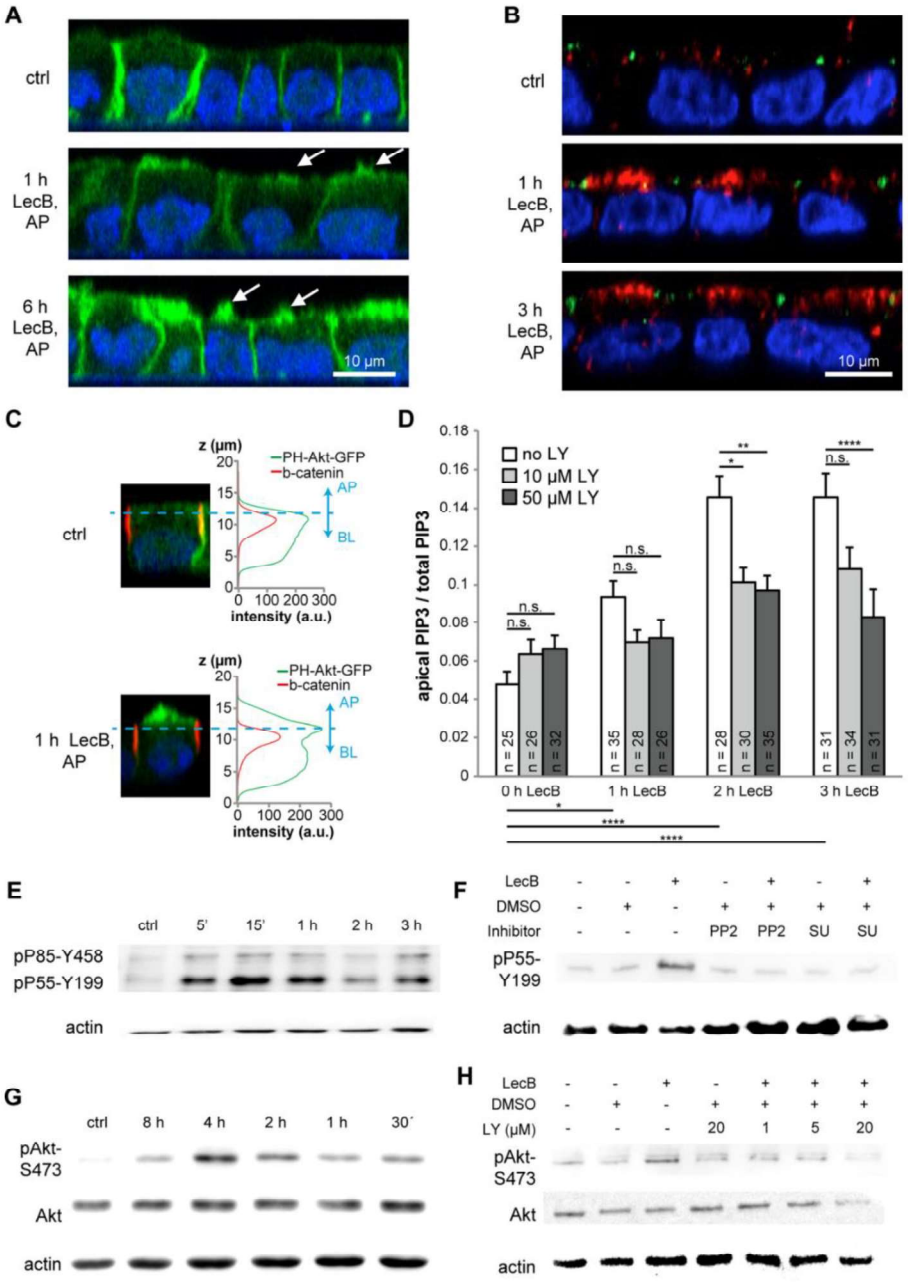

FIG 1 After binding to the apical plasma membrane of MDCK cells, LecB triggers an Src-PI3K/Akt signaling cascade. (A) MDCK cells stably expressing the PIP_3 marker PH-Akt-GFP (green) were left untreated (ctrl) or treated from the apical (AP) side with LecB for the indicated time periods; nuclei were stained with DAPI (blue). White arrows point to apical protrusions resulting from LecB treatment. (B) MDCK cells were left untreated (ctrl) or treated with LecB as indicated, fixed, and then stained for active PI3K (pP85-Y458 and pP55-Y199; red) and ZO-1 (green); nuclei were stained with DAPI (blue). (C) MDCK cells stably expressing the PIP_3

(Continued on next page)

proteins (Table S1), underscoring the property of LecB of binding to multiple receptors. However, this property also prevented us from singling out a receptor that was responsible for LecB-triggered PI3K signaling, since the list included several proteins for which a capacity to elicit PI3K signaling was known (CEACAM1 [25, 26], mucin-1 [27], ICAM1 [28], and podocalyxin [29, 30]).

Taken together, these findings show that after binding to fucosylated receptors at the plasma membrane of epithelial cells, LecB triggered an Src-PI3K/Akt signaling cascade, which replicated the cellular responses that were observed after binding of live *P. aeruginosa* cells to apical membranes (13).

Coating beads with LecB and expression of LecB by *P. aeruginosa* both enhance their apical uptake. To more realistically model the geometry during infection with *P. aeruginosa*, we utilized bacterium-sized beads that were coated with LecB. In pilot experiments using cell fixation, LecB-coated beads were seen to bind to the apical plasma membrane of polarized MDCK cells and to cause local apical accumulation of PH-Akt-GFP/PIP_3 (Fig. 2A), and many beads were found to be completely internalized by cells (Fig. 2B). Live-cell microscopy experiments revealed that apical PH-Akt-GFP/PIP_3 accumulation is a transient event that occurs before apical uptake of beads by MDCK cells (Fig. 2C, Movie S1). Detailed quantification showed that biotin-coated control beads were able to trigger apical PH-Akt-GFP/PIP_3 bursts to some extent, but at a much lower rate than LecB-coated beads (Fig. 2D). Interestingly, the PH-Akt-GFP/PIP_3 bursts caused by control beads were hardly sufficient to mediate cellular uptake, whereas the LecB-coated beads were taken up extensively (Fig. 2E). In addition, LecB treatment stimulated macropinocytotic uptake of dextran in H1975 cells (Fig. S4A and B), which provides further evidence that LecB activates cellular uptake mechanisms.

Motivated by these results, we investigated whether the expression of LecB influences host cell uptake of live *P. aeruginosa* bacteria. Indeed, abrogation of LecB expression in *P. aeruginosa* (dLecB) and blockage of LecB with L-fucose diminished the apical uptake of *P. aeruginosa* in polarized MDCK cells (Fig. 2F). In accordance with previous studies (13, 31), inhibition of Src kinases with PP2 and inhibition of PI3K with LY294002 also decreased *P. aeruginosa* uptake (Fig. 2F). Due to the easier handling, the experiments whose results are shown in Fig. 2F were carried out with MDCK cells grown in 24-well plates. For verification, we repeated them with transwell filter-grown MDCK cells, which yielded comparable results (Fig. 2G). Of note, the association of wild-type (wt) and dLecB *P. aeruginosa* with polarized MDCK cells was not significantly different (Fig. S5), which suggests that the observed decrease of invasion efficiency upon deletion of LecB was due to LecB-mediated signaling and not due to reduced host cell binding. In H1975 cells, the uptake of *P. aeruginosa* was also lowered by LecB deletion (Fig. S4C) and L-fucose treatment (Fig. S4D).

Taken together, these data demonstrate that LecB promotes the uptake of *P. aeruginosa* from the apical side in polarized epithelial cells.

LecB-mediated PI3K signaling leads to Rac activation and actin rearrangement. To better understand the cellular response upon apical LecB stimulation, we investigated how PI3K activation is linked to *P. aeruginosa* uptake. Motivated by the known

FIG 1 Legend (Continued)
marker PH-Akt-GFP were treated with LecB from the apical (AP) side, fixed, and stained with β-catenin. To distinguish the apical and basolateral portion of the PH-Akt-GFP signal, β-catenin staining was utilized as a ruler. For the experiment, PH-Akt-GFP-positive cells were mixed with wt cells before seeding in a ratio of 1:10. This enabled an unbiased quantification by measuring the signals only from PH-Akt-GFP-positive cells that were surrounded by wt cells. a.u., arbitrary units. (D) Quantification of the results of the experiment described in the legend to panel C. The numbers indicated at the bottom of each bar represent the number of individual cells that were measured for each condition. Whereas cells treated with LecB show a time-dependent increase of the apical-to-total PH-Akt-GFP/PIP_3 signal ratio, treatment with LY294002 (LY) reversed this effect. (E) MDCK cells were treated apically with LecB for the indicated times and subjected to Western blotting (WB) using an antibody recognizing active PI3K (pP85-Y458 and pP55-Y199). (F) MDCK cells were treated apically with LecB and PP2 (10 μM) or SU6656 (10 μM) for 1 h and subjected to WB utilizing an antibody recognizing active PI3K (pP55-Y199). DMSO, dimethyl sulfoxide. (G) MDCK cells were treated apically with LecB for the indicated times and subjected to WB utilizing an antibody recognizing active Akt (pAkt-S473). (H) MDCK cells were treated apically with LecB and indicated concentrations of LY294002 (LY) for 1 h and subjected to WB utilizing an antibody recognizing active Akt (pAkt-S473).

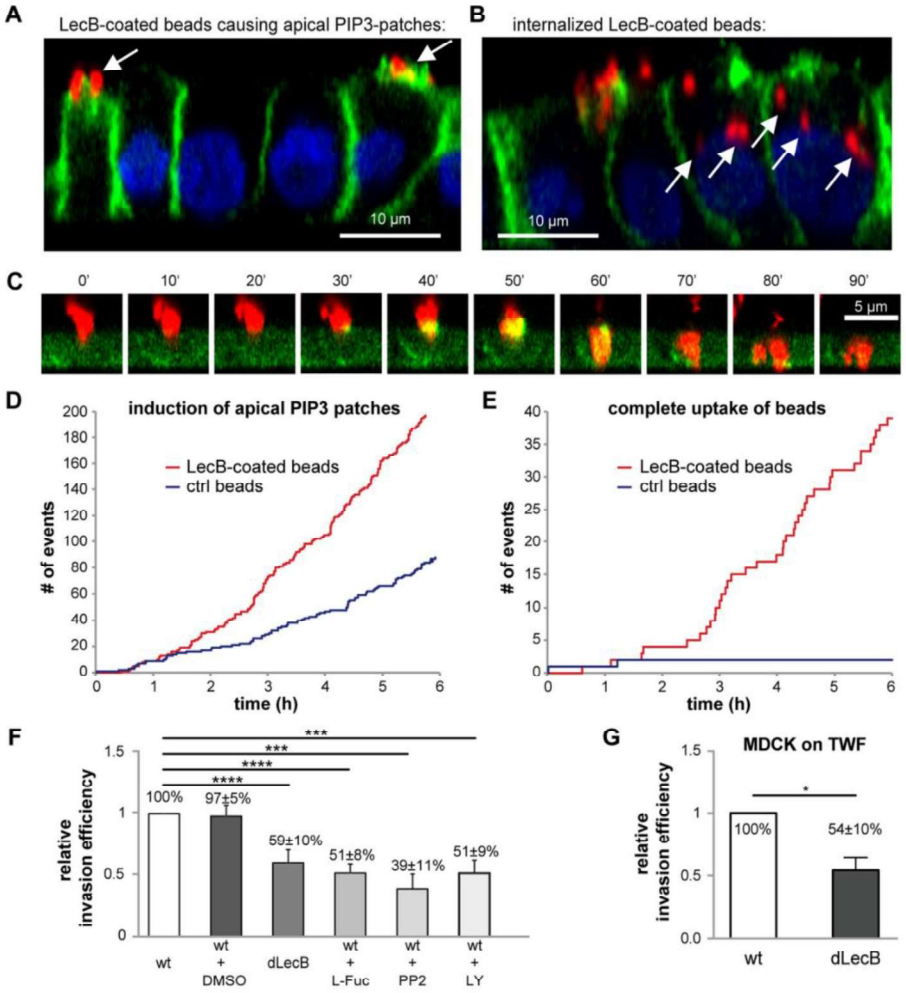

FIG 2 LecB facilitates apical uptake of beads and apical invasion of *P. aeruginosa*. (A and B) Red fluorescent LecB-coated bacterium-sized beads with 1-μm diameter were apically applied to MDCK cells stably expressing the PIP_3 marker PH-Akt-GFP (green) for 6 h; nuclei were stained with DAPI (blue). (A) Instances of beads causing apical PIP_3 patches (white arrows). (B) Fully internalized beads are depicted (white arrows). (C to E) MDCK cells stably expressing PH-Akt-GFP (green) were allowed to polarize on cover glasses. Red fluorescent beads of 1-μm diameter coated with LecB were applied, and live-cell confocal imaging was performed. The images show apicobasal cross sections extracted from confocal image stacks. (D and E) The number of induced apical PIP_3-patches (D) and the number of beads that are completely taken up over time (E) are depicted for biotin-coated beads (ctrl) and LecB-coated beads. (F) Using an amikacin protection assay, the invasion efficiencies of wild-type (wt) and LecB-deficient (dLecB) PAO1 applied at an MOI of 50 for 2 h on the apical side of polarized MDCK cells grown in 24-well plates were determined. In addition, the invasion efficiencies for bacteria preincubated with 100 mg/mL L-fucose (L-Fuc) and for cells treated with PP2 (10 μM) and LY294002 (LY; 10 μM) were measured. Mean values and SEM from $n = 8$ experiments are shown. (G) Amikacin protection assays measuring the apical invasion of PAO1-wt and PAO1-dLecB in MDCK cells grown on transwell filters. Invasion for 2 h, MOI = 50, $n = 3$.

correlations between PI3K and Rac activation (32) and the reported implication of Rac in *P. aeruginosa* internalization (31), we carried out experiments using Rac123-G-LISA assays to test the capability of LecB to activate Rac. We found that apically applied LecB activated Rac in a time-dependent manner in MDCK cells (Fig. 3A) and also in H1975 cells (Fig. 3B). The PI3K inhibitor wortmannin blocked LecB-mediated Rac activation (Fig. 3C), indicating that PI3K activation occurred upstream from Rac activation.

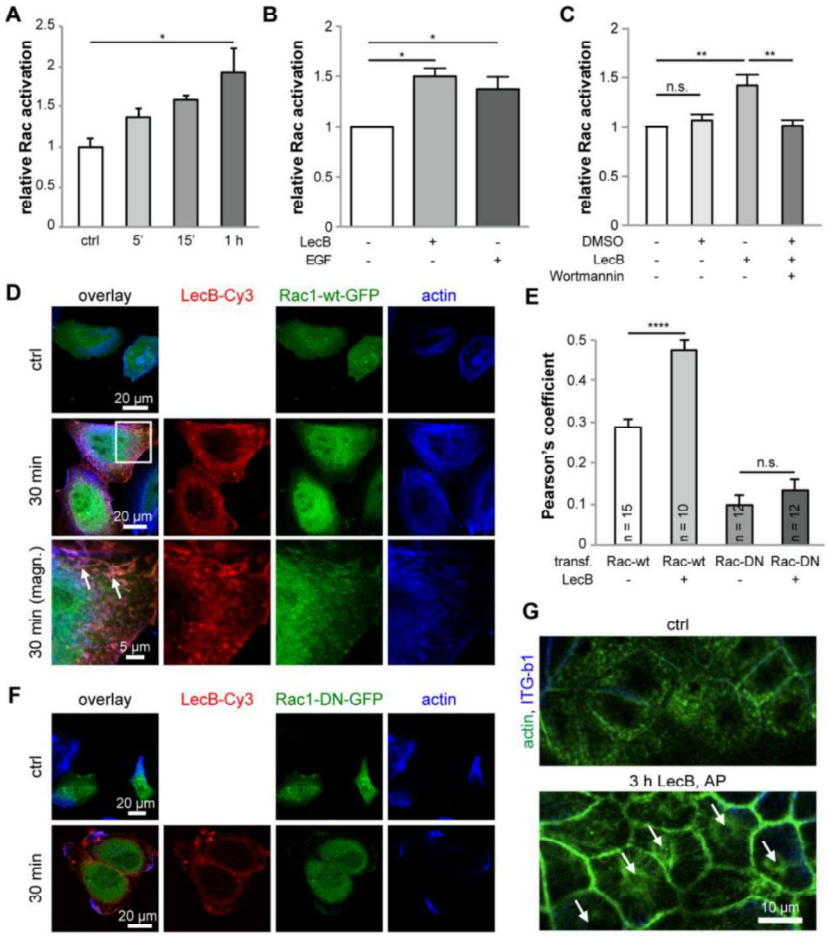

FIG 3 Apical LecB stimulation leads to Rac activation and actin rearrangement. (A) The activation of Rac upon apical LecB treatment of MDCK cells was measured using a Rac123-G-LISA assay; $n = 3$. (B) H1975 cells were treated with LecB or EGF (20 nM), and Rac activation was measured using a Rac123-G-LISA assay; $n = 3$. (C) H1975 cells were treated with LecB and wortmannin (100 nM), and Rac activation was measured using a Rac123-G-LISA assay; $n = 6$. (D to F) H1975 cells transfected with Rac1-wt-GFP (green) (D) or Rac1-DN-GFP (green) (F) were treated with LecB-Cy3 (red) as indicated, fixed, and stained for actin with phalloidin-Atto 647 (blue). (D) White arrows point to ruffle-like structures where LecB, Rac1-wt-GFP, and actin colocalized. (E) The Pearson's colocalization coefficient between Rac1-wt-GFP or Rac1-DN-GFP and actin in cells untreated or treated with LecB-Cy3 was determined in individual cells, and the average was calculated. (G) MDCK cells treated with LecB as indicated were fixed and stained with phalloidin-Atto 488 to stain actin (green) and β1-integrin (blue). Lateral confocal cross sections along the apical poles of the cells are displayed.

To investigate the consequences of LecB-mediated Rac activation on the actin cytoskeleton further, we utilized unpolarized H1975. The reason for this is that this allowed us to use overexpression of dominant-negative (DN) Rac1, which would result in unwanted side effects in polarized MDCK cells, because Rac1 also has roles during the polarization of MDCK cells (33). In sparsely seeded H1975 cells, LecB caused ruffle-like structures (Fig. 3D), and LecB colocalized with transfected Rac1-wt-GFP and actin in the ruffle-like regions (Fig. 3D, white arrows). To verify that LecB induced recruitment of Rac1-wt-GFP toward actin, we determined the Pearson's colocalization coefficient between Rac1-wt-GFP and actin, which increased significantly in LecB-treated cells

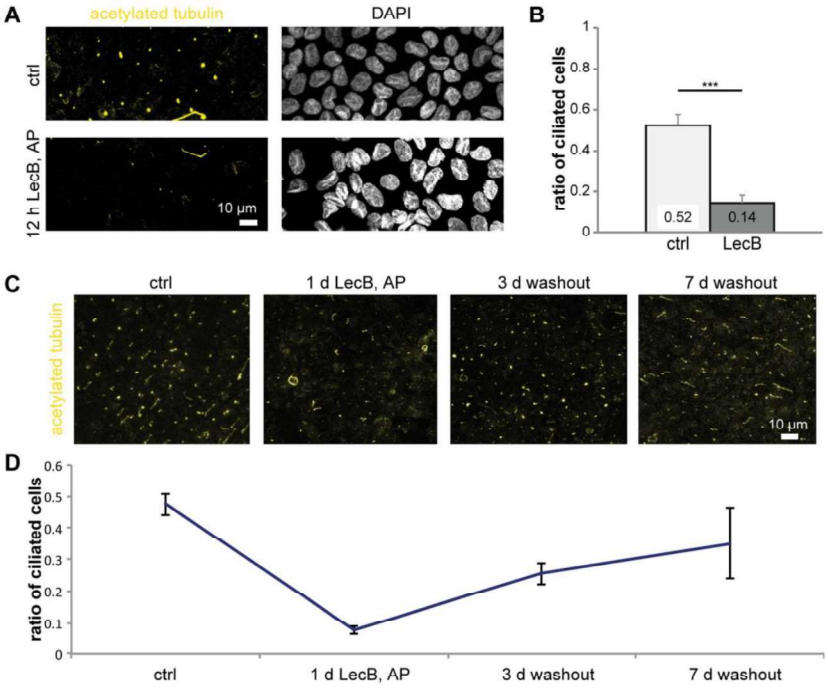

FIG 4 Apical treatment with LecB removes primary cilia in a reversible manner. (A to D) MDCK cells were grown on glass coverslips for 10 days. After the indicated treatments, cells were fixed, and immunofluorescence staining was performed for acetylated tubulin (yellow) to visualize primary cilia. (A) Nuclei were additionally stained with DAPI (white). Maximum intensity projections of confocal image stacks covering total cell heights are shown. (B) The ratio of ciliated cells was calculated by dividing the number of visible cilia by the total number of cells. Five fields of view (125 μm by 125 μm) were summed up for $n = 1$, and the results from $n = 3$ independent experiments were averaged. (C) MDCK cells were treated with LecB, followed by washout as indicated. (D) Quantification of the results of the experiment shown in panel C.

(Fig. 3E). This was not the case when DN Rac1-GFP (Rac1-DN-GFP) was overexpressed in H1975 cells (Fig. 3F and E), showing the requirement of functional Rac for this effect. For verification, we repeated the experiment in untransfected H1975 cells using antibodies recognizing endogenous Rac1 (Fig. S6). Consistently, recruitment of Rac to actin upon LecB stimulation occurred as well in this experiment.

Apical application of LecB also led to substantial rearrangement of actin at the apical cell pole of MDCK cells (Fig. 3G). In untreated cells, dotted structures representing microvilli and the central actin-devoid region of the periciliary membrane and the primary cilium (34–36) were visible. In cells treated apically for 3 h with LecB, this subapical organization of the actin cytoskeleton was completely lost. Actin was recruited to lateral aspects of the cell membrane, and actin stress fibers constricting around the central position of the outgrowth of the primary cilium (Fig. 3G, white arrows) appeared.

In summary, the results of these experiments show that LecB-triggered PI3K signaling leads to Rac activation and actin rearrangement. All these processes have been previously observed during internalization of *P. aeruginosa* (22, 31, 37), thus further underscoring the role of LecB for *P. aeruginosa* host cell invasion.

Apical LecB treatment reversibly removes primary cilia. Motivated by our observation that LecB treatment led to the formation of actin stress fibers that appeared to constrict around the basis of the primary cilium, we investigated the effects of LecB on the primary cilium. Interestingly, apical application of LecB removed primary cilia from polarized MDCK cells (Fig. 4A and B) within 12 h. This effect was reversible after

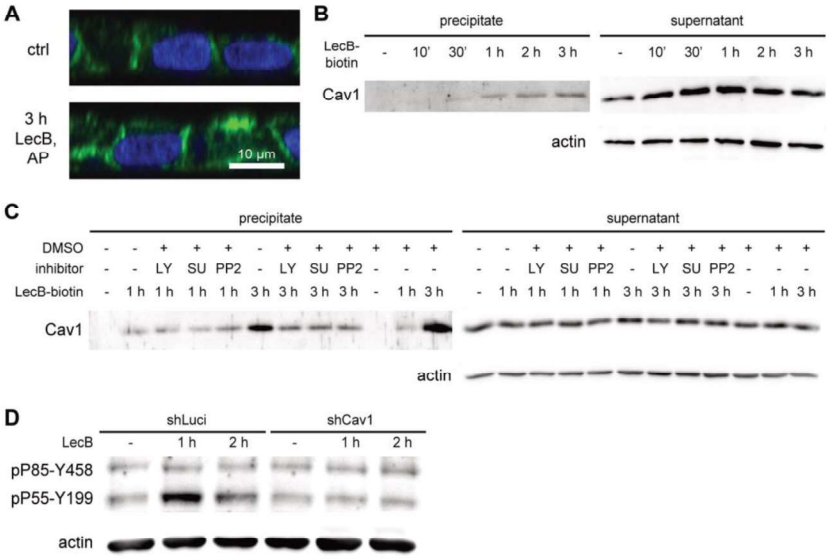

FIG 5 Caveolin-1 is essential for LecB-triggered PI3K signaling. (A) Polarized MDCK cells were treated apically (AP) with LecB as indicated, fixed, and stained for caveolin-1 (green); nuclei were stained with DAPI (blue). (B and C) LecB-biotin was apically applied to polarized MDCK cells for the indicated times. After cell lysis, LecB-biotin-receptor complexes were precipitated with streptavidin beads, and the precipitate and the supernatant were probed by WB for caveolin-1. (C) Cells were additionally treated with LY294002 (LY; 10 μM), PP2 (10 μM), or SU6656 (SU; 10 μM). (D) Polarized MDCK cells expressing a control shRNA (shLuci) and caveolin-1 knockdown MDCK cells (shCav1) were treated apically with LecB as indicated and subjected to WB using an antibody recognizing active PI3K (pP85-Y458 and pP55-Y199).

washout of LecB (Fig. 4C and D). Although the potential physiological consequences of loss of primary cilia during *P. aeruginosa* infection remain to be investigated, this finding underscores the massive extent of LecB-mediated actin rearrangement.

LecB triggers a feedback loop between caveolin-1 recruitment and PI3K activation. Interestingly, we also found caveolin-1 in the MS screen of LecB interactors (Table S1). Since caveolin-1 is a cytosolic protein, it presumably coprecipitated with LecB-interacting receptors. Motivated by this finding, we further investigated the behavior of caveolin-1 after LecB treatment. In undisturbed MDCK cells, caveolin-1 preferentially localized to the basolateral plasma membrane, as observed before (Fig. 5A) (38). However, apical LecB treatment resulted in abnormal recruitment of caveolin-1 toward the apical cell pole (Fig. 5A). In addition, the recruitment of caveolin-1 to LecB-receptor complexes was verifiable by WB and increased in a time-dependent manner (Fig. 5B). Interestingly, blocking Src kinases with SU6656 or PP2 and blocking PI3K with LY294002 diminished the coprecipitation of caveolin-1 in complexes with LecB-biotin (Fig. 5C). To directly investigate the requirement of caveolin-1 for LecB-mediated PI3K activation, we knocked down caveolin-1 in MDCK cells using small hairpin RNA (shRNA) (Fig. S7). Caveolin-1 knockdown almost completely suppressed PI3K activation upon LecB treatment (Fig. 5D).

Taken together, these data demonstrate that caveolin-1 is apically recruited by LecB stimulation and that this recruitment requires activation of Src kinases and PI3K, whereas caveolin-1 is also required for LecB-triggered PI3K activation. This constitutes a positive feedback loop between caveolin-1 recruitment and PI3K activation.

DISCUSSION

Here, we demonstrate that LecB is able to trigger an Src-PI3K-Rac signaling cascade, which is modulated by caveolin-1 and leads to actin rearrangement and protrusion formation in order to promote cellular uptake of *P. aeruginosa* bacteria. This adds LecB-

triggered signaling to the growing list of *P. aeruginosa* host cell invasion mechanisms, which provokes the question of why this bacterium has evolved so many invasion mechanisms and how LecB fits in.

The multitude of invasion mechanisms might be rooted in the adaptability of this opportunistic pathogen. *P. aeruginosa* can infect the respiratory tract, urinary tract, eye, and skin (39), and it was demonstrated that this bacterium can invade epithelial cells from the lung (9), cornea (2), and kidneys (22, 40). Considering this diversity, it makes sense that *P. aeruginosa* possesses many invasion mechanisms, which might be used by the bacterium depending on the type of host cell encountered. One example is lipid zipper-type invasion, which requires interaction between LecA from *P. aeruginosa* and the glycosphingolipid Gb3 as the host cell factor (10). However, this lipid is not expressed in all epithelial cell types. For example, the MDCK cells used in this study do not express Gb3 (Fig. S2) (41). Nevertheless, *P. aeruginosa* successfully invaded MDCK cells, and thus, it uses alternative pathways like LecB-mediated signaling, as we demonstrated here. In addition, we show that LecB deletion in *P. aeruginosa* also decreased the invasion efficiency in H1975 cells, which we identified as Gb3 positive (Fig. S2), and it has been demonstrated previously that Gb3 expression in MDCK cells increased the invasion efficiency (10). These examples suggest that invasion mechanisms, such as LecA- and LecB-dependent invasion, are not exclusive but rather function in an additive manner. Our data provide an additional line of evidence for a cooperative function of invasion mechanisms. Coating of bacterium-sized beads with LecB markedly stimulated their uptake into cells, thus demonstrating that LecB alone is sufficient for stimulating cellular uptake. But LecB deletion or blocking LecB with L-fucose did not decrease the internalization of *P. aeruginosa* bacteria to the same extent as inhibition of Src kinases and PI3K did. This hints at other bacterial factors that are also able to cause PI3K-dependent uptake into host cells. A potential candidate is type IV pili, since deletion of pili led to a small but significant reduction of PI3K/Akt activation upon apical application of *P. aeruginosa* to polarized Calu-3 cells (12).

How is LecB able to trigger the Src-PI3K-Rac-actin signaling cascade? By MS analysis, we showed that LecB binds multiple apical receptors capable of triggering PI3K signaling: CEACAM1 (25, 26), Mucin-1 (27), ICAM1 (28), and podocalyxin (29, 30). This makes it on one hand more robust for the bacterium to trigger the desired response, but it also makes it difficult for us to isolate a detailed mechanistic picture of LecB action at the apical cell membrane. We hypothesize that LecB has, due to being a tetramer that offers four binding sites (42), the capacity to cross-link and cluster different receptors (19, 43), which is a general mechanism to activate receptor-mediated signaling cascades at the cell membrane. The data we present here provide two independent lines of evidence for this hypothesis. The first line derives from our control experiments with the lectin UEA-I. UEA-I is also able to bind fucose, but it has only two binding sites (44). This makes UEA-I a less ideal cross-linker than the tetrameric LecB, which was shown to be capable of cross-linking fucosylated lipids and integrins (19, 43). Consequently, we found that UEA-I was not capable of eliciting PI3K signaling. This confirms that binding to fucosylated receptors is not enough and additional cross-linking, as in the case of LecB, is required for triggering PI3K signaling. The second line of evidence can be deduced from our experiments regarding caveolin-1. It has been shown that receptor cross-linking is sufficient to aberrantly induce caveolin-1-containing caveolae at the apical plasma membrane of epithelial cells (38, 45). LecB application at the apical plasma membrane also caused the abnormal recruitment of caveolin-1 to the apical plasma membrane, which can be explained by assuming that LecB cross-linked receptors. In addition, the fact that caveolin-1 knockdown abrogated LecB-mediated PI3K activation, together with our finding that caveolin-1 recruitment could be blocked by PI3K inhibitors, suggests that there exists a positive feedback loop between PI3K activation and caveolin-1 recruitment. This is strongly supported by our observation that caveolin-1 coprecipitation with apical LecB receptors increased in a time-dependent manner. This also offers an explanation for the previously reported role of caveolin-1 for *P. aeruginosa* host cell invasion (9).

There has been speculation in the literature about the initial events that trigger the basolateral patch formation at the apical membrane by *P. aeruginosa*, and two possible hypotheses were offered (11): Either membrane damage could be responsible, or a still unknown bacterial factor causes the required PI3K activation. Our results favor the second hypothesis. Binding and cross-linking of apical receptors by LecB offer a direct explanation for PI3K activation and, thus, identify LecB as the unknown bacterial factor. In addition, we previously reported that application of purified LecB to the apical plasma membrane of MDCK cells does not induce membrane damage, as measured by trypan blue assays that use the fluorescence of trypan blue as a sensitive readout (19). Likewise, tight junction integrity was not affected by apical application of LecB (19). This is in agreement with the finding by others that the formation of PIP_3-rich protrusions during infection with *P. aeruginosa* did not compromise tight junctions (11). This finding also excludes the possibility that LecB-triggered apical PIP_3 accumulation occurred by diffusive spreading of PIP_3 from the basolateral plasma membrane and additionally proves that apical PIP_3 accumulation was due to LecB-mediated local PI3K activity at the apical plasma membrane.

The involvement of Rac1 for *P. aeruginosa* internalization through the LecB-triggered cascade we describe here will need further clarification. Specifically, the *P. aeruginosa* exotoxin S and exotoxin T are known to contain N-terminal RhoGTPase activating protein (RhoGAP) domains, which can hydrolyze GTP to GDP in Rho, Rac, and Cdc42, leading to cytoskeletal depolymerization and countering host cell invasion (*46*, *47*). It will be interesting to investigate whether varying expression levels of LecB, exotoxin S, and exotoxin T cause more or less invasive behavior of *P. aeruginosa*.

In conclusion, our results identify LecB as a novel bacterial factor that promotes uptake of *P. aeruginosa* bacteria from the apical side of epithelial cells. Our data suggest that LecB represents a missing link that provides a unifying explanation for many observations that have been made during host cell invasion by *P. aeruginosa*. We revealed that LecB is sufficient to trigger the well-known Src-PI3K-Rac signaling cascade (11), which is required for basolateral patch formation at the apical plasma membrane and host cell invasion. LecB-mediated signaling also provides additional rationales for the previously found implication of caveolin-1 in *P. aeruginosa* invasion (9), since we identified here a LecB-triggered positive feedback loop between PI3K activation and caveolin-1 recruitment to the apical plasma membrane.

MATERIALS AND METHODS

Antibodies, plasmids, and reagents. The antibodies used are listed in Table S2. The plasmid pPH-Akt-GFP encoding PH-Akt-GFP was a gift from Tamas Balla (Addgene plasmid no. 51465). The plasmids encoding wild-type Rac1 tagged with GFP (Rac1-wt-GFP) and a mutant protein bearing a change of T to N at position 17 (Rac1-T17N) and tagged with GFP (Rac1-DN-GFP) were kindly provided by Stefan Linder (University Hospital Hamburg-Eppendorf, Germany).

Recombinant LecB was produced in *Escherichia coli* BL21(DE3) cells and purified with affinity columns as previously described (19). LecB and fluorophore-conjugated LecB were used at a concentration of 50 μg/mL (4.3 μM) unless stated otherwise. The B-subunit of Shiga toxin 1 (StxB) recombinantly produced in *Escherichia coli* was from Sigma-Aldrich. LY294002, wortmannin, PP2, SU6656, PIK-75, TGX-221, and triciribine were from Selleckchem. UEA-I was from Vector Labs. Human epidermal growth factor (EGF), L-fucose (6-deoxy-L-galactose), and fluorescein isothiocyanate (FITC)-dextran (70 kDa) were from Sigma-Aldrich. Phalloidin-Atto 488 and phalloidin-Atto 647 were from Atto-Tec.

Mammalian cell culture and creation of stable cell lines. MDCK strain II cells were cultured in Dulbecco's modified Eagle's medium (DMEM) supplemented with 5% fetal calf serum (FCS) at 37°C and 5% CO_2. H1975 cells were maintained in Roswell Park Memorial Institute (RPMI) 1640 medium supplemented with 10% FCS at 37°C and 5% CO_2. For generating polarized MDCK monolayers, 3×10^5 MDCK cells were seeded on transwell filters (12-well format, 0.4-μm pore size, polycarbonate membrane, product number 3401; Corning) and cultured for 4 days before experiments. For experiments with H1975 cells, 3×10^4 cells were seeded per 12-mm glass cover slip placed in a 24-well plate and cultured for 1 day. For the creation of the MDCK cell line stably expressing PH-Akt-GFP, cells were transfected with the plasmid pPH-Akt-GFP using lipofectamine 2000 (Thermo Fisher). After allowing the cells to express the proteins overnight, they were trypsinized and plated sparsely in medium containing 1 mg/mL G418. After single colonies had formed, GFP-positive colonies were extracted with cloning rings. At least 6 colonies were extracted for each cell line, grown on transwell filters for 4 days, fixed, and stained against the basolateral marker protein β-catenin and the tight junction marker protein ZO-1 to assay their polarized morphology. Based on these results, we chose one colony for each cell line for further experiments.

Caveolin-1 knockdown. To achieve knockdown of caveolin-1 in MDCK cells, a lentivirus-based shRNA system based on the plasmids pCMV-ΔR8.91, pMD2G-VSVG, and pLVTH was used (48). The plasmid pLVTH was modified using Gibson cloning to encode the target sequence for caveolin-1 knockdown, 5′-GATGTGATTGCAGAACCAG-3′ (49). As a control, an shRNA targeted against luciferase, which is not endogenously expressed in MDCK cells, was used (target sequence, 5′-CGTACGCGGAATACTTCGA-3′). Lentivirus was produced with HEK 293 T cells, purified with sucrose cushion centrifugation (20% sucrose, 4,000 × *g*, 14 h), resuspended in MDCK medium, and applied to freshly seeded MDCK cells. To ensure a lentivirus transduction efficiency of >80%, GFP fluorescence was checked after 48 h, since pLVTH also encodes GFP. Knockdown efficiency was then verified using WB (Fig. S7).

Immunofluorescence. Cells were washed two times with phosphate-buffered saline without Ca^{2+} and Mg^{2+} (PBS) and then fixed with 4% (wt/vol) formaldehyde (FA) for 15 min at room temperature. Samples were treated with 50 mM ammonium chloride for 5 min to quench FA and then permeabilized with a SAPO medium (PBS supplemented with 0.2% [wt/vol] bovine serum albumin and 0.02% [wt/vol] saponin) for 30 min. Primary antibodies were diluted in SAPO medium and applied on the samples for 60 min at room temperature. After three washes with PBS, secondary dye-labeled antibodies, and, if required, DAPI (4′,6-diamidino-2-phenylindole) and dye-labeled phalloidin were diluted in SAPO medium and applied to the cells for 30 min at room temperature (details for the antibodies used are listed in Table S2). After 5 washes with PBS, cells were mounted for microscopy using glycerol-based medium supplemented with DABCO (MDCK) (50) or Mowiol-based medium (H1975) (51).

Microscopy of fixed cells and live-cell experiments. For imaging, an A1R confocal microscope (Nikon) equipped with a 60× oil immersion objective (numeric aperture [NA] = 1.49) and laser lines at 405 nm, 488 nm, 561 nm, and 641 nm was utilized. Image acquisition and analysis was performed with NIS-Elements 4.10.04 (Nikon).

For live-cell experiments, MDCK cells stably expressing PH-Akt-GFP (uptake of LecB-coated beads) were grown as polarized monolayers for 3 days on Lab-Tek II chambered cover glasses (8 wells, number 1.5 borosilicate glass). The medium was changed to recording medium (Hanks' balanced salt solution [HBSS] supplemented with 1% FCS, 4.5 g/L glucose, and 20 mM HEPES).

WB. Before Western blotting, cells were starved in medium without FCS (16 h for polarized MDCK cells, 2 h for H1975 cells), and stimulation was also carried out in medium without FCS. After stimulation, cells were washed twice with PBS and lysed in radioimmunoprecipitation assay (RIPA) buffer (20 mM Tris [pH 8], 0.1% [wt/vol] SDS, 10% [vol/vol] glycerol, 13.7 mM NaCl, 2 mM EDTA, and 0.5% [wt/vol] sodium deoxycholate in water) supplemented with protease inhibitors (0.8 μM aprotinin, 11 μM leupeptin, 200 μM Pefabloc) and phosphatase inhibitor (1 mM sodium orthovanadate). Protein concentrations were analyzed using a bicinchoninic acid (BCA) assay kit (Pierce). Equal amounts of protein per sample were separated by SDS-PAGE and transferred to a nitrocellulose membrane. The membrane was blocked with tris-buffered saline (TBS) supplemented with 0.1% (vol/vol) Tween 20 and 3% (wt/vol) BSA for 1 h and incubated with primary and (HRP)-linked secondary antibodies diluted in the blocking solution. Detection was performed by a chemiluminescence reaction using the Fusion-FX7 Advance imaging system (Peqlab Biotechnologie GmbH). If not indicated otherwise, control samples were treated with the same volume of PBS that was used for dissolving LecB in the LecB-treated samples.

Rac123-G-LISA. Rac activation was measured with a Rac123-G-LISA assay (absorbance based; Cytoskeleton, Inc.) performed according to the manufacturer's protocol. Briefly, cells were serum starved, stimulated as indicated, and then lysed. The lysates were applied to provided 96-well plates, and activated Rac was detected at 490 nm using a plate reader (Tecan Safire). If not indicated otherwise, control samples were treated with the same volume of PBS that was used for dissolving LecB in the LecB-treated samples.

Bacterial culture and invasion assays. For our experiments, we used GFP-tagged *P. aeruginosa* PAO1 wild-type (PAO1-wt) and an in-frame LecB deletion mutant (PAO1-dLecB) that were described previously (52). Bacteria were cultured overnight (approximately 16 h) in LB-Miller medium containing 60 μg/mL gentamicin in a shaker (Thriller; Peqlab) at 37°C and 650 rpm. The bacteria reached an optical density (OD) measured at 600 nm of approximately 5.

MDCK cells were allowed to polarize on transwell filters or 24-well plates as indicated. H1975 cells were cultured in 24-well plates to a confluence of 70 to 80%. Overnight cultures of PAO1-wt and PAO1-dLecB were pelleted, resuspended in DMEM (MDCK) or RPMI (H1975), and incubated for 30 min at 37°C. For inhibition with L-fucose, 100 mg/mL L-fucose was added during this incubation. The inhibitors PP2 and LY294002 were preincubated for 30 min with the cells and kept on the cells during the whole experiment. Next, the concentration of bacteria was adjusted to yield the desired multiplicity of infection (MOI) of 50. For determining the total number of bacteria, cells were incubated with bacteria for 2 h at 37°C, washed three times with PBS, and then lysed with 0.25% (vol/vol) Triton X-100. Serial dilutions of the cell extracts were made and plated on LB-Miller agar plates containing gentamicin (60 μg/mL) and incubated overnight at 37°C. The number of bacterial colonies was counted on the next day. For determining the number of invading bacteria, cells were incubated with bacteria for 2 h at 37°C and washed three times with PBS. Then, extracellular bacteria were killed by treatment with 400 μg/mL amikacin sulfate (Sigma-Aldrich) for 2 h at 37°C. After lysis with 0.25% (vol/vol) Triton X-100, bacterial numbers were counted as described before. The invasion efficiencies were calculated by dividing the number of invading bacteria by the total number of bacteria. To enable comparison between different experiments, the invasion efficiencies in a single experiment were normalized to the invasion efficiency of the untreated sample and then the mean value from repeated experiments was calculated.

Labeling of lectins. LecB was labeled with Cy3 monoreactive *N*-hydroxysuccinimide (NHS) ester (GE Healthcare) or with biotin using NHS-polyethylene glycol 12 (PEG12)-biotin (Thermo Fisher) according to

the instructions of the manufacturers and purified using PD-10 desalting columns (GE Healthcare). StxB was labeled with NHS-ester conjugated with Alexa Fluor 488 (Thermo Fisher).

Preparation of LecB-coated beads. Biotinylated LecB (LecB-biotin) was incubated with a solution containing streptavidin-coated polystyrene beads containing the dye flash red with 1-μm diameter (Bangs Laboratories). To ensure homogenous coverage with LecB-biotin, a 10-fold molar excess of LecB-biotin compared to the available streptavidin binding sites on the beads was used, and then beads were washed three times with PBS. In control beads, the streptavidin binding sites were saturated with biotin.

Mass spectrometry-based identification of LecB interaction partners. MDCK cells were cultured in medium for stable-isotope labeling by amino acids in cell culture (SILAC medium) for 9 passages and then seeded on transwell filters and allowed to polarize for 4 days. For the first sample, biotinylated LecB was applied to the apical side of light-SILAC-labeled cells and on the basolateral side of medium-SILAC-labeled cells, whereas heavy-SILAC-labeled cells received no stimulation and served as a control. For the second sample, the treatment conditions were permuted. After lysis with immunoprecipitation (IP) lysis buffer, the different SILAC lysates were combined and LecB-biotin-receptor complexes were precipitated using streptavidin agarose beads as described before. Eluted LecB-biotin-receptor complexes were then prepared for MS analysis using SDS-PAGE gel electrophoresis. Gels were cut into pieces, the proteins therein digested with trypsin, and the resulting peptides were purified by stop-and-go-extraction (STAGE) tips. MS analysis was carried out as described previously (19) using a 1200 HPLC (Agilent Technologies, Waldbronn, Germany) connected online to a linear trap quadrupole (LTQ) Orbitrap XL mass spectrometer (Thermo Fisher Scientific, Bremen, Germany). From the list of MS-identified proteins generated, we defined those proteins as LecB interaction partners that showed more than 2-fold enrichment on a $\log_2$ scale over controls in both SILAC samples (Table S1).

Statistics. If not stated otherwise, data obtained from $n = 3$ independent experiments were used to calculate arithmetic means, and error bars represent standard errors of the means (SEM). Statistical significance analysis was carried out using GraphPad Prism 5. For determining the significance in experiments with multiple conditions, one-way analysis of variance (ANOVA) with Bonferroni's *post hoc* testing was applied. For determining the significance in experiments in which values were measured for one condition relative to the control condition, one-sample *t* testing was applied. n.s. denotes not significant, * denotes $P < 0.05$, ** denotes $P < 0.01$, *** denotes $P < 0.001$, and **** denotes $P < 0.0001$. All primary data are available from the authors upon request.

SUPPLEMENTAL MATERIAL

Supplemental material is available online only.

FIG S1, DOCX file, 0.1 MB.

FIG S2, DOCX file, 0.2 MB.

FIG S3, DOCX file, 0.3 MB.

FIG S4, DOCX file, 0.2 MB.

FIG S5, DOCX file, 0.04 MB.

FIG S6, DOCX file, 0.1 MB.

FIG S7, DOCX file, 0.1 MB.

TABLE S1, DOCX file, 0.01 MB.

TABLE S2, DOCX file, 0.01 MB.

MOVIE S1, AVI file, 0.04 MB.

ACKNOWLEDGMENTS

This work was supported by grants from the German Research Foundation (RO 4341/2-1 and major research instrumentation project number 438033605), the Excellence Initiative of the German Research Foundation (grants number EXC 294 and EXC 2189), the Ministry of Science, Research and the Arts of Baden-Württemberg (Az: 33-7532.20), and the Freiburg Institute for Advanced Studies (FRIAS) and a starting grant from the European Research Council (Program Ideas, ERC-2011-StG 282105). R.T. acknowledges support from the Ministry of Science, Research and the Arts of Baden-Württemberg (Az: 7533-30-10/25/36). E.W.K. acknowledges support from the German Research Foundation (grants number KFO 201, KU 1504/5-1, and SFB1140).

REFERENCES

1. WHO. 2017. WHO priority pathogens list for research and development of new antibiotics. World Health Organization, Geneva, Switzerland. http://www.who.int/mediacentre/news/releases/2017/bacteria-antibiotics-needed/en/.
2. Fleiszig SMJ, Zaidi TS, Fletcher EL, Preston MJ, Pier GB. 1994. Pseudomonas aeruginosa invades corneal epithelial cells during experimental infection. Infect Immun 62:3485–3493. https://doi.org/10.1128/iai.62.8.3485-3493.1994.
3. Heimer SR, Evans DJ, Stern ME, Barbieri JT, Yahr T, Fleiszig SMJ. 2013. Pseudomonas aeruginosa utilizes the type III secreted toxin ExoS to avoid acidified compartments within epithelial cells. PLoS One 8:e73111. https://doi.org/10.1371/journal.pone.0073111.

4. Nieto V, Kroken AR, Grosser MR, Smith BE, Metruccio MME, Hagan P, Hallsten ME, Evans DJ, Fleiszig SMJ. 2019. Type IV pili can mediate bacterial motility within epithelial cells. mBio 10:e02880-18. https://doi.org/10.1128/mBio.02880-18.
5. Fleiszig SMJ, Zaidi TS, Pier GB. 1995. Pseudomonas aeruginosa invasion of and multiplication within corneal epithelial cells in vitro. Infect Immun 63:4072–4077. https://doi.org/10.1128/iai.63.10.4072-4077.1995.
6. Garai P, Berry L, Moussouni M, Bleves S, Blanc-Potard A-B. 2019. Killing from the inside: intracellular role of T3SS in the fate of Pseudomonas aeruginosa within macrophages revealed by mgtC and oprF mutants. PLoS Pathog 15:e1007812. https://doi.org/10.1371/journal.ppat.1007812.
7. Capasso D, Pepe MV, Rossello J, Lepanto P, Arias P, Salzman V, Kierbel A. 2016. Elimination of Pseudomonas aeruginosa through efferocytosis upon binding to apoptotic cells. PLoS Pathog 12:e1006068. https://doi.org/10.1371/journal.ppat.1006068.
8. Sana TG, Baumann C, Merdes A, Soscia C, Rattei T, Hachani A, Jones C, Bennett KL, Filloux A, Superti-Furga G, Voulhoux R, Bleves S. 2015. Internalization of Pseudomonas aeruginosa strain PAO1 into epithelial cells is promoted by interaction of a T6SS effector with the microtubule network. mBio 6:e00712-15. https://doi.org/10.1128/mBio.00712-15.
9. Bajmoczi M, Gadjeva M, Alper SL, Pier GB, Golan DE. 2009. Cystic fibrosis transmembrane conductance regulator and caveolin-1 regulate epithelial cell internalization of Pseudomonas aeruginosa. Am J Physiol Cell Physiol 297:C263–C277. https://doi.org/10.1152/ajpcell.00527.2008.
10. Eierhoff T, Bastian B, Thuenauer R, Madl J, Audfray A, Aigal S, Juillot S, Rydell GE, Müller S, de Bentzmann S, Imberty A, Fleck C, Römer W. 2014. A lipid zipper triggers bacterial invasion. Proc Natl Acad Sci U S A 111:12895–12811. https://doi.org/10.1073/pnas.1402637111.
11. Ruch TR, Engel JN. 2017. Targeting the mucosal barrier: how pathogens modulate the cellular polarity network. Cold Spring Harb Perspect Biol 9:a027953. https://doi.org/10.1101/cshperspect.a027953.
12. Bucior I, Pielage JF, Engel JN. 2012. Pseudomonas aeruginosa pili and flagella mediate distinct binding and signaling events at the apical and basolateral surface of airway epithelium. PLoS Pathog 8:e1002616. https://doi.org/10.1371/journal.ppat.1002616.
13. Kierbel A, Gassama-Diagne A, Mostov K, Engel JN. 2005. The phosphoinositol-3-kinase–protein kinase B/Akt pathway is critical for Pseudomonas aeruginosa strain PAK internalization. Mol Biol Cell 16:2577–2585. https://doi.org/10.1091/mbc.e04-08-0717.
14. Tran CS, Rangel SM, Almblad H, Kierbel A, Givskov M, Tolker-Nielsen T, Hauser AR, Engel JN. 2014. The Pseudomonas aeruginosa type III translocon is required for biofilm formation at the epithelial barrier. PLoS Pathog 10:e1004479. https://doi.org/10.1371/journal.ppat.1004479.
15. Tran CS, Eran Y, Ruch TR, Bryant DM, Datta A, Brakeman P, Kierbel A, Wittmann T, Metzger RJ, Mostov KE, Engel JN. 2014. Host cell polarity proteins participate in innate immunity to Pseudomonas aeruginosa infection. Cell Host Microbe 15:636–643. https://doi.org/10.1016/j.chom.2014.04.007.
16. Imberty A, Wimmerová M, Mitchell EP, Gilboa-Garber N. 2004. Structures of the lectins from Pseudomonas aeruginosa: insights into the molecular basis for host glycan recognition. Microbes Infect 6:221–228. https://doi.org/10.1016/j.micinf.2003.10.016.
17. Tielker D, Hacker S, Loris R, Strathmann M, Wingender J, Wilhelm S, Rosenau F, Jaeger KE. 2005. Pseudomonas aeruginosa lectin LecB is located in the outer membrane and is involved in biofilm formation. Microbiology (Reading) 151:1313–1323. https://doi.org/10.1099/mic.0.27701-0.
18. Funken H, Bartels KM, Wilhelm S, Brocker M, Bott M, Bains M, Hancock REW, Rosenau F, Jaeger KE. 2012. Specific association of lectin LecB with the surface of Pseudomonas aeruginosa: role of outer membrane protein OprF. PLoS One 7:e46857. https://doi.org/10.1371/journal.pone.0046857.
19. Thuenauer R, Landi A, Trefzer A, Altmann S, Wehrum S, Eierhoff T, Diedrich B, Dengjel J, Nyström A, Imberty A, Römer W. 2020. The Pseudomonas aeruginosa lectin LecB causes integrin internalization and inhibits epithelial wound healing. mBio 11:e03260-19. https://doi.org/10.1128/mBio.03260-19.
20. Honig E, Ringer K, Dewes J, von Mach T, Kamm N, Kreitzer G, Jacob R. 2018. Galectin-3 modulates the polarized surface delivery of beta1-integrin in epithelial cells. J Cell Sci 131:jcs213199. https://doi.org/10.1242/jcs.213199.
21. Gassama-Diagne A, Yu W, ter Beest M, Martin-Belmonte F, Kierbel A, Engel J, Mostov K. 2006. Phosphatidylinositol-3,4,5-trisphosphate regulates the formation of the basolateral plasma membrane in epithelial cells. Nat Cell Biol 8:963–970. https://doi.org/10.1038/ncb1461.
22. Kierbel A, Gassama-Diagne A, Rocha C, Radoshevich L, Olson J, Mostov K, Engel J. 2007. Pseudomonas aeruginosa exploits a PIP3-dependent pathway to transform apical into basolateral membrane. J Cell Biol 177:21–27. https://doi.org/10.1083/jcb.200605142.
23. Ma J, Sawai H, Matsuo Y, Ochi N, Yasuda A, Takahashi H, Wakasugi T, Funahashi H, Sato M, Takeyama H. 2010. IGF-1 mediates PTEN suppression and enhances cell invasion and proliferation via activation of the IGF-1/PI3K/Akt signaling pathway in pancreatic cancer cells. J Surg Res 160:90–101. https://doi.org/10.1016/j.jss.2008.08.016.
24. Warfel NA, Niederst M, Newton AC. 2011. Disruption of the interface between the pleckstrin homology (PH) and kinase domains of Akt protein is sufficient for hydrophobic motif site phosphorylation in the absence of mTORC2. J Biol Chem 286:39122–39129. https://doi.org/10.1074/jbc.M111.278747.
25. Voges M, Bachmann V, Naujoks J, Kopp K, Hauck CR. 2012. Extracellular IgC2 constant domains of CEACAMs mediate PI3K sensitivity during uptake of pathogens. PLoS One 7:e39908. https://doi.org/10.1371/journal.pone.0039908.
26. Yu Q, Chow EMC, Wong H, Gu J, Mandelboim O, Gray-Owen SD, Ostrowski MA. 2006. CEACAM1 (CD66a) promotes human monocyte survival via a phosphatidylinositol 3-kinase- and AKT-dependent pathway. J Biol Chem 281:39179–39193. https://doi.org/10.1074/jbc.M608864200.
27. Raina D, Kharbanda S, Kufe D. 2004. The MUC1 oncoprotein activates the anti-apoptotic phosphoinositide 3-kinase/Akt and Bcl-xL pathways in rat 3Y1 fibroblasts. J Biol Chem 279:20607–20612. https://doi.org/10.1074/jbc.M310538200.
28. Hamaï A, Meslin F, Benlalam H, Jalil A, Mehrpour M, Faure F, Lecluse Y, Vielh P, Avril M-F, Robert C, Chouaib S. 2008. ICAM-1 has a critical role in the regulation of metastatic melanoma tumor susceptibility to CTL lysis by interfering with PI3K/AKT pathway. Cancer Res 68:9854–9864. https://doi.org/10.1158/0008-5472.CAN-08-0719.
29. Sizemore S, Cicek M, Sizemore N, Ng KP, Casey G. 2007. Podocalyxin increases the aggressive phenotype of breast and prostate cancer cells in vitro through its interaction with ezrin. Cancer Res 67:6183–6191. https://doi.org/10.1158/0008-5472.CAN-06-3575.
30. Huang Z, Huang Y, He H, Ni J. 2015. Podocalyxin promotes cisplatin chemoresistance in osteosarcoma cells through phosphatidylinositide 3-kinase signaling. Mol Med Rep 12:3916–3922. https://doi.org/10.3892/mmr.2015.3859.
31. Lepanto P, Bryant DM, Rossello J, Datta A, Mostov KE, Kierbel A. 2011. Pseudomonas aeruginosa interacts with epithelial cells rapidly forming aggregates that are internalized by a Lyn-dependent mechanism. Cell Microbiol 13:1212–1222. https://doi.org/10.1111/j.1462-5822.2011.01611.x.
32. Campa CC, Ciraolo E, Ghigo A, Germena G, Hirsch E. 2015. Crossroads of PI3K and Rac pathways. Small GTPases 6:71–80. https://doi.org/10.4161/21541248.2014.989789.
33. Rodriguez-Boulan E, Macara IG. 2014. Organization and execution of the epithelial polarity programme. Nat Rev Mol Cell Biol 15:225–242. https://doi.org/10.1038/nrm3775.
34. Francis SS, Sfakianos J, Lo B, Mellman I. 2011. A hierarchy of signals regulates entry of membrane proteins into the ciliary membrane domain in epithelial cells. J Cell Biol 193:219–233. https://doi.org/10.1083/jcb.201009001.
35. Thuenauer R, Juhasz K, Mayr R, Frühwirth T, Lipp A-M, Balogi Z, Sonnleitner A. 2011. A PDMS-based biochip with integrated sub-micrometre position control for TIRF microscopy of the apical cell membrane. Lab Chip 11:3064–3071. https://doi.org/10.1039/c1lc20458k.
36. Stroukov W, Rosch A, Schwan C, Jeney A, Romer W, Thuenauer R. 2019. Synchronizing protein traffic to the primary cilium. Front Genet 10:163. https://doi.org/10.3389/fgene.2019.00163.
37. Esen M, Grassmé H, Riethmüller J, Riehle A, Fassbender K, Gulbins E. 2001. Invasion of human epithelial cells by Pseudomonas aeruginosa involves Src-like tyrosine kinases p60Src and p59Fyn. Infect Immun 69:281–287. https://doi.org/10.1128/IAI.69.1.281-287.2001.
38. Verkade P, Harder T, Lafont F, Simons K. 2000. Induction of caveolae in the apical plasma membrane of Madin-Darby canine kidney cells. J Cell Biol 148:727–740. https://doi.org/10.1083/jcb.148.4.727.
39. Zheng S, Eierhoff T, Aigal S, Brandel A, Thuenauer R, de Bentzmann S, Imberty A, Römer W. 2017. The Pseudomonas aeruginosa lectin LecA triggers host cell signalling by glycosphingolipid-dependent phosphorylation of the adaptor protein CrkII. Biochim Biophys Acta Mol Cell Res 1864:1236–1245. https://doi.org/10.1016/j.bbamcr.2017.04.005.
40. Engel J, Eran Y. 2011. Subversion of mucosal barrier polarity by Pseudomonas aeruginosa. Front Microbiol 2:114–117. https://doi.org/10.3389/fmicb.2011.00114.
41. Müller SK, Wilhelm I, Schubert T, Zittlau K, Imberty A, Madl J, Eierhoff T, Thuenauer R, Römer W. 2017. Gb3-binding lectins as potential carriers for

transcellular drug delivery. Expert Opin Drug Deliv 14:141–153. https://doi.org/10.1080/17425247.2017.1266327.
42. Landi A, Mari M, Kleiser S, Wolf T, Gretzmeier C, Wilhelm I, Kiritsi D, Thünauer R, Geiger R, Nyström A, Reggiori F, Claudinon J, Römer W. 2019. Pseudomonas aeruginosa lectin LecB impairs keratinocyte fitness by abrogating growth factor signalling. Life Sci Alliance 2:e201900422. https://doi.org/10.26508/lsa.201900422.
43. Villringer S, Madl J, Sych T, Manner C, Imberty A, Römer W. 2018. Lectin-mediated protocell crosslinking to mimic cell-cell junctions and adhesion. Sci Rep 8:1932. https://doi.org/10.1038/s41598-018-20230-6.
44. Audette GF, Vandonselaar M, Delbaere LTJ. 2000. The 2.2 Å resolution structure of the O (H) blood-group-specific lectin I from Ulex europaeus. J Mol Biol 304:423–433. https://doi.org/10.1006/jmbi.2000.4214.
45. Thuenauer R, Müller SK, Römer W. 2017. Pathways of protein and lipid receptor-mediated transcytosis in drug delivery. Expert Opin Drug Deliv 14:341–351. https://doi.org/10.1080/17425247.2016.1220364.
46. Kroken AR, Gajenthra Kumar N, Yahr TL, Smith BE, Nieto V, Horneman H, Evans DJ, Fleiszigid SMJ. 2022. Exotoxin S secreted by internalized Pseudomonas aeruginosa delays lytic host cell death. PLoS Pathog 18:e1010306. https://doi.org/10.1371/journal.ppat.1010306.
47. Garrity-Ryan L, Kazmierczak B, Kowal R, Comolli J, Hauser A, Engel JN. 2000. The arginine finger domain of ExoT contributes to actin cytoskeleton disruption and inhibition of internalization of Pseudomonas aeruginosa by epithelial cells and macrophages. Infect Immun 68:7100–7113. https://doi.org/10.1128/IAI.68.12.7100-7113.2000.
48. Wiznerowicz M, Trono D. 2003. Conditional suppression of cellular genes: lentivirus vector-mediated drug-inducible RNA interference. J Virol 77:8957–8961. https://doi.org/10.1128/jvi.77.16.8957-8951.2003.
49. Schuck S, Manninen A, Honsho M, Füllekrug J, Simons K. 2004. Generation of single and double knockdowns in polarized epithelial cells by retrovirus-mediated RNA interference. Proc Natl Acad Sci U S A 101:4912–4917. https://doi.org/10.1073/pnas.0401285101.
50. Thuenauer R, Hsu YC, Carvajal-Gonzalez JM, Deborde S, Chuang J, Römer W, Sonnleitner A, Rodriguez-Boulan E, Sung C. 2014. Four-dimensional live imaging of apical biosynthetic trafficking reveals a post-Golgi sorting role of apical endosomal intermediates. Proc Natl Acad Sci U S A 111:4127–4132. https://doi.org/10.1073/pnas.1304168111.
51. Cott C, Thuenauer R, Landi A, Kühn K, Juillot S, Imberty A, Madl J, Eierhoff T, Römer W. 2016. Pseudomonas aeruginosa lectin LecB inhibits tissue repair processes by triggering β-catenin degradation. Biochim Biophys Acta 1863:1106–1118. https://doi.org/10.1016/j.bbamcr.2016.02.004.
52. Boukerb AM, Rousset A, Galanos N, Méar JB, Thépaut M, Grandjean T, Gillon E, Cecioni S, Abderrahmen C, Faure K, Redelberger D, Kipnis E, Dessein R, Havet S, Darblade B, Matthews SE, de Bentzmann S, Guéry B, Cournoyer B, Imberty A, Vidal S. 2014. Antiadhesive properties of glycoclusters against Pseudomonas aeruginosa lung infection. J Med Chem 57:10275–10289. https://doi.org/10.1021/jm500038p.

References

1. Chegini Z, Khoshbayan A, Taati Moghadam M, et al (2020) Bacteriophage therapy against Pseudomonas aeruginosa biofilms: a review. Ann Clin Microbiol Antimicrob 19:45. https://doi.org/10.1186/s12941-020-00389-5
2. Mielko KA, Jabłoński SJ, Milczewska J, et al (2019) Metabolomic studies of Pseudomonas aeruginosa. World J Microbiol Biotechnol 35:178. https://doi.org/10.1007/s11274-019-2739-1
3. Morin CD, Déziel E, Gauthier J, et al (2021) An Organ System-Based Synopsis of Pseudomonas aeruginosa Virulence. Virulence 12:1469–1507. https://doi.org/10.1080/21505594.2021.1926408
4. Mulani MS, Kamble EE, Kumkar SN, et al (2019) Emerging Strategies to Combat ESKAPE Pathogens in the Era of Antimicrobial Resistance: A Review. Front Microbiol 10:539. https://doi.org/10.3389/fmicb.2019.00539
5. Cott C, Thuenauer R, Landi A, et al (2016) Pseudomonas aeruginosa lectin LecB inhibits tissue repair processes by triggering β-catenin degradation. Biochim Biophys Acta - Mol Cell Res 1863(6 Pt:1106–1118. https://doi.org/10.1016/j.bbamcr.2016.02.004
6. Palmqvist N, Foster T, Tarkowski A, Josefsson E (2002) Protein A is a virulence factor in Staphylococcus aureus arthritis and septic death. Microb Pathog 33:239–249. https://doi.org/10.1006/mpat.2002.0533
7. Medzhitov R (2007) Recognition of microorganisms and activation of the immune response. Nature 449:819–826. https://doi.org/10.1038/nature06246
8. Pfalzgraff A, Brandenburg K, Weindl G (2018) Antimicrobial Peptides and Their Therapeutic Potential for Bacterial Skin Infections and Wounds. Front Pharmacol 9:. https://doi.org/10.3389/fphar.2018.00281
9. Landi A, Mari M, Kleiser S, et al (2019) Pseudomonas aeruginosa lectin LecB impairs keratinocyte fitness by abrogating growth factor signalling. Life Sci Alliance 2:e201900422. https://doi.org/10.26508/lsa.201900422
10. Thuenauer R, Landi A, Trefzer A, et al (2020) The pseudomonas aeruginosa lectin lecb causes integrin internalization and inhibits epithelial wound healing. MBio 11(2):e03260-19. https://doi.org/10.1128/mBio.03260-19
11. Prasad ASB, Shruptha P, Prabhu V, et al (2020) Pseudomonas aeruginosa virulence proteins pseudolysin and protease IV impede cutaneous wound healing. Lab Investig 100(12):1532–1550. https://doi.org/10.1038/s41374-020-00478-1
12. Ruffin M, Bilodeau C, Maillé É, et al (2016) Quorum-sensing inhibition abrogates the deleterious impact of Pseudomonas aeruginosa on airway epithelial repair. FASEB J 30:3011–25. https://doi.org/10.1096/fj.201500166R
13. Eisenbeis J, Peisker H, Backes CS, et al (2017) The extracellular adherence protein (Eap) of Staphylococcus aureus acts as a proliferation and migration repressing factor that alters the cell morphology of keratinocytes. Int J Med Microbiol 307(2):116–125. https://doi.org/10.1016/j.ijmm.2017.01.002
14. Trepat X, Chen Z, Jacobson K (2012) Cell migration. Compr Physiol 2:2369–2392. https://doi.org/10.1002/cphy.c110012
15. Goldufsky J, Wood SJ, Jayaraman V, et al (2015) Pseudomonas aeruginosa uses T3SS to inhibit diabetic wound healing. Wound Repair Regen 23(4):557–564. https://doi.org/10.1111/wrr.12310
16. Kopenhagen A, Ramming I, Camp B, et al (2022) Streptococcus pneumoniae Affects Endothelial Cell Migration in Microfluidic Circulation. Front Microbiol 13:852036. https://doi.org/10.3389/fmicb.2022.852036
17. Putra I, Rabiee B, Anwar KN, et al (2019) Staphylococcus aureus alpha-hemolysin impairs corneal epithelial wound healing and promotes intracellular bacterial invasion. Exp Eye Res 181:263–270. https://doi.org/10.1016/j.exer.2019.02.019
18. Bach MS, de Vries CR, Khosravi A, et al (2022) Filamentous bacteriophage delays healing of Pseudomonas-infected wounds. Cell Reports Med 3:100656. https://doi.org/10.1016/j.xcrm.2022.100656
19. Hess E, Duheron V, Decossas M, et al (2012) RANKL Induces Organized Lymph Node Growth by Stromal Cell Proliferation. J Immunol 188:1245–1254. https://doi.org/10.4049/jimmunol.1101513
20. Kwan W-H, Boix C, Gougelet N, et al (2007) LPS induces rapid IL-10 release by M-CSF-conditioned tolerogenic dendritic cell precursors. J Leukoc Biol 82:133–141. https://doi.org/10.1189/jlb.0406267
21. Goldmann O, Medina E (2018) Staphylococcus aureus strategies to evade the host acquired immune response. Int J Med Microbiol 308:625–630. https://doi.org/10.1016/j.ijmm.2017.09.013
22. Utay NS, Roque A, Timmer JK, et al (2016) MRSA Infections in HIV-Infected People Are Associated with Decreased MRSA-Specific Th1 Immunity. PLOS Pathog 12:e1005580. https://doi.org/10.1371/journal.ppat.1005580
23. Kurtz JR, Goggins JA, McLachlan JB (2017) Salmonella infection: Interplay between the bacteria and host immune system. Immunol Lett 190:42–50. https://doi.org/10.1016/j.imlet.2017.07.006
24. Kim T-H, Li X-H, Lee J-H (2021) Alleviation of Pseudomonas aeruginosa Infection by Propeptide-Mediated Inhibition of Protease IV. Microbiol Spectr 9:e0078221. https://doi.org/10.1128/Spectrum.00782-21
25. Moser C, Jensen PØ, Thomsen K, et al (2021) Immune Responses to Pseudomonas aeruginosa Biofilm Infections. Front Immunol 12:625597. https://doi.org/10.3389/fimmu.2021.625597
26. Vourc'h M, David G, Gaborit B, et al (2020) Pseudomonas aeruginosa Infection Impairs NKG2D-Dependent NK Cell Cytotoxicity through Regulatory T-Cell Activation. Infect Immun 88:. https://doi.org/10.1128/IAI.00363-20
27. Andonova M, Urumova V (2013) Immune surveillance mechanisms of the skin against the stealth infection strategy of Pseudomonas aeruginosa—Review. Comp Immunol Microbiol Infect Dis 36:433–448. https://doi.org/10.1016/j.cimid.2013.03.003

28. Naik S, Kumar S (2022) Lectins from plants and algae act as anti-viral against HIV, influenza and coronaviruses. Mol Biol Rep 49:12239–12246. https://doi.org/10.1007/s11033-022-07854-8
29. Singh RS, Walia AK, Khattar JS, et al (2017) Cyanobacterial lectins characteristics and their role as antiviral agents. Int J Biol Macromol 102:475–496. https://doi.org/10.1016/j.ijbiomac.2017.04.041
30. Wu AM, Liu JH (2019) Lectins and ELLSA as powerful tools for glycoconjugate recognition analyses. Glycoconj J 36:175–183. https://doi.org/10.1007/s10719-019-09865-3
31. Sharon N, Lis H (1989) Lectins as Cell Recognition Molecules. Science (80-) 246:227–234. https://doi.org/10.1126/science.2552581
32. Sharon N (2007) Lectins: Carbohydrate-specific Reagents and Biological Recognition Molecules. J Biol Chem 282:2753–2764. https://doi.org/10.1074/JBC.X600004200
33. Csávás M, Kalmár L, Szőke P, et al (2022) A Fucosylated Lactose-Presenting Tetravalent Glycocluster Acting as a Mutual Ligand of Pseudomonas aeruginosa Lectins A (PA-IL) and B (PA-IIL)-Synthesis and Interaction Studies. Int J Mol Sci 23:16194. https://doi.org/10.3390/ijms232416194
34. Grishin A V., Krivozubov MS, Karyagina AS, Gintsburg AL (2015) Pseudomonas Aeruginosa Lectins As Targets for Novel Antibacterials. Acta Naturae 7:29–41. https://doi.org/10.32607/20758251-2015-7-2-29-41
35. Gillon E, Varrot A, Imberty A (2020) LecB, a High Affinity Soluble Fucose-Binding Lectin from Pseudomonas aeruginosa. Methods Mol Biol 2132:475–482. https://doi.org/10.1007/978-1-0716-0430-4_46
36. Berthet N, Thomas B, Bossu I, et al (2013) High Affinity Glycodendrimers for the Lectin LecB from Pseudomonas aeruginosa. Bioconjug Chem 24:1598–1611. https://doi.org/10.1021/bc400239m
37. Kuhaudomlarp S, Siebs E, Shanina E, et al (2021) Non-Carbohydrate Glycomimetics as Inhibitors of Calcium(II)-Binding Lectins. Angew Chemie Int Ed 60:8104–8114. https://doi.org/10.1002/anie.202013217
38. Wojtczak K, Byrne JP (2022) Structural Considerations for Building Synthetic Glycoconjugates as Inhibitors for Pseudomonas aeruginosa Lectins. ChemMedChem 17:e202200081. https://doi.org/10.1002/cmdc.202200081
39. Mitchell E, Houles C, Sudakevitz D, et al (2002) Structural basis for oligosaccharide-mediated adhesion of Pseudomonas aeruginosa in the lungs of cystic fibrosis patients. Nat Struct Biol 9:918–921. https://doi.org/10.1038/nsb865
40. Thuenauer R, Kühn K, Guo Y, et al (2022) The Lectin LecB Induces Patches with Basolateral Characteristics at the Apical Membrane to Promote Pseudomonas aeruginosa Host Cell Invasion. MBio 13:e0081922. https://doi.org/10.1128/mbio.00819-22
41. Sommer R, Rox K, Wagner S, et al (2019) Anti-biofilm Agents against Pseudomonas aeruginosa : A Structure–Activity Relationship Study of C -Glycosidic LecB Inhibitors. J Med Chem 62:9201–9216. https://doi.org/10.1021/acs.jmedchem.9b01120
42. Sommer R, Wagner S, Rox K, et al (2018) Glycomimetic, Orally Bioavailable LecB Inhibitors Block Biofilm Formation of Pseudomonas aeruginosa. J Am Chem Soc 140:2537–2545. https://doi.org/10.1021/jacs.7b11133
43. Cecioni S, Imberty A, Vidal S (2015) Glycomimetics versus multivalent glycoconjugates for the design of high affinity lectin ligands. Chem Rev 115:525–61. https://doi.org/10.1021/cr500303t
44. Sommer R, Exner TE, Titz A (2014) A Biophysical Study with Carbohydrate Derivatives Explains the Molecular Basis of Monosaccharide Selectivity of the Pseudomonas aeruginosa Lectin LecB. PLoS One 9:e112822. https://doi.org/10.1371/journal.pone.0112822
45. Wilhelm I, Levit-Zerdoun E, Jakob J, et al (2019) Carbohydrate-dependent B cell activation by fucose-binding bacterial lectins. Sci Signal 12:. https://doi.org/10.1126/scisignal.aao7194
46. Kühn K, Cott C, Bohler S, et al (2015) The interplay of autophagy and β-Catenin signaling regulates differentiation in acute myeloid leukemia. Cell Death Discov 1:15031. https://doi.org/10.1038/cddiscovery.2015.31
47. Chemani C, Imberty A, de Bentzmann S, et al (2009) Role of LecA and LecB lectins in Pseudomonas aeruginosa-induced lung injury and effect of carbohydrate ligands. Infect Immun 77:2065–75. https://doi.org/10.1128/IAI.01204-08
48. Heino J, Kapyla J (2009) Cellular Receptors of Extracellular Matrix Molecules. Curr Pharm Des 15:1309–1317. https://doi.org/10.2174/138161209787846720
49. Ginsberg MH (2014) Integrin activation. BMB Rep 47:655–659. https://doi.org/10.5483/bmbrep.2014.47.12.241
50. Tuon FF, Dantas LR, Suss PH, Tasca Ribeiro VS (2022) Pathogenesis of the Pseudomonas aeruginosa Biofilm: A Review. Pathogens 11:300. https://doi.org/10.3390/pathogens11030300
51. Passos da Silva D, Matwichuk ML, Townsend DO, et al (2019) The Pseudomonas aeruginosa lectin LecB binds to the exopolysaccharide Psl and stabilizes the biofilm matrix. Nat Commun 10:2183. https://doi.org/10.1038/s41467-019-10201-4
52. Ruffin M, Brochiero E (2019) Repair Process Impairment by Pseudomonas aeruginosa in Epithelial Tissues: Major Features and Potential Therapeutic Avenues. Front Cell Infect Microbiol 9:. https://doi.org/10.3389/fcimb.2019.00182
53. Sponsel J, Guo Y, Hamzam L, et al (2023) Pseudomonas aeruginosa LecB suppresses immune responses by inhibiting transendothelial migration. EMBO Rep e55971. https://doi.org/10.15252/embr.202255971
54. Torigoe S, Schutt CR, Yamasaki S (2021) Immune discrimination of the environmental spectrum through C-type lectin receptors. Int Immunol 33:847–851. https://doi.org/10.1093/intimm/dxab074

55. Li Y, Pan L, Yu J (2022) The injection of one recombinant C-type lectin (LvLec) induced the immune response of hemocytes in Litopenaeus vannamei. Fish Shellfish Immunol 124:324–331. https://doi.org/10.1016/j.fsi.2022.04.017
56. Gadjeva M, Thiel S, Jensenius JC (2001) The mannan-binding-lectin pathway of the innate immune response. Curr Opin Immunol 13:74–78. https://doi.org/10.1016/S0952-7915(00)00185-0
57. Khalili A, Ahmad M (2015) A Review of Cell Adhesion Studies for Biomedical and Biological Applications. Int J Mol Sci 16:18149–18184. https://doi.org/10.3390/ijms160818149
58. Berrier AL, Yamada KM (2007) Cell–matrix adhesion. J Cell Physiol 213:565–573. https://doi.org/10.1002/jcp.21237
59. Parsons JT, Horwitz AR, Schwartz MA (2010) Cell adhesion: integrating cytoskeletal dynamics and cellular tension. Nat Rev Mol Cell Biol 11:633–643. https://doi.org/10.1038/nrm2957
60. Shinde A, Illath K, Gupta P, et al (2021) A Review of Single-Cell Adhesion Force Kinetics and Applications. Cells 10:577. https://doi.org/10.3390/cells10030577
61. Ananthakrishnan R, Ehrlicher A (2007) The forces behind cell movement. Int J Biol Sci 3:303–17. https://doi.org/10.7150/ijbs.3.303
62. Bachmann M, Kukkurainen S, Hytönen VP, Wehrle-Haller B (2019) Cell Adhesion by Integrins. Physiol Rev 99:1655–1699. https://doi.org/10.1152/physrev.00036.2018
63. Spangenberg C, Lausch EU, Trost TM, et al (2006) ERBB2-Mediated Transcriptional Up-regulation of the α5β1 Integrin Fibronectin Receptor Promotes Tumor Cell Survival Under Adverse Conditions. Cancer Res 66:3715–3725. https://doi.org/10.1158/0008-5472.CAN-05-2823
64. Jaffe AB, Hall A (2005) RHO GTPASES: Biochemistry and Biology. Annu Rev Cell Dev Biol 21:247–269. https://doi.org/10.1146/annurev.cellbio.21.020604.150721
65. Basu S, Cheriyamundath S, Ben-Ze'ev A (2018) Cell–cell adhesion: linking Wnt/β-catenin signaling with partial EMT and stemness traits in tumorigenesis. F1000Research 7:1488. https://doi.org/10.12688/f1000research.15782.1
66. LeBaron R., Athanasiou K. (2000) Ex vivo synthesis of articular cartilage. Biomaterials 21:2575–2587. https://doi.org/10.1016/S0142-9612(00)00125-3
67. Huang W, Anvari B, Torres JH, et al (2003) Temporal effects of cell adhesion on mechanical characteristics of the single chondrocyte. J Orthop Res 21:88–95. https://doi.org/10.1016/S0736-0266(02)00130-4
68. Hong S, Ergezen E, Lec R, Barbee KA (2006) Real-time analysis of cell–surface adhesive interactions using thickness shear mode resonator. Biomaterials 27:5813–5820. https://doi.org/10.1016/j.biomaterials.2006.07.031
69. Kametaka S, Moriyama K, Burgos P V., et al (2007) Canonical Interaction of Cyclin G–associated Kinase with Adaptor Protein 1 Regulates Lysosomal Enzyme Sorting. Mol Biol Cell 18:2991–3001. https://doi.org/10.1091/mbc.e06-12-1162
70. Friedrichs J, Helenius J, Müller DJ (2010) Stimulated single-cell force spectroscopy to quantify cell adhesion receptor crosstalk. Proteomics 10:1455–1462. https://doi.org/10.1002/pmic.200900724
71. Chen J, Xu Y, Shi Y, Xia T (2019) Functionalization of Atomic Force Microscope Cantilevers with Single-T Cells or Single-Particle for Immunological Single-Cell Force Spectroscopy. J Vis Exp. https://doi.org/10.3791/59609
72. Sima M, Martinkova S, Kafkova A, et al (2022) Cell-tak coating interferes with DNA-based normalization of metabolic flux data. Physiol Res 71:517–526. https://doi.org/10.33549/physiolres.934855
73. Helenius J, Heisenberg C-P, Gaub HE, Muller DJ (2008) Single-cell force spectroscopy. J Cell Sci 121:1785–1791. https://doi.org/10.1242/jcs.030999
74. Bodiou V, Moutsatsou P, Post MJ (2020) Microcarriers for Upscaling Cultured Meat Production. Front Nutr 7:10. https://doi.org/10.3389/fnut.2020.00010
75. Derakhti S, Safiabadi-Tali SH, Amoabediny G, Sheikhpour M (2019) Attachment and detachment strategies in microcarrier-based cell culture technology: A comprehensive review. Mater Sci Eng C 103:109782. https://doi.org/10.1016/j.msec.2019.109782
76. Bainer R (2022) A formalization of one of the main claims of "The cancer glycocalyx mechanically primes integrin-mediated growth and survival" by Paszek et al. 20141. Data Sci 5:65–69. https://doi.org/10.3233/DS-210050
77. Honn K V., Tang DG (1992) Adhesion molecules and tumor cell interaction with endothelium and subendothelial matrix. Cancer Metastasis Rev 11:353–375. https://doi.org/10.1007/BF01307187
78. Conway JRW, Jacquemet G (2019) Cell matrix adhesion in cell migration. Essays Biochem 63:535–551. https://doi.org/10.1042/EBC20190012
79. Ye F, Petrich BG, Anekal P, et al (2013) The Mechanism of Kindlin-Mediated Activation of Integrin αIIbβ3. Curr Biol 23:2288–2295. https://doi.org/10.1016/j.cub.2013.09.050
80. Arjonen A, Alanko J, Veltel S, Ivaska J (2012) Distinct Recycling of Active and Inactive β1 Integrins. Traffic 13:610–625. https://doi.org/10.1111/j.1600-0854.2012.01327.x
81. MEHTA JR, DIEFENBACH B, BROWN A, et al (1998) Transmembrane-truncated αvβ3 integrin retains high affinity for ligand binding: evidence for an 'inside-out' suppressor? Biochem J 330:861–869. https://doi.org/10.1042/bj3300861
82. De Franceschi N, Hamidi H, Alanko J, et al (2015) Integrin traffic – the update. J Cell Sci 128(5):839–852. https://doi.org/10.1242/jcs.161653
83. Moreno-Layseca P, Icha J, Hamidi H, Ivaska J (2019) Integrin trafficking in cells and tissues. Nat Cell Biol 21:122–132.

https://doi.org/10.1038/s41556-018-0223-z
84. FABRICIUS E-M, WILDNER G-P, KRUSE-BOITSCHENKO U, et al (2011) Immunohistochemical analysis of integrins αvβ3, αvβ5 and α5β1, and their ligands, fibrinogen, fibronectin, osteopontin and vitronectin, in frozen sections of human oral head and neck squamous cell carcinomas. Exp Ther Med 2:9–19. https://doi.org/10.3892/etm.2010.171
85. Bharadwaj M, Strohmeyer N, Colo GP, et al (2017) αV-class integrins exert dual roles on α5β1 integrins to strengthen adhesion to fibronectin. Nat Commun 8:14348. https://doi.org/10.1038/ncomms14348
86. De Pascalis C, Etienne-Manneville S (2017) Single and collective cell migration: the mechanics of adhesions. Mol Biol Cell 28:1833–1846. https://doi.org/10.1091/mbc.e17-03-0134
87. Barrow-McGee R, Kishi N, Joffre C, et al (2016) Beta 1-integrin–c-Met cooperation reveals an inside-in survival signalling on autophagy-related endomembranes. Nat Commun 7:11942. https://doi.org/10.1038/ncomms11942
88. Taddei M, Giannoni E, Fiaschi T, Chiarugi P (2012) Anoikis: an emerging hallmark in health and diseases. J Pathol 226:380–393. https://doi.org/10.1002/path.3000
89. Humphries JD, Byron A, Humphries MJ (2006) Integrin ligands at a glance. J Cell Sci 119:3901–3903. https://doi.org/10.1242/jcs.03098
90. Jones JCR, Kam CY, Harmon RM, et al (2017) Intermediate Filaments and the Plasma Membrane. Cold Spring Harb Perspect Biol 9:a025866. https://doi.org/10.1101/cshperspect.a025866
91. Veillat V, Spuul P, Daubon T, et al (2015) Podosomes: Multipurpose organelles? Int J Biochem Cell Biol 65:52–60. https://doi.org/10.1016/j.biocel.2015.05.020
92. Charras G, Sahai E (2014) Physical influences of the extracellular environment on cell migration. Nat Rev Mol Cell Biol 15:813–824. https://doi.org/10.1038/nrm3897
93. Kanchanawong P, Calderwood DA (2023) Organization, dynamics and mechanoregulation of integrin-mediated cell–ECM adhesions. Nat Rev Mol Cell Biol 24:142–161. https://doi.org/10.1038/s41580-022-00531-5
94. Horton ER, Humphries JD, Stutchbury B, et al (2016) Modulation of FAK and Src adhesion signaling occurs independently of adhesion complex composition. J Cell Biol 212:349–364. https://doi.org/10.1083/jcb.201508080
95. Revach O-Y, Grosheva I, Geiger B (2020) Biomechanical regulation of focal adhesion and invadopodia formation. J Cell Sci 133:. https://doi.org/10.1242/jcs.244848
96. De Arcangelis A (2000) Integrin and ECM functions: roles in vertebrate development. Trends Genet 16:389–395. https://doi.org/10.1016/S0168-9525(00)02074-6
97. Badaoui M, Zoso A, Idris T, et al (2020) Vav3 Mediates Pseudomonas aeruginosa Adhesion to the Cystic Fibrosis Airway Epithelium. Cell Rep 32:107842. https://doi.org/10.1016/j.celrep.2020.107842
98. Stefanelli VL, Choudhury S, Hu P, et al (2019) Citrullination of fibronectin alters integrin clustering and focal adhesion stability promoting stromal cell invasion. Matrix Biol 82:86–104. https://doi.org/10.1016/j.matbio.2019.04.002
99. Wozniak MA, Modzelewska K, Kwong L, Keely PJ (2004) Focal adhesion regulation of cell behavior. Biochim Biophys Acta - Mol Cell Res 1692:103–119. https://doi.org/10.1016/j.bbamcr.2004.04.007
100. Mishra YG, Manavathi B (2021) Focal adhesion dynamics in cellular function and disease. Cell Signal 85:110046. https://doi.org/10.1016/j.cellsig.2021.110046
101. Mitra SK, Hanson DA, Schlaepfer DD (2005) Focal adhesion kinase: in command and control of cell motility. Nat Rev Mol Cell Biol 6(1):56–68. https://doi.org/10.1038/nrm1549
102. Haining AWM, Lieberthal TJ, Hernández A del R (2016) Talin: a mechanosensitive molecule in health and disease. FASEB J 30:2073–2085. https://doi.org/10.1096/fj.201500080R
103. Yan J, Yao M, Goult BT, Sheetz MP (2015) Talin Dependent Mechanosensitivity of Cell Focal Adhesions. Cell Mol Bioeng 8:151–159. https://doi.org/10.1007/s12195-014-0364-5
104. Rainero E, Howe JD, Caswell PT, et al (2015) Ligand-Occupied Integrin Internalization Links Nutrient Signaling to Invasive Migration. Cell Rep 10:398–413. https://doi.org/10.1016/j.celrep.2014.12.037
105. Georgiadou M, Lilja J, Jacquemet G, et al (2017) AMPK negatively regulates tensin-dependent integrin activity. J Cell Biol 216:1107–1121. https://doi.org/10.1083/jcb.201609066
106. Kano Y, Katoh K, Fujiwara K (2000) Lateral Zone of Cell-Cell Adhesion as the Major Fluid Shear Stress–Related Signal Transduction Site. Circ Res 86:425–433. https://doi.org/10.1161/01.RES.86.4.425
107. Krüger-Genge, Blocki, Franke, Jung (2019) Vascular Endothelial Cell Biology: An Update. Int J Mol Sci 20:4411. https://doi.org/10.3390/ijms20184411
108. Kano Y, Katoh K, Masuda M, Fujiwara K (1996) Macromolecular Composition of Stress Fiber–Plasma Membrane Attachment Sites in Endothelial Cells In Situ. Circ Res 79:1000–1006. https://doi.org/10.1161/01.RES.79.5.1000
109. Katoh K (2020) FAK-Dependent Cell Motility and Cell Elongation. Cells 9:192. https://doi.org/10.3390/cells9010192
110. Tapial Martínez P, López Navajas P, Lietha D (2020) FAK Structure and Regulation by Membrane Interactions and Force in Focal Adhesions. Biomolecules 10:179. https://doi.org/10.3390/biom10020179
111. Dawson JC, Serrels A, Stupack DG, et al (2021) Targeting FAK in anticancer combination therapies. Nat Rev Cancer 21:313–324. https://doi.org/10.1038/s41568-021-00340-6
112. Chuang H-H, Zhen Y-Y, Tsai Y-C, et al (2022) FAK in Cancer: From Mechanisms to Therapeutic Strategies. Int J Mol Sci

23:1726. https://doi.org/10.3390/ijms23031726
113. Mitra SK, Schlaepfer DD (2006) Integrin-regulated FAK–Src signaling in normal and cancer cells. Curr Opin Cell Biol 18(5):516–523. https://doi.org/10.1016/j.ceb.2006.08.011
114. Chen XL, Nam J-O, Jean C, et al (2012) VEGF-Induced Vascular Permeability Is Mediated by FAK. Dev Cell 22:146–157. https://doi.org/10.1016/j.devcel.2011.11.002
115. Arthur WT, Petch LA, Burridge K (2000) Integrin engagement suppresses RhoA activity via a c-Src-dependent mechanism. Curr Biol 10:719–722. https://doi.org/10.1016/S0960-9822(00)00537-6
116. Hernández AJA, Reyes VL, Albores-García D, et al (2018) MeHg affects the activation of FAK, Src, Rac1 and Cdc42, critical proteins for cell movement in PDGF-stimulated SH-SY5Y neuroblastoma cells. Toxicology 394:35–44. https://doi.org/10.1016/j.tox.2017.11.019
117. Zhao M, Finlay D, Kwong E, et al (2022) Cell adhesion suppresses autophagy via Src/FAK-mediated phosphorylation and inhibition of AMPK. Cell Signal 89:110170. https://doi.org/10.1016/j.cellsig.2021.110170
118. Wu H-J, Hao M, Yeo SK, Guan J-L (2020) FAK signaling in cancer-associated fibroblasts promotes breast cancer cell migration and metastasis by exosomal miRNAs-mediated intercellular communication. Oncogene 39:2539–2549. https://doi.org/10.1038/s41388-020-1162-2
119. Zhang P-F, Li K-S, Shen Y, et al (2016) Galectin-1 induces hepatocellular carcinoma EMT and sorafenib resistance by activating FAK/PI3K/AKT signaling. Cell Death Dis 7(4):e2201–e2201. https://doi.org/10.1038/cddis.2015.324
120. Shen M, Jiang Y-Z, Wei Y, et al (2019) Tinagl1 Suppresses Triple-Negative Breast Cancer Progression and Metastasis by Simultaneously Inhibiting Integrin/FAK and EGFR Signaling. Cancer Cell 35:64-80.e7. https://doi.org/10.1016/j.ccell.2018.11.016
121. Huveneers S, Danen EHJ (2009) Adhesion signaling – crosstalk between integrins, Src and Rho. J Cell Sci 122:1059–1069. https://doi.org/10.1242/jcs.039446
122. Ackermann TF, Kempe DS, Lang F, Lang UE (2010) Hyperactivity and Enhanced Curiosity of Mice Expressing PKB/SGK-resistant Glycogen Synthase Kinase-3 (GSK-3). Cell Physiol Biochem 25:775–786. https://doi.org/10.1159/000315097
123. Crampton SP, Wu B, Park EJ, et al (2009) Integration of the beta-catenin-dependent Wnt pathway with integrin signaling through the adaptor molecule Grb2. PLoS One 4:e7841. https://doi.org/10.1371/journal.pone.0007841
124. Li L, Yuan H, Xie W, et al (1999) Dishevelled Proteins Lead to Two Signaling Pathways. J Biol Chem 274:129–134. https://doi.org/10.1074/jbc.274.1.129
125. Vivanco I, Palaskas N, Tran C, et al (2007) Identification of the JNK Signaling Pathway as a Functional Target of the Tumor Suppressor PTEN. Cancer Cell 11:555–569. https://doi.org/10.1016/j.ccr.2007.04.021
126. Gao C, Chen G, Kuan S-F, et al (2015) FAK/PYK2 promotes the Wnt/β-catenin pathway and intestinal tumorigenesis by phosphorylating GSK3β. Elife 4:e10072. https://doi.org/10.7554/eLife.10072
127. Wörthmüller J, Rüegg C (2020) The crosstalk between FAK and Wnt signaling pathways in cancer and its therapeutic implication. Int J Mol Sci 21(23):9107. https://doi.org/10.3390/ijms21239107
128. Pankov R, Cukierman E, Katz BZ, et al (2000) Integrin dynamics and matrix assembly: tensin-dependent translocation of alpha(5)beta(1) integrins promotes early fibronectin fibrillogenesis. J Cell Biol 148:1075–1090. https://doi.org/10.1083/jcb.148.5.1075
129. Diaz C, Neubauer S, Rechenmacher F, et al (2020) Recruitment of α(v)β(3) integrin to α(5)β(1) integrin-induced clusters enables focal adhesion maturation and cell spreading. J Cell Sci 133:. https://doi.org/10.1242/jcs.232702
130. Stuermer CAO (2010) The reggie/flotillin connection to growth. Trends Cell Biol 20:6–13. https://doi.org/10.1016/j.tcb.2009.10.003
131. Bodin S, Planchon D, Rios Morris E, et al (2014) Flotillins in intercellular adhesion – from cellular physiology to human diseases. J Cell Sci 127(Pt 24):5139–5147. https://doi.org/10.1242/jcs.159764
132. Langhorst MF, Reuter A, Stuermer CAO (2005) Scaffolding microdomains and beyond: the function of reggie/flotillin proteins. Cell Mol Life Sci 62:2228–2240. https://doi.org/10.1007/s00018-005-5166-4
133. Singh J, Elhabashy H, Muthukottiappan P, et al (2022) Cross-linking of the endolysosomal system reveals potential flotillin structures and cargo. Nat Commun 13(1):6212. https://doi.org/10.1038/s41467-022-33951-0
134. Morrow IC, Parton RG (2005) Flotillins and the PHB Domain Protein Family: Rafts, Worms and Anaesthetics. Traffic 6:725–740. https://doi.org/10.1111/j.1600-0854.2005.00318.x
135. Roitbak T, Surviladze Z, Tikkanen R, Wandinger-Ness A (2005) A polycystin multiprotein complex constitutes a cholesterol-containing signalling microdomain in human kidney epithelia. Biochem J 392:29–38. https://doi.org/10.1042/BJ20050645
136. Strauss K, Goebel C, Runz H, et al (2010) Exosome Secretion Ameliorates Lysosomal Storage of Cholesterol in Niemann-Pick Type C Disease. J Biol Chem 285:26279–26288. https://doi.org/10.1074/jbc.M110.134775
137. Gauthier-Rouvière C, Bodin S, Comunale F, Planchon D (2020) Flotillin membrane domains in cancer. Cancer Metastasis Rev 39:361–374. https://doi.org/10.1007/s10555-020-09873-y
138. Morrow IC, Rea S, Martin S, et al (2002) Flotillin-1/Reggie-2 Traffics to Surface Raft Domains via a Novel Golgi-independent Pathway. J Biol Chem 277:48834–48841. https://doi.org/10.1074/jbc.M209082200

139. Langhorst MF, Solis GP, Hannbeck S, et al (2007) Linking membrane microdomains to the cytoskeleton: Regulation of the lateral mobility of reggie-1/flotillin-2 by interaction with actin. FEBS Lett 581:4697–4703. https://doi.org/10.1016/j.febslet.2007.08.074
140. Banning A, Tomasovic A, Tikkanen R (2011) Functional Aspects of Membrane Association of Reggie/Flotillin Proteins. Curr Protein Pept Sci 12:725–735. https://doi.org/10.2174/138920311798841708
141. Meister M, Tikkanen R (2014) Endocytic Trafficking of Membrane-Bound Cargo: A Flotillin Point of View. Membranes (Basel) 4(3):356–371. https://doi.org/10.3390/membranes4030356
142. Kühne S, Ockenga W, Banning A, Tikkanen R (2015) Cholinergic Transactivation of the EGFR in HaCaT Keratinocytes Stimulates a Flotillin-1 Dependent MAPK-Mediated Transcriptional Response. Int J Mol Sci 16:6447–6463. https://doi.org/10.3390/ijms16036447
143. Banning A, Ockenga W, Finger F, et al (2012) Transcriptional Regulation of Flotillins by the Extracellularly Regulated Kinases and Retinoid X Receptor Complexes. PLoS One 7:e45514. https://doi.org/10.1371/journal.pone.0045514
144. Koh M, Yong H-Y, Kim E-S, et al (2016) A novel role for flotillin-1 in H-Ras-regulated breast cancer aggressiveness. Int J Cancer 138:1232–1245. https://doi.org/10.1002/ijc.29869
145. Liu J, Huang W, Ren C, et al (2020) Author Correction: Flotillin-2 promotes metastasis of nasopharyngeal carcinoma by activating NF-κB and PI3K/Akt3 signaling pathways. Sci Rep 10:6914. https://doi.org/10.1038/s41598-020-63750-w
146. Sandvig K, Kavaliauskiene S, Skotland T (2018) Clathrin-independent endocytosis: an increasing degree of complexity. Histochem Cell Biol 150:107–118. https://doi.org/10.1007/s00418-018-1678-5
147. Cremona ML, Matthies HJG, Pau K, et al (2011) Flotillin-1 is essential for PKC-triggered endocytosis and membrane microdomain localization of DAT. Nat Neurosci 14:469–477. https://doi.org/10.1038/nn.2781
148. Solis GP, Hülsbusch N, Radon Y, et al (2013) Reggies/flotillins interact with Rab11a and SNX4 at the tubulovesicular recycling compartment and function in transferrin receptor and E-cadherin trafficking. Mol Biol Cell 24(17):2689–2702. https://doi.org/10.1091/mbc.e12-12-0854
149. Meister M, Bänfer S, Gärtner U, et al (2017) Regulation of cargo transfer between ESCRT-0 and ESCRT-I complexes by flotillin-1 during endosomal sorting of ubiquitinated cargo. Oncogenesis 6:e344–e344. https://doi.org/10.1038/oncsis.2017.47
150. Stuermer CAO (2011) Reggie/flotillin and the targeted delivery of cargo. J Neurochem 116:708–713. https://doi.org/10.1111/j.1471-4159.2010.07007.x
151. Hülsbusch N, Solis GP, Katanaev VL, Stuermer CAO (2015) Reggie-1/Flotillin-2 regulates integrin trafficking and focal adhesion turnover via Rab11a. Eur J Cell Biol 94:531–545. https://doi.org/10.1016/j.ejcb.2015.07.003
152. Banning A, Babuke T, Kurrle N, et al (2018) Flotillins Regulate Focal Adhesions by Interacting with α-Actinin and by Influencing the Activation of Focal Adhesion Kinase. Cells 7:28. https://doi.org/10.3390/cells7040028
153. Langhorst MF, Jaeger FA, Mueller S, et al (2008) Reggies/flotillins regulate cytoskeletal remodeling during neuronal differentiation via CAP/ponsin and Rho GTPases. Eur J Cell Biol 87:921–931. https://doi.org/10.1016/j.ejcb.2008.07.001
154. Schleif R (1999) Arm-domain interactions in proteins: a review. Proteins Struct Funct Genet 34:1–3. https://doi.org/10.1002/(SICI)1097-0134(19990101)34:1<1::AID-PROT1>3.0.CO;2-C
155. Kurrle N, Völlner F, Eming R, et al (2013) Flotillins Directly Interact with γ-Catenin and Regulate Epithelial Cell-Cell Adhesion. PLoS One 8:e84393. https://doi.org/10.1371/journal.pone.0084393
156. Solis GP, Schrock Y, Hülsbusch N, et al (2012) Reggies/flotillins regulate E-cadherin–mediated cell contact formation by affecting EGFR trafficking. Mol Biol Cell 23:1812–1825. https://doi.org/10.1091/mbc.e11-12-1006
157. Baumann CA, Ribon V, Kanzaki M, et al (2000) CAP defines a second signalling pathway required for insulin-stimulated glucose transport. Nature 407:202–207. https://doi.org/10.1038/35025089
158. Otto GP, Nichols BJ (2011) The roles of flotillin microdomains – endocytosis and beyond. J Cell Sci 124:3933–3940. https://doi.org/10.1242/jcs.092015
159. Ridley AJ (2015) Rho GTPase signalling in cell migration. Curr Opin Cell Biol 36:103–112. https://doi.org/10.1016/j.ceb.2015.08.005
160. Thalwieser Z, Király N, Fonódi M, et al (2019) Protein phosphatase 2A–mediated flotillin-1 dephosphorylation up-regulates endothelial cell migration and angiogenesis regulation. J Biol Chem 294:20196–20206. https://doi.org/10.1074/jbc.RA119.007980
161. Huang Y, Guo Y, Xu Y, et al (2022) Flotillin-1 promotes EMT of gastric cancer via stabilizing Snail. PeerJ 10:e13901. https://doi.org/10.7717/peerj.13901
162. Zhu M, Shi W, Chen K, et al (2022) Pulsatilla saponin E suppresses viability, migration, invasion and promotes apoptosis of NSCLC cells through negatively regulating Akt/FASN pathway via inhibition of flotillin-2 in lipid raft. J Recept Signal Transduct 42:23–33. https://doi.org/10.1080/10799893.2020.1839764
163. Yang Q, Zhu M, Wang Z, et al (2016) 4.1N is involved in a flotillin-1/β-catenin/Wnt pathway and suppresses cell proliferation and migration in non-small cell lung cancer cell lines. Tumor Biol 37(9):12713–12723. https://doi.org/10.1007/s13277-016-5146-3
164. Yokoyama N, Malbon CC (2009) Dishevelled-2 docks and activates Src in a Wnt-dependent manner. J Cell Sci

122(24):4439–4451. https://doi.org/10.1242/jcs.051847
165. Megy S, Bertho G, Gharbi-Benarous J, et al (2006) STD and TRNOESY NMR studies for the epitope mapping of the phosphorylation motif of the oncogenic protein beta-catenin recognized by a selective monoclonal antibody. FEBS Lett 580:5411–5422. https://doi.org/10.1016/j.febslet.2006.08.084
166. Baczynska D, Bombik I, Malicka-Błaszkiewicz M (2016) β-Catenin Expression Regulates Cell Migration of Human Colonic Adenocarcinoma Cells Through Gelsolin. Anticancer Res 36:5249–5256. https://doi.org/10.21873/anticanres.11095
167. Xu W, Kimelman D (2007) Mechanistic insights from structural studies of β-catenin and its binding partners. J Cell Sci 120:3337–3344. https://doi.org/10.1242/jcs.013771
168. Huber AH, Nelson WJ, Weis WI (1997) Three-Dimensional Structure of the Armadillo Repeat Region of β-Catenin. Cell 90:871–882. https://doi.org/10.1016/S0092-8674(00)80352-9
169. Solanas G, Miravet S, Casagolda D, et al (2004) β-Catenin and Plakoglobin N- and C-tails Determine Ligand Specificity. J Biol Chem 279:49849–49856. https://doi.org/10.1074/jbc.M408685200
170. Bremnes RM, Veve R, Hirsch FR, Franklin WA (2002) The E-cadherin cell–cell adhesion complex and lung cancer invasion, metastasis, and prognosis. Lung Cancer 36:115–124. https://doi.org/10.1016/S0169-5002(01)00471-8
171. Kaszak I, Witkowska-Piłaszewicz O, Niewiadomska Z, et al (2020) Role of Cadherins in Cancer—A Review. Int J Mol Sci 21:7624. https://doi.org/10.3390/ijms21207624
172. Nagafuchi A, Takeichi M (1988) Cell binding function of E-cadherin is regulated by the cytoplasmic domain. EMBO J 7:3679–3684. https://doi.org/10.1002/j.1460-2075.1988.tb03249.x
173. Kourtidis A, Lu R, Pence LJ, Anastasiadis PZ (2017) A central role for cadherin signaling in cancer. Exp Cell Res 358:78–85. https://doi.org/10.1016/j.yexcr.2017.04.006
174. Guillaume E, Comunale F, Do Khoa N, et al (2013) Flotillin micro-domains stabilize Cadherins at cell-cell junctions. J Cell Sci 126(Pt 22):5293–5304. https://doi.org/10.1242/jcs.133975
175. Baranwal S, Alahari SK (2009) Molecular mechanisms controlling E-cadherin expression in breast cancer. Biochem Biophys Res Commun 384:6–11. https://doi.org/10.1016/j.bbrc.2009.04.051
176. Renner G, Noulet F, Mercier M-C, et al (2016) Expression/activation of α5β1 integrin is linked to the β-catenin signaling pathway to drive migration in glioma cells. Oncotarget 7:62194–62207. https://doi.org/10.18632/oncotarget.11552
177. You Y, Zheng Q, Dong Y, et al (2015) Higher Matrix Stiffness Upregulates Osteopontin Expression in Hepatocellular Carcinoma Cells Mediated by Integrin β1/GSK3β/β-Catenin Signaling Pathway. PLoS One 10:e0134243. https://doi.org/10.1371/journal.pone.0134243
178. Couffinhal T, Dufourcq P, Duplàa C (2006) β-Catenin Nuclear Activation. Circ Res 99:1287–1289. https://doi.org/10.1161/01.RES.0000253139.82251.31
179. Wu Y, Chiang Y, Chou S, Pan C (2021) Wnt signalling and endocytosis: Mechanisms, controversies and implications for stress responses. Biol Cell 113:95–106. https://doi.org/10.1111/boc.202000099
180. Muñoz-Descalzo S, Hadjantonakis A-K, Arias AM (2015) Wnt/ß-catenin signalling and the dynamics of fate decisions in early mouse embryos and embryonic stem (ES) cells. Semin Cell Dev Biol 47–48:101–109. https://doi.org/10.1016/j.semcdb.2015.08.011
181. Gayrard C, Bernaudin C, Déjardin T, et al (2018) Src- and confinement-dependent FAK activation causes E-cadherin relaxation and β-catenin activity. J Cell Biol 217:1063–1077. https://doi.org/10.1083/jcb.201706013
182. Valenta T, Hausmann G, Basler K (2012) The many faces and functions of β-catenin. EMBO J 31:2714–2736. https://doi.org/10.1038/emboj.2012.150
183. Yang P, Anastas JN, Toroni RA, et al (2012) WLS inhibits melanoma cell proliferation through the β-catenin signalling pathway and induces spontaneous metastasis. EMBO Mol Med 4:1294–1307. https://doi.org/10.1002/emmm.201201486
184. Karrasch T, Spaeth T, Allard B, Jobin C (2011) PI3K-Dependent GSK3ß(Ser9)-Phosphorylation Is Implicated in the Intestinal Epithelial Cell Wound-Healing Response. PLoS One 6:e26340. https://doi.org/10.1371/journal.pone.0026340
185. Brandel A, Aigal S, Lagies S, et al (2020) The Gb3-enriched CD59/flotillin plasma membrane domain regulates host cell invasion by Pseudomonas aeruginosa. bioRxiv 78(7):3637–3656. https://doi.org/10.1101/2020.06.26.173336
186. Azzopardi EA, Azzopardi E, Camilleri L, et al (2014) Gram negative wound infection in hospitalised adult burn patients-systematic review and metanalysis. PLoS One 9(4):e95042. https://doi.org/10.1371/journal.pone.0095042
187. Neumann-Glesen C, Fernow I, Amaddii M, Tikkanen R (2007) Role of EGF-induced tyrosine phosphorylation of reggie-1/flotillin-2 in cell spreading and signaling to the actin cytoskeleton. J Cell Sci 120(Pt 3):395–406. https://doi.org/10.1242/jcs.03336
188. Gomez D, Natan S, Shokef Y, Lesman A (2019) Mechanical Interaction between Cells Facilitates Molecular Transport. Adv Biosyst. https://doi.org/10.1002/adbi.201900192
189. Inada N, Ueda T (2014) Membrane Trafficking Pathways and their Roles in Plant–Microbe Interactions. Plant Cell Physiol 55:672–686. https://doi.org/10.1093/pcp/pcu046
190. Sarangi NK, Shafaq-Zadah M, Berselli GB, et al (2022) Galectin-3 Binding to α5β1 Integrin in Pore Suspended Biomembranes. J Phys Chem B 126:10000–10017. https://doi.org/10.1021/acs.jpcb.2c05717

191. Hönig E, Schneider K, Jacob R (2015) Recycling of galectin-3 in epithelial cells. Eur J Cell Biol 94(7–9):309–315. https://doi.org/10.1016/j.ejcb.2015.05.004
192. Naslavsky N, Caplan S (2018) The enigmatic endosome – sorting the ins and outs of endocytic trafficking. J Cell Sci 131(13):jcs216499. https://doi.org/10.1242/jcs.216499
193. Janik ME, Lityńska A, Vereecken P (2010) Cell migration—The role of integrin glycosylation. Biochim Biophys Acta - Gen Subj 1800:545–555. https://doi.org/10.1016/j.bbagen.2010.03.013
194. Chierchia L, Tussellino M, Guarino D, et al (2015) Cytoskeletal proteins associate with components of the ribosomal maturation and translation apparatus in Xenopus stage I oocytes. Zygote 23(5):669–682. https://doi.org/10.1017/S0967199414000409
195. Dietrich C, Scherwat J, Faust D, Oesch F (2002) Subcellular localization of beta-catenin is regulated by cell density. Biochem Biophys Res Commun 292:195–199. https://doi.org/10.1006/bbrc.2002.6625
196. Banning A, Kurrle N, Meister M, Tikkanen R (2014) Flotillins in Receptor Tyrosine Kinase Signaling and Cancer. Cells 3:129–149. https://doi.org/10.3390/cells3010129
197. Xu R, Song X, Su P, et al (2017) Identification and characterization of the lamprey Flotillin-1 gene with a role in cell adhesion. Fish Shellfish Immunol 71:286–294. https://doi.org/10.1016/j.fsi.2017.06.061
198. Lakshminarayan R, Wunder C, Becken U, et al (2014) Galectin-3 drives glycosphingolipid-dependent biogenesis of clathrin-independent carriers. Nat Cell Biol 16:592–603. https://doi.org/10.1038/ncb2970
199. Boscher C, Zheng YZ, Lakshminarayan R, et al (2012) Galectin-3 Protein Regulates Mobility of N-cadherin and GM1 Ganglioside at Cell-Cell Junctions of Mammary Carcinoma Cells. J Biol Chem 287:32940–32952. https://doi.org/10.1074/jbc.M112.353334
200. Furtak V, Hatcher F, Ochieng J (2001) Galectin-3 Mediates the Endocytosis of β-1 Integrins by Breast Carcinoma Cells. Biochem Biophys Res Commun 289:845–850. https://doi.org/10.1006/bbrc.2001.6064
201. Burkhalter RJ, Symowicz J, Hudson LG, et al (2011) Integrin Regulation of β-Catenin Signaling in Ovarian Carcinoma. J Biol Chem 286(26):23467–23475. https://doi.org/10.1074/jbc.M110.199539
202. Chairoungdua A, Smith DL, Pochard P, et al (2010) Exosome release of β-catenin: a novel mechanism that antagonizes Wnt signaling. J Cell Biol 190(6):1079–1091. https://doi.org/10.1083/jcb.201002049
203. Maldonado-García D, Salgado-Lucio ML, Roa-Espitia AL, et al (2017) Calpain inhibition prevents flotillin re-ordering and Src family activation during capacitation. Cell Tissue Res 369(2):395–412. https://doi.org/10.1007/s00441-017-2591-2
204. Krause-Gruszczynska M, Boehm M, Rohde M, et al (2011) The signaling pathway of Campylobacter jejuni-induced Cdc42 activation: Role of fibronectin, integrin beta1, tyrosine kinases and guanine exchange factor Vav2. Cell Commun Signal 9(1):32. https://doi.org/10.1186/1478-811X-9-32
205. Zahorska E, Rosato F, Stober K, et al (2023) Neutralisation der Auswirkungen des Virulenzfaktors LecA aus Pseudomonas aeruginosa auf Humanzellen durch neue glykomimetische Inhibitoren. Angew Chemie 135:. https://doi.org/10.1002/ange.202215535
206. Fu Q, Chen K, Zhu Q, et al (2017) β-catenin promotes intracellular bacterial killing via suppression of Pseudomonas aeruginosa -triggered macrophage autophagy. J Int Med Res 45(2):556–569. https://doi.org/10.1177/0300060517692147
207. Li Y, Jin K, van Pelt GW, et al (2016) c-Myb Enhances Breast Cancer Invasion and Metastasis through the Wnt/β-Catenin/Axin2 Pathway. Cancer Res 76:3364–3375. https://doi.org/10.1158/0008-5472.CAN-15-2302
208. Nagaoka T, Kaburagi Y, Hamaguchi Y, et al (2000) Delayed Wound Healing in the Absence of Intercellular Adhesion Molecule-1 or L-Selectin Expression. Am J Pathol 157:237–247. https://doi.org/10.1016/S0002-9440(10)64534-8
209. Liu X, Gao J, Sun Y, et al (2017) Mutation of N-linked glycosylation in EpCAM affected cell adhesion in breast cancer cells. Biol Chem 398:1119–1126. https://doi.org/10.1515/hsz-2016-0232
210. Kikkawa Y, Ogawa T, Sudo R, et al (2013) The Lutheran/Basal Cell Adhesion Molecule Promotes Tumor Cell Migration by Modulating Integrin-mediated Cell Attachment to Laminin-511 Protein. J Biol Chem 288:30990–31001. https://doi.org/10.1074/jbc.M113.486456
211. Devis L, Moiola CP, Masia N, et al (2017) Activated leukocyte cell adhesion molecule (ALCAM) is a marker of recurrence and promotes cell migration, invasion, and metastasis in early-stage endometrioid endometrial cancer. J Pathol 241:475–487. https://doi.org/10.1002/path.4851
212. Lobert VH, Brech A, Pedersen NM, et al (2010) Ubiquitination of α5β1 Integrin Controls Fibroblast Migration through Lysosomal Degradation of Fibronectin-Integrin Complexes. Dev Cell 19:148–159. https://doi.org/10.1016/j.devcel.2010.06.010
213. Faridi MH, Altintas MM, Gomez C, et al (2013) Small molecule agonists of integrin CD11b/CD18 do not induce global conformational changes and are significantly better than activating antibodies in reducing vascular injury. Biochim Biophys Acta - Gen Subj 1830:3696–3710. https://doi.org/10.1016/j.bbagen.2013.02.018
214. Riccio G, Bottone S, La Regina G, et al (2018) A Negative Allosteric Modulator of WNT Receptor Frizzled 4 Switches into an Allosteric Agonist. Biochemistry 57:839–851. https://doi.org/10.1021/acs.biochem.7b01087
215. Hofmann A, Sommer R, Hauck D, et al (2015) Synthesis of mannoheptose derivatives and their evaluation as inhibitors

of the lectin LecB from the opportunistic pathogen Pseudomonas aeruginosa. Carbohydr Res 412:34–42. https://doi.org/10.1016/j.carres.2015.04.010
216. Liao S, von der Weid PY (2015) Lymphatic system: An active pathway for immune protection. Semin Cell Dev Biol 38:83–89. https://doi.org/10.1016/j.semcdb.2014.11.012
217. Hu D, Li L, Li S, et al (2019) Lymphatic system identification, pathophysiology and therapy in the cardiovascular diseases. J Mol Cell Cardiol 133:99–111. https://doi.org/10.1016/j.yjmcc.2019.06.002
218. Yousef M, Silva D, Bou Chacra N, et al (2021) The Lymphatic System: A Sometimes-Forgotten Compartment in Pharmaceutical Sciences. J Pharm Pharm Sci 24:533–547. https://doi.org/10.18433/jpps32222
219. Margaris KN, Black RA (2012) Modelling the lymphatic system: challenges and opportunities. J R Soc Interface 9:601–612. https://doi.org/10.1098/rsif.2011.0751
220. Swartz M (2001) The physiology of the lymphatic system. Adv Drug Deliv Rev 50:3–20. https://doi.org/10.1016/S0169-409X(01)00150-8
221. Petrova T V., Koh GY (2020) Biological functions of lymphatic vessels. Science (80-) 369:. https://doi.org/10.1126/science.aax4063
222. Leak L V. (1976) The structure of lymphatic capillaries in lymph formation. Fed Proc 35:1863–71
223. McLafferty E, Hendry C, Farley A (2012) The lymphatic system. Nurs Stand 27:37–42. https://doi.org/10.7748/ns2012.12.27.15.37.c9482
224. Stephens M, Liao S (2018) Neutrophil–lymphatic interactions during acute and chronic disease. Cell Tissue Res 371:599–606. https://doi.org/10.1007/s00441-017-2779-5
225. Baluk P, Fuxe J, Hashizume H, et al (2007) Functionally specialized junctions between endothelial cells of lymphatic vessels. J Exp Med 204:2349–2362. https://doi.org/10.1084/jem.20062596
226. Nakashima BJ, Hong Y-K (2022) VE-Cadherin: A Critical Sticking Point for Lymphatic System Maintenance: Role of VE-Cadherin in Lymphatic Maintenance. Circ Res 130:24–26. https://doi.org/10.1161/CIRCRESAHA.121.320497
227. Lutter S, Xie S, Tatin F, Makinen T (2012) Smooth muscle–endothelial cell communication activates Reelin signaling and regulates lymphatic vessel formation. J Cell Biol 197:837–849. https://doi.org/10.1083/jcb.201110132
228. Lutter S, Makinen T (2014) Regulation of lymphatic vasculature by extracellular matrix. Adv Anat Embryol Cell Biol 214:55–65. https://doi.org/10.1007/978-3-7091-1646-3_5
229. Dudás B (2023) Lymphatic System. In: Dudás B (ed) Human Histology. Elsevier, pp 35–53
230. Ohtani O, Ohtani Y (2008) Structure and function of rat lymph nodes. Arch Histol Cytol 71:69–76. https://doi.org/10.1679/aohc.71.69
231. Willard-Mack CL (2006) Normal Structure, Function, and Histology of Lymph Nodes. Toxicol Pathol 34:409–424. https://doi.org/10.1080/01926230600867727
232. Knoop KA, Butler BR, Kumar N, et al (2011) Distinct Developmental Requirements for Isolated Lymphoid Follicle Formation in the Small and Large Intestine. Am J Pathol 179:1861–1871. https://doi.org/10.1016/j.ajpath.2011.06.004
233. Műzes G, Bohusné Barta B, Sipos F (2022) Colitis and Colorectal Carcinogenesis: The Focus on Isolated Lymphoid Follicles. Biomedicines 10:226. https://doi.org/10.3390/biomedicines10020226
234. Fenton TM, Jørgensen PB, Niss K, et al (2020) Immune Profiling of Human Gut-Associated Lymphoid Tissue Identifies a Role for Isolated Lymphoid Follicles in Priming of Region-Specific Immunity. Immunity 52:557-570.e6. https://doi.org/10.1016/j.immuni.2020.02.001
235. Escobedo N, Oliver G (2016) Lymphangiogenesis: Origin, Specification, and Cell Fate Determination. Annu Rev Cell Dev Biol 32:677–691. https://doi.org/10.1146/annurev-cellbio-111315-124944
236. Trevaskis NL, Hu L, Caliph SM, et al (2015) The mesenteric lymph duct cannulated rat model: application to the assessment of intestinal lymphatic drug transport. J Vis Exp 52389. https://doi.org/10.3791/52389
237. Alexander JS, Ganta VC, Jordan PA, Witte MH (2010) Gastrointestinal lymphatics in health and disease. Pathophysiology 17:315–335. https://doi.org/10.1016/j.pathophys.2009.09.003
238. Jiang X, Nicolls MR, Tian W, Rockson SG (2018) Lymphatic Dysfunction, Leukotrienes, and Lymphedema. Annu Rev Physiol 80:49–70. https://doi.org/10.1146/annurev-physiol-022516-034008
239. OLIVER G, SOSAPINEDA B, GEISENDORF S, et al (1993) Prox 1, a prospero-related homeobox gene expressed during mouse development. Mech Dev 44:3–16. https://doi.org/10.1016/0925-4773(93)90012-M
240. Hong Y-K, Detmar M (2003) Prox1, master regulator of the lymphatic vasculature phenotype. Cell Tissue Res 314:85–92. https://doi.org/10.1007/s00441-003-0747-8
241. Wigle JT (2002) An essential role for Prox1 in the induction of the lymphatic endothelial cell phenotype. EMBO J 21:1505–1513. https://doi.org/10.1093/emboj/21.7.1505
242. Jackson DG, Prevo R, Clasper S, Banerji S (2001) LYVE-1, the lymphatic system and tumor lymphangiogenesis. Trends Immunol 22:317–321. https://doi.org/10.1016/S1471-4906(01)01936-6
243. Johnson LA, Banerji S, Lawrance W, et al (2017) Dendritic cells enter lymph vessels by hyaluronan-mediated docking to the endothelial receptor LYVE-1. Nat Immunol 18:762–770. https://doi.org/10.1038/ni.3750
244. Hamrah P, Chen L, Zhang Q, Dana MR (2003) Novel Expression of Vascular Endothelial Growth Factor Receptor

(VEGFR)-3 and VEGF-C on Corneal Dendritic Cells. Am J Pathol 163:57–68. https://doi.org/10.1016/S0002-9440(10)63630-9
245. Ammar A, Mohammed RAA, Salmi M, et al (2011) Lymphatic expression of CLEVER-1 in breast cancer and its relationship with lymph node metastasis. Anal Cell Pathol (Amst) 34:67–78. https://doi.org/10.3233/ACP-2011-0002
246. Kzhyshkowska J, Gratchev A, Goerdt S (2006) Stabilin-1, a homeostatic scavenger receptor with multiple functions. J Cell Mol Med 10:635–649. https://doi.org/10.1111/j.1582-4934.2006.tb00425.x
247. Irjala H, Elima K, Johansson E-L, et al (2003) The same endothelial receptor controls lymphocyte traffic both in vascular and lymphatic vessels. Eur J Immunol 33:815–824. https://doi.org/10.1002/eji.200323859
248. Roh S-E, Jeong Y, Kang M-H, Bae Y-S (2018) Junctional adhesion molecules mediate transendothelial migration of dendritic cell vaccine in cancer immunotherapy. Cancer Lett 434:196–205. https://doi.org/10.1016/j.canlet.2018.07.029
249. Jalkanen S, Salmi M (2020) Lymphatic endothelial cells of the lymph node. Nat Rev Immunol 20:566–578. https://doi.org/10.1038/s41577-020-0281-x
250. Buettner M, Bode U (2012) Lymph node dissection – understanding the immunological function of lymph nodes. Clin Exp Immunol 169:205–212. https://doi.org/10.1111/j.1365-2249.2012.04602.x
251. Ager A (2017) High Endothelial Venules and Other Blood Vessels: Critical Regulators of Lymphoid Organ Development and Function. Front Immunol 8:. https://doi.org/10.3389/fimmu.2017.00045
252. du Bois H, Heim TA, Lund AW (2021) Tumor-draining lymph nodes: At the crossroads of metastasis and immunity. Sci Immunol 6:. https://doi.org/10.1126/sciimmunol.abg3551
253. Lucas ED, Finlon JM, Burchill MA, et al (2018) Type 1 IFN and PD-L1 Coordinate Lymphatic Endothelial Cell Expansion and Contraction during an Inflammatory Immune Response. J Immunol 201:1735–1747. https://doi.org/10.4049/jimmunol.1800271
254. Angeli V, Ginhoux F, Llodrà J, et al (2006) B Cell-Driven Lymphangiogenesis in Inflamed Lymph Nodes Enhances Dendritic Cell Mobilization. Immunity 24:203–215. https://doi.org/10.1016/j.immuni.2006.01.003
255. Comerford I, Harata-Lee Y, Bunting MD, et al (2013) A myriad of functions and complex regulation of the CCR7/CCL19/CCL21 chemokine axis in the adaptive immune system. Cytokine Growth Factor Rev 24:269–283. https://doi.org/10.1016/j.cytogfr.2013.03.001
256. Schineis P, Runge P, Halin C (2019) Cellular traffic through afferent lymphatic vessels. Vascul Pharmacol 112:31–41. https://doi.org/10.1016/j.vph.2018.08.001
257. Braun A, Worbs T, Moschovakis GL, et al (2011) Afferent lymph–derived T cells and DCs use different chemokine receptor CCR7–dependent routes for entry into the lymph node and intranodal migration. Nat Immunol 12:879–887. https://doi.org/10.1038/ni.2085
258. Britschgi MR, Favre S, Luther SA (2010) CCL21 is sufficient to mediate DC migration, maturation and function in the absence of CCL19. Eur J Immunol 40:1266–1271. https://doi.org/10.1002/eji.200939921
259. Achen MG, Jeltsch M, Kukk E, et al (1998) Vascular endothelial growth factor D (VEGF-D) is a ligand for the tyrosine kinases VEGF receptor 2 (Flk1) and VEGF receptor 3 (Flt4). Proc Natl Acad Sci 95:548–553. https://doi.org/10.1073/pnas.95.2.548
260. Salameh A, Galvagni F, Bardelli M, et al (2005) Direct recruitment of CRK and GRB2 to VEGFR-3 induces proliferation, migration, and survival of endothelial cells through the activation of ERK, AKT, and JNK pathways. Blood 106:3423–3431. https://doi.org/10.1182/blood-2005-04-1388
261. Shalaby F, Rossant J, Yamaguchi TP, et al (1995) Failure of blood-island formation and vasculogenesis in Flk-1-deficient mice. Nature 376:62–66. https://doi.org/10.1038/376062a0
262. Fong G-H, Rossant J, Gertsenstein M, Breitman ML (1995) Role of the Flt-1 receptor tyrosine kinase in regulating the assembly of vascular endothelium. Nature 376:66–70. https://doi.org/10.1038/376066a0
263. Olariu R, Tsai C, Abd El Hafez M, et al (2021) Presence of Donor Lymph Nodes Within Vascularized Composite Allotransplantation Ameliorates VEGF-C-mediated Lymphangiogenesis and Delays the Onset of Acute Rejection. Transplantation 105:1747–1759. https://doi.org/10.1097/TP.0000000000003601
264. Wong BW (2020) Lymphatic vessels in solid organ transplantation and immunobiology. Am J Transplant 20:1992–2000. https://doi.org/10.1111/ajt.15806
265. Secker GA, Harvey NL (2015) VEGFR signaling during lymphatic vascular development: From progenitor cells to functional vessels. Dev Dyn 244:323–331. https://doi.org/10.1002/dvdy.24227
266. Lee JY, Kim H-J (2014) (Lymph)angiogenic influences on hematopoietic cells in acute myeloid leukemia. Exp Mol Med 46:e122–e122. https://doi.org/10.1038/emm.2014.72
267. Gasteiger G, Ataide M, Kastenmüller W (2016) Lymph node - an organ for T-cell activation and pathogen defense. Immunol Rev 271:200–220. https://doi.org/10.1111/imr.12399
268. Mackay CR, Marston WL, Dudler L (1990) Naive and memory T cells show distinct pathways of lymphocyte recirculation. J Exp Med 171:801–817. https://doi.org/10.1084/jem.171.3.801
269. Girard J-P, Moussion C, Förster R (2012) HEVs, lymphatics and homeostatic immune cell trafficking in lymph nodes. Nat

Rev Immunol 12:762–773. https://doi.org/10.1038/nri3298
270. Tomura M, Yoshida N, Tanaka J, et al (2008) Monitoring cellular movement in vivo with photoconvertible fluorescence protein “Kaede” transgenic mice. Proc Natl Acad Sci 105:10871–10876. https://doi.org/10.1073/pnas.0802278105
271. Zhu J, Yamane H, Paul WE (2010) Differentiation of Effector CD4 T Cell Populations. Annu Rev Immunol 28:445–489. https://doi.org/10.1146/annurev-immunol-030409-101212
272. Duckworth BC, Qin RZ, Groom JR (2022) Spatial determinates of effector and memory CD8 + T cell fates*. Immunol Rev 306:76–92. https://doi.org/10.1111/imr.13044
273. Borst J, Ahrends T, Bąbała N, et al (2018) CD4+ T cell help in cancer immunology and immunotherapy. Nat Rev Immunol 18:635–647. https://doi.org/10.1038/s41577-018-0044-0
274. Arasa J, Collado-Diaz V, Halin C (2021) Structure and Immune Function of Afferent Lymphatics and Their Mechanistic Contribution to Dendritic Cell and T Cell Trafficking. Cells 10:1269. https://doi.org/10.3390/cells10051269
275. Watanabe R, Gehad A, Yang C, et al (2015) Human skin is protected by four functionally and phenotypically discrete populations of resident and recirculating memory T cells. Sci Transl Med 7:. https://doi.org/10.1126/scitranslmed.3010302
276. Salmi M, Koskinen K, Henttinen T, et al (2004) CLEVER-1 mediates lymphocyte transmigration through vascular and lymphatic endothelium. Blood 104:3849–3857. https://doi.org/10.1182/blood-2004-01-0222
277. Karikoski M, Irjala H, Maksimow M, et al (2009) Clever-1/Stabilin-1 regulates lymphocyte migration within lymphatics and leukocyte entrance to sites of inflammation. Eur J Immunol 39:3477–3487. https://doi.org/10.1002/eji.200939896
278. Brinkman CC, Iwami D, Hritzo MK, et al (2016) Treg engage lymphotoxin beta receptor for afferent lymphatic transendothelial migration. Nat Commun 7:12021. https://doi.org/10.1038/ncomms12021
279. Teijeira A, Hunter MC, Russo E, et al (2017) T Cell Migration from Inflamed Skin to Draining Lymph Nodes Requires Intralymphatic Crawling Supported by ICAM-1/LFA-1 Interactions. Cell Rep 18:857–865. https://doi.org/10.1016/j.celrep.2016.12.078
280. Randolph GJ, Angeli V, Swartz MA (2005) Dendritic-cell trafficking to lymph nodes through lymphatic vessels. Nat Rev Immunol 5:617–628. https://doi.org/10.1038/nri1670
281. Alvarez D, Vollmann EH, von Andrian UH (2008) Mechanisms and Consequences of Dendritic Cell Migration. Immunity 29:325–342. https://doi.org/10.1016/j.immuni.2008.08.006
282. Radtke AJ, Kastenmüller W, Espinosa DA, et al (2015) Lymph-Node Resident CD8α+ Dendritic Cells Capture Antigens from Migratory Malaria Sporozoites and Induce CD8+ T Cell Responses. PLOS Pathog 11:e1004637. https://doi.org/10.1371/journal.ppat.1004637
283. Hor JL, Whitney PG, Zaid A, et al (2015) Spatiotemporally Distinct Interactions with Dendritic Cell Subsets Facilitates CD4+ and CD8+ T Cell Activation to Localized Viral Infection. Immunity 43:554–565. https://doi.org/10.1016/j.immuni.2015.07.020
284. Ohl L, Mohaupt M, Czeloth N, et al (2004) CCR7 Governs Skin Dendritic Cell Migration under Inflammatory and Steady-State Conditions. Immunity 21:279–288. https://doi.org/10.1016/j.immuni.2004.06.014
285. Förster R, Schubel A, Breitfeld D, et al (1999) CCR7 Coordinates the Primary Immune Response by Establishing Functional Microenvironments in Secondary Lymphoid Organs. Cell 99:23–33. https://doi.org/10.1016/S0092-8674(00)80059-8
286. Mandell KJ, Babbin BA, Nusrat A, Parkos CA (2005) Junctional Adhesion Molecule 1 Regulates Epithelial Cell Morphology through Effects on β1 Integrins and Rap1 Activity. J Biol Chem 280:11665–11674. https://doi.org/10.1074/jbc.M412650200
287. Matsutani T, Tanaka T, Tohya K, et al (2007) Plasmacytoid dendritic cells employ multiple cell adhesion molecules sequentially to interact with high endothelial venule cells - molecular basis of their trafficking to lymph nodes. Int Immunol 19:1031–1037. https://doi.org/10.1093/intimm/dxm088
288. Vigl B, Aebischer D, Nitschké M, et al (2011) Tissue inflammation modulates gene expression of lymphatic endothelial cells and dendritic cell migration in a stimulus-dependent manner. Blood 118:205–215. https://doi.org/10.1182/blood-2010-12-326447
289. Worbs T, Hammerschmidt SI, Förster R (2017) Dendritic cell migration in health and disease. Nat Rev Immunol 17:30–48. https://doi.org/10.1038/nri.2016.116
290. Eisenbarth SC (2019) Dendritic cell subsets in T cell programming: location dictates function. Nat Rev Immunol 19:89–103. https://doi.org/10.1038/s41577-018-0088-1
291. Bousso P (2008) T-cell activation by dendritic cells in the lymph node: lessons from the movies. Nat Rev Immunol 8:675–684. https://doi.org/10.1038/nri2379
292. Gaud G, Lesourne R, Love PE (2018) Regulatory mechanisms in T cell receptor signalling. Nat Rev Immunol 18:485–497. https://doi.org/10.1038/s41577-018-0020-8
293. Alcover A, Alarcón B, Di Bartolo V (2018) Cell Biology of T Cell Receptor Expression and Regulation. Annu Rev Immunol 36:103–125. https://doi.org/10.1146/annurev-immunol-042617-053429
294. Alcover A, Alarcon B (2000) Internalization and Intracellular Fate of TCR-CD3 Complexes. Crit Rev Immunol 20:22.

https://doi.org/10.1615/CritRevImmunol.v20.i4.20
295. Fujii Y, Fujii K, Iwata S, et al (2006) Abnormal intracellular distribution of NFAT1 in T lymphocytes from patients with systemic lupus erythematosus and characteristic clinical features. Clin Immunol 119:297–306. https://doi.org/10.1016/j.clim.2006.01.001
296. Hatchi EM, Poalas K, Cordeiro N, et al (2014) Participation of the E3-ligase TRIM13 in NF-κB p65 activation and NFAT-dependent activation of c-Rel upon T-cell receptor engagement. Int J Biochem Cell Biol 54:217–222. https://doi.org/10.1016/j.biocel.2014.07.012
297. Leung S, Smith D, Myc A, et al (2013) OT-II TCR transgenic mice fail to produce anti-ovalbumin antibodies upon vaccination. Cell Immunol 282:79–84. https://doi.org/10.1016/j.cellimm.2012.12.006
298. Park H-B, Lim S-M, Hwang J, et al (2020) Cancer immunotherapy using a polysaccharide from Codium fragile in a murine model. Oncoimmunology 9:1772663. https://doi.org/10.1080/2162402X.2020.1772663
299. Schnorrer P, Behrens GMN, Wilson NS, et al (2006) The dominant role of CD8 + dendritic cells in cross-presentation is not dictated by antigen capture. Proc Natl Acad Sci 103:10729–10734. https://doi.org/10.1073/pnas.0601956103
300. Jongbloed SL, Kassianos AJ, McDonald KJ, et al (2010) Human CD141+ (BDCA-3)+ dendritic cells (DCs) represent a unique myeloid DC subset that cross-presents necrotic cell antigens. J Exp Med 207:1247–1260. https://doi.org/10.1084/jem.20092140
301. Jafri S, Moore SD, Morrell NW, Ormiston ML (2017) A sex-specific reconstitution bias in the competitive CD45.1/CD45.2 congenic bone marrow transplant model. Sci Rep 7:3495. https://doi.org/10.1038/s41598-017-03784-9
302. Basu S, Ray A, Dittel BN (2013) Differential representation of B cell subsets in mixed bone marrow chimera mice due to expression of allelic variants of CD45 (CD45.1/CD45.2). J Immunol Methods 396:163–167. https://doi.org/10.1016/j.jim.2013.07.008
303. Spangrude GJ, Heimfeld S, Weissman IL (1988) Purification and Characterization of Mouse Hematopoietic Stem Cells. Science (80-) 241:58–62. https://doi.org/10.1126/science.2898810
304. Mercier FE, Sykes DB, Scadden DT (2016) Single Targeted Exon Mutation Creates a True Congenic Mouse for Competitive Hematopoietic Stem Cell Transplantation: The C57BL/6-CD45.1STEM Mouse. Stem Cell Reports 6:985–992. https://doi.org/10.1016/j.stemcr.2016.04.010
305. Silva PDM, Bier J, Paiatto LN, et al (2015) Tolerogenic Dendritic Cells on Transplantation: Immunotherapy Based on Second Signal Blockage. J Immunol Res 2015:1–15. https://doi.org/10.1155/2015/856707
306. Nagai S, Azuma M (2019) The CD28–B7 Family of Co-signaling Molecules. In: Advances in Experimental Medicine and Biology. pp 25–51
307. Hubo M, Trinschek B, Kryczanowsky F, et al (2013) Costimulatory Molecules on Immunogenic Versus Tolerogenic Human Dendritic Cells. Front Immunol 4:. https://doi.org/10.3389/fimmu.2013.00082
308. Corse E, Allison JP (2012) Cutting Edge: CTLA-4 on Effector T Cells Inhibits In Trans. J Immunol 189:1123–1127. https://doi.org/10.4049/jimmunol.1200695
309. Perez N, Karumuthil-Melethil S, Li R, et al (2008) Preferential costimulation by CD80 results in IL-10 dependent TGF-beta1+ adaptive regulatory T cell generation. FASEB J 22:405–405. https://doi.org/10.1096/fasebj.22.2_supplement.405
310. Elgueta R, Benson MJ, de Vries VC, et al (2009) Molecular mechanism and function of CD40/CD40L engagement in the immune system. Immunol Rev 229:152–172. https://doi.org/10.1111/j.1600-065X.2009.00782.x
311. Jordan-Williams KL, Ramanujam N, Farr AG, Ruddell A (2016) The Lymphatic Endothelial mCLCA1 Antibody Induces Proliferation and Growth of Lymph Node Lymphatic Sinuses. PLoS One 11:e0156079. https://doi.org/10.1371/journal.pone.0156079
312. Ruddell A, Croft A, Kelly-Spratt K, et al (2014) Tumors induce coordinate growth of artery, vein, and lymphatic vessel triads. BMC Cancer 14:354. https://doi.org/10.1186/1471-2407-14-354
313. Ruddell A, Mezquita P, Brandvold KA, et al (2003) B Lymphocyte-Specific c-Myc Expression Stimulates Early and Functional Expansion of the Vasculature and Lymphatics during Lymphomagenesis. Am J Pathol 163:2233–2245. https://doi.org/10.1016/S0002-9440(10)63581-X
314. Furuya M, Kirschbaum SB, Paulovich A, et al (2010) Lymphatic Endothelial Murine Chloride Channel Calcium-Activated 1 Is a Ligand for Leukocyte LFA-1 and Mac-1. J Immunol 185:5769–5777. https://doi.org/10.4049/jimmunol.1002226
315. Farr AG, Cho Y, De Bruyn PP (1980) The structure of the sinus wall of the lymph node relative to its endocytic properties and transmural cell passage. Am J Anat 157:265–284. https://doi.org/10.1002/aja.1001570304
316. Pfeiffer F, Kumar V, Butz S, et al (2008) Distinct molecular composition of blood and lymphatic vascular endothelial cell junctions establishes specific functional barriers within the peripheral lymph node. Eur J Immunol 38:2142–2155. https://doi.org/10.1002/eji.200838140
317. Wallez Y, Huber P (2008) Endothelial adherens and tight junctions in vascular homeostasis, inflammation and angiogenesis. Biochim Biophys Acta 1778:794–809. https://doi.org/10.1016/j.bbamem.2007.09.003
318. Breier G, Breviario F, Caveda L, et al (1996) Molecular cloning and expression of murine vascular endothelial- cadherin in early stage development of cardiovascular system. Blood 87:630–641.

https://doi.org/10.1182/blood.V87.2.630.bloodjournal872630
319. Lampugnani MG, Corada M, Caveda L, et al (1995) The molecular organization of endothelial cell to cell junctions: differential association of plakoglobin, beta-catenin, and alpha-catenin with vascular endothelial cadherin (VE-cadherin). J Cell Biol 129:203–217. https://doi.org/10.1083/jcb.129.1.203
320. Jannaway M, Scallan JP (2021) VE-Cadherin and Vesicles Differentially Regulate Lymphatic Vascular Permeability to Solutes of Various Sizes. Front Physiol 12:. https://doi.org/10.3389/fphys.2021.687563
321. Lagendijk AK, Hogan BM (2015) VE-cadherin in Vascular Development. In: Current Topics in Developmental Biology. pp 325–352
322. Baumeister U, Funke R, Ebnet K, et al (2005) Association of Csk to VE-cadherin and inhibition of cell proliferation. EMBO J 24:1686–1695. https://doi.org/10.1038/sj.emboj.7600647
323. Belvitch P, Htwe YM, Brown ME, Dudek S (2018) Cortical Actin Dynamics in Endothelial Permeability. Curr Top Membr 82:141–195. https://doi.org/10.1016/bs.ctm.2018.09.003
324. Viswanathan P, Ephstein Y, Garcia JGN, et al (2016) Differential elastic responses to barrier-altering agonists in two types of human lung endothelium. Biochem Biophys Res Commun 478:599–605. https://doi.org/10.1016/j.bbrc.2016.07.112
325. Doggett TM, Breslin JW (2011) Study of the actin cytoskeleton in live endothelial cells expressing GFP-actin. J Vis Exp. https://doi.org/10.3791/3187
326. Harris ES, Nelson WJ (2010) VE-cadherin: at the front, center, and sides of endothelial cell organization and function. Curr Opin Cell Biol 22:651–658. https://doi.org/10.1016/j.ceb.2010.07.006
327. Srinivasan RS, Dillard ME, Lagutin O V, et al (2007) Lineage tracing demonstrates the venous origin of the mammalian lymphatic vasculature. Genes Dev 21:2422–2432. https://doi.org/10.1101/gad.1588407
328. Mehta D, Malik AB (2006) Signaling Mechanisms Regulating Endothelial Permeability. Physiol Rev 86:279–367. https://doi.org/10.1152/physrev.00012.2005
329. Gündüz D, Troidl C, Tanislav C, et al (2019) Role of PI3K/Akt and MEK/ERK Signalling in cAMP/Epac-Mediated Endothelial Barrier Stabilisation. Front Physiol 10:. https://doi.org/10.3389/fphys.2019.01387
330. Garcia JGN, Davis HW, Patterson CE (1995) Regulation of endothelial cell gap formation and barrier dysfunction: Role of myosin light chain phosphorylation. J Cell Physiol 163:510–522. https://doi.org/10.1002/jcp.1041630311
331. Vestweber D (2008) VE-Cadherin. Arterioscler Thromb Vasc Biol 28:223–232. https://doi.org/10.1161/ATVBAHA.107.158014
332. Potter MD, Barbero S, Cheresh DA (2005) Tyrosine phosphorylation of VE-cadherin prevents binding of p120- and beta-catenin and maintains the cellular mesenchymal state. J Biol Chem 280:31906–31912. https://doi.org/10.1074/jbc.M505568200
333. Broman MT, Kouklis P, Gao X, et al (2006) Cdc42 regulates adherens junction stability and endothelial permeability by inducing alpha-catenin interaction with the vascular endothelial cadherin complex. Circ Res 98:73–80. https://doi.org/10.1161/01.RES.0000198387.44395.e9
334. Freemont AJ (1989) Endothelial cell biology in health and disease, N. Simionescu and M. Simionescu (Eds). Plenum Press, New York, 1988. No. of pages: xvii + 458. Price: $89.50. ISBN: 0 306 42761 6. J Pathol 158:359–360. https://doi.org/10.1002/path.1711580414
335. Maltabe V, Kouklis P (2022) Vascular Endothelial (VE)-cadherin-mediated adherens junctions involvement in cardiovascular progenitor cell specification. Int J Dev Biol 66:77–83. https://doi.org/10.1387/ijdb.210167pk
336. Li B, Huang X, Wei J, et al (2022) Role of moesin and its phosphorylation in VE-cadherin expression and distribution in endothelial adherens junctions. Cell Signal 100:110466. https://doi.org/10.1016/j.cellsig.2022.110466
337. Morsing SKH, Al-Mardini C, van Stalborch A-MD, et al (2020) Double-Hit–Induced Leukocyte Extravasation Driven by Endothelial Adherens Junction Destabilization. J Immunol 205:511–520. https://doi.org/10.4049/jimmunol.1900816
338. Giannotta M, Trani M, Dejana E (2013) VE-Cadherin and Endothelial Adherens Junctions: Active Guardians of Vascular Integrity. Dev Cell 26:441–454. https://doi.org/10.1016/j.devcel.2013.08.020
339. Giampietro C, Taddei A, Corada M, et al (2012) Overlapping and divergent signaling pathways of N-cadherin and VE-cadherin in endothelial cells. Blood 119:2159–2170. https://doi.org/10.1182/blood-2011-09-381012
340. Bazigou E, Lyons OTA, Smith A, et al (2011) Genes regulating lymphangiogenesis control venous valve formation and maintenance in mice. J Clin Invest 121:2984–2992. https://doi.org/10.1172/JCI58050
341. Terrén I, Orrantia A, Vitallé J, et al (2020) CFSE dilution to study human T and NK cell proliferation in vitro. Methods Enzymol 631:239–255. https://doi.org/10.1016/bs.mie.2019.05.020
342. Parish CR (1999) Fluorescent dyes for lymphocyte migration and proliferation studies. Immunol Cell Biol 77:499–508. https://doi.org/10.1046/j.1440-1711.1999.00877.x
343. Simenc J, Juric DM, Lipnik-Stangelj M (2019) NADPH oxidase inhibitor VAS2870 prevents staurosporine-induced cell death in rat astrocytes. Radiol Oncol 53:69–76. https://doi.org/10.2478/raon-2019-0002
344. Kirkeby S, Wimmerová M, Moe D, Hansen AK (2007) The mink as an animal model for Pseudomonas aeruginosa adhesion: binding of the bacterial lectins (PA-IL and PA-IIL) to neoglycoproteins and to sections of pancreas and lung

tissues from healthy mink. Microbes Infect 9:566–573. https://doi.org/10.1016/j.micinf.2007.01.025
345. Lameignere E, Malinovská L, Sláviková M, et al (2008) Structural basis for mannose recognition by a lectin from opportunistic bacteria Burkholderia cenocepacia. Biochem J 411:307–318. https://doi.org/10.1042/BJ20071276
346. Napimoga MH, Cavada BS, Alencar NMN, et al (2007) Lonchocarpus sericeus lectin decreases leukocyte migration and mechanical hypernociception by inhibiting cytokine and chemokines production. Int Immunopharmacol 7:824–835. https://doi.org/10.1016/j.intimp.2007.02.001
347. Kawata K, Suzuki T, Ozawa K, Sekiguchi M (2021) Features of T-cell subset composition in a D-galactose-induced senescence mouse model. Exp Anim 70:20–0095. https://doi.org/10.1538/expanim.20-0095
348. Alobaid MA, Richards S-J, Alexander MR, et al (2020) Developing immune-regulatory materials using immobilized monosaccharides with immune-instructive properties. Mater Today Bio 8:100080. https://doi.org/10.1016/j.mtbio.2020.100080
349. Toor SM, Saleh R, Sasidharan Nair V, et al (2021) T-cell responses and therapies against SARS-CoV-2 infection. Immunology 162:30–43. https://doi.org/10.1111/imm.13262
350. Haydar D, Gonzalez R, Garvy BA, et al (2021) Myeloid arginase-1 controls excessive inflammation and modulates T cell responses in Pseudomonas aeruginosa pneumonia. Immunobiology 226:152034. https://doi.org/10.1016/j.imbio.2020.152034
351. Walma DAC, Yamada KM (2020) The extracellular matrix in development. Development 147:. https://doi.org/10.1242/dev.175596
352. Kim EJY, Sorokin L, Hiiragi T (2022) ECM-integrin signalling instructs cellular position sensing to pattern the early mouse embryo. Development 149:. https://doi.org/10.1242/dev.200140
353. Ludwig A, Otto GP, Riento K, et al (2010) Flotillin microdomains interact with the cortical cytoskeleton to control uropod formation and neutrophil recruitment. J Cell Biol 191:771–781. https://doi.org/10.1083/jcb.201005140

Université de Strasbourg

Yubing GUO

L'impact de la lectine LecB de la bactérie Pseudomonas aeruginosa sur la cicatrisation et la réponse immunitaire

École doctorale Sciences de la vie et de la santé | ED 414
Université de Strasbourg

Résumé

Pseudomonas aeruginosa (P. aeruginosa) est une bactérie environnementale Gram-négative omniprésente et est connue comme un pathogène opportuniste et nosocomial. Elle peut provoquer une grande variété d'infections, qui peuvent affecter tous les organes du corps humain, telles que la pneumonie associée à la ventilation et les lésions pulmonaires aiguës. En raison des toxines extracellulaires de P. aeruginosa, il est virulent pour les cellules ou organes hôtes. Il a été rapporté que P. aeruginosa et ses protéines de virulence peuvent entraver la cicatrisation des plaies et altérer les processus de réparation, entraînant des plaies chroniques. De plus, l'infection à P. aeruginosa peut altérer la réponse immunitaire, comme les cellules NK, les cellules T et les cellules B. La première étape dans l'établissement d'une infection à P. aeruginosa consiste à adhérer aux cellules hôtes via des facteurs extracellulaires, tels que les lectines. Les lectines sont des glycoprotéines qui forment des liaisons réversibles lors de l'interaction avec des sucres/glycoprotéines liées à la membrane de la cellule hôte. P. aeruginosa possède deux lectines solubles, LecA et LecB (aussi communément appelées PA-IL et PA-IIL). À ce jour, plusieurs données laissent à supposer que LecB est un facteur de virulence important. Par exemple, LecB joue un rôle essentiel dans les plaies humaines chroniques avec surinfection. LecB peut bloquer la cicatrisation des cellules épithéliales et la migration des cellules cancéreuses du poumon avec la réduction du niveau de β-caténine, cependant, les mécanismes moléculaires induits par LecB ne sont pas clairs. En outre, LecB provoque également la mort induite par l'activation dépendante du BCR des cellules B in vitro, cependant, son impact sur le système immunitaire reste peut étudié. LecB est un tétramère, et chaque monomère possède une poche de liaison avec la plus grande affinité pour le L-fucose et ses dérivés10. En conséquence, le L-fucose et ses dérivés sont utilisés comme antagonistes de LecB dans plusieurs études. Par exemple, le L-fucose récuse la migration cellulaire collective inhibée et la cicatrisation des plaies dans les monocouches MDCK induites par LecB, et il inhibe l'invasion apicale de P. aeruginosa dans les cellules MDCK polarisées. les projets sont séparés en deux parties pour étudier les questions. Une partie concerne l'effet de LecB sur l'adhésion cellulaire et la migration cellulaire in vitro, et une autre partie concerne l'impact de LecB sur la réponse immunitaire in vivo, impliquant les cellules DC et T.

Mots clés :

P. aeruginosa, lectine LecB, migration cellulaire, réponse immunitaire

Résumé en anglais

Pseudomonas aeruginosa (P. aeruginosa) is a ubiquitous Gram-negative environmental bacterium and is known as an opportunistic and nosocomial pathogen. It can cause a wide variety of infections, which can affect all organs of the human body, such as ventilator-associated pneumonia and acute lung injury. Due to the extracellular toxins of P. aeruginosa, it is virulent to host cells or organs. It has been reported that P. aeruginosa and its virulence proteins can impede wound healing and alter repair processes, leading to chronic wounds. In addition, P. aeruginosa infection can alter the immune response, such as NK cells, T cells and B cells. The first step in establishing a P. aeruginosa infection is to adhere to host cells via extracellular factors, such as lectins. Lectins are glycoproteins that form reversible bonds when interacting with sugars/glycoproteins bound to the host cell membrane. P. aeruginosa has two soluble lectins, LecA and LecB (also known as PA-IL and PA-IIL). To date, several

data suggest that LecB is an important virulence factor. For example, LecB plays an essential role in chronic human wounds with superinfection. LecB can block epithelial cell healing and lung cancer cell migration with the reduction of β-catenin levels, however, the molecular mechanisms induced by LecB are unclear. Furthermore, LecB also induces BCR-dependent activation-induced death of B cells in vitro, however, its impact on the immune system remains unexplored. LecB is a tetramer, and each monomer has a binding pocket with the highest affinity for L-fucose and its derivatives10. As a result, L-fucose and its derivatives have been used as LecB antagonists in several studies. For example, L-fucose challenges inhibited collective cell migration and wound healing in LecB-induced MDCK monolayers, and it inhibits apical invasion of P. aeruginosa in polarised MDCK cells. the projects are split into two parts to investigate the issues. One part concerns the effect of LecB on cell adhesion and cell migration in vitro, and another part concerns the impact of LecB on the immune response in vivo, involving DC and T cells.

Keywords :

P. aeruginosa, lectin LecB, cell migration, immune response